New Optimisation Methods for Machine Learning

Aaron Defazio

A thesis submitted for the degree of
Doctor of Philosophy
of The Australian National University

October 2015

Except where otherwise indicated, this thesis is my own original work.

Aaron Defazio

7 October 2015

Acknowledgements

I would like to thank several NICTA researchers for conversations and brainstorming sessions during the course of my PhD, particularly Scott Sanner and my supervisor Tiberio Caetano.

I would like to thank Justin Domke for many discussions about the Finito algorithm, and his assistance with developing and checking the proof. Likewise, for the SAGA algorithm I would like to thank Francis Bach and Simon Lacoste-Julien for discussion and assistance with the proofs. The SAGA algorithm was discovered in collaboration with them while visiting the INRIA lab, with some financial support from INRIA.

I would also like to thank my family for all their support during the course of my PhD. Particularly my mother for giving me a place to stay for part of the duration of the PhD as well as food, love and support. I do not thank her often enough.

I also would like to thank NICTA for their scholarship during the course of the PhD. NICTA is funded by the Australian Government through the Department of Communications and the Australian Research Council through the ICT Centre of Excellence Program.

Abstract

In this work we introduce several new optimisation methods for problems in machine learning. Our algorithms broadly fall into two categories: optimisation of finite sums and of graph structured objectives. The finite sum problem is simply the minimisation of objective functions that are naturally expressed as a summation over a large number of terms, where each term has a similar or identical weight. Such objectives most often appear in machine learning in the empirical risk minimisation framework in the non-online learning setting. The second category, that of graph structured objectives, consists of objectives that result from applying maximum likelihood to Markov random field models. Unlike the finite sum case, all the non-linearity is contained within a *partition function* term, which does not readily decompose into a summation.

For the finite sum problem, we introduce the Finito and SAGA algorithms, as well as variants of each. The Finito algorithm is best suited to strongly convex problems where the number of terms is of the same order as the condition number of the problem. We prove the fast convergence rate of Finito for strongly convex problems and demonstrate its state-of-the-art empirical performance on 5 datasets.

The SAGA algorithm we introduce is complementary to the Finito algorithm. It is more generally applicable, as it can be applied to problems without strong convexity, and to problems that have a non-differentiable regularisation term. In both cases we establish strong convergence rate proofs. It is also better suited to sparser problems than Finito. The SAGA method has a broader and simpler theory than any existing fast method for the problem class of finite sums, in particular it is the first such method that can provably be applied to non-strongly convex problems with non-differentiable regularisers without introduction of additional regularisation.

For graph-structured problems, we take three complementary approaches. We look at learning the parameters for a fixed structure, learning the structure independently, and learning both simultaneously. Specifically, for the combined approach, we introduce a new method for encouraging graph structures with the "scale-free" property. For the structure learning problem, we establish SHORTCUT, a $O(n^{2.5})$ expected time approximate structure learning method for Gaussian graphical models. For problems where the structure is known but the parameters unknown, we introduce an approximate maximum likelihood learning algorithm that is capable of learning a useful subclass of Gaussian graphical models.

Our thesis as a whole introduces a new suit of techniques for machine learning practitioners that increases the size and type of problems that can be efficiently solved. Our work is backed by extensive theory, including proofs of convergence for each method discussed.

Contents

Chapter 1

Introduction and Overview

Numerical optimisation is in many ways the core problem in modern machine learning. Virtually all learning problems can be tackled by formulating a real valued objective function expressing some notation of loss or suboptimality which can be optimised over. Indeed approaches that don't have well founded objective functions are rare, perhaps contrastive divergence (Hinton, 2002) and some sampling schemes being notable examples.

Many methods that started as heuristics were able to be significantly improved once well-founded objectives were discovered and exploited. Often a convex variant can be developed. A prime example is belief propagation, the relation to the Bethe approximation (Yedidia et al., 2000), and the later development of tree weighted variants (Wainwright et al., 2003) which allowed a convex formulation. The core of this thesis is the development of several new numerical optimisation schemes, primarily focusing on convex objectives, which either address limitations of existing approaches, or improve on the performance of state-of-the-art algorithms. These methods increase the breadth and depth of machine learning problems that are tractable on modern computers.

1.1 Convex Machine Learning Problems

In this work we particularly focus on problems that have convex objectives. This is a major restriction, and one at the core of much of modern optimisation theory, but one that nevertheless requires justification. The primary reasons for targeting convex problems is their ubiquitousness in applications and their relative ease of solving them. Logistic regression, least-squares, support vector machines, conditional random fields and tree-weighted belief propagation all involve convex models. All of these techniques have seen real world application, although their use has been overshadowed in recent years by non-convex models such as neural networks.

Convex optimisation is still of interest when addressing non-convex problems though. Many algorithms that were developed for convex problems, motivated by their provably fast convergence have later been applied to non-convex problems with good

empirical results. Additionally, often the best approach to solving a non-convex problem is through the repeated solution of convex sub-problems, or by replacing the problem entirely with a close convex surrogate.

The class of convex numerical problems is sometimes considered synonymous with that of computationally tractable problems. This is not strictly true in the usual compute science sense of tractability as some convex problems on complicated but convex sets can still be NP-hard (de Klerk and Pasechnik, 2006).

On the other hand, we can sometimes approximately solve non-convex problems of massive scale using modern approaches (e.g. Dean et al., 2012). Instead, convex problems can be better thought of as the *reliably solvable* problems. For convex problems we can almost always establish theoretical results giving a practical bound on the amount of computation time required to solve a given convex problem (Nesterov and Nemirovski, 1994). For non-convex problems we can rarely do better than finding a locally optimal solution.

Together with the small or no tuning required by convex optimisation algorithms, they can be used as building blocks within larger programs; details of the problem can be abstracted away from the users. This is rarely the case for non-convex problems, where the most commonly used methods require substantial hand tuning.

When tasked with solving a convex problem, we have at our disposal powerful and flexible algorithms such as interior point methods and in particular Newton's method. While Newton's method is strikingly successful on small problems, its approximately cubic running time per iteration resulting from the need to do a linear solve means that it scales extremely poorly to problems with large numbers of variables. It is also unable to directly handle non-differentiable problems common in machine learning. Both of these shortcomings have been addressed to some degree (Nocedal, 1980; Liu and Nocedal, 1989; Andrew and Gao, 2007), by the use of low-rank approximations and tricks for specific non-differentiable structures, although problems remain.

An additional complication is a divergence in between the numerical optimisation and machine learning communities. Numerical convex optimisation researchers in the 80s and 90s largely focused on solving problems with large numbers of complex constraints, particularly Quadratic Programming (QP) and Linear Programming (LP) problems. These advances were applicable to the kernel methods of the early 2000s, but at odds with many of the more modern machine learning problems which are characterised by large numbers of potentially non-differentiable terms. The core examples would be linear support vector machines, other max-margin methods and neural networks with non-differentiable activation functions. The problem we address in Chapter 7 also fits into this class.

In this thesis we will focus on smooth optimisation problems, allowing only a controlled level of non-smooth structure in the form of certain non-differentiable regularisation terms (detailed in Section 1.2). The notion of smoothness we use is that

of Lipschitz smoothness. A function f is Lipschitz smooth with constant L if its gradients are Lipschitz continuous. That is, for all $x, y \in \mathbb{R}^d$:

$$\left\| f'(x) - f'(y) \right\| \leq L \left\| x - y \right\|.$$

Lipschitz smooth functions are differentiable, and if their Hessian matrix exists it is bounded in spectral norm. The other assumption we will sometimes make is that of strong convexity. A function f is strongly convex with constant μ if for all $x, y \in \mathbb{R}^d$ and $\alpha \in [0, 1]$:

$$f\left(\alpha x + (1-\alpha)y\right) \leq \alpha f(x) + (1-\alpha) f(y) - \alpha\left(1-\alpha\right) \frac{\mu}{2} \left\| x - y \right\|^2.$$

Essentially rather than the usual convexity interpolation bound $f\left(\alpha x + (1-\alpha)y\right) \leq \alpha f(x) + (1-\alpha) f(y)$, we have it strengthened by a quadratic term.

1.2 Problem Structure and Black Box Methods

The last few years have seen a resurgence in convex optimisation centred around the technique of exploiting problem structure, an approach we take as well. When no structure is assumed by the optimisation method about the problem other than the degree of convexity, very strong results are known about the best possible convergence rates obtainable. These results date back to the seminal work of Nemirovsky and Yudin (1983) and Nesterov (1998, earlier work in Russian). These results have contributed to the widely held attitude that convex optimisation is a solved problem.

But when the problem has some sort of additional structure these worst-case theoretical results are no longer applicable. Indeed, a series of recent results suggest that practically all problems of interest have such structure, allowing advances in theoretical, not just practical convergence. For example, non-differentiable problems under reasonable Lipschitz smoothness assumptions can be solved with an error reduction of $O(\sqrt{t})$ times after t iterations, for standard measures of convergence rate, at best (Nesterov, 1998, Theorem 3.2.1). In practice, virtually all non-differentiable problems can be treated by a smoothing transformation, giving a $O(t)$ reduction in error after t iterations when an optimal algorithm is used (Nesterov, 2005).

Many problems of interest have a structure where most terms in the objective involve only a small number of variables. This is the case for example in inference problems on graphical models. In such cases block coordinate descent methods can give better theoretical and practical results (Richtarik and Takac, 2011).

Another exploitable structure involves a sum of two terms $F(x) = f(x) + h(x)$, where the first term $f(x)$ is structurally nice, say smooth and differentiable, but potentially

complex to evaluate, and where the second term $h(x)$ is non-differentiable. As long as $h(x)$ is simple in the sense that its *proximal operator* is easy to evaluate, then algorithms exist with the same theoretical convergence rate as if $h(x)$ was not part of the objective at all ($F(x) = f(x)$) (Beck and Teboulle, 2009). The proximal operator is a key construction in this work, and indeed in modern optimisation theory. It is defined for a function h and constant γ as:

$$\text{prox}_{\gamma}^{h}(v) = \arg\min_{x} \left\{ h(x) + \frac{\gamma}{2} \|x - v\|^2 \right\}.$$

Some definitions of the proximal operator use the weighting $\frac{1}{2\gamma}$ instead of $\frac{\gamma}{2}$; we use this form throughout this work. The proximal operator is itself an optimisation problem, and so in general it is only useful when the function h is simple. In many cases of interest the proximal operator has a closed form solution.

The first four chapters of this work focus on quite possibly the simplest problem structure, that of a finite summation. This occurs when there is a large number of terms with similar structure added together or averaged in the objective. Recent results have shown that for strongly convex problems better convergence rates are possible under such summation structures than is possible for black box problems (Schmidt et al., 2013; Shalev-Shwartz and Zhang, 2013b). We provide three new algorithms for this problem structure, discussed in Chapters 3 and 4. We also discuss properties of problems in the finite sum class extensively in Chapter 5.

1.3 Early & Late Stage Convergence

When dealing with problems with a finite sum structure, practitioners have traditionally had to make a key trade-off between stochastic methods which access the objective one term at a time, and batch methods which work directly with the full objective. Stochastic methods such as SGD (stochastic gradient descent, Robbins and Monro, 1951) exhibit rapid convergence during early stages of optimisation, yielding a good approximate solution quickly, but this convergence slows down over time; getting a high accuracy solution is nearly impossible with SGD. Fortunately, in machine learning it is often the case that a low accuracy solution gives just as a good a result as a high accuracy solution for minimising the test loss on held out data. A high accuracy solution can effectively over-fit to the training data. Running SGD for a small number of epochs is common in practice.

Batch methods on the other hand are slowly converging but steady; if run for long enough they yield a high accuracy solution. For strongly convex problems, the difference in convergence is between a $O(1/t)$ error after t iterations for SGD versus

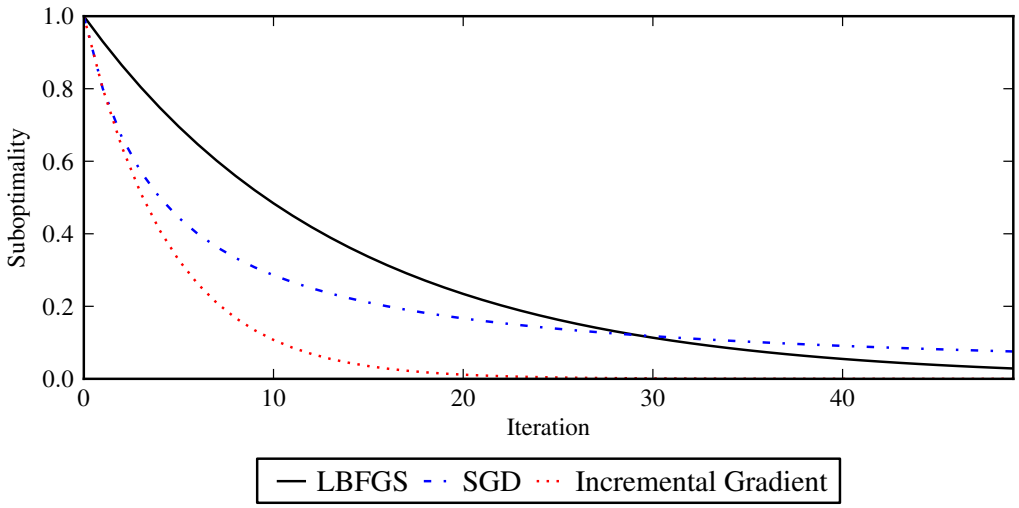

Figure 1.1: Schematic illustration of convergence rates

a $O(\rho^t)$ error ($\rho < 1$) for LBFGS[1], the most popular batch method (Nocedal, 1980). We have illustrated the difference schematically in Figure 1.1. The SGD and LBFGS lines here are typical of simple prediction problems, where SGD gives acceptable solutions after 5-10 epochs (passes over the data), where LBFGS eventually gives a better solution, taking 30-100 iterations to do so. LBFGS is particularly well suited to use in a distributed computing setting, and it is sometimes the case LBFGS will give better results ultimately on the test loss, particularly for poorly conditioned (high-curvature) problems.

Figure 1.1 also illustrates the kind of convergence that the recently developed class of incremental gradient methods potentially offers. Incremental gradient methods have the same linear $O(\rho^t)$ error after t epochs as a batch method, but with a coefficient ρ dramatically better. The difference being in theory thousands of times faster convergence, and in practice usually 10-20 times better. With favorable problem structure incremental gradient have the potential to offer the best of both worlds, having rapid initial convergence without the later stage slow-down of SGD.

Another traditional advantage of batch methods over stochastic methods is their ease of use. Methods such as LBFGS require no hand tuning to be applied to virtually any smooth problem. Some tuning of the memory constant that holds the number of past gradients to remember at each step can give faster convergence, but bad choices of this constant still result in convergence. SGD and other traditional stochastic methods on the other hand require a step size parameter and a parameter annealing schedule to be set. SGD is sensitive to these choices, and will diverge for poor choices.

[1]Quasi-newton methods are often cited as having local super-linear convergence. This is only true if the dimensionality of the underlying parameter space is comparable to the number of iterations used. In machine learning the parameter space is usually much larger in effective dimension than the number of iterations.

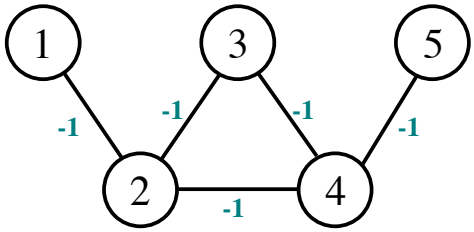

$$C = \frac{1}{100}\begin{bmatrix} 10 & 1 & 0.1 & 0.1 & 0.01 \\ 1 & 10 & 1 & 1 & 0.1 \\ 0.1 & 1 & 10 & 1 & 0.0 \\ 0.1 & 1 & 1 & 10 & 1 \\ 0.01 & 0.1 & 0.1 & 1 & 10 \end{bmatrix} \qquad P = C^{-1} = \begin{bmatrix} 10 & -1 & 0 & 0 & 0 \\ -1 & 10 & -1 & -1 & 0 \\ 0 & -1 & 10 & -1 & 0 \\ 0 & -1 & -1 & 10 & -1 \\ 0 & 0 & 0 & -1 & 10 \end{bmatrix}$$

Figure 1.2: Gaussian graphical model defined by the precision matrix P, together with the non-sparse covariance matrix C it induces with rounding to 1 significant figure. Correlations are indicated by negative edge weights in a Gaussian model.

Incremental gradient methods offer a solution to the tuning problem as well. Most incremental gradient algorithms have only a single step size parameter that needs to be set. Fortunately the convergence rate is fairly robust to the value of this parameter. The SDCA algorithm (Shalev-Shwartz and Zhang 2013b) reduces this to 0 parameters, but at the expense of being limited to problems with efficient to compute proximal operators.

1.4 Approximations

The exploitation of problem structure is not always directly possible with the objectives we encounter in machine learning. A case we focus on in this work is the learning of weight parameters in a Gaussian graphical model structure. This is an undirected graph structure with weights associated with both edges and nodes. These weights are the entries of the precision matrix (inverse covariance matrix) of a Gaussian distribution. Absent edges effectively have a weight of zero (Figure 1.2). A formal definition is given in Chapter 6. A key approach to such problems is the use of approximations that introduce additional structure in the objective which we can exploit.

The regularised maximum likelihood objective for fitting a Gaussian graphical model can require time $O(n^3)$ to evaluate[2]. This is prohibitively long on many problems of interest. Instead, approximations can be introduced that decompose the objective, allowing more efficient techniques to be used. In Chapter 9 we show how the *Bethe approximation* may be applied for learning the edge weights on restricted classes of

[2]Theoretically it takes time equivalent to the big-O cost of a fast matrix multiplication such as Strassen's algorithm ($\approx O(n^{2.8})$), but in practice simpler $O(n^3)$ techniques are used.

Gaussian graphical models. This approximation allows for the use of an efficient dual decomposition optimisation method, and has direct practical applicability in the domain of recommendation systems.

Besides parameter learning, the other primary task involving graphs is directly learning the structure. Structure learning for Gaussian graphical models is problem that has seen a lot of interest in machine learning. The structure can be used in a machine learning pipeline as the precursor to parameter learning, or it can be used for its own sake as indicator of correlation structure in a dataset. The use of approximations in structure learning is more widespread than in parameter learning, and we give an overview of approaches in Chapter 6. We improve on an existing technique in Chapter 8, where we show that an existing approximation can be *further approximated*, giving a substantial practical and theoretical speed-up by a factor of $O(\sqrt{n})$.

1.5 Non-differentiability in Machine Learning

As mentioned, machine learning problems tend to have substantial non-differentiable structure compared to the constraint structures more commonly addressed in numerical optimisation. These two forms of structure are in a sense two sides of the same coin, as for convex problems the transformation to the dual problem can often convert from one to the other. The primary example being support vector machines, where non-differentiability in the primal hinge loss is converted to a constraint set when the dual is considered.

Recent progress in optimisation has seen the use of proximal methods as the tool of choice for handling both structures in machine learning problems. When using a regularised loss objective of the form $F(x) = f(x) + h(x)$ as mentioned above in Section 1.2, the non-differentiability can be in the regulariser $h(x)$ or the loss term $f(x)$. We introduce methods addressing both cases in this work. The SAGA algorithm of Chapter 4 is a new primal method, the first primal incremental gradient method able to be used on non-strongly convex problems with non-differentiable regularisers directly. It makes use of the proximal operator of the regulariser. It can also be used on problems with constraints, where the function $h(x)$ is the indicator function of the constraint set, and proximal operator is projection onto the constraint set.

In this work we also introduce a new non-differentiable regulariser for the above mentioned graph structure learning problem, which can also be attacked using proximal methods. Its non-differentiable structure is atypically complex compared to other regularisers used in machine learning, requiring a special optimisation procedure to be used just to evaluate the proximal operator.

For non-differentiable losses, we introduce the Prox-Finito algorithm (Section 3.6). This incremental gradient algorithm uses the proximal operator of the single datapoint loss. It provides a bridge between the Finito algorithm (Section 3.1) and

the SDCA algorithm (Shalev-Shwartz and Zhang, 2013b), having properties of both methods.

1.6 Publications Related to This Thesis

The majority of the content in this thesis has been published as conference articles. For the work on incremental gradient methods, the Finito method has been published as Defazio et al. (2014b), and the SAGA method as Defazio et al. (2014a). Chapters 3 & 4 contain much more detailed theory than has been previously published. Some of the discussion in Chapter 5 appears in Defazio et al. (2014b) also. For the portion of this thesis on Gaussian graphical models, Chapter 7 largely follows the publication Defazio and Caetano (2012a). Chapter 9 is based on the work in Defazio and Caetano (2012b), although heavily revised.

Chapter 2

Incremental Gradient Methods

In this chapter we give an introduction to the class of incremental gradient (IG) methods. Incremental gradient methods are simply a class of methods that can take advantage of known summation structure in an optimisation objective by accessing the objective one term at a time. Objectives that are decomposable as a sum of a number of terms come up often in applied mathematics and scientific computing, but are particularly prevalent in machine learning applications. Research in the last two decades on optimisation problems with a summation structure has focused more on the stochastic approximation setting, where the summation is assumed to be over an infinite set of terms. The *finite* sum case that incremental gradient methods cover has seen a resurgence in recent years after the discovery that there exist *fast* incremental gradient methods whose convergence rates are better than any possible black box method for finite sums with particular (common) structures. We provide an extensive overview of all known fast incremental gradient methods in the later parts of this chapter. Building on the described methods, in Chapters 3 & 4 we introduce three novel fast incremental gradient methods. Depending on the problem structure, each of these methods can have state-of-the-art performance.

2.1 Problem Setup

We are interested in minimising functions of the form

$$f(x) = \frac{1}{n}\sum_{i=1}^{n} f_i(x),$$

where $x \in \mathbb{R}^d$ and each f_i is convex and Lipschitz smooth with constant L. We will also consider the case where each f_i is additionally strongly convex with constant μ. See Appendix A.1 for defintions of Lipschitz smoothness and strong convexity. Incremental gradient methods are algorithms that at each step evaluate the gradient and function value of only a single f_i.

We will measure convergence rates in terms of the number of $(f_i(x), f_i'(x))$ evaluations, normally these are much cheaper computationally than evaluations of the whole function gradient f', such as performed by the *gradient descent* algorithm. We use the notation x^* to denote a minimiser of f. For strongly convex problems this is the unique minimiser.

This setup differs from the traditional black box smooth convex optimisation problem only in that we are assuming that our function is decomposable into a *finite sum* structure. This finite sum structure is widespread in machine learning applications. For example, the standard framework of Empirical Risk Minimisation (ERM) takes this form, where for a loss function $L : \mathbb{R}^d \times \mathbb{R} \to \mathbb{R}$ and data label tuples (x_i, y_i), we have:

$$R_{\text{emp}}(h) = \frac{1}{n} \sum_{i}^{n} L(h(x_i), y_i),$$

where h is the hypothesis function that we intend to optimise over. The most common case of ERM is minimisation of the negative log-likelihood, for instance the classical logistic regression problem (See standard texts such as Bishop 2006). Often ERM is an approximation to an underlying stochastic programming problem, where the summation is replaced with an expectation over a population of data tuples from which we can sample from.

2.1.1 Exploiting problem structure

Given the very general nature of the finite sum structure, we can not expect to get faster convergence than we would by accessing the whole gradient without additional assumptions. For example, suppose the summation only has one term, or alternatively each f_i is the zero function except one of the n.

Notice that the Lipschitz smoothness and strong convexity assumptions we made are on each f_i rather than on f. This is a key point. If the directions of maximum curvature of each term are aligned and of similar magnitude, then we can expect the term Lipschitz smoothness to be similar to the smoothness of the whole function. However, it is easy to construct problems for which this is not the case, in fact the Lipschitz smoothness of f may be n times smaller than that of each f_i. In that case the incremental gradient methods will give no improvement over black box optimisation methods.

For machine learning problems, and particularly the empirical risk minimisation problem, this worst case behavior is not common. The curvature and hence the Lipschitz constants are defined largely by the loss function, which is shared between the terms, rather than the data point. Common data preprocessing methods such as data whitening can improve this even further.

The requirement that the magnitude of the Lipschitz constants be approximately balanced can be relaxed in some cases. It is possible to formulate IG methods where the convergence is stated in terms of the average of the Lipschitz constants of the f_i instead of the maximum. This is the case for the Prox-Finito algorithm described in Section 3.6. All known methods that make use of the average Lipschitz constant require knowledge of the ratios of the Lipschitz constants of the f_i terms, which limits their practicality unfortunately.

Regardless of the condition number of the problem, if we have a summation with enough terms optimisation becomes easy. This in made precise in the definition that follows.

Definition 2.1. The big data condition: For some known constant $\beta \geq 1$,

$$n \geq \beta \frac{L}{\mu}.$$

This condition obviously requires strong convexity and Lipschitz smoothness so that L/μ is well defined. It is a very strong assumption for small n, as the condition number L/μ in typical machine learning problems is at least in the thousands. For applications of this assumption, β is typically between 1 and 8. Several of the methods we describe below have a fixed and very fast convergence rate independent of the condition number when this big-data condition holds.

2.1.2 Randomness and expected convergence rates

This thesis works extensively with optimisation methods that make random decisions during the course of the algorithm. Unlike the stochastic approximation setting, we are dealing with deterministic, known optimisation problems; the stochasticity is introduced by our optimisation methods, it is not inherent in the problem. We introduce randomness because it allows us to get convergence rates faster than that of any currently known deterministic methods. The caveat is that these convergence rates are in *expectation*, so they don't always hold precisely. This is not as bad as it first seems though. Determining that the expectation of a general random variable converges is normally quite a weak result, as its value may vary around the expectation substantially in practice, potentially by far more than it converges by. The reason why this is not an issue for the optimisation methods we consider is that all the random variables we bound are *non-negative*. A non-negative random variable X with a very small expectation, say:

$$E[X] = 1 \times 10^{-5},$$

is with high probability close to its expectation. This is a fundamental result implied by Markov's inequality. For example, suppose $E[X] = 1 \times 10^{-5}$ and we want to bound the probability that X is greater than 1×10^{-3}, i.e. a factor of 100 worse than

its expectation. Then Markov's inequality tells us that:

$$P(X \geq 1 \times 10^{-3}) \leq \frac{1}{100}.$$

So there is only a 1% chance of X being larger than 100 times its expected value here. We will largely focus on methods with linear convergence in the following chapters, so in order to increase the probability of the value X holding by a factor ρ, only a logarithmic number of additional iterations in ρ is required ($O(\log \rho)$).

We would also like to note that Markov's inequality can be quite conservative. Our experiments in later chapters show little in the way of random noise attributable to the optimisation procedure, particularly when the amount of data is large.

2.1.3 Data access order

The source of randomness in all the methods considered in this chapter is the order of accessing the f_i terms. By *access* we mean the evaluation of $f_i(x)$ and $f_i'(x)$ at an x of our choice. This is more formally known as an oracle evaluation (see Section 5.1), and typically constitutes the most computationally expensive part of the main loop of each algorithm we consider. The access order is defined on a per-*epoch* basis, where an epoch is n evaluations. Only three different access orders are considered in this work:

Cyclic Each step with $j = 1 + (k \mod n)$. Effectively we access f_i in the order they appear, then loop to the beginning and the end of every epoch.

Permuted Each epoch with j is sampled without replacement from the set of indices not accessed yet in that epoch. This is equivalent to permuting the f_i at the beginning of each epoch, then using the cyclic order within the epoch.

Randomised The value of j is sampled uniformly at random with replacement from $1, \ldots, n$.

The "permuted" terminology is our nomenclature, whereas the other two terms are standard.

2.2 Early Incremental Gradient Methods

The classical incremental gradient (IG) method is simply a step of the form:

$$x^{k+1} = x^k - \gamma_k f_j'(x^k),$$

where at step k we use cyclic access, taking $j = 1 + (k \mod n)$. This is similar to the more well known stochastic gradient descent, but with a cyclic order of access of the data instead of a random order. We have introduced here a superscript notation x^k for the variable x at step k. We use this notation throughout this work.

It turns out to be much easier to analyse such methods under a random access ordering. For the random order IG method (i.e. SGD) on smooth strongly convex problems, the following rate holds for an appropriately chosen step sizes:

$$\mathbb{E}\left[f(x^k) - f(x^*)\right] \leq \frac{L}{2k}\left\|x^0 - x^*\right\|^2.$$

The step size scheme required is of the form $\gamma_k = \frac{\theta}{k}$, where θ is a constant that depends on the gradient norm bound R as well as the degree of strong convexity μ. It may be required to be quite small in some cases. This is what's known as a *sublinear* rate of convergence, as the dependence on k is of the form $O(\frac{L}{2k})$, which is slower than the linear rate $O((1-\alpha)^k)$ for any $\alpha \in (0,1)$ asymptotically.

Incremental gradient methods for strongly convex smooth problems were of less practical utility in machine learning up until the development of fast variants (discussed below), as the sublinear rates for the previously known methods did not compare favourably to the (super-)linear rate of quasi-Newton methods. For non-strongly convex problems, or strongly convex but non-smooth problems, the story is quite different. In those cases, the theoretical and practical rates are hard to beat with full (sub-)gradient methods. The non-convex case is of particular interest in machine learning. SGD has been the de facto standard optimisation method for neural networks for example since the 1980s (Rumelhart et al., 1986).

Such incremental gradient methods have a long history, having been applied to specific problems as far back as the 1960s (Widrow and Hoff, 1960). An up-to-date survey can be found in Bertsekas (2012).

2.3 Stochastic Dual Coordinate Descent (SDCA)

The stochastic dual coordinate descent method (Shalev-Shwartz and Zhang, 2013b) is based on the principle that for problems with explicit quadratic regularisers, the dual takes a particularly easy to work with form. Recall the finite sum structure $f(x) = \frac{1}{n}\sum_{i=1}^n f_i(x)$ defined earlier. Instead of assuming that each f_i is strongly convex, we instead need to consider the regularised objective:

$$f(x) = \frac{1}{n}\sum_{i=1}^n f_i(x) + \frac{\mu}{2}\left\|x\right\|^2.$$

For any strongly convex f_i, we may transform our function to this form by replacing each f_i with $f_i - \frac{\mu}{2}\|x\|^2$, then including a separate regulariser. This changes the Lipschitz smoothness constant for each f_i to $L - \mu$, and preserves convexity. We are now ready to consider the dual transformation. We apply the technique of **dual decomposition**, where we decouple the terms in our objective as follows:

$$\min_{x,x_1,\dots x_i,\dots,x_n} f(x) = \frac{1}{n}\sum_{i=1}^{n} f_i(x_i) + \frac{\mu}{2}\|x\|^2,$$

$$s.t.\ x = x_i\ i = 1\dots n.$$

This reformulation initially achieves nothing, but the key idea is that we now have a constrained optimisation problem, and so we may apply Lagrangian duality (Section A.3). The Lagrangian function is:

$$\begin{aligned} L(x, x_1, \dots \alpha_1, \dots) &= \frac{1}{n}\sum_{i=1}^{n} f_i(x_i) + \frac{\mu}{2}\|x\|^2 + \frac{1}{n}\sum_{i}^{n}\langle \alpha_i, x - x_i\rangle \\ &= \frac{1}{n}\sum_{i=1}^{n}\left(f_i(x_i) - \langle \alpha_i, x_i\rangle\right) + \frac{\mu}{2}\|x\|^2 + \left\langle \frac{1}{n}\sum_{i}^{n}\alpha_i, x\right\rangle, \end{aligned} \quad (2.1)$$

where $\alpha_i \in \mathbb{R}^d$ are the introduced dual variables. The Lagrangian dual function is formed by taking the minimum of L with respect to each x_i, leaving α, the set of α_i $i = 1\dots n$ free:

$$D(\alpha) = \frac{1}{n}\sum_{i=1}^{n}\min_{x_i}\left\{f_i(x_i) - \langle \alpha_i, x_i\rangle\right\} + \min_{x}\left\{\frac{\mu}{2}\|x\|^2 + \left\langle \frac{1}{n}\sum_{i}\alpha_i, x\right\rangle\right\}, \quad (2.2)$$

Now recall that the definition of the convex conjugate (Section A.2) says that:

$$\min\left\{f(x) - \langle a, x\rangle\right\} = -\sup_x\left\{\langle a, x\rangle - f(x)\right\} = -f^*(\alpha).$$

Clearly we can plug this in for each f_i to get:

$$D(\alpha) = -\frac{1}{n}\sum_{i=1}^{n} f_i^*(\alpha_i) + \min_{x}\left[\frac{\mu}{2}\|x\|^2 + \left\langle \frac{1}{n}\sum_{i}\alpha_i, x\right\rangle\right].$$

We still need to simplify the remaining min term, which is also in the form of a convex conjugate. We know that squared norms are self-conjugate, and scaling a function by a positive constant β transforms its conjugate from $f^*(a)$ to $\beta f^*(a/\beta)$, so we in fact have:

$$D(\alpha) = -\frac{1}{n}\sum_{i=1}^{n} f_i^*(\alpha_i) - \frac{\mu}{2}\left\|\frac{1}{\mu n}\sum_{i}\alpha_i\right\|^2.$$

Algorithm 2.1 SDCA (exact coordinate descent)

Initialise x^0 and α_i^0 as the zero vector, for all i.
Step $k+1$:

1. Pick an index j uniformly at random.
2. Update α_j, leaving the other α_i unchanged:

$$\alpha_j^{k+1} = \arg\min_y \left[f_j^*(y) + \frac{\mu n}{2} \left\| x^k - \frac{1}{\mu n} \left(y - \alpha_j^k \right) \right\|^2 \right].$$

3. Update $x^{k+1} = x^k - \frac{1}{\mu n} \left(\alpha_j^{k+1} - \alpha_j^k \right)$.

At completion, for smooth f_i return x^k. For non-smooth, return a tail average of the x^k sequence.

This is the objective directly maximised by SDCA. As the name implies, SDCA is randomised (block) coordinate ascent on this objective, where only one α_i is changed each step.

In coordinate descent we have the option of performing a gradient step in a coordinate direction, or an exact minimisation. For the exact coordinate minimisation, the update is easy to derive:

$$\begin{aligned} \alpha_j^{k+1} &= \arg\min_{\alpha_j} \left[\frac{1}{n} \sum_{i=1}^n f^*(\alpha_i) + \frac{\mu}{2} \left\| \frac{1}{\mu n} \sum_i^n \alpha_i \right\|^2 \right] \\ &= \arg\min_{\alpha_j} \left[f_j^*(\alpha_j) + \frac{\mu n}{2} \left\| \frac{1}{\mu n} \sum_i^n \alpha_i \right\|^2 \right]. \end{aligned} \tag{2.3}$$

The primal point x^k corresponding to the dual variables α_i^k at step k is the minimiser of the conjugate problem $x^k = \arg\min_x \left[\frac{\mu}{2} \|x\|^2 + \left\langle \frac{1}{n} \sum_i^n \alpha_i^k, x \right\rangle \right]$, which in closed form is simply $x^k = -\frac{1}{\mu n} \sum_i^n \alpha_i^k$. This can be used to further simplify Equation 2.3. The full method is Algorithm 2.1.

The SDCA method has a geometric convergence rate in the dual objective D of the form:

$$\mathbb{E}\left[D(\alpha^k) - D(\alpha^*) \right] \leq \left(1 - \frac{\mu}{L + \mu n} \right)^k \left[D(\alpha^0) - D(\alpha^*) \right].$$

This is easily extended to a statement about the duality gap $f(x^k) - D(\alpha^k)$ and hence the suboptimality $f(x^k) - f(x^*)$ by using the relation:

$$f(x^k) - D(\alpha^k) \leq \frac{L + \mu n}{\mu} \left(D(\alpha^k) - D(\alpha^*) \right).$$

2.3.1 Alternative steps

The full coordinate minimisation step discussed in the previous section is not always practical. If we are treating each element f_i in the summation $\frac{1}{n}\sum_i^n f_i(x)$ as a single data point loss, then even for the simple binary logistic loss there is not a closed form solution for the exact coordinate step. We can use a black-box 1D optimisation method to find the coordinate minimiser, but this will generally require 20-30 exponential function evaluations, together with one vector dot product.

For multiclass logistic loss, the subproblem solve is not fast enough to yield a usable algorithm. In the case of non-differentiable losses, the situation is better. Most non-differentiable functions we use in machine learning, such as the hinge loss, yield closed form solutions.

For performance reasons we often want to treat each f_i as a minibatch loss, in which case we virtually never have a closed form solution for the subproblem, even in the non-differentiable case.

Shalev-Shwartz and Zhang (2013a) describe a number of other possible steps which lead to the same theoretical convergence rate as the exact minimisation step, but which are more usable in practice:

Interval Line search: It turns out that it is sufficient to perform the minimisation in Equation 2.3 along the interval between the current dual variable α_j^k and the point $u = f_j'(x^k)$. The update takes the form:

$$s = \arg\min_{s\in[0,1]} \left[f_j^* \left(\alpha_j^k + s(u - \alpha_j^k)\right) + \frac{\mu n}{2} \left\| x^k + \frac{s}{\mu n}\left(u - \alpha_j^k\right)\right\|^2 \right],$$

$$\alpha_j^{k+1} = \alpha_j^k + s(u - \alpha_j^k).$$

Constant step: If the value of the Lipschitz smoothness constant L is known, we can calculate a conservative value for the parameter s instead of optimising over it with an interval line search. This gives an update of the form:

$$\alpha_j^{k+1} = \alpha_j^k + s(u - \alpha_j^k)$$

$$\text{where } s = \frac{\mu n}{\mu n + L}.$$

This method is much slower in practice than performing a line-search, just as a $\frac{1}{L}$ step size with gradient descent is much slower than performing a line search.

2.3.2 Reducing storage requirements

We have presented the SDCA algorithm in full generality above. This results in dual variables of dimension d, for which the total storage $d \times n$ can be prohibitive. In practice, the dual variables often lie on a low-dimensional subspace. This is the case with linear classifiers and regressors, where a r class problem has gradients on a $r-1$ dimensional subspace.

A linear classifier takes the form $f_i(x) = \phi\left(X_i^T x\right)$, for a fixed loss $\phi : \mathbb{R}^r \to \mathbb{R}$ and data instance matrix $X_i : d \times r$. In the simplest case X_i is just the data point duplicated as r rows. Then the dual variables are r dimensional, and the x^k updates change to:

$$x^k = -\frac{1}{\mu n} \sum_i^n X_i \alpha_i.$$

$$\alpha_j^{k+1} = \arg\min_\alpha \left[\phi_j^*(\alpha) + \frac{\mu n}{2} \left\| x^k + \frac{1}{\mu n} X_i \left(\alpha - \alpha_j^k \right) \right\|^2 \right].$$

This is the form of SDCA presented by Shalev-Shwartz and Zhang (2013a), although with the negation of our dual variables.

2.3.3 Accelerated SDCA

The SDCA method is also currently the only fast incremental gradient method to have a known accelerated variant. By acceleration, we refer to the modification of an optimisation method to improve the convergence rate by an amount greater than any constant factor. This terminology is common in optimisation although a precise definition is not normally given.

The **A**SDCA method (Shalev-Shwartz and Zhang, 2013a) works by utilising the regular SDCA method as a sub-procedure. It has an outer loop, which at each step invokes SDCA on a modified problem $x^{k+1} = \min_x f(x) + \frac{\lambda}{2} \|x - y\|^2$, where y is chosen as an over-relaxed step of the form:

$$y = x^k + \beta(x^k - x^{k-1}),$$

for some known constant β. The constant λ is likewise computed from the Lipschitz smoothness and strong convexity constants. These regularised sub-problems $f(x) + \frac{\lambda}{2} \|x - y\|^2$ have a greater degree of strong convexity than $f(x)$, and so individually are much faster to solve. By a careful choice of the accuracy at which they are computed to, the total number of steps made between all the subproblem solves is

much smaller than would be required if regular SDCA is applied directly to $f(x)$ to reach the same accuracy.

In particular, they state that to reach an accuracy of ϵ in expectation for the function value, they need k iterations, where:

$$k = \tilde{O}\left(dn + \min\left\{\frac{dL}{\mu}, d\sqrt{\frac{nL}{\mu}}\right\}\right)\log(1/\epsilon).$$

The $\tilde{O}$ notation hides constant factors. This rate is not of the same precise form as the other convergence rates we will discuss in this chapter. We can make some general statements though. When n is in the range of the big-data condition, this rate is no better than regular SDCA's rate, and probably worse in practice due to overheads hidden by the $\tilde{O}$ notation. When n is much smaller than $\frac{L}{\mu}$, then potentially it can be much faster than regular SDCA.

Unfortunately, the ASDCA procedure has significant computational overheads that make it not necessarily the best choice in practice. Probably the biggest issue however is a sensitivity to the Lipschitz smoothness and strong convexity constants. It assumes these are known, and if the used values differ from the true values, it may be significantly slower than regular SDCA. In contrast, regular SDCA requires no knowledge of the Lipschitz smoothness constants (for the prox variant at least), just the strong convexity (regularisation) constant.

2.4 Stochastic Average Gradient (SAG)

The SAG algorithm (Schmidt et al., 2013) is the closest in form to the classical SGD algorithm among the fast incremental gradient methods. Instead of storing dual variables α_i like SDCA above, we store a table of past gradients y_i, which has the same storage cost in general, $n \times d$. The SAG method is given in Algorithm 2.2. The key equation for SAG is the step:

$$x^{k+1} = x^k - \frac{1}{\gamma n}\sum_i^n y_i^k.$$

Essentially we move in the direction of the average of the past gradients. Note that this average contains one past gradient for each term, and they are equally weighted. This can be contrasted to the SGD method with momentum, which uses a geometrically decaying weighted sum of all past gradient evaluations. SGD with momentum however is not a linearly convergent method. It is surprising that using equal weights like this actually yields a much faster converging algorithm, even though some of the gradients in the summation can be extremely out of date.

Algorithm 2.2 SAG

Initialise x^0 as the zero vector, and $y_i = f_i'(x^0)$ for each i.
Step $k+1$:

1. Pick an index j uniformly at random.
2. Update x using step length constant γ:

$$x^{k+1} = x^k - \frac{1}{\gamma n} \sum_i^n y_i^k.$$

3. Set $y_j^{k+1} = f_j'(x^{k+1})$. Leave $y_i^{k+1} = y_i^k$ for $i \neq j$.

SAG is an evolution of the earlier incremental averaged gradient method (IAG, Blatt et al., 2007) which has the same update with a different constant factor, and with cyclic access used instead of randomised. IAG has a more limited convergence theory covering quadratic or bounded gradient problems, and a much slower rate of convergence.

The convergence rate of SAG for strongly convex problems is of the same order as SDCA, although the constants are not quite as good. In particular, we have an expected convergence rate in terms of function value suboptimality of:

$$\mathbb{E}[f(x^k) - f(x^*)] \leq \left(1 - \min\left\{\frac{1}{8n}, \frac{\mu}{16L}\right\}\right)^k L_0,$$

Where L_0 is a complex expression involving $f(x^0 + \frac{1}{\gamma n}\sum_i^n y_i^0)$ and a quadratic form of x^0 and each y_i^0. This theoretical convergence rate is between 8 and 16 times worse than SDCA. In practice SAG is often faster than SDCA though, suggesting that the SAG theory is not tight. A nice feature of SAG is that unlike SDCA, it can be directly applied to non-strongly convex problems. Differentiability is still required though. The convergence rate is then in terms of the average iterate $\bar{x}^k = \frac{1}{k}\sum_l^k x^l$:

$$\mathbb{E}[f(\bar{x}^k) - f(x^*)] \leq \frac{32n}{k} L_0.$$

The SAG algorithm has great practical performance, but it is surprisingly difficult to analyse theoretically. The above rates are likely conservative by a factor of between 4 and 8. Due to the difficulty of analysis, the proximal version for composite losses has not yet had its theoretical convergence established.

Algorithm 2.3 SVRG

Initialise x^0 as the zero vector, $g^k = \frac{1}{n}\sum_i f_i'(x^0)$ and $\tilde{x}^0 = x^0$.
Step $k+1$:

1. Pick j uniformly at random.
2. Update x:
$$x^{k+1} = x^k - \frac{1}{\eta} f_j'(x^k) + \frac{1}{\eta}\left[f_j'(\tilde{x}^k) - g^k\right].$$
3. Every m iterations, set $\tilde{x}$ and recalculate the full gradient at that point:
$$\tilde{x}^{k+1} = x^{k+1}.$$
$$g^k = \frac{1}{n}\sum_i f_i'(\tilde{x}^{k+1}).$$
Otherwise leave $\tilde{x}^{k+1} = \tilde{x}^k$ and $g^{k+1} = g^k$.

At completion return $\tilde{x}$.

2.5 Stochastic Variance Reduced Gradient (SVRG)

The SVRG method (Johnson and Zhang, 2013) is a recently developed fast incremental gradient method. It was developed to address the potentially high storage costs of SDCA and SAG, by trading off storage against computation. The SVRG method is given in Algorithm 2.3. Unlike the other methods discussed, there is a tunable parameter m, which specifies the number of iterations to complete before the current gradient approximation is "recalibrated" by computing a full gradient $f'(\tilde{x})$ at the last iterate before the recalibration, $\tilde{x} := x^k$. Essentially, instead of maintaining a table of past gradients y_i for each i like SAG does, the algorithm just stores the location $\tilde{x}$ at which those gradients should be evaluated, then re-evaluates them when needed by just computing $f_j'(\tilde{x})$.

Like the SAG algorithm, at each step we need to know the updated term gradient $f_j'(x^k)$, the old term gradient $f_j'(\tilde{x})$ and the average of the old gradients $f'(\tilde{x})$. Since we are not storing the old term gradient, just its average, we need to calculate two term gradients instead of the one term gradient calculated by SAG at each step.

The S2GD method (Konečný and Richtárik, 2013) was concurrently developed with SVRG. It has the same update as SVRG, just differing in that the theoretical choice of $\tilde{x}$ discussed in the next paragraph. We use SVRG henceforth to refer to both methods.

The update $\tilde{x}^{k+1} = x^{k+1}$ in step 3 above is technically not supported by the theory. Instead, one of the following two updates are used:

1. $\tilde{x}$ is the average of the x values from the last m iterations. This is the variant suggested by Johnson and Zhang (2013).

2. $\tilde{x}$ is a randomly sampled x from the last m iterations. This is used in the S2GD variant (Konečný and Richtárik, 2013).

These alternative updates are required theoretically as the convergence between re-calibrations is expressed in terms of the average of function values of the last m points,

$$\frac{1}{m}\sum_{r=k-m}^{k}\left[f(x^r)-f(x^*)\right],$$

instead of in terms of $f(x^k)-f(x^*)$ directly. Variant 1 avoids this issue by using Jensen's inequality to pull the summation inside:

$$\frac{1}{m}\sum_{r=k-m}^{k}\left[f(x^r)-f(x^*)\right] \geq f(\frac{1}{m}\sum_{r=k-m}^{k}x^r)-f(x^*).$$

Variant 2 uses a sampled x, which in expectation will also have the required value. In practice, there is a very high probability that $f(x^k)-f(x^*)$ is less than the last-m average, so just taking $\tilde{x}=x^k$ works.

The SVRG method has the following convergence rate if k is a multiple of m:

$$\mathbb{E}[f(\tilde{x}^k)-f(x^*)] \leq \rho^{k/m}\left[f(\tilde{x}^0)-f(x^*)\right],$$

$$\text{where } \rho=\frac{\eta}{\mu(1-4L/\eta)m}+\frac{4L(m+1)}{\eta(1-4L/\eta)m}.$$

Note also that each step requires two term gradients, so the rate must be halved when comparing against the other methods described in this chapter. There is also the cost of the recalibration pass, which (depending on m) can further increase the run time to three times that of SAG per step. This convergence rate has quite a different form from that of the other methods considered in this section, making direct comparison difficult. However, for most parameter values this theoretical rate is worse than that of the other fast incremental gradient methods. In Section 4.7 we give an analysis of SVRG that requires additional assumptions, but gives a rate that is directly comparable to the other fast incremental gradient methods.

Chapter 3

New Dual Incremental Gradient Methods

In this chapter we introduce a novel fast incremental gradient method for strongly convex problems that we call *Finito*. Like SDCA, SVRG and SAG, Finito is a stochastic method that is able to achieve linear convergence rates for strongly convex problems. Although the Finito algorithm only uses primal quantities directly, the proof of its convergence rate uses lower bounds extensively, so it can be considered a dual method, like SDCA. Similar to SDCA, its theory does not support its use on non-strongly convex problems, although there are no practical issues with its application.

In Section 3.7 we prove the convergence rate of the Finito method under the big-data condition described in the previous chapter. This theoretical rate is better than the SAG and SVRG rates but not quite as good as the SDCA rate. In Section 3.3 we compare Finito empirically against SAG and SDCA, showing that it converges faster. This difference is most pronounced when using a permuted access order, which unfortunately is not covered by current convergence theory.

The relationship between Finito and SDCA allows a kind of midpoint algorithm to be constructed, which has favourable properties of both methods. We call this midpoint Prox-Finito. It is described in Section 3.6.

An earlier version of the work in this chapter has been published as Defazio et al. (2014b).

3.1 The Finito Algorithm

As discussed in Chapter 2, we are interested in convex functions of the form

$$f(w) = \frac{1}{n} \sum_{i=1}^{n} f_i(w).$$

We assume that each f_i is Lipschitz smooth with constant L and is strongly convex with constant μ. We will focus on the *big data* setting:

$$n \geq \beta \frac{L}{\mu}$$

with $\beta = 2$, as described in Section 2.1.1.

3.1.1 Additional notation

We omit the n superscript on summations throughout, and subscript i with the implication that indexing starts at 1. When we use separate arguments for each f_i, we denote them ϕ_i. Let $\bar{\phi}^k$ denote the average $\bar{\phi}^k = \frac{1}{n}\sum_{i=1}^n \phi_i^k$. Our step length constant, which depends on β (the big-data constant), is denoted α. Note that α is an inverse step length, in the sense that large α results in smaller steps. We use angle bracket notation for dot products $\langle \cdot, \cdot \rangle$.

3.1.2 Method

We start with a table of known ϕ_i^0 values, and a table of known gradients $f_i'(\phi_i^0)$, for each i. We will update these two tables during the course of the algorithm. The Finito method is described in Algorithm 3.1.

Algorithm 3.1 Finito Algorithm

Initialise $\phi_i^0 = \phi^0$ for some ϕ^0 and all i, and calculate and store each $f_i'(\phi_i^0)$.
The step for iteration k, is:

1. Update w using the step:

$$w^k = \bar{\phi}^k - \frac{1}{\alpha\mu n}\sum_i f_i'(\phi_i^k). \tag{3.1}$$

2. Pick an index j uniformly at random, or using without-replacement sampling as discussed in Section 3.2.
3. Set $\phi_j^{k+1} = w^k$ in the table and leave the other variables the same ($\phi_i^{k+1} = \phi_i^k$ for $i \neq j$).
4. Calculate and store $f_j'(\phi_j^{k+1})$ in the table.

We have established the theoretical convergence rate of Finito under the big-data condition:

Theorem 3.1. *When the big-data condition holds with $\beta = 2$, $\alpha = 2$ may be used. In that setting, the expected convergence rate is:*

$$\mathbb{E}\left[f(\bar{\phi}^k) - f(w^*)\right] \leq \left(1 - \frac{1}{2n}\right)^k \frac{3}{4\mu} \left\|f'(\phi^0)\right\|^2.$$

See Section 3.7 for the proof. This can be compared to the SAG method, which achieves a $1 - \frac{1}{8n}$ geometric rate when $\beta = 2$. The SDCA method has a $1 - \frac{2L/n}{2L+L} = 1 - \frac{2}{3n}$ rate, which is very slightly better rate ($0.666\ldots$ v.s. 0.5) than Finito.

Note that on a per epoch basis, the Finito rate is $\left(1 - \frac{1}{2n}\right)^n \approx \exp(-1/2) = 0.606$. Lemma B.7 discusses this $\exp(\ldots)$ approximation in more detail. To put that rate into context, 10 epochs will see the error bound reduced by more than 148x.

One notable feature of our method is the fixed step size. In typical machine learning problems the strong convexity constant is given by the strength constant of the quadratic regulariser used. Since this is a known quantity, as long as the big-data condition holds $\alpha = 2$ may be used without any tuning or adjustment of Finito required. This lack of tuning is a major feature of Finito.

Our theory is not as complete as for SDCA and SAG. In cases where the big-data condition does not hold, we conjecture that the step size must be reduced proportionally to the violation of the big-data condition. In practice, the most effective step size can be found by testing a number of step sizes, as is usually done with other stochastic optimisation methods. We do not have any convergence theory for when the big-data condition doesn't hold, except for when very small step sizes are used, such as by setting the inverse step size constant α to $\alpha = \frac{L}{\mu}$ (Section 5.3).

3.1.3 Storage costs

Another difference compared to the SAG method is that we store both gradients $f_i'(\phi_i)$ and points ϕ_i. We do not actually need twice as much memory however, as they can be stored summed together. In particular we can store the quantities $p_i = f_i'(\phi_i) - \alpha\mu\phi_i$, and use the update rule $w = -\frac{1}{\alpha\mu n}\sum_i p_i$. This trick does not work when step lengths are adjusted during optimisation unfortunately.

When using this trick it would on the surface appear that storage of ϕ_i is a disadvantage when the gradients $f_i'(\phi_i)$ are sparse but the ϕ_i values are not. However, when is f_i is strongly convex (which is one of our assumptions) this can not occur.

There is an additional possible method for avoiding the storage of the ϕ_i values. If we can easily evaluate the gradient of the convex conjugate of each f_i, then we can use the relation (Section A.2):

$$\phi_i = f_i^{*\prime}\left(f_i'(\phi_i)\right).$$

This is possible because for strongly convex functions there is an isomorphism between the dual space that the gradients live in and the primal space.

3.2 Permutation & the Importance of Randomness

One of the most interesting aspects Finito and the other fast incremental gradient methods is the random choice of index at each iteration. We are not in a stochastic approximation setting, so there is no inherent randomness in the problem. Yet it seems that randomisation is required for Finito. It diverges in practice if a cyclic access order is used. It is hard to emphasise enough the importance of randomness here. The technique of pre-permuting the data, then doing in order passes after that, is not enough. Even reducing the step size in SAG or Finito by 1 or 2 orders of magnitude does not fix convergence.

The permuted ordering described in Section 2.1.3 is particularly well suited to use with Finito. Recall that for the permuted ordering, each step within an epoch the data is sampled without replacement from the points not accessed yet in that epoch. In practice, this approach does not give any speed-up with SAG, however it works spectacularly well with Finito. We see speed-ups of up to a factor of two using this approach. This is one of the major differences in practice between SAG and Finito. We should note that we have no theory to support this case however.

The SDCA method is also sometimes used with a permuted ordering (Shalev-Shwartz and Zhang, 2013b), our experiments in Section 3.3 show that this sometimes results in a speed-up over uniform random sampling, although it does not appear to be as reliable as with Finito.

3.3 Experiments

In this section we compare Finito, SAG, SDCA and LBFGS. The SVRG method was not published at the time these experiments where run. We only consider problems where the regulariser is large enough so that the big-data condition holds, as this is the case our theory supports. However, in practice our method can be used with smaller step sizes in the more general case, in much the same way as SAG.

Since we do not know the Lipschitz smoothness constant for these problems exactly, the SAG method was run for a variety of step sizes, with the one that gave the fastest rate of convergence plotted. The best step size for SAG is usually not what the theory suggests. Schmidt et al. (2013) suggest using $\frac{1}{L}$ instead of the theoretical rate $\frac{1}{16L}$. For Finito, we find that using $\alpha = 2$ is the fastest rate when the big-data condition holds for any $\beta > 1$. This is the step suggested by our theory when $\beta = 2$. Interestingly, reducing α to 1 does not improve the convergence rate. Instead, we see no further improvement in our experiments.

For both SAG and Finito we used a different step size rule than suggested by the theory for the first pass. For Finito, during the first pass, since we do not have derivatives for each ϕ_i yet, we simply sum over the k terms seen so far

$$w^k = \frac{1}{k}\sum_i^k \phi_i^k - \frac{1}{\alpha\mu k}\sum_i^k f_i'(\phi_i^k),$$

where we process data points in cyclic order for the first pass only. A similar trick is suggested by Schmidt et al. (2013) for SAG.

For our test problems we choose log loss for 3 binary classification datasets, and quadratic loss for 2 regression tasks. For classification, we tested on the ijcnn1 and covtype datasets [1], as well as MNIST[2] classifying 0-4 against 5-9. For regression, we choose the two datasets from the UCI repository: the million song year regression dataset, and the slice-localisation dataset. The training portion of the datasets are of size 5.3×10^5, 5.0×10^4, 6.0×10^4, 4.7×10^5 and 5.3×10^4 respectively.

Figures 3.1 & 3.2 shows the results of our experiments. Firstly we can see that LB-FGS is not competitive with any of the incremental gradient methods considered. Secondly, the non-permuted SAG, Finito and SDCA often converge at very similar rates. The observed differences are usually down to the speed of the very first pass, where SAG and Finito are using the above mentioned trick to speed their convergence. After the first pass, the slopes of the line are usually comparable. When considering the methods with permutation each pass, we see a clear advantage for Finito. Interestingly, it gives very flat lines, indicating very stable convergence. SAG with permutation is not shown as it is much slower and unstable than randomised SAG.

3.4 The MISO Method

The MISO (Mairal, 2013) method is an incremental gradient method applicable when each of the terms f_i can easily be majorised (that is upper bounded everywhere) by known functions. When quadratic functions are chosen for the majorisation step, the method has the same update as Finito but with an alternative and much smaller step size. MISO maintains the following upper bound on $f(x)$ at each step:

$$B(x) = \frac{1}{n}\sum_i f_i(\phi_i) + \frac{1}{n}\sum_i \left\langle f_i'(\phi_i), x - \phi_i \right\rangle + \frac{L}{2n}\sum_i \|x - \phi_i\|^2 .$$

[1] http://www.csie.ntu.edu.tw/~cjlin/libsvmtools/datasets/binary.html
[2] http://yann.lecun.com/exdb/mnist/

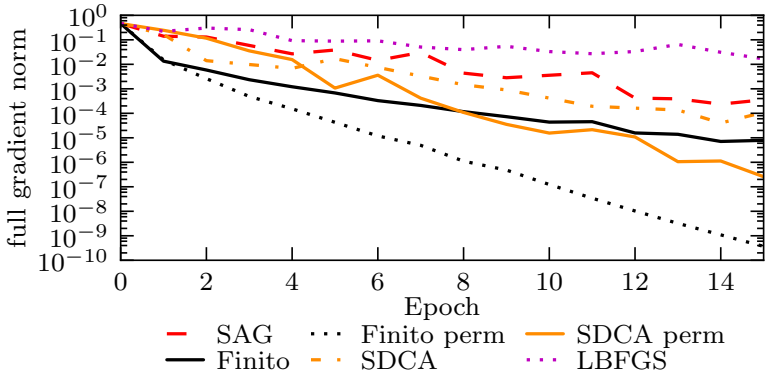

(a) MNIST

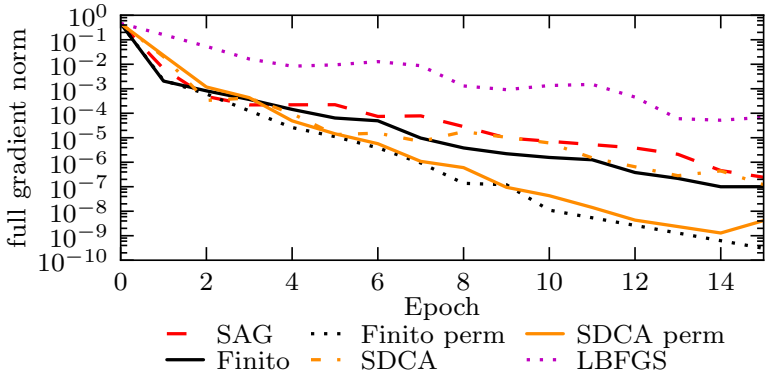

(b) ijcnn1

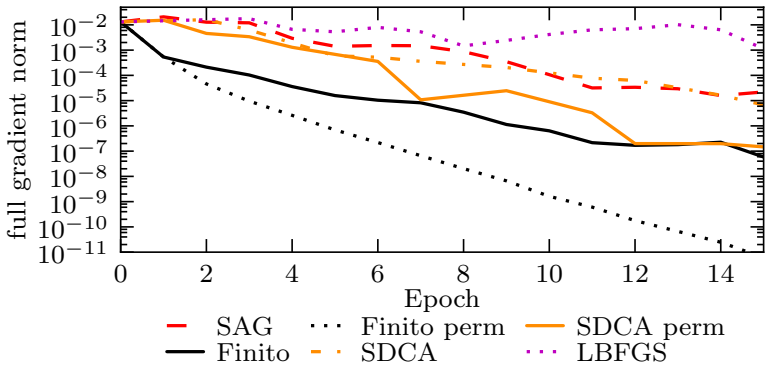

(c) covtype

Figure 3.1: Classification tasks

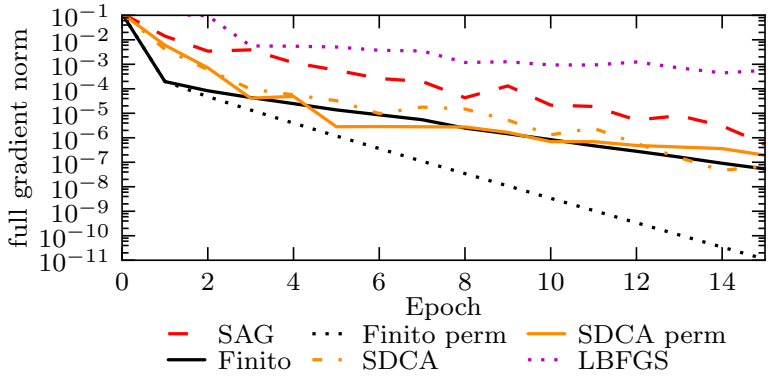

(a) million song

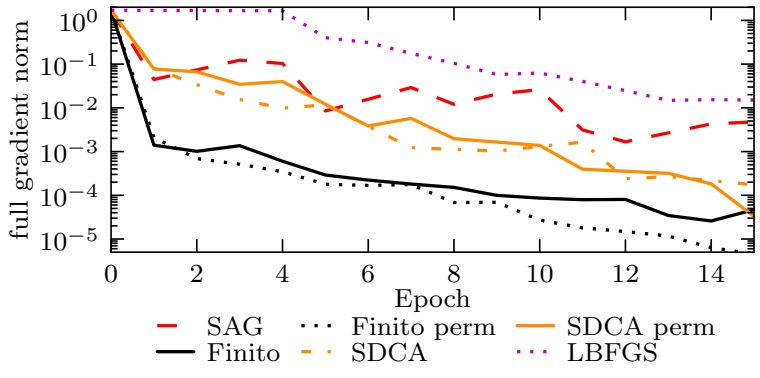

(b) slice

Figure 3.2: Regression tasks

This is just the sum of the Lipschitz smoothness upper bounds around each f_i, at different points ϕ_i. The method alternates updating randomly chosen ϕ_j values, using the update:

$$\phi_j^{k+1} = w^k \triangleq \arg\min_x B^k(x).$$

This update is sensible. We are using the minimum of the upper bound as our best guess at the solution, just like in gradient descent and Newton's method. Taking the gradient of B to zero gives an explicit formula for w^k of:

$$w^k = \bar{\phi} - \frac{1}{Ln}\sum_i f_i'(\phi_i), \tag{3.2}$$

which is identical to Finito but with an inverse step size of L instead of 2μ. Since the condition number of practical problems is large, generally in the thousands to millions, this step size is dramatically smaller.

Mairal (2013) establishes the following convergence rate for this method in the strongly convex case:

$$\mathbb{E}\left[f(x^k) - f(x^*)\right] \leq \left(1 - \frac{\mu}{(\mu+L)n}\right)^{k-1} \frac{L}{2}\left\|w^0 - w^*\right\|^2. \tag{3.3}$$

Note that on a per epoch basis, this rate essentially matches that of gradient descent, as $\left(1 - \frac{\mu}{(\mu+L)n}\right)^n \approx \left(1 - \frac{\mu}{L}\right)$. This approximation is described further in Lemma B.4. Gradient descent is not considered a competitive method for optimisation, and likewise, experiments suggest that this method is even slower in practice than gradient descent with line searches. In Theorem 5.8 (Chapter 5) we improve on this result, establishing a convergence rate with a factor of 2 better geometric constant:

$$\mathbb{E}\left[f(x^k) - f(x^*)\right] \leq \left(1 - \frac{\mu}{(\mu+L)n}\right)^{2k} \frac{2n}{\mu}\left\|f'(\phi^0)\right\|^2,$$

although this result is for the specific form of MISO given in Equation 3.2 rather than the general upper bound minimisation scheme they describe.

A recent technical report (Mairal, 2014) gives a proof of the MISO method's convergence rate under the larger step sizes we consider with Finito. Although this no longer fits into the upper bound minimisation framework of MISO, they refer to this as the MISOμ method. Their report was released while Finito was under peer review. They establish for a step size $\alpha = 1$ (Compared to our $\alpha = 2$ rate used in the Finito proof, see Equation 3.1) a rate of

$$\mathbb{E}\left[f(x^k) - f(x^*)\right] \leq \left(1 - \frac{1}{3n}\right)^k \frac{2n}{\mu}\left\|f'(\phi^0)\right\|^2.$$

This $1 - \frac{1}{3n}$ constant is slightly worse than the $1 - \frac{1}{2n}$ constant we get. They make the same big-data assumption $n \geq 2L/\mu$ that we do.

Algorithm 3.2 Primal SDCA

Initialise $\phi_i^0 = \phi^0$ for some initialϕ^0 and compute the table of gradients $f_i'(\phi_i^0)$ for each i .
At step $k+1$:

1. Pick an index j uniformly at random.
2. Compute $\phi_j^{k+1} = \text{prox}_{1/\lambda}^{f_j}(z)$, where

$$z = -\lambda \sum_{i \neq j}^{n} f_i'(\phi_i^k), \tag{3.4}$$

$$\text{and} \quad \lambda = \frac{1}{\mu n}.$$

3. Store the gradient $f_j'(\phi_j^{k+1}) = \frac{1}{\lambda}\left(z - \phi_j^{k+1}\right)$ in the table at location j. For $i \neq j$, the table entries are unchanged ($f_i'(\phi_i^{k+1}) = f_i'(\phi_i^k)$).

At completion, return $x^k = -\lambda \sum_i^n f_i'(\phi_i^k)$.

3.5 A Primal Form of SDCA

At first glance, the SDCA method bears no obvious relation to Finito. However, there is a simple transformation that can be applied to SDCA, that makes the relation clear. This leads to a novel primal formulation of SDCA. This also allows us to construct an algorithm that sits at the midpoint between SDCA and Finito.

The primal version of SDCA is given as Algorithm 3.2. At each step, this algorithm evaluates the proximal operator of a term f_j at a particular point z, yielding the new point ϕ_j^{k+1}. The gradient table is then updated with $f_j'(\phi_j^{k+1})$. The point z is just a constant times the table's average gradient, excluding location j. Compare this to the other fast incremental gradient methods that use a table average, such as SDCA and Finito, where in those cases the average includes the location j.

It's not immediately obvious that the $f_j'(\phi_j^{k+1})$ update is actually computing $f_j'(\phi_j^{k+1})$ in Algorithm 3.2. To see why it works, consider the optimality condition of the proximal operator from Step 2, found by taking the definition of the proximal operator and setting its gradient to zero:

$$f_j'(\phi_j^{k+1}) + \frac{1}{\lambda}(\phi_j^{k+1} - z) = 0.$$

Relating this to the update in Step 3 shows that the step does indeed compute the gradient.

We claim that this algorithm is exactly equivalent to SDCA when exact coordinate minimisation is used (the standard variant). In fact, the simple relation $\alpha_i^k = f_i'(\phi_i^k)$ holds. Note that in SDCA the quantities ϕ_i are not used explicitly, whereas in our notation here we have made them explicit.

Theorem 3.2. *Primal SDCA (Algorithm 3.2) is equivalent to SDCA (Algorithm 2.1) when each α_i^0 is initialised to $f_i'(\phi_i^0)$.*

In particular the iterate x^k defined as $x^k = -\lambda \sum_i^n f_i'(\phi_i^k)$ is identical to the SDCA iterate $x^k = -\frac{1}{\mu n} \sum_i^n \alpha_i$, due to the relation $\alpha_i^k = f_i'(\phi_i^k)$.

Proof. We will prove this by induction, by showing that $\alpha_i^k = f_i'(\phi_i^k)$ at each step. For the base case, we have assumed that α_i^0 is initialised to $f_i'(\phi_i^0)$, so it holds by construction. Next suppose that at step k, $\alpha_i^k = f_i'(\phi_i^k)$. Then we just need to show that a single step in Algorithm 3.2 gives $\alpha_j^{k+1} = f_j'(\phi_j^{k+1})$.

The relation between the SDCA and the primal variant we describe stems from the fact that the standard dual version performs a minimisation of the following form at each step:

$$\alpha_j^{k+1} = \arg\min_{\alpha} \left[f_j^*(\alpha) + \frac{\mu n}{2} \left\| x^k - \frac{1}{\mu n} \left(\alpha - \alpha_j^k \right) \right\|^2 \right]. \tag{3.5}$$

Here α are dual variables and x^k the current primal point. As noted by Shalev-Shwartz and Zhang (2013a), this is actually an instance of the proximal operator of the convex conjugate of f_j. Recall the definition of the proximal operator of a function f with weight γ:

$$\text{prox}_\gamma^f(v) = \arg\min_x \left\{ f(x) + \frac{\gamma}{2} \|x - v\|^2 \right\}.$$

Clearly the exact coordinate step (Equation 3.5) is the proximal operator of f^* in the following form:

$$\begin{aligned} \alpha_j^{k+1} &= \mu n \cdot \text{prox}_{\mu n}^{f^*}(x^k + \frac{1}{\mu n} \alpha_j^k). && (3.6) \\ &= \mu n \cdot \text{prox}_{\mu n}^{f^*}(-\frac{1}{\mu n} \sum_{i \neq j} \alpha_i^k). && (3.7) \\ &= \frac{1}{\lambda} \text{prox}_{1/\lambda}^{f^*}(z^k) \quad \text{(in notation from Eq 3.4)} && (3.8) \end{aligned}$$

In the last step we have used our assumption that $\alpha_i^k = f_i'(\phi_i^k)$. Our primal formulation exploits this definition of α_j^{k+1} using a relation between the proximal operator of a function and its convex conjugate known as the Moreau decomposition:

$$\text{prox}^{f^*}(v) = v - \text{prox}^f(v).$$

See Section A.2 for more details on the Moreau decomposition. This decomposition allows us to compute the proximal operator of conjugate via the primal proximal operator. As this is the only use in the basic SDCA method of the conjugate function, applying this decomposition allows us to completely eliminate the "dual" aspect of the algorithm. The same trick can be used to interpret Dykstra's set intersection as a primal algorithm instead of a dual block coordinate descent algorithm (Combettes and Pesquet, 2011).

We now apply the Moreau decomposition to our primal SDCA (Algorithm 3.2) formulation's update : $\phi_j^{k+1} = \text{prox}_{1/\lambda}^{f_j}(-\lambda \sum_{i \neq j}^n f_i'(\phi_i^k))$, giving:

$$\begin{aligned} \phi_j^{k+1} &= \text{prox}_{1/\lambda}^{f_j}(z) \\ &= z - \text{prox}_{1/\lambda}^{f_j^*}(z). \end{aligned}$$

$$\therefore \text{prox}_{1/\lambda}^{f_j^*}(z) = z - \phi_j^{k+1}. \tag{3.9}$$

Now consider Step 3 of Algorithm 3.2. Combining with Equation 3.9 and $\alpha_j^{k+1} = f_j'(\phi_j^{k+1})$ we have:

$$\begin{aligned} \frac{1}{\lambda}\left(z - \phi_j^{k+1}\right) &= \frac{1}{\lambda} \cdot \text{prox}_{1/\lambda}^{f_j^*}(z). \\ &= \alpha_j^{k+1} \text{ (Equation 3.8).} \end{aligned}$$

This gives that the update for α_j^{k+1} in SDCA is identical to the $f_j'(\phi_j^{k+1})$ update in Algorithm 3.2. □

Remark 3.3. The initialisation of SDCA typically takes each α_i as the zero vector. This is a somewhat unnatural initialisation to use in the primal variant, where it is more natural to take $\phi_i^0 = 0$ for all i. The SDCA style initialisation can be done using the assignment $\phi_i^0 = f_i^{*\prime}(0)$ if desired, but that requires working with the convex conjugate function.

3.6 Prox-Finito: a Novel Midpoint Algorithm

The primal form of SDCA has some resemblance to Finito; the primary difference being that it assumes strong convexity is induced by a separate strongly convex regulariser, rather than each f_i being strongly convex. We now show how to modify SDCA so that it works without a separate regulariser.

Consider the dual problem maximised by SDCA, using our relation $\alpha_i = f_i'(\phi_i)$, and $x^k = -\lambda \sum_i^n f_i'(\phi_i^k)$. Using the Lagrangian from Equation 2.1:

$$\begin{aligned} D &= \min_{w,x_1,\dots x_n,} \left\{ \frac{1}{n}\sum_{i=1}^{n} f_i(x_i) + \frac{\mu}{2}\|w\|^2 + \frac{1}{n}\sum_i \langle \alpha_i, w - x_i\rangle \right\} \\ &= \min_{w} \left\{ \frac{1}{n}\sum_{i=1}^{n} \min_{x_i} \left[f_i(x_i) + \left\langle f_i'(\phi_i^k), w - x_i \right\rangle \right] + \frac{\mu}{2}\|w\|^2 \right\}. \end{aligned}$$

Notice now that a minimiser of each inner problem can be found by setting the gradient to zero: $f'(x_i) - f'(\phi_i^k) = 0$, therefore we can take $x_i = \phi_i^k$.

$$\begin{aligned} D &= \min_{w} \left\{ \frac{1}{n}\sum_{i=1}^{n} \left[f_i(\phi_i^k) + \left\langle f_i'(\phi_i^k), w - \phi_i^k \right\rangle \right] + \frac{\mu}{2}\|w\|^2 \right\}. \\ &= \frac{1}{n}\sum_{i=1}^{n} \left[f_i(\phi_i^k) + \left\langle f_i'(\phi_i^k), x^k - \phi_i^k \right\rangle \right] + \frac{\mu}{2}\left\|x^k\right\|^2. \end{aligned} \tag{3.10}$$

Using this form of the dual, the coordinate step for coordinate j can be seen as the minimiser of the following function with respect to x:

$$A_j^k(x) = \frac{1}{n} f_j(x) + \frac{1}{n}\sum_{i\neq j}^{n} \left[f_i(\phi_i^k) + \left\langle f_i'(\phi_i^k), x - \phi_i^k \right\rangle \right] + \frac{\mu}{2}\|x\|^2.$$

So each step of SDCA:

1. Replaces the linear lower bound around one of the functions f_j with the explicit function f_j, yielding the global lower bound A_j^k;
2. Sets x^{k+1} to be the minimiser of A_j^k;
3. Then re-linearises f_j around the point x^{k+1} by taking $\phi_j^{k+1} = x^{k+1}$.

Now notice that Equation 3.10 is the standard convexity lower bound in terms of each f_i summed together, added to the explicit regulariser term. Since Finito works with strongly convex functions without an explicit regulariser, it is natural to replace this expression with the strong convexity lower bound:

$$B = \frac{1}{n}\sum_{i=1}^{n} \left[f_i(\phi_i^k) + \left\langle f_i'(\phi_i^k), x^k - \phi_i^k \right\rangle + \frac{\mu}{2}\left\|x^k - \phi_i^k\right\|^2 \right].$$

Now applying the same procedure as SDCA uses to this alternative expression yields Algorithm 3.3.

Like SDCA, Prox-Finito has a linear convergence rate. The geometric factor is $1 - \frac{\mu}{\mu n + L - \mu}$ instead of $1 - \frac{\mu}{\mu n + L}$, as the Lipschitz smoothness constant now includes the strong convexity constant due to the assumption that strong convexity is induced by each f_i instead of a separate regulariser. We establish this convergence rate directly in Section 3.8.

Algorithm 3.3 Prox-Finito

1. Pick an index j uniformly at random.
2. Compute $\phi_j^{k+1} = \text{prox}_\eta^{f_j}(z)$, where:

$$z = \frac{1}{n-1}\sum_{i\neq j}^{n}\phi_i^k - \frac{1}{\eta}\sum_{i\neq j}^{n} f_i'(\phi_i^k), \tag{3.11}$$

$$\text{and} \quad \eta = \mu(n-1).$$

3. Store the gradient $f_j'(\phi_j^{k+1}) = \eta\left(z - \phi_j^{k+1}\right)$ in the table at location j. For $i \neq j$, the table entries are unchanged ($f_i'(\phi_i^{k+1}) = f_i'(\phi_i^k)$).

At completion, return $x^k = \frac{1}{n}\sum_i \phi_i^k - \frac{1}{\mu n}\sum_i f_i'(\phi_i^k)$.

3.6.1 Prox-Finito relation to Finito

We constructed Prox-Finito as a natural modification of the SDCA algorithm. We now show how it is closely related to Finito. Consider again the lower bound used in Prox-Finito:

$$B = \frac{1}{n}\sum_{i=1}^{n}\left[f_i(\phi_i^k) + \left\langle f_i'(\phi_i^k), x^k - \phi_i^k\right\rangle + \frac{\mu}{2}\left\|x^k - \phi_i^k\right\|^2\right].$$

The update of Finito is also a minimisation involving this bound. Instead of replacing f_j with the true function then minimising, the minimisation is done as-is on B with respect to x^k. That yields the equation:

$$x^k = \frac{1}{n}\sum_{i}^{n}\phi_i^k - \frac{1}{\mu n}\sum_{i}^{n} f_i'(\phi_i^k).$$

Instead of using this update directly, Finito takes a more conservative step, smaller by a factor of $\alpha = 2$:

$$x^k = \frac{1}{n}\sum_{i}^{n}\phi_i^k - \frac{1}{\alpha\mu n}\sum_{i}^{n} f_i'(\phi_i^k).$$

After each minimisation of B with respect to x^k, we may then minimise with respect to ϕ_j, which yields $\phi_j = x^k$ as the update.

3.6.2 Non-Uniform Lipschitz Constants

The standard Prox-Finito method does not rely on the Lipschitz smoothness constant of the gradient in the actual algorithm, just its convergence rate is dependent on L. So

it potentially does not require knowledge of L to be used. Suppose instead that we know separate Lipschitz smoothness constants L_i for each f_i function's gradient. Let $\bar{L}$ be the average of these. This is also a bound on the Lipschitz smoothness constant of the entire function's gradient f'. A straightforward modification of the Prox-Finito algorithm gives a convergence rate dependent on $\bar{L}$ instead of L:

Theorem 3.4. *Define $c_i = \frac{\mu n + L_i - \mu}{\mu}$. Modify the Prox-Finito algorithm so that sampling of j is done with probabilities*

$$p_i = \frac{1}{Z} \cdot c_i,$$

with Z the normalisation constant so $\sum_i p_i = 1$. Then the expected convergence rate becomes:

$$f(w^*) - \mathbb{E}\left[B^k(w^k)\right] \leq \left(1 - \frac{\mu}{(\mu n + \bar{L} - \mu)}\right)^k \left[f(w^*) - B^0(w^0)\right].$$

Proof. See Section 3.8.2. □

Remark 3.5. This modification to allow for non-uniform sampling strongly resembles the non-uniform sampling scheme described by Nesterov (2010). Note that for the other fast gradient methods, non-uniform sampling does not have a proven convergence rate yet. For SAG, Schmidt et al. (2013) consider a simple $c_i = L_i$ weighting, which they say can diverge in practice.

3.7 Finito Theory

This section is highly technical. The main result is in Theorem 3.12. We start by examining the expectation of a single Finito step. All expectations in the following are over the choice of index j at step k, conditioned on all ϕ_i and w from previous steps. Quantities without superscripts are at their values at iteration k. Note if we combine the $\bar{\phi}$ and w updates together, we get:

$$w^{k+1} - w = \frac{1}{n}(w - \phi_j) + \frac{1}{\alpha\mu n}\left[f_j'(\phi_j) - f_j'(w)\right]. \tag{3.12}$$

Lemma 3.6. *The expectation of the Finito step is:*

$$\mathbb{E}[w^{k+1}] - w = -\frac{1}{\alpha\mu n} f'(w).$$

I.e. the w step is a gradient descent step in expectation ($\frac{1}{\alpha\mu n} \propto \frac{1}{L}$). A similar equality also holds for SGD and SVRG, but not for SAG or SDCA.

Proof.

$$\begin{aligned}\mathbb{E}[w^{k+1}] - w &= \mathbb{E}\left[\frac{1}{n}(w-\phi_j) - \frac{1}{\alpha\mu n}\left(f_j'(w) - f_j'(\phi_j)\right)\right] \\ &= \frac{1}{n}(w-\bar{\phi}) - \frac{1}{\alpha\mu n}f'(w) + \frac{1}{\alpha\mu n^2}\sum_i f_i'(\phi_i).\end{aligned}$$

Now simplify $\frac{1}{n}(w-\bar{\phi})$ as $-\frac{1}{\alpha\mu n^2}\sum_i f_i'(\phi_i)$, so the only term that remains is $-\frac{1}{\alpha\mu n}f'(w)$. □

3.7.1 Main proof

Our proof proceed by construction of a Lyapunov function T. That is, a function that bounds a quantity of interest, and that decreases each iteration in expectation. Our Lyapunov function $T = T_1 + T_2 + T_3 + T_4$ is composed of the sum of the following terms:

$$T_1 = f(\bar{\phi}),$$

$$T_2 = -\frac{1}{n}\sum_i f_i(\phi_i) - \frac{1}{n}\sum_i \left\langle f_i'(\phi_i), w - \phi_i \right\rangle,$$

$$T_3 = -\frac{\mu}{2n}\sum_i \|w-\phi_i\|^2,$$

$$T_4 = \frac{\mu}{2n}\sum_i \|\bar{\phi}-\phi_i\|^2.$$

In the following set of Lemmas we determine how each term changes between steps $k+1$ and k in expectation. We use extensively that $\phi_j^{k+1} = w$, and that $\phi_i^{k+1} = \phi_i$ for $i \neq j$.

Lemma 3.7. *Between steps k and $k+1$, the $T_1 = f(\bar{\phi})$ term changes as follows:*

$$\mathbb{E}[T_1^{k+1}] - T_1 \leq \frac{1}{n}\left\langle f'(\bar{\phi}), w - \bar{\phi}\right\rangle + \frac{L}{2n^3}\sum_i \|w-\phi_i\|^2.$$

Proof. First we use the standard Lipschitz smoothness upper bound (Theorem A.5):

$$f(y) \leq f(x) + \left\langle f'(x), y-x\right\rangle + \frac{L}{2}\|x-y\|^2.$$

We can apply this using $y = \bar{\phi}^{k+1} = \bar{\phi} + \frac{1}{n}(w-\phi_j)$ and $x = \bar{\phi}$:

$$f(\bar{\phi}^{k+1}) \leq f(\bar{\phi}) + \frac{1}{n}\left\langle f'(\bar{\phi}), w-\phi_j\right\rangle + \frac{L}{2n^2}\|w-\phi_j\|^2.$$

We now take expectations over j, giving:

$$\mathbb{E}[f(\bar{\phi}^{k+1})] - f(\bar{\phi}) \leq \frac{1}{n}\left\langle f'(\bar{\phi}), w - \bar{\phi}\right\rangle + \frac{L}{2n^3}\sum_i \|w - \phi_i\|^2 .$$

□

Lemma 3.8. *Between steps k and $k+1$, the $T_2 = -\frac{1}{n}\sum_i f_i(\phi_i) - \frac{1}{n}\sum_i \left\langle f_i'(\phi_i), w - \phi_i\right\rangle$ term changes as follows:*

$$\begin{aligned}\mathbb{E}[T_2^{k+1}] - T_2 &\leq -\frac{1}{n}T_2 - \frac{1}{n}f(w) \\ &+ (\frac{1}{\alpha} - \frac{\beta}{n})\frac{1}{sn^3}\sum_i \left\|f_i'(w) - f_i'(\phi_i)\right\|^2 \\ &+ \frac{1}{n}\left\langle \bar{\phi} - w, f'(w)\right\rangle - \frac{1}{n^3}\sum_i \left\langle f_i'(w) - f_i'(\phi_i), w - \phi_i\right\rangle .\end{aligned}$$

Proof. We introduce the notation $T_{21} = -\frac{1}{n}\sum_i f_i(\phi_i)$ and $T_{22} = -\frac{1}{n}\sum_i \left\langle f_i'(\phi_i), w - \phi_i\right\rangle$. We simplify the change in T_{21} first using $\phi_j^{k+1} = w$:

$$\begin{aligned}T_{21}^{k+1} - T_{21} &= -\frac{1}{n}\sum_i f_i(\phi_i^{k+1}) + \frac{1}{n}\sum_i f_i(\phi_i) \\ &= -\frac{1}{n}\sum_i f_i(\phi_i) + \frac{1}{n}f_j(\phi_j) - \frac{1}{n}f_j(w) + \frac{1}{n}\sum_i f_i(\phi_i) \\ &= \frac{1}{n}f_j(\phi_j) - \frac{1}{n}f_j(w).\end{aligned}$$

Now we simplify the change in T_{22}:

$$T_{22}^{k+1} - T_{22} = -\frac{1}{n}\sum_i \left\langle f_i'(\phi_i^{k+1}), w^{k+1} - w + w - \phi_i^{k+1}\right\rangle - T_{22}$$

$$\therefore T_{22}^{k+1} - T_{22} = -\frac{1}{n}\sum_i \left\langle f_i'(\phi_i^{k+1}), w - \phi_i^{k+1}\right\rangle - T_{22} - \frac{1}{n}\sum_i \left\langle f_i'(\phi_i^{k+1}), w^{k+1} - w\right\rangle . \tag{3.13}$$

We now simplify the first two terms using $\phi_j^{k+1} = w$:

$$\begin{aligned}-\frac{1}{n}\sum_i \left\langle f_i'(\phi_i^{k+1}), w - \phi_i^{k+1}\right\rangle - T_{22} &= T_{22} - \frac{1}{n}\left\langle f_j'(\phi_j), w - \phi_j\right\rangle \\ &\quad + \frac{1}{n}\left\langle f_j'(w), w - w\right\rangle - T_{22} \\ &= \frac{1}{n}\left\langle f_j'(\phi_j), w - \phi_j\right\rangle .\end{aligned}$$

The last term of Equation 3.13 expands further:

$$\begin{aligned} & -\frac{1}{n}\sum_i \left\langle f_i'(\phi_i^{k+1}), w^{k+1} - w \right\rangle \\ = \; & -\frac{1}{n}\left\langle \sum_i f_i'(\phi_i) - f_j'(\phi_j) + f_j'(w), w^{k+1} - w \right\rangle \qquad (3.14) \\ = \; & -\frac{1}{n}\left\langle \sum_i f_i'(\phi_i), w^{k+1} - w \right\rangle - \frac{1}{n}\left\langle f_j'(w) - f_j'(\phi_j), w^{k+1} - w \right\rangle. \qquad (3.15) \end{aligned}$$

The second inner product term in 3.15 simplifies further using Equation 3.12:

$$\begin{aligned} & -\frac{1}{n}\left\langle f_j'(w) - f_j'(\phi_j), w^{k+1} - w \right\rangle \\ = \; & -\frac{1}{n}\left\langle f_j'(w) - f_j'(\phi_j), \frac{1}{n}(w - \phi_j) + \frac{1}{\alpha\mu n}\left[f_j'(\phi_j) - f_j'(w)\right] \right\rangle \\ = \; & -\frac{1}{n^2}\left\langle f_j'(w) - f_j'(\phi_j), w - \phi_j \right\rangle - \frac{1}{\alpha\mu n^2}\left\langle f_j'(w) - f_j'(\phi_j), f_j'(\phi_j) - f_j'(w) \right\rangle. \end{aligned}$$

We simplify the second term:

$$-\frac{1}{\alpha\mu n^2}\left\langle f_j'(w) - f_j'(\phi_j), f_j'(\phi_j) - f_j'(w) \right\rangle = \frac{1}{\alpha\mu n^2}\left\| f_j'(w) - f_j'(\phi_j) \right\|^2.$$

Grouping all remaining terms gives:

$$\begin{aligned} T_2^{k+1} - T_2 \leq \; & \frac{1}{n} f_j(\phi_j) + \frac{1}{n}\left\langle f_j'(\phi_j), w - \phi_j \right\rangle - \frac{1}{n} f_j(w) \\ + \; & \frac{1}{\alpha\mu n^2}\left\| f_j'(w) - f_j'(\phi_j) \right\|^2 - \frac{1}{n^2}\left\langle f_j'(w) - f_j'(\phi_j), w - \phi_j \right\rangle \\ - \; & \frac{1}{n}\left\langle \sum_i f_i'(\phi_i), w^{k+1} - w \right\rangle. \end{aligned}$$

We now take expectations of each remaining term. For the bottom inner product we use Lemma 1:

$$\begin{aligned} -\frac{1}{n}\left\langle \sum_i f_i'(\phi_i), w^{k+1} - w \right\rangle &= \frac{1}{\alpha\mu n^2}\left\langle \sum_i f_i'(\phi_i), f'(w) \right\rangle \\ &= \frac{1}{n}\left\langle \bar{\phi} - w, f'(w) \right\rangle. \end{aligned}$$

Taking expectations of the remaining terms is straight forward. We get:

$$\begin{aligned}\mathbb{E}[T_2^{k+1}] - T_2 &\leq \frac{1}{n^2}\sum_i f_i(\phi_i) - \frac{1}{n}f(w) + \frac{1}{n^2}\sum_i \left\langle f_i'(\phi_i), w - \phi_i \right\rangle \\ &+ \frac{1}{\alpha\mu n^3}\sum_i \left\| f_i'(w) - f_i'(\phi_i) \right\|^2 - \frac{1}{n^3}\sum_i \left\langle f_i'(w) - f_i'(\phi_i), w - \phi_i \right\rangle \\ &+ \frac{1}{n}\left\langle \bar{\phi} - w, f'(w) \right\rangle.\end{aligned}$$

□

Lemma 3.9. *Between steps k and k+1, the* $T_3 = -\frac{\mu}{2n}\sum_i \|w - \phi_i\|^2$ *term changes as follows:*

$$\begin{aligned}\mathbb{E}[T_3^{k+1}] - T_3 &= -(1 + \frac{1}{n})\frac{1}{n}T_3 \\ &+ \frac{1}{\alpha n}\left\langle f'(w), w - \bar{\phi} \right\rangle - \frac{1}{2\alpha^2\mu n^3}\sum_i \left\| f_i'(\phi_i) - f_i'(w) \right\|^2.\end{aligned}$$

Proof. We expand as:

$$\begin{aligned}T_3^{k+1} &= -\frac{\mu}{2n}\sum_i \left\| w^{k+1} - \phi_i^{k+1} \right\|^2 \\ &= -\frac{\mu}{2n}\sum_i \left\| w^{k+1} - w + w - \phi_i^{k+1} \right\|^2 \qquad (3.16) \\ &= -\frac{\mu}{2}\left\| w^{k+1} - w \right\|^2 - \frac{\mu}{2n}\sum_i \left\| w - \phi_i^{k+1} \right\|^2 \qquad (3.17) \\ &\quad -\frac{\mu}{n}\sum_i \left\langle w^{k+1} - w, w - \phi_i^{k+1} \right\rangle. \qquad (3.18)\end{aligned}$$

We expand the three terms on the right separately. For the first term:

$$\begin{aligned}-\frac{\mu}{2}\left\| w^{k+1} - w \right\|^2 &= -\frac{\mu}{2}\left\| \frac{1}{n}(w - \phi_j) + \frac{1}{\alpha\mu n}\left(f_j(\phi_j) - f_j(w) \right) \right\|^2 \\ &= -\frac{\mu}{2n^2}\left\| w - \phi_j \right\|^2 - \frac{1}{2\alpha^2\mu n^2}\left\| f_j(\phi_j) - f_j(w) \right\|^2 \\ &\quad -\frac{1}{\alpha n^2}\left\langle f_j(\phi_j) - f_j(w), w - \phi_j \right\rangle. \qquad (3.19)\end{aligned}$$

For the second term of Equation 3.17, using $\phi_j^{k+1} = w$:

$$\begin{aligned}-\frac{\mu}{2n}\sum_i \left\| w - \phi_i^{k+1} \right\|^2 &= -\frac{\mu}{2n}\sum_i \left\| w - \phi_i \right\|^2 + \frac{\mu}{2n}\left\| w - \phi_j \right\|^2 \\ &= T_3 + \frac{\mu}{2n}\left\| w - \phi_j \right\|^2.\end{aligned}$$

For the third term of Equation 3.17:

$$\begin{aligned} & -\frac{\mu}{n}\sum_i \left\langle w^{k+1}-w, w-\phi_i^{k+1}\right\rangle \\ = \; & -\frac{\mu}{n}\sum_i \left\langle w^{k+1}-w, w-\phi_i\right\rangle + \frac{\mu}{n}\left\langle w^{k+1}-w, w-\phi_j\right\rangle \qquad (3.20) \\ = \; & -\mu\left\langle w^{k+1}-w, w-\frac{1}{n}\sum_i \phi_i\right\rangle + \frac{\mu}{n}\left\langle w^{k+1}-w, w-\phi_j\right\rangle. \qquad (3.21) \end{aligned}$$

The second inner product term in Equation 3.21 becomes (using Equation 3.12):

$$\begin{aligned} \frac{\mu}{n}\left\langle w^{k+1}-w, w-\phi_j\right\rangle &= \frac{\mu}{n}\left\langle \frac{1}{n}(w-\phi_j)+\frac{1}{\alpha\mu n}\left[f_j'(\phi_j)-f_j'(w)\right], w-\phi_j\right\rangle \\ &= \frac{\mu}{n^2}\left\|w-\phi_j\right\|^2+\frac{1}{\alpha n^2}\left\langle f_j'(\phi_j)-f_j'(w), w-\phi_j\right\rangle. \end{aligned}$$

Notice that the inner product term here cancels with the one in 3.19.

Now we can take expectations of each remaining term. Recall that $\mathbb{E}[w^{k+1}]-w = -\frac{1}{\alpha\mu n}f'(w)$, so the first inner product term in 3.21 becomes:

$$-\mu\mathbb{E}\left[\left\langle w^{k+1}-w, w-\frac{1}{n}\sum_i\phi_i\right\rangle\right] = \frac{1}{\alpha n}\left\langle f'(w), w-\bar{\phi}\right\rangle.$$

All other terms don't simplify under expectations. So the result is:

$$\begin{aligned} \mathbb{E}[T_3^{k+1}]-T_3 &= (\frac{1}{2}-\frac{1}{n})\frac{\mu}{n^2}\sum_i\|w-\phi_i\|^2 \\ &+ \frac{1}{\alpha n}\left\langle f'(w), w-\bar{\phi}\right\rangle - \frac{1}{2\alpha^2\mu n^3}\sum_i\|f_i(\phi_i)-f_i(w)\|^2. \end{aligned}$$

□

Lemma 3.10. *Between steps k and $k+1$, the $T_4 = \frac{\mu}{2n}\sum_i\|\bar{\phi}-\phi_i\|^2$ term changes as follows:*

$$\mathbb{E}[T_4^{k+1}]-T_4 = -\frac{\mu}{2n^2}\sum_i\|\bar{\phi}-\phi_i\|^2+\frac{\mu}{2n}\|\bar{\phi}-w\|^2-\frac{\mu}{2n^3}\sum_i\|w-\phi_i\|^2.$$

Proof. Note that $\bar{\phi}^{k+1} - \bar{\phi} = \frac{1}{n}(w - \phi_j)$, so:

$$\begin{aligned} T_4^{k+1} &= \frac{\mu}{2n}\sum_i \left\|\bar{\phi}^{k+1} - \bar{\phi} + \bar{\phi} - \phi_i^{k+1}\right\|^2 \\ &= \frac{\mu}{2n}\sum_i \left(\left\|\bar{\phi}^{k+1} - \bar{\phi}\right\|^2 + \left\|\bar{\phi} - \phi_i^{k+1}\right\|^2 + 2\left\langle \bar{\phi}^{k+1} - \bar{\phi}, \bar{\phi} - \phi_i^{k+1}\right\rangle\right) \\ &= \frac{\mu}{2n}\sum_i \left(\left\|\frac{1}{n}(w - \phi_j)\right\|^2 + \left\|\bar{\phi} - \phi_i^{k+1}\right\|^2 + \frac{2}{n}\left\langle w - \phi_j, \bar{\phi} - \phi_i^{k+1}\right\rangle\right). \end{aligned}$$

Now using $\frac{1}{n}\sum_i \left(\bar{\phi} - \phi_i^{k+1}\right) = \bar{\phi} - \bar{\phi}^{k+1} = -\frac{1}{n}(w - \phi_j)$ to simplify the inner product term:

$$\begin{aligned} &= \frac{\mu}{2n^2}\left\|w - \phi_j\right\|^2 + \frac{\mu}{2n}\sum_i \left\|\bar{\phi} - \phi_i^{k+1}\right\|^2 + \frac{\mu}{n^2}\left\langle w - \phi_j, \phi_j - w\right\rangle \\ &= \frac{\mu}{2n^2}\left\|w - \phi_j\right\|^2 + \frac{u}{2n}\sum_i \left\|\bar{\phi} - \phi_i^{k+1}\right\|^2 - \frac{\mu}{n}\left\|w - \phi_j\right\|^2 \\ &= \frac{\mu}{2n}\sum_i \left\|\bar{\phi} - \phi_i^{k+1}\right\|^2 - \frac{\mu}{2n}\left\|w - \phi_j\right\|^2 \\ &= \frac{\mu}{2n}\sum_i \left\|\bar{\phi} - \phi_i\right\|^2 - \frac{\mu}{2n}\left\|\bar{\phi} - \phi_j\right\|^2 + \frac{\mu}{2n}\left\|\bar{\phi} - w\right\|^2 - \frac{\mu}{2n^2}\left\|w - \phi_j\right\|^2. \quad (3.22) \end{aligned}$$

Taking expectations gives the result. □

Lemma 3.11. *Take $f(x) = \frac{1}{n}\sum_i f_i(x)$, with the big-data condition holding with constant β. Then for any x and ϕ_i vectors:*

$$\begin{aligned} f(x) \geq\ & \frac{1}{n}\sum_i f_i(\phi_i) + \frac{1}{n}\sum_i \left\langle f_i'(\phi_i), x - \phi_i\right\rangle + \frac{\beta}{2\mu n^2}\sum_i \left\|f_i'(x) - f_i'(\phi_i)\right\|^2 \\ &+ \frac{\beta L}{2n^2}\sum_i \left\|x - \phi_i\right\|^2 + \frac{\beta}{n^2}\sum_i \left\langle f_i'(x) - f_i'(\phi_i), \phi_i - x\right\rangle. \end{aligned}$$

Proof. We apply Lemma A.14 to each f_i , but instead of using the actual constant L, we use $\frac{\mu n}{\beta} + \mu$, which under the big-data assumption is larger than L:

$$\begin{aligned} f_i(x) \geq\ & f_i(\phi_i) + \left\langle f_i'(\phi_i), x - \phi_i\right\rangle + \frac{\beta}{2\mu n}\left\|f_i'(x) - f_i'(\phi_i)\right\|^2 \\ &+ \frac{\beta L}{2n}\left\|x - \phi_i\right\|^2 + \frac{\beta}{n}\left\langle f_i'(x) - f_i'(\phi_i), \phi_i - x\right\rangle. \end{aligned}$$

Averaging over i gives the result. □

We are now ready to prove our main result:

Theorem 3.12. *Between steps k and k + 1 of the Finito algorithm, if* $\frac{2}{\alpha} - \frac{1}{\alpha^2} - \beta + \frac{\beta}{\alpha} \leq 0$, $\alpha \geq 2$ *and* $\beta \geq 2$ *then*

$$\mathbb{E}[T^{k+1}] - T \leq -\frac{1}{\alpha n} T.$$

Proof. First recall from the Lemmas above the change in each term:

$$\mathbb{E}[T_1^{k+1}] - T_1 \leq \frac{1}{n} \left\langle f'(\bar{\phi}), w - \bar{\phi} \right\rangle + \frac{L}{2n^3} \sum_i \|w - \phi_i\|^2,$$

$$\begin{aligned} \mathbb{E}[T_2^{k+1}] - T_2 \quad \leq \quad & -\frac{1}{n} T_2 - \frac{1}{n} f(w) + (\frac{1}{\alpha} - \frac{\beta}{n}) \frac{1}{\mu n^3} \sum_i \left\| f_i'(w) - f_i'(\phi_i) \right\|^2 \\ & + \frac{1}{n} \left\langle \bar{\phi} - w, f'(w) \right\rangle - \frac{1}{n^3} \sum_i \left\langle f_i'(w) - f_i'(\phi_i), w - \phi_i \right\rangle, \end{aligned}$$

$$\mathbb{E}[T_3^{k+1}] - T_3 = -(\frac{1}{n} + \frac{1}{n^2}) T_3 + \frac{1}{\alpha n} \left\langle f'(w), w - \bar{\phi} \right\rangle - \frac{1}{2\alpha^2 \mu n^3} \sum_i \left\| f_i'(\phi_i) - f_i'(w) \right\|^2,$$

$$\mathbb{E}[T_4^{k+1}] - T_4 = -\frac{\mu}{2n^2} \sum_i \|\bar{\phi} - \phi_i\|^2 + \frac{\mu}{2n} \|\bar{\phi} - w\|^2 - \frac{\mu}{2n^3} \sum_i \|w - \phi_i\|^2.$$

We now combine these and group like terms to get:

$$\begin{aligned} \mathbb{E}[T^{k+1}] - T \quad \leq \quad & \frac{1}{n} \left\langle f'(\bar{\phi}), w - \bar{\phi} \right\rangle + \frac{1}{n^2} \sum_i f_i(\phi_i) \\ & - \frac{1}{n} f(w) + \frac{1}{n^2} \sum_i \left\langle f_i'(\phi_i), w - \phi_i \right\rangle \\ & + (1 - \frac{1}{\alpha}) \frac{1}{n} \left\langle f'(w), \bar{\phi} - w \right\rangle \\ & + (\frac{L}{\mu n} + 1) \frac{\mu}{2n^2} \sum_i \|w - \phi_i\|^2 \\ & - \frac{1}{n^3} \sum_i \left\langle f_i'(w) - f_i'(\phi_i), w - \phi_i \right\rangle \\ & + (1 - \frac{1}{2\alpha}) \frac{1}{\alpha \mu n^3} \sum_i \left\| f_i'(\phi_i) - f_i'(w) \right\|^2 \\ & + \frac{\mu}{2n} \|w - \bar{\phi}\|^2 - \frac{\mu}{2n^2} \sum_i \|\bar{\phi} - \phi_i\|^2. \end{aligned} \tag{3.23}$$

Next we cancel part of the first line using the strong convexity lower bound:

$$\frac{1}{\alpha n} \left\langle f'(\bar{\phi}), w - \bar{\phi} \right\rangle \leq \frac{1}{\alpha n} f(w) - \frac{1}{\alpha n} f(\bar{\phi}) - \frac{\mu}{2\alpha n} \|w - \bar{\phi}\|^2,$$

We then pull terms occurring in $-\frac{1}{\alpha n}T$ together, giving

$$\begin{aligned}\mathbb{E}[T^{k+1}] - T \quad \leq \quad & -\frac{1}{\alpha n}T + (1-\frac{1}{\alpha})\frac{1}{n}\left\langle f'(\bar{\phi}) - f'(w), w - \bar{\phi}\right\rangle \\ & +(1-\frac{1}{\alpha})\left[-\frac{1}{n}f(w) - \frac{1}{n}T_2\right] \\ & +(\frac{L}{\mu n} + 1 - \frac{1}{\alpha})\frac{\mu}{2n^2}\sum_i \|w-\phi_i\|^2 \\ & -\frac{1}{n^3}\sum_i \left\langle f_i'(w) - f_i'(\phi_i), w - \phi_i\right\rangle \\ & +(1-\frac{1}{2\alpha})\frac{1}{\alpha\mu n^3}\sum_i \left\|f_i'(\phi_i) - f_i'(w)\right\|^2 \\ & +(1-\frac{1}{\alpha})\frac{\mu}{2n}\|w-\bar{\phi}\|^2 - (1-\frac{1}{\alpha})\frac{\mu}{2n^2}\sum_i \|\bar{\phi}-\phi_i\|^2 . \qquad (3.24)\end{aligned}$$

Next we use the standard inequality $\langle f'(x) - f'(y), x-y\rangle \geq \mu\|x-y\|^2$ in the form:

$$(1-\frac{1}{\alpha})\frac{1}{n}\left\langle f'(\bar{\phi}) - f'(w), w-\bar{\phi}\right\rangle \leq -(1-\frac{1}{\alpha})\frac{\mu}{n}\|w-\bar{\phi}\|^2 ,$$

which changes the bottom row of Equation 3.24 to

$$-(1-\frac{1}{\alpha})\frac{\mu}{2n}\|w-\bar{\phi}\|^2 - (1-\frac{1}{\alpha})\frac{\mu}{2n^2}\sum_i \|\bar{\phi}-\phi_i\|^2 .$$

These two terms can then be grouped using Lemma B.9 to give

$$\begin{aligned}\mathbb{E}[T^{k+1}] - T \quad \leq \quad & -\frac{1}{\alpha n}T + \frac{L}{2n^3}\sum_i \|w-\phi_i\|^2 \\ & +(1-\frac{1}{\alpha})\left[-\frac{1}{n}f(w) - \frac{1}{n}T_2\right] \\ & -\frac{1}{n^3}\sum_i \left\langle f_i'(w) - f_i'(\phi_i), w-\phi_i\right\rangle \\ & +(1-\frac{1}{2\alpha})\frac{1}{\alpha\mu n^3}\sum_i \left\|f_i'(\phi_i) - f_i'(w)\right\|^2 .\end{aligned}$$

We now use Lemma 3.11 in the following scaled form to cancel against the $\sum_i \|w-\phi_i\|^2$ term:

$$\begin{aligned}\frac{1}{\beta}\left[-\frac{1}{n}f(w) - \frac{1}{n}T_2\right] \quad \leq \quad & \frac{1}{n^3}\sum_i \left\langle f_i'(w) - f_i'(\phi_i), w-\phi_i\right\rangle \\ & -\frac{L}{2n^3}\sum_i \|w-\phi_i\|^2 - \frac{1}{2\mu n^3}\sum_i \left\|f_i'(w) - f_i'(\phi_i)\right\|^2 ,\end{aligned}$$

and then apply the following standard equality (Theorem A.8) to partially cancel $\sum_i \|f_i(\phi_i) - f_i(w)\|^2$:

$$\left(1 - \frac{1}{\alpha} - \frac{1}{\beta}\right)\left[-\frac{1}{n}f(w) - \frac{1}{n}T_2\right] \leq -\left(1 - \frac{1}{\alpha} - \frac{1}{\beta}\right)\frac{\beta}{2\mu n^3}\sum_i \left\|f_i'(\phi_i) - f_i'(w)\right\|^2.$$

Leaving us with

$$\mathbb{E}[T^{k+1}] - T \leq -\frac{1}{\alpha n}T + (\frac{2}{\alpha} - \frac{1}{\alpha^2} - \beta + \frac{\beta}{\alpha})\frac{1}{2\mu n^3}\sum_i \left\|f_i'(\phi_i) - f_i'(w)\right\|^2.$$

The remaining gradient norm term is non-positive under the conditions specified in our assumptions. □

Theorem 3.13. *The Finito Lyapunov function bounds $f(\bar{\phi}) - f(w^*)$ as follows:*

$$f(\bar{\phi}^k) - f(w^*) \leq \alpha T^k.$$

Proof. Consider the following function, which we will call $R(x)$:

$$R(x) = \frac{1}{n}\sum_i f_i(\phi_i) + \frac{1}{n}\sum_i \left\langle f_i'(\phi_i), x - \phi_i\right\rangle + \frac{\mu}{2n}\sum_i \|x - \phi_i\|^2.$$

When evaluated at its minimum with respect to x, which we denote $w' = \bar{\phi} - \frac{1}{\mu n}\sum_i f_i'(\phi_i)$, it is a lower bound on $f(w^*)$ by strong convexity. However, we are evaluating at $w = \bar{\phi} - \frac{1}{\alpha\mu n}\sum_i f_i'(\phi_i)$ instead in the (negated) Lyapunov function. R is convex with respect to x, so by definition

$$R(w) = R\left(\left(1 - \frac{1}{\alpha}\right)\bar{\phi} + \frac{1}{\alpha}w'\right) \leq \left(1 - \frac{1}{\alpha}\right)R(\bar{\phi}) + \frac{1}{\alpha}R(w').$$

Therefore, by the lower bounding property

$$\begin{aligned} f(\bar{\phi}) - R(w) &\geq f(\bar{\phi}) - \left(1 - \frac{1}{\alpha}\right)R(\bar{\phi}) - \frac{1}{\alpha}R(w') \\ &\geq f(\bar{\phi}) - \left(1 - \frac{1}{\alpha}\right)f(\bar{\phi}) - \frac{1}{\alpha}f(w^*) \\ &= \frac{1}{\alpha}\left(f(\bar{\phi}) - f(w^*)\right). \end{aligned}$$

Now note that $T \geq f(\bar{\phi}) - R(w)$. So

$$f(\bar{\phi}) - f(w^*) \leq \alpha T.$$

□

Theorem 3.14. *If the Finito method is initialised with all ϕ_i^0 the same, $\phi_i^0 = \phi^0$, and the assumptions of Theorem 3.12 hold, then the expected convergence rate is:*

$$\mathbb{E}\left[f(\bar{\phi}^k)\right] - f(w^*) \leq \frac{c}{\mu}\left(1 - \frac{1}{\alpha n}\right)^k \left\|f'(\phi^0)\right\|^2,$$

with $c = \left(1 - \frac{1}{2\alpha}\right)$.

Proof. By unrolling Theorem 3.12, we get

$$\mathbb{E}[T^k] \leq \left(1 - \frac{1}{\alpha n}\right)^k T^0.$$

Now using Theorem 3.13:

$$\mathbb{E}\left[f(\bar{\phi}^k)\right] - f(w^*) \leq \alpha\left(1 - \frac{1}{\alpha n}\right)^k T^0.$$

We need to control T^0 as well. Since we are assuming that all ϕ_i^0 start the same, we have that

$$\begin{aligned}
T^0 &= f(\phi^0) - \frac{1}{n}\sum_i f_i(\phi^0) - \frac{1}{n}\sum_i \left\langle f_i'(\phi^0), w^0 - \phi^0\right\rangle - \frac{\mu}{2}\left\|w^0 - \phi^0\right\|^2 \\
&= 0 - \left\langle f'(\phi^0), w^0 - \phi^0\right\rangle - \frac{\mu}{2}\left\|-\frac{1}{\alpha\mu}f'(\phi^0)\right\|^2 \\
&= \frac{1}{\alpha\mu}\left\|f'(\phi^0)\right\|^2 - \frac{1}{2\alpha^2\mu}\left\|f'(\phi^0)\right\|^2 \\
&= \left(1 - \frac{1}{2\alpha}\right)\frac{1}{\alpha\mu}\left\|f'(\phi^0)\right\|^2.
\end{aligned}$$

□

3.8 Prox-Finito Theory

The Prox-Finito algorithm is very closely related to SDCA. Instead of giving a proof in the spirit of SDCA, we now present a convergence proof using a novel primal argument. This argument has a geometric feel to it which we believe is clearer than the SDCA proof, although it is a little longer. The main result is in Theorem 3.17.

Lemma 3.15. *We consider a set of possible functions (F). F is $S_{\mu,L}$, the set of μ strong convex and L smooth functions, with the additional restriction that each $f \in F$ is lower bounded by a quadratic function l with curvature μ that we know ($l \in S_{\mu,\mu}$), and that for all $f \in F$, $f(w) - l(w) = \delta$, for a single known w and δ. For each unit vector direction r, we define the function:*

$$b(x) = l(v) + \langle l'(v), x - v \rangle + \frac{L}{2} \|x - v\|^2,$$

where v is the point in the direction r such that $\frac{L-\mu}{2} \|w - v\|^2 = \delta$. More precisely, $v = w + \alpha r$, for $\alpha = \sqrt{\frac{2\delta}{L-\mu}}$. Then define the line segment L as the segment between w and v, $\left(L = \left\{w + \alpha r \,:\, 0 \leq \alpha \leq \sqrt{\frac{2\delta}{L-\mu}}\right\}\right)$, Then for all $f \in F$ and points $x \in L$:

$$f(x) \geq b(x) \geq l(x),$$

i.e. $b(x)$ is at least as tight a lower bound on the interval L as $l(x)$. Furthermore, we have:

$$\forall x \in L,\ b(x) - l(x) = \frac{L-\mu}{2} \|x - v\|^2.$$

The above points also imply that:

$$f(w) - l(w) = \frac{L-\mu}{2} \|w - v\|^2. \tag{3.25}$$

Proof. The situation is depicted in Figure 3.3. Since l is quadratic with curvature μ, it can be written as

$$l(x) = l(v) + \langle l'(v), x - v \rangle + \frac{\mu}{2} \|x - v\|^2.$$

By cancelling like terms, $b(x) - l(x) = \frac{L-\mu}{2} \|x - v\|^2$. Let f be any function in F. Now suppose that there exists a $y \in L$ such that $f(y) < b(y)$. Then we consider the possible derivatives in the direction r. Let $f_r'(x)$ denote the directional derivative $\langle f'(x), r \rangle$.

1. Suppose that $f_r'(w) < b_r'(w)$. Then taking the Lipschitz smoothness upper bound about point w of f, for all $x \in L$:

$$\begin{aligned} f(x) &\leq f(w) + \langle f'(w), x - w \rangle + \frac{L}{2} \|x - w\|^2 \\ &< f(w) + \langle b'(w), x - w \rangle + \frac{L}{2} \|x - w\|^2 \\ &= b(x), \end{aligned}$$

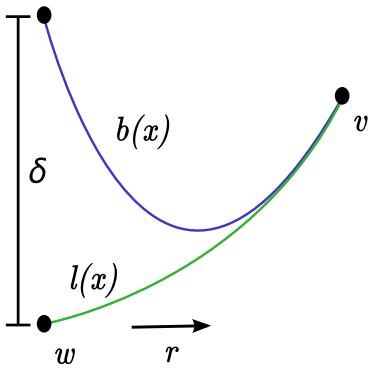

Figure 3.3: Lemma 3.15 schematic. The vertical axis is function value, and the horizontal axis is change along the direction r.

which holds since $b(x)$ can be reparameterised as

$$b(w) + \langle b'(w), x - w \rangle + \frac{L}{2} \|x - w\|^2,$$

and $b(w) = f(w)$. Since $b(v) = l(v)$, this implies $f(v) < l(v)$, which is a contradiction.

2. Suppose that $f'_r(w) > b'_r(w)$. Then f lies above b at some point in the direction r from w. In order that our assumption $f(y) < b(y)$ holds, f must equal b somewhere in the interval L, which we denote u, i.e. the curves cross. Then at the crossing point f is more negative than b ($f'_r(u) < b'_r(u)$), and the argument from case (1) applies with u instead of w.

3. Suppose that $f'_r(w) = b'_r(w)$. Then consider the Lipschitz smoothness upper bound around y:

$$f(x) \leq f(y) + \langle f'(y), x - y \rangle + \frac{L}{2} \|x - y\|^2. \tag{3.26}$$

Recall that we can reparameterise b around y as $b(x) = b(y) + \langle b'(y), x - y \rangle + \frac{L}{2} \|x - y\|^2$. Since we require that $f(v) \geq b(v)$, the inner product term in Equation 3.26 when evaluating at v must be greater than that in b to offset the $b(y) - f(y)$ difference, i.e. $\langle f'(y), v - y \rangle > \langle b'(y), v - y \rangle$, therefore $f'_r(y) > b'_r(y)$. But this violates the Lipschitz smoothness condition $\|f'(y) - f'(w)\| \leq L \|y - w\|$ on the gradients of f, as $b'(y)$ is as different as possible for a gradient of f at that distance from w along r, by its construction.

□

Lemma 3.16. *For any v_j and w^k, the minimum of*

$$g_j(w_j^{k+1}) = \frac{\mu}{2} \left\| w_j^{k+1} - w^k \right\|^2 + \frac{L - \mu}{2n} \left\| w_j^{k+1} - v_j \right\|^2,$$

with respect to w_j^{k+1} *is:*

$$\frac{\mu\frac{L-\mu}{n}}{2\left(\mu+\frac{L-\mu}{n}\right)}\left\|w^k-v_j\right\|^2.$$

Proof. Let the minimiser be x. We find the value of x by setting the gradient to zero of g_j:

$$\begin{aligned}\mu(x-w^k)+\frac{L-\mu}{n}(x-v_j)&=0,\\ \mu w^k+\frac{L-\mu}{n}v_j&=(\mu+\frac{L-\mu}{n})x,\\ \therefore x&=\frac{\mu w^k+\frac{L-\mu}{n}v_j}{\mu+\frac{L-\mu}{n}}.\end{aligned}$$

So the minimum for the first term is:

$$\begin{aligned}\frac{\mu}{2}\left\|\frac{\mu w^k+\frac{L-\mu}{n}v_j-\mu w^k-\frac{L-\mu}{n}w^k}{\mu+\frac{L-\mu}{n}}\right\|^2 &= \frac{\mu}{2}\left\|(\frac{L-\mu}{n})\frac{v_j-w^k}{\mu+\frac{L-\mu}{n}}\right\|^2\\ &= \frac{\mu}{2}\left(\frac{L-\mu}{n(\mu+\frac{L-\mu}{n})}\right)^2\left\|w^k-v_j\right\|^2,\end{aligned}$$

for the second term:

$$\begin{aligned}\frac{L-\mu}{2n}\left\|\frac{\mu w^k+\frac{L-\mu}{n}v_j-\mu v_j-\frac{L-\mu}{n}v_j}{\mu+\frac{L-\mu}{n}}\right\|^2 &= \frac{L-\mu}{2n}\left\|\mu\frac{w^k-v_j}{\mu+\frac{L-\mu}{n}}\right\|^2\\ &= \frac{L-\mu}{2n}\left(\frac{\mu}{\mu+\frac{L-\mu}{n}}\right)^2\left\|w^k-v_j\right\|^2,\end{aligned}$$

Combining the constants:

$$\begin{aligned}\frac{\mu}{2}\left(\frac{L-\mu}{n(\mu+\frac{L-\mu}{n})}\right)^2+\frac{L-\mu}{2n}\left(\frac{\mu}{\mu+\frac{L-\mu}{n}}\right)^2 &= \frac{\mu}{2\left(\mu+\frac{L-\mu}{n}\right)^2}\left(\left(\frac{L-\mu}{n}\right)^2+\mu\frac{L-\mu}{n}\right)\\ &= \frac{\mu\frac{L-\mu}{n}}{2\left(\mu+\frac{L-\mu}{n}\right)^2}\left(\left(\frac{L-\mu}{n}\right)+\mu\right)\\ &= \frac{\mu\frac{L-\mu}{n}}{2\left(\mu+\frac{L-\mu}{n}\right)}.\end{aligned}$$

□

3.8.1 Main result

Theorem 3.17. *Define the Lyapunov function T^k at step k as $T^k = f(w^*) - B^k(w^k)$. Then the expected change in T between steps k and $k+1$ for the Prox-Finito algorithm is:*

$$\mathbb{E}[T^{k+1}] \leq \left(1 - \frac{\mu}{(\mu n + L - \mu)}\right) T^k.$$

Proof. Let

$$l_i^k(x) = f_i(\phi_i^k) + \left\langle f_i'(\phi_i^k), x - \phi_i^k \right\rangle + \frac{\mu}{2} \left\| x - \phi_i^k \right\|^2,$$

so that $B^k(x) = \frac{1}{n}\sum_i l_i(x)$. Let w_j^{k+1} be the minimiser of B^{k+1}, which of course depends on the choice of index j.

Now using the fact that B^k is quadratic, we get that for all x:

$$B^k(x) = B^k(w^k) + \left\langle \left(B^k\right)'(w^k), x - w^k \right\rangle + \frac{\mu}{2} \left\| w^k - x \right\|^2,$$

so using that $\left(B^k\right)'(w^k) = 0$ by construction, and evaluating at w_j^{k+1}, we have:

$$B^k(w_j^{k+1}) - B^k(w^k) = \frac{\mu}{2} \left\| w_j^{k+1} - w^k \right\|^2. \tag{3.27}$$

We also need to bound the change between B^{k+1} and B^k at the point w_j^{k+1}. Using the key property $\phi_j^{k+1} = w_j^{k+1}$, the added lower bound $l_j^{k+1}(w_j^{k+1})$ is tight at w_j^{k+1} by construction, so:

$$\begin{aligned} B^{k+1}(w_j^{k+1}) - B^k(w_j^{k+1}) &= \frac{1}{n} l_j^{k+1}(\phi_j^{k+1}) - \frac{1}{n} l_j^k(w_j^{k+1}) \\ &= \frac{1}{n} f_j(w_j^{k+1}) - \frac{1}{n} l_j^k(w_j^{k+1}). \end{aligned} \tag{3.28}$$

The change in the $B^k(w^k)$ term in the Lyapunov function between steps is given by combining 3.27 and 3.28:

$$\begin{aligned} B^{k+1}(w_j^{k+1}) - B^k(w^k) &= \left[B^{k+1}(w_j^{k+1}) - B^k(w_j^{k+1})\right] + \left[B^k(w_j^{k+1}) - B^k(w^k)\right] \\ &= \frac{\mu}{2} \left\| w_j^{k+1} - w^k \right\|^2 + \frac{1}{n} f_j(w_j^{k+1}) - \frac{1}{n} l_j^k(w_j^{k+1}). \end{aligned}$$

Since our Lyapunov function is $f(w^*) - B^k(w^k)$ and $f(w^*)$ is fixed, our goal is to lower bound the expectation of the change in the B^k function's minimum with respect to the choice of index j:

$$\mathbb{E}\left[B^{k+1}(w_j^{k+1}) - B^k(w^k)\right] = \mathbb{E}\left[\frac{\mu}{2} \left\| w_j^{k+1} - w^k \right\|^2 + \frac{1}{n} f_j(w_j^{k+1}) - \frac{1}{n} l_j^k(w_j^{k+1})\right]. \tag{3.29}$$

Let us fix the choice of j. We proceed by determining the minimum over w_j^{k+1} of the quantity inside the expectation. We will also fix the unit vector direction r_j from w^k that w_j^{k+1} is in. Then we can apply Lemma 3.15 with $\delta = f_j(w^k) - l_j(w^k)$, to give:

$$\frac{1}{n} f_j(w_j^{k+1}) - \frac{1}{n} l_j^k(w_j^{k+1}) \geq \frac{1}{n} b(w_j^{k+1}) - \frac{1}{n} l_j(w_j^{k+1}) = \frac{L-\mu}{2n} \left\| w_j^{k+1} - v_j \right\|^2,$$

where v_j and b are given in Lemma 3.15. Note that v_j is coplanar with w^k and w_j^{k+1}, namely in direction r_j from w^k. Applying this result:

$$\begin{aligned}
B^{k+1}(w_j^{k+1}) - B^k(w^k) &= \frac{\mu}{2} \left\| w_j^{k+1} - w^k \right\|^2 + \frac{1}{n} f_j(w_j^{k+1}) - \frac{1}{n} l_j^k(w_j^{k+1}) \\
&\geq \frac{\mu}{2} \left\| w_j^{k+1} - w^k \right\|^2 + \frac{L-\mu}{2n} \left\| w_j^{k+1} - v_j \right\|^2 \\
&= g_j(w_j^{k+1}) \quad \text{(Lemma 3.16)} \\
&\geq \frac{\mu \frac{L-\mu}{n}}{2\left(\mu + \frac{L-\mu}{n}\right)} \left\| w^k - v_j \right\|^2 \quad \text{(Lemma 3.16)} \\
&= \frac{2}{L-\mu} \cdot \frac{\mu \frac{L-\mu}{n}}{2\left(\mu + \frac{L-\mu}{n}\right)} \left(f_j(w^k) - l_j(w^k) \right) \quad \text{(Lem. 3.15, Eq 3.25)} \\
&= \frac{\mu}{(\mu n + L - \mu)} \left(f_j(w^k) - l_j(w^k) \right).
\end{aligned}$$

We now take expectations of this quantity with respect to the choice of index j, and note that the above argument holds for all possible choices of the direction r_j. So:

$$\begin{aligned}
\mathbb{E}[B^{k+1}(w^{k+1})] - B^k(w^k) &\geq \mathbb{E}\left[\frac{\mu}{(\mu n + L - \mu)} \left(f_j(w^k) - l_j(w^k) \right) \right] && (3.30) \\
&= \frac{\mu}{(\mu n + L - \mu)} \left(f(w^k) - B^k(w^k) \right) && (3.31) \\
&\geq \frac{\mu}{(\mu n + L - \mu)} \left(f(w^*) - B^k(w^k) \right).
\end{aligned}$$

So we have established a bound on Expression 3.29. Stating in terms of the Lyapunov function:

$$\mathbb{E}[T^{k+1}] \leq \left(1 - \frac{\mu}{(\mu n + L - \mu)} \right) T^k.$$

□

Theorem 3.18. *The expected convergence rate of the Prox-Finito algorithm for $n > 1$ stopping at iteration k is:*

$$E\left[f(w^k) - f(w^*)\right] \leq \left(1 - \frac{\mu}{(\mu n + L - \mu)}\right)^k \frac{\mu n + L - \mu}{\mu} \left[f(w^*) - B^0(w^0)\right].$$

Proof. From here the proof follows closely the SDCA proof. Taking the expectation of Theorem 3.17 with respect to all k, then summing from 0 to $k-1$ gives: □

$$f(w^*) - \mathbb{E}\left[B^k(w^k)\right] \leq \left(1 - \frac{\mu}{(\mu n + L - \mu)}\right)^k \left[f(w^*) - B^0(w^0)\right]. \tag{3.32}$$

This expectation is unconditional. We now need to bound $f(w^k) - f(w^*)$ by some constant times $f(w^*) - B^k(w^k)$. Recall Equation 3.31:

$$\mathbb{E}[B^{k+1}(w^{k+1})] - B^k(w^k) \geq \frac{\mu}{(\mu n + L - \mu)} \left(f(w^k) - B^k(w^k)\right).$$

Rearranging gives:

$$\begin{aligned} f(w^k) - B^k(w^k) &\leq \frac{\mu n + L - \mu}{\mu} \left[\mathbb{E}[B^{k+1}(w^{k+1})] - B^k(w^k)\right] \\ &= \frac{\mu n + L - \mu}{\mu} \left[\left(\mathbb{E}[B^{k+1}(w^{k+1})] - f(w^*)\right) - \left(B^k(w^k) - f(w^*)\right)\right]. \\ &\leq \frac{\mu n + L - \mu}{\mu} \left[-\left(B^k(w^k) - f(w^*)\right)\right]. \end{aligned}$$

We have used the negativity of $B^k(w^k) - f(w^*)$ in the last step. Since $B^k(w^k) \leq f(w^*)$, we have by taking expectations over all previous steps that:

$$\mathbb{E}\left[f(w^k) - f(w^*)\right] \leq \frac{\mu n + L - \mu}{\mu} \mathbb{E}\left[f(w^*) - B^k(w^k)\right].$$

This expectation is also unconditional. Combining with Equation 3.32 gives the result.

3.8.2 Proof of Theorem 3.4

Proof. The key change in the proof of Theorem 3.17 is in the calculation of the following Expectation in Equation 3.30:

$$\mathbb{E}\left[\frac{1}{c_j}\left(f_j(w^k) - l_j(w^k)\right)\right].$$

Applying the weighted probabilities to this expectation yields:

$$\begin{aligned}\mathbb{E}\left[\frac{1}{c_j}\left(f_j(w^k) - l_j(w^k)\right)\right] &= \frac{1}{Z}\sum_i c_i \frac{1}{c_i}\left(f_i(w^k) - l_i(w^k)\right) \\ &= \frac{1}{Z}\sum_i \left(f_i(w^k) - l_i(w^k)\right).\end{aligned}$$

The value of Z is:

$$\sum_i \frac{\mu n + L_i - \mu}{\mu} = n\frac{\mu n + \bar{L} - \mu}{\mu},$$

so we have

$$\begin{aligned}\mathbb{E}\left[\frac{1}{c_j}\left(f_j(w^k) - l_j(w^k)\right)\right] &= \frac{\mu}{(\mu n + \bar{L} - \mu)} \cdot \frac{1}{n}\sum_i \left(f_i(w^k) - l_i(w^k)\right) \\ &= \frac{\mu}{(\mu n + \bar{L} - \mu)}\left(f(w^k) - B^k(w^k)\right).\end{aligned}$$

The remaining steps mirror the proof of Theorem 3.17 and 3.18. □

Chapter 4

New Primal Incremental Gradient Methods

The fast primal incremental gradient methods in the existing literature have a number of deficiencies. The SAG method has a complex theory, and no theoretical support for its use on composite objectives (defined in Section 4.1). The SVRG method avoids those problems, but it has an awkward theoretical convergence rate in terms of the number of gradient evaluations, and it does not natively support non-strongly convex problems. In this chapter we present the SAGA method, which has none of these deficiencies. The SAGA method has a simple theory, with a theoretical convergence rate directly comparable to SDCA ($2\times$ worse) and SAG ($2\times$ better). It is also adaptive to strong convexity, as it may be used without modification and with the same step size on both convex and strongly convex problems. If the problem is strongly convex, it will converge at a fast linear rate, falling back to an $O(1/k)$ rate otherwise. This avoids one of the main deficiencies of SDCA.

An interesting property of SAGA is that the algorithm can be written in a number of different ways, making the update similar to either SVRG, SAG or Finito. This sheds light on the relationships between the currently known fast incremental gradient methods.

An earlier version of the work in this chapter has been published as Defazio et al. (2014a).

4.1 Composite Objectives

Several of the fast incremental gradient methods can be extended to support *composite* objectives (Table 4.1). A composite problem is just the usual finite sum structure $f(x) = \frac{1}{n}\sum_{i=1}^{n} f_i(x)$, together with an additional term h:

$$F(x) = f(x) + h(x),$$

where $h\colon \mathbb{R}^d \to \mathbb{R}^d$ is convex but potentially non-differentiable. For the SAGA algorithm we will solve this problem using a *proximal* approach, making use of the proximal operator of the function h. For most problems, known convergence rates of composite objectives are as good as those for the non-composite case (Combettes and Pesquet, 2011) when we have access to the proximal operator of h. Although the problem is not necessarily smooth, by accessing the non-smooth portion through the proximal operator it is still possible to converge linearly, which is not the case when we only have access to (sub-)gradients.

4.2 SAGA Algorithm

We start with some known initial vector $x^0 \in \mathbb{R}^d$ and known derivatives $f_i'(\phi_i^0) \in \mathbb{R}^d$ with $\phi_i^0 = x^0$ for each i. These derivatives are stored in a table data-structure of length n, or alternatively a $n \times d$ matrix. For many problems of interest, such as binary classification and least-squares, only a single floating point value instead of a full gradient vector needs to be stored (see Section 4.4). The update is given in Algorithm 4.1.

Algorithm 4.1 SAGA

Given the value of x^k and of each $f_i'(\phi_i^k)$ at the end of iteration k, the updates for iteration $k+1$ is as follows:

1. Pick a j uniformly at random.
2. Take $\phi_j^{k+1} = x^k$, and store $f_j'(\phi_j^{k+1})$ in the table. All other entries in the table remain unchanged. The quantity ϕ_j^{k+1} is not explicitly stored.
3. Update x using $f_j'(\phi_j^{k+1})$, $f_j'(\phi_j^k)$ and the table average:

$$w^{k+1} = x^k - \gamma \left[f_j'(\phi_j^{k+1}) - f_j'(\phi_j^k) + \frac{1}{n} \sum_{i=1}^{n} f_i'(\phi_i^k) \right], \tag{4.1}$$

$$x^{k+1} = \text{prox}_{1/\gamma}^{h} \left(w^{k+1} \right).$$

We establish the following theoretical results in Section 4.6:

In the strongly convex case, when a step size of $\gamma = 1/(2(\mu n + L))$ is chosen, we have the following convergence rate in the composite and hence also the non-composite case:

$$\mathbb{E} \left\| x^k - x^* \right\|^2 \leq \left(1 - \frac{\mu}{2(\mu n + L)} \right)^k \left[\left\| x^0 - x^* \right\|^2 + \frac{n}{\mu n + L} \left[f(x^0) - \left\langle f'(x^*), x^0 - x^* \right\rangle - f(x^*) \right] \right].$$

We prove this result in Section 4.6.1. The requirement of strong convexity can be relaxed from needing to hold for each f_i to just holding on average, but at the expense of a worse geometric rate $(1 - \frac{\mu}{6(\mu n+L)})$, requiring a step size of $\gamma = 1/(3(\mu n + L))$.

In the non-strongly convex case, we have established the convergence rate in terms of the average iterate, excluding step 0: $\bar{x}^k = \frac{1}{k}\sum_{t=1}^{k} x^t$. Using a step size of $\gamma = 1/(3L)$ we have

$$\mathbb{E}\left[F(\bar{x}^k)\right] - F(x^*) \leq \frac{10n}{k}\left[\frac{2L}{n}\left\|x^0 - x^*\right\|^2 + f(x^0) - \left\langle f'(x^*), x^0 - x^*\right\rangle - f(x^*)\right].$$

This result is proved in Section 4.6. Importantly, when this step size $\gamma = 1/(3L)$ is used, our algorithm *automatically adapts* to the level of strong convexity $\mu > 0$ naturally present, giving a convergence rate of:

$$\mathbb{E}\left\|x^k - x^*\right\|^2 \leq \left(1 - \min\left\{\frac{1}{4n}, \frac{\mu}{3L}\right\}\right)^k \left[\left\|x^0 - x^*\right\|^2 + \frac{2n}{3L}\left[f(x^0) - \left\langle f'(x^*), x^0 - x^*\right\rangle - = f(x^*)\right]\right].$$

Although any incremental gradient method can be applied to non-strongly convex problems via the addition of a small quadratic regularisation, the amount of regularisation is an additional tunable parameter which our method avoids.

4.3 Relation to Existing Methods

In the non-composite case, it is possible to write the SAGA algorithm in terms of two quantities at each step instead of one: x^k and u^k.

Algorithm 4.2 2 variable SAGA

Given the value of u^k and of each $f_i'(\phi_i^k)$ at the end of iteration k the updates for iteration $k+1$, is as follows:

1. Calculate x^k:
$$x^k = u^k - \gamma\sum_{i=1}^{n} f_i'(\phi_i^k). \tag{4.2}$$
2. Update u with $u^{k+1} = u^k + \frac{1}{n}(x^k - u^k)$.
3. Pick a j uniformly at random.
4. Take $\phi_j^{k+1} = x^k$, and store $f_j'(\phi_j^{k+1})$ in the table replacing $f_j'(\phi_j^k)$. All other entries in the table remain unchanged. The quantity ϕ_j^{k+1} is not explicitly stored.

Writing the algorithm in this form makes the relationship with prior methods more apparent. We explore the relationship between SAGA and the other fast incremental

gradient methods in this section. By using SAGA as a midpoint, we are able to provide a more unified view than is available in the existing literature. A brief summary of the properties of each method considered in this section is given in Table 4.1.

4.3.1 SAG

If we eliminate x^k we get an update for u in SAGA of:

$$u^{k+1} = u^k - \frac{\gamma}{n} \sum_{i=1}^{n} f_i'(\phi_i^k). \tag{4.3}$$

After translating notation, this is identical to the Stochastic Average Gradient (SAG, Schmidt et al., 2013) update discussed in Section 2.4, except instead of setting $\phi_j^{k+1} = u^k$, we are using a more aggressive update of $\phi_j^{k+1} = x^k = u^k - \gamma \sum_i f_i'(\phi_i^k)$. The order of the steps is also changed, as in SAG the jth gradient is updated before the x step is taken, whereas above it is updated after. The order of the steps for SAG doesn't affect the algorithm as it only has two steps, so the ordering change is not significant.

The$\phi_j^{k+1} = x^k$ change has a large effect on the estimate of the gradient. In SAG, the gradient approximation $\frac{1}{n} \sum_i f_i'(\phi_i^k)$ is biased away from the true gradient, whereas for all the other methods considered here, including SAGA, the gradient approximation is unbiased. The trade-off for the increased bias is a decreased variance in the $f_i'(\phi_i^k)$ gradients, due to the less aggressive ϕ_i^k updates used.

There is another way of interpreting the SAG algorithm in relation to the SAGA algorithm. We can rewrite the SAG update to make it more directly comparable:

$$\text{(SAG)} \qquad x^{k+1} = x^k - \gamma \left[\frac{f_j'(x^k) - f_j'(\phi_j^k)}{n} + \frac{1}{n} \sum_{i=1}^{n} f_i'(\phi_i^k) \right], \tag{4.4}$$

$$\text{(SAGA)} \qquad x^{k+1} = x^k - \gamma \left[f_j'(x^k) - f_j'(\phi_j^k) + \frac{1}{n} \sum_{i=1}^{n} f_i'(\phi_i^k) \right], \tag{4.5}$$

Notice that the central terms are weighted by $1/n$ for SAG, in comparison to SAGA. The lower variance of the SAG update arises because of the smaller magnitude of those two terms.

The per update computation and storage costs of SAGA and SAG is essentially the same. They both require a gradient evaluation and a gradient storage (although the storage cost can usually be ameliorated for both, see Section 4.4). The advantage over SAG is that SAGA has a much more complete, simple and tight theory. The

theoretical and practical convergence rate is better for SAGA, and no theory exists for the use of proximal operators in SAG whereas we establish such a theory for SAGA in this work. Based also on our superior experimental results in Section 4.5, we consider SAGA as a replacement for SAG in most situations.

4.3.2 SVRG

Recall the x^{k+1} update for SAGA (Equation 4.1) in the non-composite case:

$$x^{k+1} = x^k - \gamma f_j'(x^k) + \gamma \left[f_j'(\phi_j^k) - \frac{1}{n} \sum_{i=1}^{n} f_i'(\phi_i^k) \right].$$

This can be directly compared against the SVRG (Stochastic Variance Reduced Gradient) (Johnson and Zhang, 2013) update from Section 2.5, if we translate the notation:

$$x^{k+1} = x^k - \gamma f_j'(x^k) + \gamma \left[f_j'(\tilde{x}) - \frac{1}{n} \sum_{i=1}^{n} f_i'(\tilde{x}) \right].$$

The vector $\tilde{x}$ is not updated every step, but rather the loop over k appears inside an outer loop, where $\tilde{x}$ is updated at the start of each outer iteration. Essentially SAGA is at the midpoint between SVRG and SAG; it updates the ϕ_j value each time index j is picked, whereas SVRG updates all of ϕ function's as a batch.

The SVRG algorithm has been previously motivated as being a form of variance reduction (Johnson and Zhang, 2013), similar to approaches used for Monte Carlo estimation of integrals. The SAGA algorithm can also be interpreted as a form of variance reduction, see Defazio et al. (2014a).

SVRG makes a trade-off between time and space. For the equivalent practical convergence rate it makes 2x-3x more gradient evaluations, but in doing so it does not need to store a table of gradients, but a single average gradient. The usage of SAG v.s. SVRG is problem dependent. For example for linear predictors where gradients can be stored as a reduced vector of dimension $p - 1$ for p classes, SAGA is preferred over SVRG both theoretically and in practice. For neural networks, where no theory is available for either method, the storage of gradients is generally more expensive than the additional backwards propagations, giving SVRG the advantage.

SVRG also has an additional parameter besides step size that needs to be set, namely the number of iterations per inner loop (m). This parameter can be set via the theory, or conservatively as $m = n$, however doing so does not give anywhere near the best practical performance. Having to tune one parameter instead of two is a practical advantage for SAGA.

	SAGA	SAG	SDCA	SVRG	FINITO
Strongly Convex (SC)	✓	✓	✓	✓	✓
Convex, Non-SC*	✓	✓	✗	?	?
Prox Reg.	✓	?	✓?	✓	✗
Non-smooth	✗	✗	✓	✗	✗
Low Storage Cost	✗	✗	✗	✓	✗
Simple(-ish) Proof	✓	✗	✓	✓	✓
Adaptive to SC	✓	✓	✗	?	?

Table 4.1: Basic summary of method properties. Question marks denote unproven, but not experimentally ruled out cases. A tick indicates that the method can be applied in that setting, or that the property holds. (*) Note that any method can be applied to non-strongly convex problems by adding a small amount of L_2 regularisation, this row describes methods that do not require this trick.

4.3.3 Finito

The Finito method (Section 3.1) is also closely related to SAGA. Recall that Finito uses a step of the following form:

$$x^{k+1} = \bar{\phi}^k - \gamma \sum_{i=1}^{n} f_i'(\phi_i^k).$$

Note that the step sized used is of the order of $\gamma = 1/\mu n$, roughly comparable to the γ in SAGA.

Using the two variable SAGA formulation, SAGA can be interpreted as Finito, but with the quantity $\bar{\phi}$ replaced with u, which is updated in the same way as $\bar{\phi}$, but *in expectation*. To see this, consider how $\bar{\phi}$ changes in value and in expectation, conditioned on the previous step:

$$\mathbb{E}\left[\bar{\phi}^{k+1}\right] = \mathbb{E}\left[\bar{\phi}^k + \frac{1}{n}\left(x^k - \phi_j^k\right)\right] = \bar{\phi}^k + \frac{1}{n}\left(x^k - \bar{\phi}^k\right).$$

The update is identical in expectation to the update for u, $u^{k+1} = u^k + \frac{1}{n}(x^k - u^k)$.

There are three advantages of SAGA over Finito. SAGA doesn't require strong convexity to work, it has support for proximal operators, and it doesn't require storing the ϕ_i values. The big advantage of Finito is that when it is applicable, it can be used with a permuted access ordering, which can make it up to two times faster. Finito is particularly useful when f_i is computationally expensive to compute compared to the extra storage costs required for it over the other methods.

4.4 Implementation

We briefly discuss some implementation concerns:

1. For many problems each derivative f_i' is just a simple weighting of the ith data vector. Logistic regression and least squares have this property. In such cases, instead of storing the full derivative f_i' for each i, we need only store the weighting constants. This reduces the storage requirements to be the same as the SDCA method in practice. A similar trick can be applied to multi-class classifiers with p classes by storing $p-1$ values for each i.

2. Our algorithm assumes that initial gradients are known for each f_i at the starting point x^0. Instead, a heuristic may be used where during the first pass, data-points are introduced one-by-one, in a non-randomized order, with averages computed in terms of those data-points processed so far. This procedure has been successfully used with SAG (Schmidt et al., 2013).

3. The SAGA update as stated is slower than necessary when derivatives are sparse. A just-in-time updating of u or x may be performed just as is suggested for SAG (Schmidt, Roux, and Bach, 2013), which ensures that only sparse updates are done at each iteration.

4. We give the form of SAGA for the case where each f_i are strongly convex. In practice however, we usually have only convex f_i, with strong convexity in f induced by the addition of a quadratic regulariser. This quadratic regulariser may be split amount the f_i functions evenly, to satisfy our assumptions. It is perhaps easier to use a variant of SAGA where the regulariser $\frac{\mu}{2}||x||^2$ is explicit, such as the following modification of Equation 4.1:

$$x^{k+1} = (1-\mu\gamma)\, x^k - \gamma f_j'(x^k) + \gamma \left[f_j'(\phi_j^k) - \frac{1}{n}\sum_i f_i'(\phi_i^k) \right].$$

   For sparse implementations instead of scaling x^k at each step, a separate scaling constant β^k may be scaled instead, with $\beta^k x^k$ being used in place of x^k. This is a standard trick used with stochastic gradient methods.

4.5 Experiments

We performed a series of experiments to validate the effectiveness of SAGA. We tested a binary classifier on MNIST, COVTYPE, IJCNN1 and a least squares predictor on MILLIONSONG. Details of these datasets are in Section 3.3. We used the same code base for each method, just changing the main update rule. SVRG was tested

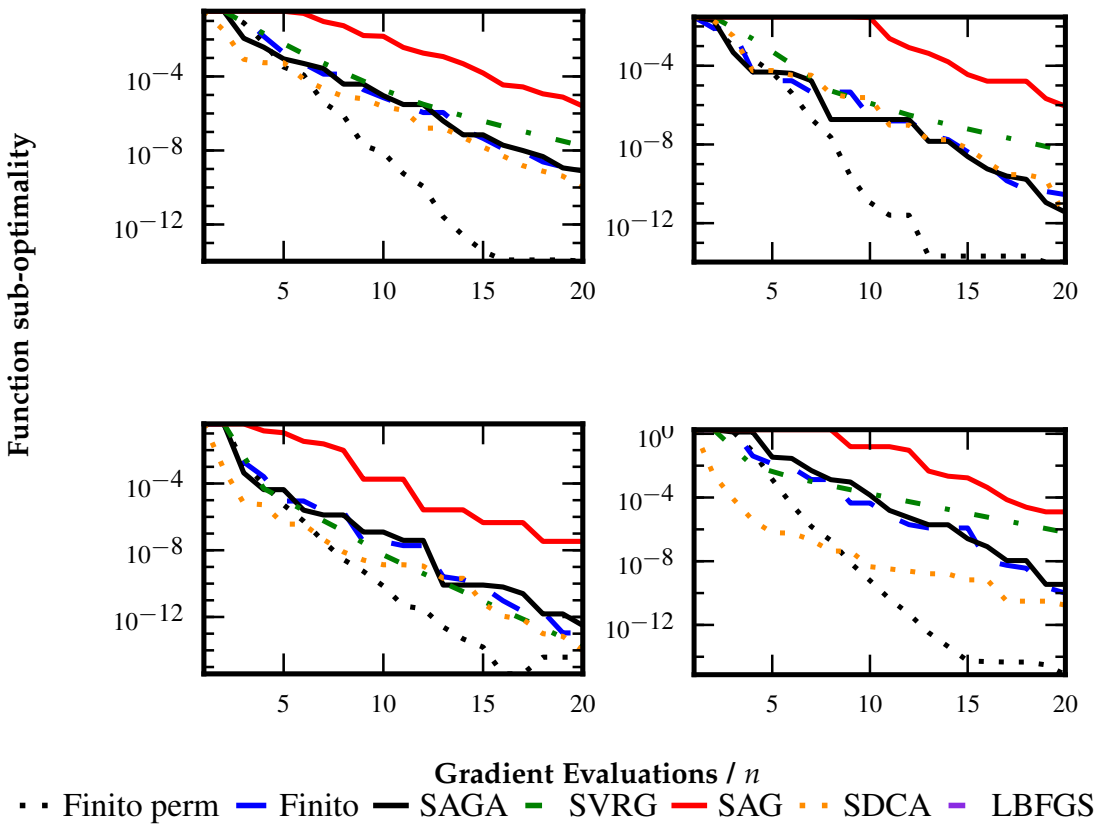

Figure 4.1: From left to right, top to bottom we have the MNIST, COVTYPE, IJCNN1 and MILLIONSONG datasets with L_2 regularisation.

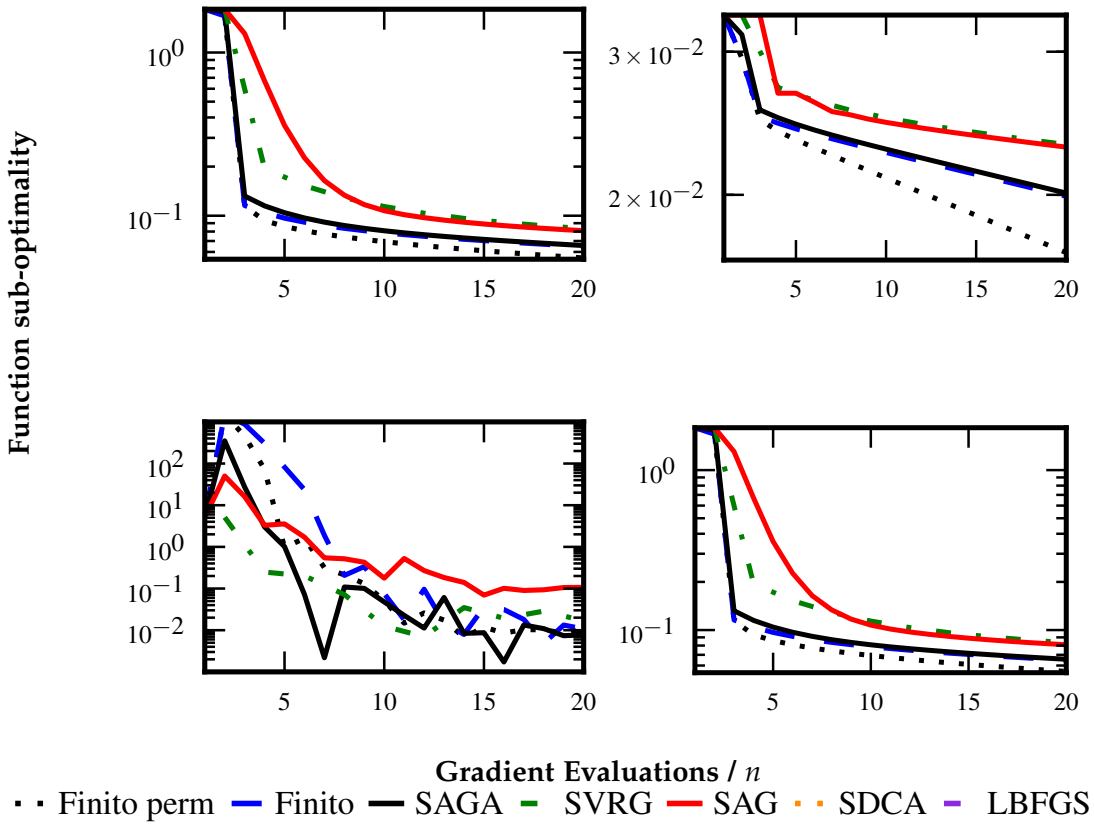

Figure 4.2: From left to right, top to bottom we have the MNIST, COVTYPE, IJCNN1 and MILLIONSONG datasets with L_1 regularisation.

with the recalibration pass used every n iterations, as suggested by Konečný and Richtárik (2013). Each method had its step size parameter chosen to give the fastest convergence. In contrast to Section 3.3, we consider non-strongly convex problems, as well as the SVRG method, which was not published at the time those earlier experiments were run.

We tested with a L_2 regulariser, which all methods support, and with a L_1 regulariser on a subset of the methods. The results are shown in Figures 4.1 & 4.2. We can see that Finito (perm) performs the best on a per epoch equivalent basis, but it can be the most expensive method per step. We have observed that Finito (perm) has the advantage in general on problems where strong regularisation is used. SVRG is similarly fast on a per epoch basis, but when considering the number of gradient evaluations per epoch is double that of the other methods for this problem, it is middle of the pack. SAGA can be seen to perform similar to the non-permuted Finito case, and to SDCA. Note that SAG is slower than the other methods at the beginning. To get the optimal results for SAG, an adaptive step size rule needs to be used rather than the constant step size we used.

In general, these tests confirm that the choice of methods should be done based on their properties as discussed in Section 4.3, rather than small constant factors in their convergence rates.

4.6 SAGA Theory

In this section, all expectations are taken with respect to the choice of j at iteration $k+1$ and conditioned on x^k and each $f_i'(\phi_i^k)$ unless stated otherwise. The main results are in Theorems 4.6 (strongly convex case) and 4.8.

We start with Corollaries of standard convexity results.

Corollary 4.1. *We can apply Theorem A.14 to our finite sum structure (using $y \leftarrow x$ and $x \leftarrow x^*$), where each f_i is μ-strongly convex and is Lipschitz smooth with constant L. We get that for all x and x^*:*

$$\begin{aligned}\left\langle f'(x), x^* - x \right\rangle \quad \leq \quad & \frac{L-\mu}{L}\left[f(x^*) - f(x)\right] - \frac{\mu}{2}\left\|x^* - x\right\|^2 \\ & -\frac{1}{2Ln}\sum_i \left\|f_i'(x^*) - f_i'(x)\right\|^2 - \frac{\mu}{L}\left\langle f'(x^*), x - x^*\right\rangle.\end{aligned}$$

Corollary 4.2. *By applying Theorem A.8:*

$$f(y) \geq f(x) + \left\langle f'(x), y - x\right\rangle + \frac{1}{2L}\left\|f'(x) - f'(y)\right\|^2$$

with $y \leftarrow \phi_i$ and $x \leftarrow x^*$, for each f_i and summing, we have that for all ϕ_i and x^*:

$$\frac{1}{n}\sum_i \left\|f_i'(\phi_i) - f_i'(x^*)\right\|^2 \leq 2L\left[\frac{1}{n}\sum_i f_i(\phi_i) - f(x^*) - \frac{1}{n}\sum_i \left\langle f_i'(x^*), \phi_i - x^*\right\rangle\right].$$

Lemma 4.3. *It holds that for any ϕ_i,x^* and $\beta > 0$, with w^{k+1} and x^k as defined in Equation 4.1:*

$$\begin{aligned}\mathbb{E}\left\|w^{k+1} - x^k - \gamma f'(x^*)\right\|^2 \;&\leq\; \gamma^2\left(1+\beta^{-1}\right)\mathbb{E}\left\|f_j'(\phi_j^k) - f_j'(x^*)\right\|^2 \\ &+\; \gamma^2(1+\beta)\,\mathbb{E}\left\|f_j'(x^k) - f_j'(x^*)\right\|^2 - \gamma^2\beta\left\|f'(x^k) - f'(x^*)\right\|^2.\end{aligned}$$

Proof. We follow a similar argument as occurs in the SVRG proof (Johnson and Zhang, 2013) for this term, but with a tighter argument. The tightening comes from using $\|x+y\|^2 \leq (1+\beta^{-1})\|x\|^2 + (1+\beta)\|y\|^2$ instead of the simpler $\beta = 1$ case they use. The other key trick is the use of the standard variance decomposition $\mathbb{E}[\|X - \mathbb{E}[X]\|^2] = \mathbb{E}[\|X\|^2] - \|\mathbb{E}[X]\|^2$ three times.

$$\begin{aligned}&\mathbb{E}\left\|w^{k+1} - x^k + \gamma f'(x^*)\right\|^2 \\ =&\mathbb{E}\Bigg\|\underbrace{-\frac{\gamma}{n}\sum_i f_i'(\phi_i^k) + \gamma f'(x^*) + \gamma\left[f_j'(\phi_j^k) - f_j'(x^k)\right]}_{:=\gamma X}\Bigg\|^2 \\ =&\gamma^2\mathbb{E}\Bigg\|\overbrace{\left[f_j'(\phi_j^k) - f_j'(x^*) - \frac{1}{n}\sum_i f_i'(\phi_i^k) + f'(x^*)\right] - \left[f_j'(x^k) - f_j'(x^*)\right]}^{X} - \overbrace{\left[f'(x^k) + f'(x^*)\right]}^{\mathbb{E}[X]}\Bigg\|^2 \\ &+\gamma^2\left\|\overbrace{f'(x^k) - f'(x^*)}^{\mathbb{E}[X]}\right\|^2 \\ \leq&\gamma^2(1+\beta^{-1})\mathbb{E}\left\|f_j'(\phi_j^k) - f_j'(x^*) - \frac{1}{n}\sum_i f_i'(\phi_i) + f'(x^*)\right\|^2 \\ &+\gamma^2(1+\beta)\mathbb{E}\left\|f_j'(x^k) - f_j'(x^*) - f'(x^k) + f'(x^*)\right\|^2 + \gamma^2\left\|f'(x^k) - f'(x^*)\right\|^2 \\ &\qquad\text{(use variance decomposition twice more):} \\ \leq&\gamma^2(1+\beta^{-1})\mathbb{E}\left\|f_j'(\phi_j^k) - f_j'(x^*)\right\|^2 + \gamma^2(1+\beta)\mathbb{E}\left\|f_j'(x^k) - f_j'(x^*)\right\|^2 \\ &-\gamma^2\beta\left\|f'(x^k) - f'(x^*)\right\|^2.\end{aligned}$$

□

Lemma 4.4. *Define $\Delta = -\frac{1}{\gamma}\left(w^{k+1} - x^k\right) - f'(x^k)$, the difference between our approxima-*

tion to the gradient at x and true gradient. Then using the SAGA step:

$$\mathbb{E}\left\|x^{k+1}-x^*\right\|^2 \leq \left\|x^k-x^*\right\|^2 - 2\gamma\mathbb{E}\left[F(x^{k+1})-F(x^*)\right] + 2\gamma^2\mathbb{E}\left\|\Delta\right\|^2.$$

Proof. This Lemma's proof is based on a similar Lemma 3 for SVRG (2nd eq. on p.11 Xiao and Zhang, 2014). The optimality condition of the proximal operator:

$$z = \text{prox}^h_{1/\gamma}(y) := \text{argmin}_{x\in\mathbb{R}^d}\left\{h(x) + \frac{1}{2\gamma}\|x-y\|^2\right\}$$

implies that there exists a subgradient ξ of h at z such that:

$$\frac{1}{\gamma}(z-y)+\xi = 0.$$

Applying this to our setting, where $x^{k+1} = \text{prox}^h_{1/\gamma}\left(w^{k+1}\right)$, and

$$w^{k+1} = x^k - \gamma\left(f'(x^k)+\Delta\right),$$

we have ξ as a subgradient of h at x^{k+1}. Now we proceed to lower bound $F(x^*) = f(x^*)+h(x^*)$, by treating the two parts separately. Firstly the regulariser about x^{k+1}, using the subgradient of h defined above:

$$h(x^*) \geq h(x^{k+1}) + \left\langle \xi, x^*-x^{k+1}\right\rangle. \tag{4.6}$$

Next the loss about x^k:

$$f(x^*) \geq f(x^k) + \left\langle f'(x^k), x^*-x^k\right\rangle. \tag{4.7}$$

We want x^{k+1} on the right, so we further lower bound around x^{k+1} by using the negated Lipschitz smoothness upper bound (Theorem A.5):

$$f(x^k) \geq f(x^{k+1}) - \left\langle f'(x^k), x^{k+1}-x^k\right\rangle - \frac{L}{2}\left\|x^{k+1}-x^k\right\|^2. \tag{4.8}$$

Combining Equation 4.6 with 4.7 and 4.8 gives:

$$\begin{aligned}
F(x^*) &\geq f(x^{k+1}) + h(x^{k+1}) - \left\langle f'(x^k), x^{k+1}-x\right\rangle - \frac{L}{2}\left\|x^{k+1}-x^k\right\|^2 \\
&\quad + \left\langle f'(x^k), x^*-x^k\right\rangle + \left\langle \xi, x^*-x^{k+1}\right\rangle \\
&= F(x^{k+1}) - \left\langle f'(x^k), x^{k+1}-x^k-x^*+x^k\right\rangle - \frac{L}{2}\left\|x^{k+1}-x^k\right\|^2 - \left\langle \xi, x^{k+1}-x^*\right\rangle \\
&= F(x^{k+1}) - \left\langle f'(x^k), x^{k+1}-x^*\right\rangle - \frac{L}{2}\left\|x^{k+1}-x^k\right\|^2 - \left\langle \xi, x^{k+1}-x^*\right\rangle.
\end{aligned}$$

Now we do some careful manipulation of the two inner product terms, using the

optimality condition

$$\begin{aligned}\xi &= \frac{1}{\gamma}(w^{k+1} - x^{k+1}) \\ &= \frac{1}{\gamma}(x^k - \gamma\left(f'(x^k) + \Delta\right) - x^{k+1}) \\ &= \frac{1}{\gamma}(x^k - x^{k+1}) - \left(f'(x^k) + \Delta\right),\end{aligned}$$

to simplify:

$$\begin{aligned}&= -\left\langle f'(x^k), x^{k+1} - x^* \right\rangle - \left\langle \xi, x^{k+1} - x^* \right\rangle \\ &\quad -\left\langle f'(x^k) + \xi, x^{k+1} - x^* \right\rangle \\ &= -\left\langle f'(x^k) + \frac{1}{\gamma}(x^k - x^{k+1}) - \left(f'(x^k) + \Delta\right), x^{k+1} - x^* \right\rangle\end{aligned}$$

$$\begin{aligned}&= -\frac{1}{\gamma}\left\langle x^k - x^{k+1}, x^{k+1} - x^* \right\rangle + \left\langle \Delta, x^{k+1} - x^* \right\rangle \\ &= -\frac{1}{\gamma}\left\langle x^k - x^{k+1}, x^{k+1} - x^k + x^k - x^* \right\rangle + \left\langle \Delta, x^{k+1} - x^* \right\rangle \\ &= \frac{1}{\gamma}\left\| x^{k+1} - x^k \right\|^2 - \frac{1}{\gamma}\left\langle x^k - x^{k+1}, x^k - x^* \right\rangle + \left\langle \Delta, x^{k+1} - x^* \right\rangle.\end{aligned}$$

So we have using $\frac{1}{\gamma} \geq L$:

$$F(x^*) \geq F(x^{k+1}) + \frac{1}{\gamma}\left\langle x^{k+1} - x^k, x^k - x^* \right\rangle + \left\langle \Delta, x^{k+1} - x^* \right\rangle + \frac{1}{2\gamma}\left\| x^{k+1} - x^k \right\|^2. \tag{4.9}$$

Now using:

$$\begin{aligned}\left\| x^{k+1} - x^* \right\|^2 &= \left\| x^{k+1} - x^k + x^k - x^* \right\|^2 \\ &= \left\| x^{k+1} - x^k \right\|^2 + 2\left\langle x^{k+1} - x^k, x^k - x^* \right\rangle + \left\| x^k - x^* \right\|^2,\end{aligned}$$

we have:

$$F(x^*) \geq F(x^{k+1}) + \frac{1}{2\gamma}\left\| x^{k+1} - x^* \right\|^2 - \frac{1}{2\gamma}\left\| x^k - x^* \right\|^2 + \left\langle \Delta, x^{k+1} - x^* \right\rangle.$$

Now we just need to bound the $\langle \Delta, x^{k+1} - x^* \rangle$ term. We do this by introducing a new point y^{k+1} which is the result of a non-stochastic proximal gradient step from x^k:

$$y^{k+1} = \text{prox}^h_{1/\gamma}\left(x^k - \gamma f'(x^k)\right).$$

So to lower bound $\langle \Delta, x^{k+1} - x^* \rangle$ we will look at upper bounding it's negation. We start by adding and subtracting y^{k+1}, then we apply Cauchy-Schwarz:

$$\begin{aligned} -\left\langle \Delta, x^{k+1} - x^* \right\rangle &= -\left\langle \Delta, x^{k+1} - y^{k+1} \right\rangle - \left\langle \Delta, y^{k+1} - x^* \right\rangle \\ &= -\left\langle \Delta, x^{k+1} - y^{k+1} \right\rangle - \left\langle \Delta, y^{k+1} - x^* \right\rangle \\ &\leq \|\Delta\| \left\| x^{k+1} - y^{k+1} \right\| - \left\langle \Delta, y^{k+1} - x^* \right\rangle \end{aligned}$$

Now note that the term $\langle \Delta, y^{k+1} - x^* \rangle$ has expectation zero as the right hand side is independent of the j choice, and $\mathbb{E}[\Delta] = 0$. We next apply non-expansivity of the proximal operator for $x^{k+1} - y^{k+1}$, and plug in the definitions of w^{k+1} in terms of Δ:

$$\begin{aligned} \|\Delta\| \left\| x^{k+1} - y^{k+1} \right\| &\leq \|\Delta\| \left\| w^{k+1} - x^k + \gamma f'(x^k) \right\| \\ &= \|\Delta\| \left\| x^k - \gamma \left(f'(x^k) + \Delta \right) - x^k + \gamma f'(x^k) \right\| \\ &= \|\Delta\| \left\| -\gamma (\Delta) \right\| \\ &= \gamma \|\Delta\|^2 \end{aligned}$$

Plugging this back into Equation 4.9 gives a scaling of the result:

$$F(x^*) \geq \mathbb{E}\left[F(x^{k+1}) \right] + \frac{1}{2\gamma} \mathbb{E} \left\| x^{k+1} - x^* \right\|^2 - \frac{1}{2\gamma} \left\| x^k - x^* \right\|^2 - \gamma \mathbb{E} \|\Delta\|^2 .$$

Multiplying through by 2γ and rearranging gives the result. □

Lemma 4.5. *We will also need to use a simple modification of Lemma 4.3 to bound Δ as defined in Lemma 4.4 directly above:*

$$\mathbb{E} \|\Delta\|^2 \leq \left(1 + \beta^{-1} \right) \mathbb{E} \left\| f_j'(\phi_j^k) + f_j'(x^*) \right\|^2 + (1 + \beta) \mathbb{E} \left\| f_j'(x^k) - f_j'(x^*) \right\|^2 .$$

Proof. We first expand and group terms:

$$\begin{aligned} &= \mathbb{E} \|\Delta\|^2 \\ &= \mathbb{E} \left\| \frac{1}{\gamma} \left(w^{k+1} - x^k \right) + f'(x^k) \right\|^2 \\ &= \mathbb{E} \left\| - \left[f_j'(\phi_j^{k+1}) - f_j'(\phi_j^k) + \frac{1}{n} \sum_{i=1}^n f_i'(\phi_i^k) \right] + f'(x^k) \right\|^2 \\ &= \mathbb{E} \left\| - \left[f_j'(x^k) - f_j'(\phi_j^k) \right] + f'(x^k) - \frac{1}{n} \sum_{i=1}^n f_i'(\phi_i^k) \right\|^2 \\ &= \mathbb{E} \left\| \left[f_j'(x^k) - f_j'(\phi_j^k) \right] - \left[f'(x^k) - \frac{1}{n} \sum_{i=1}^n f_i'(\phi_i^k) \right] \right\|^2 . \end{aligned}$$

Now let $X = f_j'(x^k) - f_j'(\phi_j^k)$. Note that $E[X] = f'(x^k) - \frac{1}{n}\sum_{i=1}^n f_i'(\phi_i^k)$, which is the other term, so we have $\mathbb{E}\left\|\Delta\right\|^2 = \mathbb{E}\left\|X - E[X]\right\|^2$. Applying decomposition of variance, $\mathbb{E}[\|X - \mathbb{E}[X]\|^2] = \mathbb{E}[\|X\|^2] - \|\mathbb{E}[X]\|^2$. We drop the 2nd term $-\|\mathbb{E}[X]\|^2$ since we want an upper bound:

$$\mathbb{E}\left\|\Delta\right\|^2 \leq \mathbb{E}\left\|f_j'(x^k) - f_j'(\phi_j^k)\right\|^2.$$

Now add and subtract $f_j'(x^*)$:

$$\begin{aligned}\mathbb{E}\left\|\Delta\right\|^2 &\leq \mathbb{E}\left\|f_j'(x^k) - f_j'(x^*) - \left[f_j'(\phi_j^k) + f_j'(x^*)\right]\right\|^2 \\ &\leq \left(1+\beta^{-1}\right)\mathbb{E}\left\|f_j'(\phi_j^k) + f_j'(x^*)\right\|^2 + (1+\beta)\mathbb{E}\left\|f_j'(x^k) - f_j'(x^*)\right\|^2.\end{aligned}$$

□

4.6.1 Linear convergence for strongly convex problems

Theorem 4.6. *With x^* the optimal solution, we define the Lyapunov function:*

$$T^k = \frac{1}{n}\sum_i f_i(\phi_i^k) - f(x^*) - \frac{1}{n}\sum_i \left\langle f_i'(x^*), \phi_i^k - x^*\right\rangle + c\left\|x^k - x^*\right\|^2.$$

with $c = \frac{1}{2\gamma(1-\gamma\mu)n}$. It is implicitly a function of x^k and each ϕ_i^k. Then under the SAGA algorithm it holds that:

$$\mathbb{E}[T^{k+1}] \leq (1 - \frac{1}{\kappa})T^k,$$

where $\frac{1}{\kappa} = \gamma\mu = \frac{\mu}{2(\mu n + L)}$ for step size $\gamma = \frac{1}{2(\mu n+L)}$ and $\frac{1}{\kappa} = \min\left\{\frac{1}{4n}, \frac{\mu}{3L}\right\}$ for step size $\gamma = \frac{1}{3L}$.

Proof. The first three terms in T^{k+1} are straightforward to simplify:

$$\begin{aligned}\mathbb{E}\left[\frac{1}{n}\sum_i f_i(\phi_i^{k+1})\right] &= \frac{1}{n}f(x^k) + \left(1 - \frac{1}{n}\right)\frac{1}{n}\sum_i f_i(\phi_i^k). \\ \mathbb{E}\left[-\frac{1}{n}\sum_i \left\langle f_i'(x^*), \phi_i^{k+1} - x^*\right\rangle\right] &= -\frac{1}{n}\left\langle f'(x^*), x^k - x^*\right\rangle \\ &\quad - \left(1 - \frac{1}{n}\right)\frac{1}{n}\sum_i \left\langle f_i'(x^*), \phi_i^k - x^*\right\rangle.\end{aligned}$$

For the change in the last term of T we apply the non-expansiveness of the proximal operator. Note that this is the only place in the proof where we use the fact that x^* is an optimality point.

$$\begin{aligned} c\left\|x^{k+1}-x^*\right\|^2 &= c\left\|\mathrm{prox}_{1/\gamma}(w^{k+1})-\mathrm{prox}_{1/\gamma}(x^*-\gamma f'(x^*))\right\|^2 \\ &\leq c\left\|w^{k+1}-x^*+\gamma f'(x^*)\right\|^2. \end{aligned}$$

Then we expand the quadratic and apply $\mathbb{E}[w^{k+1}] = x^k - \gamma f'(x^k)$ to simplify the inner product term:

$$\begin{aligned} & c\mathbb{E}\left\|w^{k+1}-x^*+\gamma f'(x^*)\right\|^2 \\ =& c\mathbb{E}\left\|x^k-x^*+w^{k+1}-x^k+\gamma f'(x^*)\right\|^2 \\ =& c\left\|x^k-x^*\right\|^2+2c\mathbb{E}\left[\left\langle w^{k+1}-x^k+\gamma f'(x^*),x^k-x^*\right\rangle\right]+c\mathbb{E}\left\|w^{k+1}-x^k+\gamma f'(x^*)\right\|^2 \\ =& c\left\|x^k-x^*\right\|^2-2c\gamma\left\langle f'(x^k)-f'(x^*),x^k-x^*\right\rangle+c\mathbb{E}\left\|w^{k+1}-x^k+\gamma f'(x^*)\right\|^2 \end{aligned}$$

We now apply Lemma 4.3 to bound the error term $c\mathbb{E}\left\|w^{k+1}-x^k+\gamma f'(x^*)\right\|^2$, giving:

$$\begin{aligned} & c\mathbb{E}\left\|x^{k+1}-x^*\right\|^2 \\ \leq\ & c\left\|x^k-x^*\right\|^2-c\gamma^2\beta\left\|f'(x^k)-f'(x^*)\right\|^2 \\ & -2c\gamma\left\langle f'(x^k),x^k-x^*\right\rangle+2c\gamma\left\langle f'(x^*),x^k-x^*\right\rangle \\ & +\left(1+\beta^{-1}\right)c\gamma^2\mathbb{E}\left\|f_j'(\phi_j^k)-f_j'(x^*)\right\|^2+(1+\beta)\,c\gamma^2\mathbb{E}\left\|f_j'(x^k)-f_j'(x^*)\right\|^2. \end{aligned}$$

The value of β shall be fixed later. Now we bound $-2c\gamma\left\langle f'(x),x-x^*\right\rangle$ with Corollary 4.1 and then apply Corollary 4.2 to bound $\mathbb{E}\left\|f_j'(\phi_j)-f_j'(x^*)\right\|^2$:

$$\begin{aligned} c\mathbb{E}\left\|x^{k+1}-x^*\right\|^2 \leq{}& (c-c\gamma\mu)\left\|x^k-x^*\right\|^2 \\ & +\left((1+\beta)c\gamma^2-\frac{c\gamma}{L}\right)\mathbb{E}\left\|f_j'(x^k)-f_j'(x^*)\right\|^2-c\gamma^2\beta\left\|f'(x^k)-f'(x^*)\right\|^2 \\ & -\frac{2c\gamma(L-\mu)}{L}\left[f(x^k)-f(x^*)-\left\langle f'(x^*),x^k-x^*\right\rangle\right] \\ & +2\left(1+\beta^{-1}\right)c\gamma^2L\left[\frac{1}{n}\sum_i f_i(\phi_i)-f(x^*)-\frac{1}{n}\sum_i\left\langle f_i'(x^*),\phi_i-x^*\right\rangle\right]. \end{aligned}$$

We can now combine the bounds we have derived for each term in T, and pull out a fraction $\frac{1}{\kappa}$ of T^k (for any κ at this point). Together with the inequality from Theorem

A.6:

$$-\left\|f'(x)-f'(x^*)\right\|^2 \leq -2\mu\left[f(x)-f(x^*)-\left\langle f'(x^*), x-x^*\right\rangle\right],$$

that yields:

$$\begin{aligned}\mathbb{E}[T^{k+1}]-T^k \leq & -\frac{1}{\kappa}T^k+\left(\frac{1}{n}-\frac{2c\gamma(L-\mu)}{L}-2c\gamma^2\mu\beta\right)\left[f(x^k)-f(x^*)-\left\langle f'(x^*), x^k-x^*\right\rangle\right] \\ & +\left(\frac{1}{\kappa}+2(1+\beta^{-1})c\gamma^2L-\frac{1}{n}\right)\left[\frac{1}{n}\sum_i f_i(\phi_i^k)-f(x^*)-\frac{1}{n}\sum_i\left\langle f_i'(x^*), \phi_i^k-x^*\right\rangle\right] \\ & +\left(\frac{1}{\kappa}-\gamma\mu\right)c\left\|x^k-x^*\right\|^2+\left((1+\beta)\gamma-\frac{1}{L}\right)c\gamma\mathbb{E}\left\|f_j'(x^k)-f_j'(x^*)\right\|^2.\end{aligned} \tag{4.10}$$

Note that each of the terms in square brackets are positive. In Section 4.8 we verify that for the step size $\gamma=\frac{1}{2(\mu n+L)}$, the constants $c=\frac{1}{2\gamma(1-\gamma\mu)n}$, and $\kappa=\frac{1}{\gamma\mu}$ together with $\beta=\frac{2\mu n+L}{L}$ ensure that each of the quantities in the round brackets are non-positive. Likewise in Section 4.8.2 we show that for the step size $\gamma=\frac{1}{3L}$, the same $c=\frac{1}{2\gamma(1-\gamma\mu)n}$ as above can be used with $\beta=2$ and $\frac{1}{\kappa}=\min\left\{\frac{1}{4n},\frac{\mu}{3L}\right\}$ to ensure non-positive terms. □

Theorem 4.7. *For step size $\gamma=\frac{1}{2(\mu n+L)}$ it holds that:*

$$\mathbb{E}\left[\left\|x^k-x^*\right\|^2\right] \leq \left(1-\frac{\mu}{2(\mu n+L)}\right)^k\left[\left\|x^0-x^*\right\|^2+\frac{n}{\mu n+L}\left[f(x^0)-\left\langle f'(x^*), x^0-x^*\right\rangle-f(x^*)\right]\right],$$

and for step size $\gamma=\frac{1}{3L}$ it holds that:

$$\mathbb{E}\left\|x^k-x^*\right\|^2 \leq \left(1-\min\left\{\frac{1}{4n},\frac{\mu}{3L}\right\}\right)^k\left[\left\|x^0-x^*\right\|^2+\frac{2n}{3L}\left[f(x^0)-\left\langle f'(x^*), x^0-x^*\right\rangle-f(x^*)\right]\right].$$

Here the expectation is over all choices of index j^k up to step k.

Proof. In both cases we have from Theorem 4.6 directly above that:

$$\mathbb{E}[T^{k+1}] \leq (1-\frac{1}{\kappa})T^k,$$

where the expectation is with respect to choices made at step $k+1$, conditioning on the x^k and ϕ^k values from step k. We now take expectation with respect to those quantities also, giving:

$$\mathbb{E}[T^{k+1}] \leq (1-\frac{1}{\kappa})\mathbb{E}[T^k].$$

Now we may chain this inequality over k:

$$\begin{aligned}\mathbb{E}[T^k] &\leq (1-\frac{1}{\kappa})\mathbb{E}[T^{k-1}] \\ &\leq (1-\frac{1}{\kappa})^2\mathbb{E}[T^{k-2}] \\ &\cdots \\ &\leq (1-\frac{1}{\kappa})^k T^0.\end{aligned}$$

Now looking at the definition of T^k:

$$\begin{aligned}T^k &= \frac{1}{n}\sum_i f_i(\phi_i^k) - f(x^*) - \frac{1}{n}\sum_i \left\langle f_i'(x^{k*}), \phi_i^k - x^* \right\rangle + c\left\|x^k - x^*\right\|^2 \\ &\geq c\left\|x^k - x^*\right\|^2.\end{aligned}$$

So:

$$c\left\|x^k - x^*\right\|^2 \leq (1-\frac{1}{\kappa})^k T^0.$$

Now for the two step size cases, we simplify plug in the explicit constant values for c and κ, and divide the whole expression through by c. □

4.6.2 $1/k$ convergence for non-strongly convex problems

Theorem 4.8. *When each f_i is Lipschitz smooth with constant L and convex, using $\gamma = 1/3L$, we have for $\bar{x}^k = \frac{1}{k}\sum_{t=1}^k x^t$ that:*

$$\mathbb{E}\left[F(\bar{x}^k)\right] - F(x^*) \leq \frac{10n}{k}\left[\frac{2L}{n}\left\|x^0 - x^*\right\|^2 + f(x^0) - \left\langle f'(x^*), x^0 - x^*\right\rangle - f(x^*)\right].$$

Here the expectation is over all choices of index j^k up to step k.

Proof. We proceed by using a similar argument as in Theorem 4.6, but with an additional $\alpha\left\|x - x^*\right\|^2$ together with the existing $c\left\|x - x^*\right\|^2$ term in the Lyapunov function. I.e.

$$T = \frac{1}{n}\sum_i f_i(\phi_i^k) - f(x^*) - \frac{1}{n}\sum_i \left\langle f_i'(x^*), \phi_i^k - x^*\right\rangle + (c+\alpha)\left\|x^k - x^*\right\|^2.$$

We will bound $\alpha \left\|x^k - x^*\right\|^2$ in a different manner to $c \left\|x^k - x^*\right\|^2$. Instead of use the non-expansiveness property, we apply Lemma 4.4 scaled by α, using $\Delta = -\frac{1}{\gamma}\left(w^{k+1} - x^k\right) - f'(x^k)$ as defined in that lemma:

$$\alpha \mathbb{E}\left\|x^{k+1} - x^*\right\|^2 \leq \alpha \left\|x^k - x^*\right\|^2 - 2\alpha\gamma \mathbb{E}\left[F(x^{k+1}) - F(x^*)\right] + 2\alpha\gamma^2 \mathbb{E}\left\|\Delta\right\|^2.$$

Recall the bound on Δ from Lemma 4.5:

$$\mathbb{E}\left\|\Delta\right\|^2 \leq \left(1 + \beta^{-1}\right) \mathbb{E}\left\|f_j'(\phi_j^k) - f_j'(x^*)\right\|^2 + (1+\beta)\,\mathbb{E}\left\|f_j'(x^k) - f_j'(x^*)\right\|^2,$$

applying this gives

$$\begin{aligned}
\alpha \mathbb{E}\left\|x^{k+1} - x^*\right\|^2 \quad \leq \quad & \alpha \left\|x - x^*\right\|^2 - 2\alpha\gamma \mathbb{E}\left[F(x^{k+1}) - F(x^*)\right] \\
& + 2(1 + \beta^{-1})\alpha\gamma^2 \mathbb{E}\left\|f_j'(\phi_j^k) - f_j'(x^*)\right\|^2 \\
& + 2\left(1+\beta\right)\alpha\gamma^2 \mathbb{E}\left\|f_j'(x^k) - f_j'(x^*)\right\|^2.
\end{aligned}$$

now combining with the rest of the Lyapunov function change from Equation 4.10, using $\mu = 0$ and bounding $\mathbb{E}\left\|f_j'(\phi_j^k) - f_j'(x^*)\right\|^2$ with Corollary 4.2:

$$\begin{aligned}
& \mathbb{E}[T^{k+1}] - T^k \\
\leq \quad & \left(\frac{1}{n} - 2c\gamma\right)\left[f(x^k) - f(x^*) - \left\langle f'(x^*), x^k - x^*\right\rangle\right] - 2\alpha\gamma \mathbb{E}\left[F(x^{k+1}) - F(x^*)\right] \\
& + \left(4(1+\beta^{-1})\alpha L\gamma^2 + 2(1+\beta^{-1})cL\gamma^2 - \frac{1}{n}\right)\left[\frac{1}{n}\sum_i f_i(\phi_i^k) - f(x^*)\right. \\
& \left. - \frac{1}{n}\sum_i \left\langle f_i'(x^*), \phi_i^k - x^*\right\rangle\right] \\
& + \left((1+\beta)c\gamma + 2(1+\beta)\alpha\gamma - \frac{c}{L}\right)\gamma \mathbb{E}\left\|f_j'(x^k) - f_j'(x^*)\right\|^2.
\end{aligned}$$

If we take $\gamma = 1/3L$, $c = \frac{3L}{2n}$ and $\alpha = \frac{3L}{20n}$ and $\beta = \frac{3}{2}$ (See Section 4.8.3), then we are left with

$$\mathbb{E}[T^{k+1}] - T^k \leq -\frac{1}{10n}\mathbb{E}\left[F(x^{k+1}) - F(x^*)\right]. \tag{4.11}$$

These expectations are conditional on information from step k. We now take the expectation with respect to all previous steps, yielding

$$\mathbb{E}[T^{k+1}] - \mathbb{E}[T^k] \quad \leq \quad -\frac{1}{10n}\mathbb{E}\left[F(x^{k+1}) - F(x^*)\right],$$

where all expectations are unconditional. We want to sum Equation 4.11 from 0 to $k-1$. For the left hand side this results in telescoping of the T terms:

$$\begin{aligned}\sum_{t=0}^{k-1}\Big[\mathbb{E}[T^{t+1}]-\mathbb{E}[T^t]\Big] &= \mathbb{E}[T^k]-\mathbb{E}[T^{k-1}]+\mathbb{E}[T^{k-1}]-\mathbb{E}[T^{k-2}]+\cdots-\mathbb{E}[T^0]\\ &= \mathbb{E}[T^k]-\mathbb{E}[T^0],\end{aligned}$$

For the right hand side we simply get $-\frac{1}{10n}\mathbb{E}\left[\sum_{t=0}^{k-1}\left[F(x^{t+1})-F(x^*)\right]\right]$. So it holds that:

$$\frac{1}{10n}\mathbb{E}\left[\sum_{t=1}^{k}\left[F(x^t)-F(x^*)\right]\right]\leq T^0-\mathbb{E}[T^k].$$

We can drop the $-\mathbb{E}\left[T^k\right]$ term since T^k is always positive. For the right hand side we apply Jensen's inequality to pull the summation inside of F:

$$\mathbb{E}\left[F(\frac{1}{k}\sum_{t=1}^{k}x^t)-F(x^*)\right]\leq\frac{1}{k}\mathbb{E}\left[\sum_{t=1}^{k}\left[F(x^t)-F(x^*)\right]\right].$$

Further multiplying through by $10n/k$ gives:

$$\mathbb{E}\left[F(\frac{1}{k}\sum_{t=1}^{k}x^t)-F(x^*)\right]\leq\frac{10n}{k}T^0.$$

Plugging in the T^0 expression and using the rough bound $c+\alpha\leq\frac{2L}{n}$ gives the result. □

Remark 4.9. The convergence rate in the non-strongly convex case is given in terms of the average iterate instead of the last iterate. This is a fairly common problem that arises in stochastic optimisation theory. In practice the last iterate is still a good choice for the method to return, despite the fact that it is not backed by the theory. Doing so allows the method to be identical in the strongly convex and non-strongly convex cases.

For a more theoretically sound approach, the SAGA algorithm can compute the full function value at $F(x^k)$ and at $F(\frac{1}{k}\sum_{t=1}^{k}x^t)$, and return the one that yields the lower function value.

4.7 Understanding the Convergence of the SVRG Method

Recall from Section 2.5 that SVRG has the following convergence rate in terms of the number of recalibrations $r=k/m$:

$$E[f(\tilde{x}^k) - f(x^*)] \leq \left(\frac{\eta}{\mu(1-4L/\eta)m} + \frac{4L(m+1)}{\eta(1-4L/\eta)m}\right)^r \left[f(\tilde{x}^0) - f(x^*)\right].$$

Our analysis of the SAGA method uses some of the same techniques as the SVRG analysis, so we would like to make a direct comparison of the convergence rates of the two methods. However, the complexity of the above expression makes the true convergence rate quite opaque. In this section we provide a convergence rate proof of the SVRG method that is tighter, and gives a rate directly relatable to the other fast incremental gradient methods. Unfortunately, we have to impose some assumptions on the behaviour of the iterates x^k in order to do so.

As discussed in Section 2.5, in a practical implementation of the SVRG method, it is assumed that

$$f(x^k) - f(x^*) \leq \frac{1}{m} \sum_{r=k-m}^{k} \left[f(x^r) - f(x^*)\right], \tag{4.12}$$

so that the last point x^k may be returned by the method. This is not directly supported by the theory, but empirically is overwhelmingly likely. We will encode a similar assumption directly into our theory, namely that

$$f(x^k) - f(x^*) \leq \frac{1}{\sum_{t=0}^{m-1} c_1^t} \sum_{t=0}^{m-1} c_1^t \left[f(x^{k-1-t}) - f(x^*)\right], \tag{4.13}$$

$$\text{where } c_1 = \left(1 - \frac{\mu}{\eta}\right).$$

Instead of the uniform weighting of Equation 4.12 we use a geometric weighting. In practice the weight of c_1^0 v.s. c_1^m will only a factor of 2 difference, so the practical difference between this geometric weighting and a uniform weighting is quite small.

Under this assumption, we establish in Theorem 4.10 a convergence rate of the form:

$$\mathbb{E}\left\|x^k - x^*\right\|^2 \leq \left(\max\left\{\frac{1}{2}, \left(1 - \frac{\mu}{4L}\right)^m\right\}\right)^{k/m} \left[\left\|x^0 - x^*\right\|^2 + \frac{c_4}{2L}\left[f(x^0) - f(x^*)\right]\right],$$

for some constant c^4. Recall that the recalibration pass is performed every m iterations. This rate tells us that we should set m so that $\left(1 - \frac{\mu}{4L}\right)^m = \frac{1}{2}$, as using a larger m will just lead to a slower convergence rate. If we use that value, we get a convergence rate of simply:

$$\mathbb{E}\left\|x^k - x^*\right\|^2 \leq \left(1 - \frac{\mu}{4L}\right)^k \left[\left\|x^0 - x^*\right\|^2 + \frac{c_4}{2L}\left[f(x^0) - f(x^*)\right]\right].$$

This is directly comparable to the slightly faster $1 - \frac{\mu}{3L}$ rate for SAGA outside the big-data regime. Note that the effective number of gradient calculations is larger for SVRG than SAGA as well, as during each recalibration pass it does n additional term-gradient evaluations. In cases where $m \gg n$, the efficiency of the methods is broadly comparable.

Theorem 4.10. *We define the following Lyapunov function at the rth recalibration:*

$$T^r = \mathbb{E}\left\|\tilde{x}^r - x^*\right\|^2 + \frac{c_4}{2L}\left[f(\tilde{x}^r) - f(x^*)\right].$$

Where $c_4 = \sum_{t=0}^{m} c_1^t$ with $c_1 = 1 - \frac{\mu}{\eta}$. Then between recalibrations r and $r+1$ when using step size $\eta = 4L$ and Assumption 4.13:

$$\mathbb{E}[T^{r+1}] \leq \max\left\{\frac{1}{2}, \left(1 - \frac{\mu}{4L}\right)^m\right\} T^r.$$

This expectation is conditioned on $\tilde{x}^r$.

Proof. Recall the SVRG step:

$$x^{k+1} = x^k - \frac{1}{\eta} f_j'(x^k) + \frac{1}{\eta}\left[f_j'(\tilde{x}^k) - g^k\right]$$

Define:

$$g_j(x) = f_j'(x) - f_j'(\tilde{x}) + \mathbb{E}[f_j'(\tilde{x})].$$

Now like in the regular SVRG proof as well as the SAGA proof, we start by expanding $\mathbb{E}\left\|x^{k+1} - x^*\right\|^2$.

$$\begin{aligned}
\mathbb{E}\left\|x^{k+1} - x^*\right\|^2 &= \mathbb{E}\left\|x - \frac{1}{\eta} g_j(x) - x^*\right\|^2 \\
&= \|x - x^*\|^2 - \frac{2}{\eta}\mathbb{E}\left\langle g_j(x), x - x^*\right\rangle + \frac{1}{\eta^2}\left\|g_j(x)\right\|^2 \\
&= \|x - x^*\|^2 - \frac{2}{\eta}\left\langle f'(x), x - x^*\right\rangle + \frac{1}{\eta^2}\left\|g_j(x)\right\|^2
\end{aligned}$$

Now we apply Corollary 4.1 giving:

$$\begin{aligned}
\mathbb{E}\left\|x^{k+1} - x^*\right\|^2 \leq\ & \left(1 - \frac{\mu}{\eta}\right)\|x - x^*\|^2 + \frac{1}{\eta^2}\mathbb{E}\left\|g_j(x)\right\|^2 \\
& \frac{2(L-\mu)}{\eta L}\left[f(x^*) - f(x)\right] - \frac{1}{L\eta}\mathbb{E}\left\|f_j'(x^*) - f_j'(x)\right\|^2.
\end{aligned}$$

Now we bound the gradient norm term $\left\|g_j(x)\right\|^2$, using a straightforward modification of Lemma 4.3 to apply to SVRG instead of SAGA:

$$\begin{aligned}\mathbb{E}\left\|g_j(x)\right\|^2 &\leq \left(1+\beta^{-1}\right)\mathbb{E}\left\|f_j'(\tilde{x})-f_j'(x^*)\right\|^2+(1+\beta)\,\mathbb{E}\left\|f_j'(x)-f_j'(x^*)\right\|^2\\ &\quad -\beta\left\|f'(x)\right\|^2.\end{aligned}$$

Giving:

$$\begin{aligned}\mathbb{E}\left\|x^{k+1}-x^*\right\|^2 &\leq \left(1-\frac{\mu}{\eta}\right)\|x-x^*\|^2-\frac{\beta}{\eta^2}\left\|f'(x)\right\|^2\\ &\quad +\frac{1+\beta^{-1}}{\eta^2}\mathbb{E}\left\|f_j'(\tilde{x})-f_j'(x^*)\right\|^2+\frac{1+\beta}{\eta^2}\mathbb{E}\left\|f_j'(x)-f_j'(x^*)\right\|^2\\ &\quad +\frac{2\left(L-\mu\right)}{\eta L}\left[f(x^*)-f(x)\right]-\frac{1}{L\eta}\mathbb{E}\left\|f_j'(x^*)-f_j'(x)\right\|^2.\end{aligned}$$

Next we apply the following three inequalities

$$-\left\|f'(x)\right\|^2\leq -2\mu\left[f(x)-f(x^*)\right]\text{ (Theorem A.6),}$$

$$\mathbb{E}\left\|f_j'(x)-f_j'(x^*)\right\|^2\leq 2L\left[f(x)-f(x^*)\right]\text{ (Theorem A.8),}$$

$$\text{and }\mathbb{E}\left\|f_j'(\tilde{x})-f_j'(x^*)\right\|^2\leq 2L\left[f(\tilde{x})-f(x^*)\right]\text{ (Corollary 4.2).}$$

Doing so gives:

$$\mathbb{E}\left\|x^{k+1}-x^*\right\|^2 \leq c_1\|x-x^*\|^2+c_2\left[f(\tilde{x})-f(x^*)\right]-c_3\left[f(x)-f(x^*)\right].$$

Where for convenience we have introduced the constants:

$$c_1=1-\frac{\mu}{\eta},$$

$$c_2=\frac{2L\left(1+\beta^{-1}\right)}{\eta^2},$$

$$c_3=\frac{2\left(L-\mu\right)}{\eta L}+\frac{2\mu\beta}{\eta^2}+\frac{2}{\eta}-\frac{2L\left(1+\beta\right)}{\eta^2}.$$

We want to use this equation recursively on the squared norm $\|x-x^*\|^2$, between recalibration steps $r+1$ and r. Note that $\tilde{x}^{r+1}=x^k$ and $\tilde{x}^r=x^{k-m}$. Doing the

substitution yields:

$$\mathbb{E}\left\|\tilde{x}^{r+1}-x^*\right\|^2 \leq c_1^m\left\|\tilde{x}^r-x^*\right\|^2+c_2\left(\sum_{t=0}^{m-1}c_1^t\right)\left[f(\tilde{x})-f(x^*)\right] -c_3\sum_{t=0}^{m-1}c_1^t\left[f(x^{k-1-t})-f(x^*)\right].$$

Now to simplify the notation further we define $c_4 := \sum_{t=0}^{m-1} c_1^t$. and use Assumption 4.13 in the form $c_4\mathbb{E}\left[f(\tilde{x}^{r+1})-f(x^*)\right] \leq \sum_{t=0}^{m-1} c_1^t\left[f(x^{k-1-t})-f(x^*)\right]$:

$$\mathbb{E}\left\|\tilde{x}^{r+1}-x^*\right\|^2+c_3c_4\mathbb{E}\left[f(\tilde{x}^{r+1})-f(x^*)\right] \leq c_1^m\left\|\tilde{x}^r-x^*\right\|^2+c_2c_4\left[f(\tilde{x})-f(x^*)\right].$$

Now we have two rates of descent to consider here. The squared norm terms have a decrease of $\left(1-\frac{\mu}{\eta}\right)^m$ and the function values descent by c_2/c_3. Our Lyapunov function decrease is going to be the worst of the two. We can now plug in the step size $\eta = 4L$ and use $\beta = 1$:

$$c_2 = \frac{2L\left(1+\beta^{-1}\right)}{\eta^2} = \frac{1}{4L}.$$

Then:

$$\begin{aligned} c_3 &= \frac{2(L-\mu)}{\eta L}+\frac{2\mu\beta}{\eta^2}+\frac{2}{\eta}-\frac{2L(1+\beta)}{\eta^2} \\ &= \frac{2(L-\mu)}{4L^2}+\frac{2\mu}{16L^2}+\frac{2}{4L}-\frac{4}{16L} \\ &= \frac{(L-\mu)}{2L^2}+\frac{\mu}{8L^2}+\frac{1}{2L}-\frac{1}{4L} \\ &= \frac{1}{2L}-\frac{\mu}{2L^2}+\frac{\mu}{8L^2}+\frac{1}{4L} \\ &\geq \frac{1}{2L}. \end{aligned}$$

So we have $c_2/c_3 \leq \frac{1}{2}$, giving a per recalibration reduction of $\max\left\{\frac{1}{2}, \left(1-\frac{\mu}{4L}\right)^m\right\}$. □

4.8 Verifying SAGA Constants

This section covers the somewhat laborious task of checking the constants work out in the SAGA proofs. For each step size, constants need to be found so that the following constraints hold:

$$c_1 = \frac{1}{n}-\frac{2c\gamma(L-\mu)}{L}-2c\gamma^2\mu\beta \leq 0,$$

$$c_2 = \frac{1}{\kappa} + 2(1+\beta^{-1})c\gamma^2 L - \frac{1}{n} \leq 0,$$

$$c_3 = \frac{c}{\kappa} - \gamma\mu c \leq 0,$$
$$c_4 = (1+\beta)c\gamma^2 - \frac{c\gamma}{L} \leq 0.$$

4.8.1 Strongly convex step size $\gamma = 1/2(\mu n + L)$

We proceed by determining the values for the each of the constants that ensure c_1, c_3 and c_4 are exactly equal to 0. We then verify that those constants leave c_2 as negative. Some experimentation suggests this approach provides the best constants. If we look at the constraints in the order c_4,c_1,c_3 then c_2 , each constrain restricts a single variable to a particular value, assuming we want the first tree constraints to be equalities. There is then very little looseness in the resulting c_2 constrain, suggesting we are near optimal values for the constants.

First consider c_4. Under the assumed $\gamma = 1/2(\mu n + L)$ value:

$$(1+\beta)\gamma^2 - \frac{\gamma}{L} = 0,$$

$$\therefore (1+\beta) = \frac{1}{\gamma L},$$

$$\begin{aligned} \therefore \beta &= \frac{1}{\gamma L} - 1 \\ &= \frac{2(\mu n + L)}{L} - \frac{L}{L} \\ &= \frac{2\mu n + L}{L}. \end{aligned}$$

So that locks in the value of β. Next consider c_1. Given β and γ, we can determine the constant c from c_1:

$$c_1 = \frac{1}{n} - \frac{2c(L-\mu)\gamma}{L} - 2c\mu\beta\gamma^2 = 0.$$

$$\begin{aligned} \therefore \frac{L}{2\gamma n} &= c\left((L-\mu) + \mu\gamma(2\mu n + L)\right) \\ &= c\left((L-\mu) + 2\mu\gamma(\mu n + L) - \mu\gamma L\right) \\ & \quad c\left((L-\mu) + \mu - \mu\gamma L\right) \\ &= cL\left(1 - \mu\gamma\right). \end{aligned}$$

Rearranging in terms of c :

$$\begin{aligned} c &= \frac{1}{2n\gamma} / \left(1-\mu\gamma\right) \\ &= \frac{1}{2\gamma\left(1-\gamma\mu\right)n}. \end{aligned}$$

Now to determine κ we take $c_3 = 0$:

$$c_3 = \frac{c}{\kappa} - \frac{\mu c}{n} = 0,$$

$$\therefore \frac{1}{\kappa} = \mu\gamma.$$

Now for c_2, we first calculate the value of $1+\beta^{-1}$:

$$1+\beta^{-1} = 1 + \frac{L}{2\mu n + L} = \frac{2\mu n + 2L}{2\mu n + L} = \frac{1}{\gamma\left(2\mu n + L\right)}.$$

Plugging this into c_2:

$$\begin{aligned} c_2 &= \mu\gamma + 2(1+\beta^{-1})cL\gamma^2 - \frac{1}{n} \\ &= \mu\gamma + \frac{2(1+\beta^{-1})L\gamma^2}{2\gamma\left(1-\gamma\mu\right)n} - \frac{1}{n} \\ &= \mu\gamma + \frac{(1+\beta^{-1})L\gamma}{\left(1-\gamma\mu\right)n} - \frac{1}{n} \\ &= \mu\gamma + \frac{L\gamma}{\gamma\left(1-\gamma\mu\right)\left(2\mu n + L\right)n} - \frac{1}{n} \\ &= \mu\gamma + \frac{L}{n\left(1-\gamma\mu\right)\left(2\mu n + L\right)} - \frac{1}{n}. \end{aligned}$$

Now multiplying through by $n\left(1-\gamma\mu\right)\left(2\mu n + L\right)$ gives the right hand side:

$$\begin{aligned} & L + (\mu\gamma - \frac{1}{n})n\left(1-\gamma\mu\right)\left(2\mu n + L\right) \\ = \;& L + \left(\mu\gamma n - 1\right)\left(1-\gamma\mu\right)\left(2\mu n + L\right) \\ = \;& L + \mu\gamma n\left(1-\gamma\mu\right)\left(2\mu n + L\right) - \left(1-\gamma\mu\right)\left(2\mu n + L\right) \\ = \;& L + \mu\gamma n\left(2\mu n + L\right) - \mu^2\gamma^2 n\left(2\mu n + L\right) - \left(1-\gamma\mu\right)\left(2\mu n + L\right) \\ \leq \;& L + \mu\gamma n\left(2\mu n + L\right) - \left(1-\gamma\mu\right)\left(2\mu n + L\right) \\ = \;& \mu\gamma n\left(2\mu n + L\right) + \gamma\mu\left(2\mu n + L\right) - 2\mu n. \end{aligned}$$

Now note that:

$$\gamma\left(2\mu n + L\right) = \frac{\left(2\mu n + L\right)}{2\mu n + 2L} \leq 1.$$

So plugging that into the c_2 bound:

$$\begin{aligned} c_2 &\leq \mu n + \mu - 2\mu n \\ &\leq 0. \end{aligned}$$

So we have verified that each of c_1 to c_4 is non-positive for the derived constants.

4.8.2 Strongly convex step size $\gamma = 1/3L$

This step size is of interest because it does not involve μ. Using such a step size we can hope to achieve a level of *adaptivity*, where the algorithm automatically speeds up based on the unknown level of strong convexity.

First we look at c_4:

$$\begin{aligned} c_4 &= (1+\beta)c\gamma^2 - \frac{c\gamma}{L} \\ &\propto (1+\beta)\gamma - \frac{1}{L} \\ &\propto \frac{(1+\beta)}{3} - 1, \\ \therefore 1 + \beta &= 3, \\ \beta &= 2. \end{aligned}$$

So we can use the value $\beta = 2$. Now to determine c we look at c_1:

$$\begin{aligned} c_1 &= \frac{1}{n} - \frac{2c\gamma(L-\mu)}{L} - 2c\gamma^2\mu\beta \\ &= \frac{1}{n} - c\left(\frac{2(L-\mu)}{3L^2} + \frac{4\mu}{9L^2}\right) \\ &= \frac{1}{n} - c\left(\frac{2}{3L} + \left(\frac{4}{9} - \frac{2}{3}\right)\frac{\mu}{L^2}\right) \\ &= \frac{1}{n} - c\left(\frac{2}{3L} - \frac{2\mu}{9L^2}\right) \\ &= \frac{1}{n} - 2c\left(\gamma - \mu\gamma^2\right) \\ &= \frac{1}{n} - 2c\gamma\left(1 - \mu\gamma\right), \\ \therefore c &= \frac{1}{2\gamma\left(1-\gamma\mu\right)n}. \end{aligned}$$

Note that this is the same constant as we got for the $\gamma = 1/2(\mu n + L)$ step size, when put in terms of γ.

To determine the next constant, rather than fixing the descent rate κ using c_3 like in Section 4.8.1, we will consider c_2 first:

$$\begin{aligned} c_2 &= \frac{1}{\kappa} + 2(1+\beta^{-1})cL\gamma^2 - \frac{1}{n} \\ &= \frac{1}{\kappa} + \frac{2(1+\beta^{-1})L\gamma^2}{2\gamma\left(1-\gamma\mu\right)n} - \frac{1}{n} \\ &= \frac{1}{\kappa} + \frac{(1+\frac{1}{2})L\gamma}{\left(1-\gamma\mu\right)n} - \frac{1}{n} \\ &= \frac{1}{\kappa} + \frac{3L\gamma}{2\left(1-\gamma\mu\right)n} - \frac{1}{n} \\ &= \frac{1}{\kappa} + \frac{1}{2\left(1-\mu/3L\right)n} - \frac{1}{n} \end{aligned}$$

$$\begin{aligned} &= \frac{1}{\kappa} + \frac{3L}{2\left(3L-\mu\right)n} - \frac{1}{n} \\ &\leq \frac{1}{\kappa} + \frac{3L}{2\left(3L-L\right)n} - \frac{1}{n} \\ &= \frac{1}{\kappa} + \frac{3}{4n} - \frac{1}{n} \\ &= \frac{1}{\kappa} - \frac{1}{4n}. \end{aligned}$$

So in order that c_2 be non-positive, we require that:

$$\frac{1}{\kappa} \leq \frac{1}{4n}.$$

Now we need to consider the set of possible κ values carefully. In addition to this bound on $1/\kappa$, have the restriction on $1/\kappa$ from c_3 of:

$$\frac{1}{\kappa} \leq \frac{\mu}{3L}.$$

So we can take $\frac{1}{\kappa}$ as the minimum of the two quantities:

$$\frac{1}{\kappa} = \min\left\{\frac{1}{4n}, \frac{\mu}{3L}\right\}.$$

So our constants are $\gamma = 1/3L$, $\beta = 2$, $c = \frac{1}{2\gamma(1-\gamma\mu)n}$ and $\frac{1}{\kappa} = \min\left\{\frac{1}{4n}, \frac{\mu}{3L}\right\}$.

4.8.3 Non-strongly convex step size $\gamma = 1/3L$

The constraints are a little different here than the strongly convex case. We will name each as τ:

$$\tau_1 = \frac{1}{n} - 2c\gamma,$$

$$\tau_2 = 4(1+\beta^{-1})\alpha L\gamma^2 + 2(1+\beta^{-1})cL\gamma^2 - \frac{1}{n},$$

$$\tau_3 = (1+\beta)c\gamma + 2(1+\beta)\alpha\gamma - \frac{c}{L}.$$

A set of constants that work here are $\alpha = \frac{3L}{20n}$, $c = \frac{3L}{2n}$, $\beta = \frac{3}{2}$ and $\gamma = \frac{1}{3L}$. These are not quite as tight to the constraints as in the strongly convex case. We will derive these by examining each of these τ expressions in turn. We will start with $\beta = \frac{3}{2}$ as a fixed variable, since $\beta = 2$ (used above) doesn't quite work.

For τ_1

$$\frac{1}{n} - 2c\gamma = \frac{1}{n} - \frac{2}{3L}c,$$

So τ_1 is equal to zero when:

$$c = \frac{3L}{2n}.$$

Now lets look at τ_3:

$$\begin{aligned}
(1+\beta)c\gamma + 2(1+\beta)\alpha\gamma - \frac{c}{L} &= (1+\frac{3}{2})c\gamma + 2(1+\frac{3}{2})\alpha\gamma - \frac{c}{L} \\
&\quad \frac{5}{2}c\gamma + 5\alpha\gamma - \frac{c}{L} \\
&= \frac{5}{6}\frac{c}{L} + \frac{5\alpha}{3L} - \frac{c}{L} \\
&= \frac{5\alpha}{3L} - \frac{c}{6L} \\
&\propto 5\alpha - \frac{c}{2}.
\end{aligned}$$

$$\begin{aligned}
\therefore \alpha &\leq \frac{1}{10}c \\
&\leq \frac{3L}{20n}.
\end{aligned}$$

So we can take $\alpha = \frac{3L}{20n}$. We are now ready to look at τ_2:

$$\begin{aligned}
4(1+\beta^{-1})\alpha L\gamma^2 + 2(1+\beta^{-1})cL\gamma^2 - \frac{1}{n} &= 4(1+\frac{2}{3})\alpha L\gamma^2 + 2(1+\frac{2}{3})cL\gamma^2 - \frac{1}{n} \\
&= \frac{8L}{3}\alpha L\gamma^2 + \frac{10}{3}cL\gamma^2 - \frac{1}{n} \\
&= \frac{8L}{3}\alpha L\gamma^2 + \frac{10}{3*9L}c - \frac{1}{n} \\
&= \frac{8L}{3}\alpha L\gamma^2 + \frac{10}{3*9L}c - \frac{1}{n} \\
&= \frac{8L}{3}\alpha L\gamma^2 + \frac{10*3}{3*9*2n} - \frac{1}{n} \\
&= \frac{8}{3*9L}\alpha + \frac{15}{27n} - \frac{1}{n} \\
&= \frac{8*3}{3*9*20n} + \frac{15}{27n} - \frac{1}{n} \\
&\leq (0.599...)\frac{1}{n} - \frac{1}{n} \leq 0.
\end{aligned}$$

So each of the constraints are satisfied.

Chapter 5

Access Orders and Complexity Bounds

In this chapter we take a high level view of the class of fast incremental gradient methods. We start by formalising the class of lower complexity bounds for finite sum problems. We discuss the best possible convergence rates that can achieved by an incremental gradient method on such problems, and we prove one such bound. In Section 5.1.3 we show that incremental gradient methods can not be faster than batch optimisation methods when dealing with non-strongly convex problems, unless further assumptions are placed on the problem class.

The necessity of randomisation in incremental gradient methods is also discussed in this chapter. We give an overview of which of the commonly used optimisation methods have theoretical or practical speed-ups under randomised access orders. For the SAG method, it is known that using much smaller step sizes removes the need for randomisation. We prove a similar result for Finito in Section 5.3, showing that other access patterns are at least as fast as random access when using small enough step sizes.

5.1 Lower Complexity Bounds

The convergence rate bounds we have established so far for the fast incremental gradient methods give us an idea of the worst case convergence rate, for *any problem* satisfying our assumptions, under a particular algorithm. Lower complexity bounds are the opposite side of the coin. They show the best possible convergence rate for *any algorithm* on the hardest problems in class considered. In equational form they resemble convergence rate estimates but with the inequality $\geq$ instead of $\leq$. Convergence rates are a property of an algorithm, applied to a class, whereas lower complexity bounds are a property of the class of problems, for all algorithms[1].

[1] We usually need some assumptions on the algorithm's possible behaviour, but these are typically very weak.

If we are able to establish lower complexity bounds that match our convergence rate bounds for a particular method within a constant, then by convention we call that method *optimal* for the class of problems under consideration.

It is helpful to formalise what information about a function that an optimisation method has access to at each step. This is normally done using the notion of an *oracle*. An oracle is simply an ancillary function $\mathcal{O}$ that when queried returns some specific information about the function f. The simplest case we consider is a first order oracle, where $\mathcal{O} : \mathbb{R}^d \to (\mathbb{R}, \mathbb{R}^d)$ just takes some point x in the domain of f as input and returns the function value and gradient at x. From a software development point of view, the oracle is the *interface* specification of our problem. An optimisation algorithm can only interact with the objective function through the interface defined by the oracle. We state the lower complexity bounds on a class of problems in terms of the accuracy that can be obtained after k invocations to a particular oracle.

The theory for the class of L-smooth μ-strongly convex problems under the first order oracle (known as $S^{1,1}_{s,L}$) is well developed[2]. These results require the technical condition that the dimensionality of the input space $\mathbb{R}^d$ is much larger than the number of iterations we will take. For simplicity we will assume this is the case in the following discussions.

It has been proven (Nemirovsky and Yudin, 1983) that problems exist in $S^{1,1}_{s,L}$ for which the lower complexity bound is:

$$\left\|w^k - w^*\right\|^2 \geq \left(\frac{\sqrt{L/\mu} - 1}{\sqrt{L/\mu} + 1}\right)^{2k} \left\|w^0 - w^*\right\|^2.$$

In fact, when μ and L are known in advance, this rate is achieved up to a small constant factor by several methods, most notably by Nesterov's accelerated gradient descent method (Nesterov, 1988). So in order to achieve convergence rates faster than this, additional assumptions must be made on the class of functions considered.

In this work we have considered problems in $S^{1,1}_{s,L}$ with an additional finite sum structure. Under this structure, we have established convergence rates that in expectation are can be substantially better than the above lower complexity bound. Ideally we would like to establish a tight lower complexity bound for our new class.

To be precise, we now define the (stochastic) oracle class $FS^{1,1}_{s,L,n}(\mathbb{R}^d)$ for which SAG and Finito most naturally fit.

Function class: $f(w) = \frac{1}{n}\sum_{i=1}^n f_i(w)$, with $f_i \in S^{1,1}_{s,L}(\mathbb{R}^d)$.
Oracle: Each query takes a point $x \in \mathbb{R}^d$, and returns j, $f_j(w)$ and $f_j'(w)$, with j chosen uniformly at random.
Accuracy: Find w such that $\mathbb{E}[\left\|w^k - w^*\right\|^2] \leq \epsilon$.

[2]The 1, 1 in $S^{1,1}_{s,L}$ refers to the problem being at least once differentiable, and the oracle being first order

The main choice made in formulating this definition is putting the random choice inside the oracle. This restricts the methods allowed quite strongly. The alternative case, where the index j is input to the oracle in addition to x, is also interesting. Assuming that the method has access to a source of true random indices, we call that class $DS^{1,1}_{s,L,n}(\mathbb{R}^d)$. In Section 3.3 we showed empirical evidence that suggests that faster rates are possible in $DS^{1,1}_{s,L,n}(\mathbb{R}^d)$ than for $FS^{1,1}_{s,L,n}(\mathbb{R}^d)$.

It should first be noted that there is a simple lower bound rate for $f \in FS^{1,1}_{s,L,n}(\mathbb{R}^d)$ of $\left(1 - \frac{1}{n}\right)$ reduction per step. We establish this in Section 5.1.2. Finito is only a factor of 2 off this rate, when the big-data condition holds, namely $\left(1 - \frac{1}{2n}\right)$. SDCA also achieves the rate asymptotically as the amount of data is increased.

Another case to consider is the smooth convex but non-strongly convex setting. We still assume Lipschitz smoothness. In this setting we will show in Section 5.1.3 that for sufficiently high dimensional input spaces, the (non-stochastic) lower complexity bound is the same for the finite sum case and cannot be better than that given by treating f as a single black box function. Essentially, strongly convexity is crucial to the construction of a fast incremental gradient method.

5.1.1 Technical assumptions

In the remainder of this section we use the following technical assumption, as used in Nesterov (1998):

Assumption 1: An optimisation method at step k may only invoke the oracle with a point x^k that is of the form:

$$x^k = x^0 + \sum_i a_i g^{(i)},$$

where $g^{(i)}$ is the derivative returned by the oracle at step i, and $a_i \in \mathbb{R}$.

This assumption prevents an optimisation method from just guessing the correct solution without doing any work. Virtually all optimisation methods satisfy this assumption.

5.1.2 Simple $(1 - \frac{1}{n})^k$ bound

Any procedure that minimises a sum of the form $f(w) = \frac{1}{n}\sum_i f_i(w)$ by uniform random access of f_i is restricted by the requirement that it has to actually see each term at least once in order to find the minimum. This leads to a $\left(1 - \frac{1}{n}\right)^k$ rate in expectation. We now formalise such an argument. We will work in $\mathbb{R}^n$, matching the dimensionality of the problem to the number of terms in the summation.

Theorem 5.1. *For any $f \in FS^{1,1}_{1,n,n}(\mathbb{R}^d)$, and initial point $w^0 \in \mathbb{R}^d$ we have that a k step optimisation procedure gives an expected sub-optimality of at best:*

$$\mathbb{E}[f(w)] - f(w^*) \geq \left(1 - \frac{1}{n}\right)^k \left(f(w^0) - f(w^*)\right).$$

Proof. We will exhibit a simple worst-case problem. Without loss of generality we assume that the first oracle access by the optimisation procedure is at $w = 0$. In any other case, we shift our space in the following argument appropriately.

Let $f(w) = \frac{1}{n}\sum_i \left[\frac{n}{2}\left(w_i - 1\right)^2 + \frac{1}{2}\left\|w\right\|^2\right]$. Then clearly the solution is $w_i = \frac{1}{2}$ for each i, with minimum of $f(w^*) = \frac{n}{4}$. For $w = 0$ we have $f0 = \frac{n}{2}$. Since the derivative of each f_j is 0 on the ith component if we have not yet seen f_i, the value of each w_i remains 0 unless term i has been seen.

Let v^k be the number of unique terms we have not seen up to step k. Between steps k and $k+1$, v decreases by 1 with probably $\frac{v}{n}$ and stays the same otherwise. So

$$\mathbb{E}[v^{k+1}|v^k] = v^k - \frac{v^k}{n} = \left(1 - \frac{1}{n}\right) v^k.$$

So we may define the sequence $X^k = \left(1 - \frac{1}{n}\right)^{-k} v^k$, which is then martingale with respect to v, as

$$\begin{aligned}
\mathbb{E}[X^{k+1}|v^k] &= \left(1 - \frac{1}{n}\right)^{-k-1} \mathbb{E}[v^{k+1}|v^k] \\
&= \left(1 - \frac{1}{n}\right)^{-k} v^k \\
&= X^k.
\end{aligned}$$

Now since k is chosen in advance, stopping time theory gives that $\mathbb{E}[X^k] = \mathbb{E}[X^0]$. So

$$\mathbb{E}[\left(1 - \frac{1}{n}\right)^{-k} v^k] = n,$$

$$\therefore \mathbb{E}[v^k] = \left(1 - \frac{1}{n}\right)^k n.$$

By Assumption 1, the function can be at most minimised over the dimensions seen up to step k. The seen dimensions contribute a value of $\frac{1}{4}$ and the unseen terms $\frac{1}{2}$ to

the function. So we have that:

$$\begin{aligned}\mathbb{E}[f(w^k)] - f(w^*) &\geq \frac{1}{4}\left(n - \mathbb{E}[v^k]\right) + \frac{1}{2}\mathbb{E}[v^k] - \frac{n}{4} \\ &= \frac{1}{4}\mathbb{E}[v^k] \\ &= \left(1 - \frac{1}{n}\right)^k \frac{n}{4} \\ &= \left(1 - \frac{1}{n}\right)^k \left[f(w^0) - f(w^*)\right].\end{aligned}$$

□

5.1.3 Minimisation of non-strongly convex finite sums

Consider the class of convex & differentiable problems, with L Lipschitz smoothness $F_L^{1,1}(\mathbb{R}^d)$. For every f in $F_L^{1,1}(\mathbb{R}^d)$, the following lower complexity bound holds when $k < d$, for any $x^0 \in \mathbb{R}^d$ and for every minimiser x^* of f:

$$f(x^k) - f(x^*) \geq \frac{L\left\|x^0 - x^*\right\|^2}{8\left(k+1\right)^2},$$

which is proved via explicit construction of a worst-case function f where it holds with equality (Nesterov, 1998). Let this worst case function be denoted h^k at step k.

We will show that the same bound applies for the finite-sum case, on a per pass equivalent basis, by a simple construction.

Theorem 5.2. *The following lower bound holds for k a multiple of n, for any $x^0 \in \mathbb{R}^d$:*

$$f(x^k) - f(x^*) \geq \frac{L\left\|x^0 - x^*\right\|^2}{8(\frac{k}{n}+1)^2},$$

when f is a finite sum of n terms $f(x) = \frac{1}{n}\sum_i f_i(x)$, with each $f_i \in F_L^{1,1}(\mathbb{R}^d)$, and with $d > kn$, under the oracle model where the optimisation method may choose the index i to access at each step.

Proof. Let h_i be a copy of h^k redefined to be acting on the subset of dimensions $i + jn$, for $j = 1 \ldots k$, or in other words, $h_i^k(x) = h^k([x_i, x_{i+n}, \ldots x_{i+jn}, \ldots])$. Then we will use:

$$f^k(x) = \frac{1}{n}\sum_i h_i^k(x),$$

as a worst case function for step k.

Since the derivatives are orthogonal between h_i and h_j for $i \neq j$, by Assumption 1, the bound on $h_i^k(x^k) - h_i^k(x^*)$ depends only on the number of times the oracle has been invoked with index i, for each i. Let this be denoted c_i. Then we have that:

$$f^k(x^k) - f^k(x^*) \geq \frac{L}{8n} \sum_i \frac{\left\|x^0 - x^*\right\|_{(i)}^2}{(c_i + 1)^2}.$$

Where $\|\cdot\|_{(i)}^2$ is the norm on the dimensions $i + jn$ for $j = 1 \dots k$. We can combine these norms into a regular Euclidean norm:

$$f^k(x^k) - f^k(x^*) \geq \frac{L \left\|x^0 - x^*\right\|^2}{8n} \sum_i \frac{1}{(c_i + 1)^2}.$$

Now notice that $\sum_i \frac{1}{(c_i+1)^2}$ under the constraint $\sum c_i = k$ is minimised when each $c_i = \frac{k}{n}$. So we have:

$$\begin{aligned} f^k(x^k) - f^k(x^*) \quad \geq \quad & \frac{L \left\|x^0 - x^*\right\|^2}{8n} \sum_i \frac{1}{(\frac{k}{n} + 1)^2}, \\ & \frac{L \left\|x^0 - x^*\right\|^2}{8(\frac{k}{n} + 1)^2}, \end{aligned}$$

which is the same lower bound as for k/n iterations of an optimisation method on f directly. □

5.1.4 Open problems

The above lower complexity theory is unfortunately far from complete. For example, we do not know a tight complexity estimate for the random access case $FS_{s,L,n}^{1,1}(\mathbb{R}^d)$. We conjecture the lower complexity bound will have a geometric constant of

$$1 - \sqrt{\frac{\mu}{n(\mu n + L)}}. \tag{5.1}$$

When the condition number is small compared to n, then $1 - \sqrt{\frac{\mu}{n(\mu n+L)}} \approx 1 - \sqrt{\frac{\mu}{\mu n^2}} = 1 - \frac{1}{n}$, which we know is the best possible rate, and is achieved up to a constant for known methods when $n \geq 2\frac{L}{\mu}$. When n is small, say $n = 1$, then we

get $1 - \sqrt{\frac{\mu}{\mu+L}} \approx 1 - \sqrt{\frac{\mu}{L}}$, which is the best possible rate in the black box setting, which is identical to $FS^{1,1}_{s,L,n}(\mathbb{R}^d)$ when $n = 1$. We also have known methods that achieve this rate. The in-between setting is what is interesting here. There exists the ASDCA method (Section2.3.3) which is applicable in this setting, unfortunately its known convergence rate is not in the simple geometric form of Equation 5.1; it includes additional constants and logarithmic factors.

There is also the non-randomised class $DS^{1,1}_{s,L,n}(\mathbb{R}^d)$. It's not clear if the lower complexity bound for this more general class is actually any different. Perhaps the most important question is if a deterministic method exists with a convergence rate matching the expected rate for those two classes.

5.2 Access Orderings

As discussed in the previous chapters, the order of accessing the f_i terms in an incremental gradient method can have a dramatic effect on the convergence rate. In this section we compare and contrast the various access orders on the most commonly used randomised optimisation methods.

An access order is defined on a per-*epoch* basis. An epoch is just defined as n steps for an incremental gradient algorithm, or d coordinate steps for a coordinate descent algorithm. Recall the three most common access orderings (Section 2.1.3):

Cyclic Each step, $j = 1 + (k \mod n)$.

Permuted Each epoch, j is sampled without replacement from the set of indices not accessed yet in that epoch.

Randomised The value of j is sampled with replacement from $1, \ldots, n$.

We now summarise the behaviour of incremental and coordinate methods under the random, permuted and cyclic orderings for strongly convex problems:

Finito Empirically converges rapidly under randomised ordering. Is always faster under permuted ordering. Can diverge under cyclic ordering. Theory covers randomised ordering only.

SAGA Empirically converges rapidly under randomised ordering. Cyclic ordering converges but extremely slowly. The permuted ordering converges at a similar rate to randomised ordering, but sometimes 50% slower or faster. Theory covers randomised ordering only.

Method	Empirical convergence (Randomised)	Empirical convergence (Permuted)	Empirical convergence (Cyclic)	*Fast* Rate on strong convex problems	Theory covers cyclic/permuted
Finito	✓	✓	✗	✓	✗
SAGA	✓	✓	✗	✓	✗
SVRG	✓	✓	✗/Slow	✓	✗
SAG	✓	✓/Slower	✗	✓	✗
SDCA	✓	✓	Slow Rate	✓	Slow Rate
MISO	✓	✓	✓	✗	✓(Sec 5.3)
SGD	✓	✓	✓/Slower	✗	✓/Slow
CD	✓	✓	✓	✗	✓/Slower

Table 5.1: The effect of different access orders on a selection of optimisation methods

SVRG Situation is identical to SAGA. Interestingly, even when the recalibration step of SVRG is run every pass, using a cyclic ordering is still much slower, although less so than if the recalibration is done less frequently. The "memory" of the previous ordering carries through between epochs even though only a single vector is actually passed.

SAG Empirically converges rapidly under randomised ordering. Cyclic ordering can diverge. The permuted ordering is extremely slow, sometimes diverging, particularly if aggressive step sizes are used. Theory covers randomised ordering only.

SDCA Empirically converges rapidly under randomised ordering. The permuted ordering is sometimes faster, sometimes the same as randomised ordering. Cyclic ordering is extremely slow but convergent. Theory for fast convergence covers randomised ordering only. Convergence under cyclic and permuted orders is provable, but rates unknown.

MISO MISO is the small step size variant of Finito. Empirically it converges under randomised, cyclic and permuted ordering. Previous theory covers randomised ordering (Mairal, 2014). We show in Section 5.3 that cyclic and permuted orders have the same theoretical rate as the randomised ordering.

SGD Empirically fast under randomised ordering, but generally faster under permuted ordering. Cyclic order convergent with small enough step sizes, but slower. Theoretical convergence under cyclic ordering known, slower than randomised ordering by a factor n, for both non-smooth and smooth strongly convex (Nedic and Bertsekas, 2000).

CD Coordinate descent is applied in different circumstances than the above methods, but it can also be compared based on its properties under different access orders. Empirically, cyclic can be better than randomised in some cases. Permuted at least as fast as randomised. Classical convergence proof covers randomised ordering. Theory establishes cyclic and permuted ordering convergence rates, with slower constants dependent on how uniform the Lipschitz smoothness constants are between the f_i functions. This clashes somewhat with the practical results (Beck and Tetruashvili, 2013). There is an additional access order, the Gauss-Soutwell rule, that can be applied to CD problems. At each step the coordinate with the largest gradient is chosen. Nutini et al. (2015) show quite extensive theretical and practical results supporting the GS rule and its variants.

Unfortunately, there is no general pattern to be seen from these results. It appears that the effect of the ordering between two methods can be radically different, even when the methods have otherwise similar performance using a different ordering. One thing is clear though, for all fast incremental gradient methods, the cyclic ordering is extremely inferior.

It is interesting that for Finito and SAG, if we reduce the step size by a factor of n, they then work with cyclic and permuted orderings. SDCA doesn't have a step size, but using the cyclic ordering automatically has a similar effect, lowering the convergence rate to that of small-step-size Finito and SAG.

The permuted ordering is rarely covered explicitly in the existing literature. When the rate is known for the permuted ordering, it is because the cyclic ordering proof also applies to the permuted case. That kind of rate is unsatisfactory, as for those same methods the permuted ordering is faster than randomised in practice, whereas the cyclic rate is slower.

For the SGD method, the permuted case has been explicitly considered by Recht and Re (2012). They show that a cyclic ordering can be exponentially slower than the randomised ordering. They also give a simple conjecture that would imply that permuted ordering is at least as fast as the randomised ordering.

5.3 MISO Robustness

As noted above, the MISO method (the small step size case of Finito) is robust to the use of alternative data access patterns. Both cyclic and permuted orderings work in practice as fast as the randomised ordering. This behaviour is quite unlike the other incremental gradient methods and coordinate descent methods discussed above.

In this section we provide an extension of the theory of MISO to cover these two alternate access orderings. Normally in the incremental gradient literature for cyclic orderings, the analysis is performed on a whole epoch at a time. In our novel analysis, we provide a simple single-step proof for random access ordering, then we show that the alternative access patterns give as least as much descent each step. In particular, the expected convergence rate under each of the three orderings is

$$E\left[f(x^k) - f(x^*)\right] \leq \left(1 - \frac{\mu}{(\mu + L)n}\right)^{2k} \frac{2n}{\mu} \left\|f'(\phi^0)\right\|^2,$$

where the expectation is over the choice of index at each step for that ordering.

The key trick is the introduction of a new metric, which replaces the use of the Euclidean metric in our proof.

Definition 5.3. The path distance $d(\cdot, \cdot)$ is defined for a sequence of points $w^0, \ldots, w^k$ as follows. for any pair w^i and w^j, we assume without loss of generality that $i \leq j$. Then:

$$d(w^i, w^j) = \sum_{l=i}^{j-1} \left\| w^l - w^{l+1} \right\|.$$

This function has the simple interpretation as measuring distance of points in the sequence as the distance along the ordered path between the two points. It is easily verified that all requirements of a distance function are satisfied here. Most importantly the triangle inequality. The other key property we use is that the path distance always dominates the Euclidean distance. Note also that our distance measure is defined on a set, not on the actual vector space. This matters if an identical point appears twice in the sequence, as then it is disambiguated by its index.

For the purposes of this work we will only use the path distance along the sequence of points $\phi^0, w^0, w^1, w^2, \ldots, w^k$, which includes the initial point ϕ^0 , as well as all iterates occurring during the MISO algorithm. Note that each ϕ update sets $\phi_j = w^k$, so all ϕ_i the algorithm uses are included in this path as well. For reference, the MISO update is:

$$w^k = \bar{\phi}^k - \frac{1}{Ln}\sum_i f_i'(\phi_i^k).$$

Now we establish a lemma on the change in w between steps:

Lemma 5.4. *For the MISO method the distance between successive iterates is bounded by:*

$$\left\|w^{k+1} - w\right\| \leq \left(1 - \frac{\mu}{(\mu + L)}\right)\frac{1}{n}\left\|w - \phi_j\right\|.$$

Note that $d(w^{k+1}, w) = \left\|w^{k+1} - w\right\|$, and $\left\|w - \phi_j\right\| \leq d(w, \phi_j)$ by domination. So this theorem holds under the path distance as well as Euclidean distance.

Proof.

$$\begin{aligned}
\left\|w^{k+1} - w\right\|^2 &= \left\|\bar{\phi}^{k+1} - \frac{1}{Ln}\sum_i f_i'(\phi_i^{k+1}) - \bar{\phi} + \frac{1}{Ln}\sum_i f_i'(\phi_i)\right\|^2 \\
&= \left\|\frac{1}{n}(w - \phi_j) - \frac{1}{Ln}f_j'(w) + \frac{1}{Ln}f_j'(\phi_j)\right\|^2 \\
&= \frac{1}{n^2}\left\|w - \phi_j\right\|^2 + \frac{1}{L^2n^2}\left\|f_j'(w) - f_j'(\phi_j)\right\|^2 \\
&\quad -\frac{2}{n^2L}\left\langle w - \phi_j, f_j'(w) - f_j'(\phi_j)\right\rangle.
\end{aligned}$$

We now apply the inner product bound $\langle f'(x) - f'(y), x - y\rangle \geq \frac{\mu L}{\mu + L}\left\|x - y\right\|^2 +$

$\frac{1}{\mu+L}\left\|f'(x)-f'(y)\right\|^2$:

$$\begin{aligned}\left\|w^{k+1}-w\right\|^2 &\leq \left(\frac{1}{n^2}-\frac{2\mu L}{n^2L(\mu+L)}\right)\left\|w-\phi_j\right\|^2 \\ &\quad+\left(\frac{1}{L^2n^2}-\frac{2}{n^2L(\mu+L)}\right)\left\|f_j'(w)-f_j'(\phi_j)\right\|^2 \\ &= \left(1-\frac{2\mu}{(\mu+L)}\right)\frac{1}{n^2}\left\|w-\phi_j\right\|^2+\left(\frac{1}{L}-\frac{2}{\mu+L}\right)\frac{1}{n^2L}\left\|f_j'(w)-f_j'(\phi_j)\right\|^2 \\ &\leq \left(1-\frac{2\mu}{(\mu+L)}\right)\frac{1}{n^2}\left\|w-\phi_j\right\|^2.\end{aligned}$$

Now we use that $\sqrt{1-\frac{1}{a}}\leq 1-\frac{1}{2a}$ for $a\geq 1$ (Lemma B.6) to get the result. □

We now establish the convergence rate of MISO under the path distance for the standard random sampling ordering for MISO.

Theorem 5.5. *For the MISO method, conditioning on information at step k, the expected descent in the quantity $\frac{1}{n}\sum_i d(w,\phi_i)$ after one step is:*

$$\mathbb{E}\left[\frac{1}{n}\sum_i d(w^{k+1},\phi_i^{k+1})\right]\leq\left(1-\frac{\mu}{(\mu+L)n}\right)\frac{1}{n}\sum_i d(w,\phi_i).$$

This theorem holds under the Euclidean distance as well, with the same proof technique.

Proof. We will start by an application of the triangle inequality:

$$\begin{aligned}\frac{1}{n}\sum_i d(w^{k+1},\phi_i^{k+1}) &\leq \frac{1}{n}\sum_i d(w,\phi_i^{k+1})+d(w^{k+1},w) \\ &= \frac{1}{n}\sum_i d(w,\phi_i)+\left[\frac{1}{n}d(w,w)-\frac{1}{n}d(w,\phi_j)\right]+d(w^{k+1},w). \\ &= \frac{1}{n}\sum_i d(w,\phi_i)-\frac{1}{n}d(w,\phi_j)+d(w^{k+1},w).\end{aligned}$$

Now we apply Lemma 5.4:

$$\begin{aligned}\frac{1}{n}\sum_i d(w^{k+1},\phi_i^{k+1}) &\leq \frac{1}{n}\sum_i d(w,\phi_i)+\left(1-\frac{\mu}{(\mu+L)}-1\right)\frac{1}{n}d(w,\phi_j) \\ &= \frac{1}{n}\sum_i d(w,\phi_i)-\frac{\mu}{(\mu+L)n}d(w,\phi_j).\end{aligned}$$

Taking expectations with respect to the choice of j gives:

$$\mathbb{E}\left[\frac{1}{n}\sum_i d(w^{k+1}, \phi_i^{k+1})\right] \leq \left(1 - \frac{\mu}{(\mu+L)n}\right)\frac{1}{n}\sum_i d(w, \phi_i).$$

□

We are now ready to extend our result to alternative access orderings

Theorem 5.6. *If the MISO algorithm is used with a cyclic access pattern then the one-step convergence rate is no worse than the expected rate for a random ordering:*

$$\frac{1}{n}\sum_i d(w^{k+1}, \phi_i^{k+1}) \leq \left(1 - \frac{\mu}{(\mu+L)n}\right)\frac{1}{n}\sum_i d(w, \phi_i).$$

Proof. The only point in the proof of Theorem 5.5 where we use the access ordering is when we simplify with:

$$\mathbb{E}\left[d(w, \phi_j)\right] = \frac{1}{n}\sum_i d(w, \phi_i).$$

This appears negated and on the right in the proof, so we need to show that when j is chosen via the cyclic pattern that $\frac{1}{n}\sum_i d(w, \phi_i) \leq d(w, \phi_j)$. Now under the cyclic access pattern, the point ϕ_j is the furthest (or tied for furthest) of the ϕ_i^k points in the path under which our path distance is defined. In other words, it is always the least recently accessed index. So for all ϕ_i, $i \neq j$:

$$d(w, \phi_i) \leq d(w, \phi_j).$$

$$\therefore d(w, \phi_j) \geq \frac{1}{n}\sum_i d(w, \phi_i).$$

The rest of the proof follows through as for Theorem 5.5 . □

Theorem 5.7. *If the MISO algorithm is used with the permuted ordering then the one-step convergence rate is no worse than the expected rate for a random ordering:*

$$\mathbb{E}_{perm}\left[\frac{1}{n}\sum_i d(w^{k+1}, \phi_i^{k+1})\right] \leq \left(1 - \frac{\mu}{(\mu+L)n}\right)\frac{1}{n}\sum_i d(w, \phi_i).$$

Proof. As in the previous theorem, we just need to prove that:

$$\frac{1}{n}\sum_i d(w, \phi_i) \leq \mathbb{E}_{\text{perm}}\left[d(w, \phi_j)\right].$$

So suppose we are at the $(r+1)$th step within an epoch. Let A be the set of r indices updated so far in this epoch. Now note that for each $i \in A$, $d(w, \phi_i)$ is less than $d(w, \phi_j)$ for any $j \notin A$, as they are further back in the path for which the path norm is defined. This implies that $\frac{1}{r}\sum_{i\in A} d(w,\phi_i) \leq \frac{1}{n-r}\sum_{i\notin A} d(w,\phi_i)$. So:

$$\begin{aligned}
\frac{1}{n}\sum_i d(w,\phi_i) &= \frac{1}{n}\sum_{i\in A} d(w,\phi_i) + \frac{1}{n}\sum_{i\notin A} d(w,\phi_i) \\
&\leq \frac{1}{n}\cdot\frac{r}{n-r}\sum_{i\notin A} d(w,\phi_i) + \frac{1}{n}\sum_{i\notin A} d(w,\phi_i) \\
&= \frac{1}{n}\cdot\frac{r}{n-r}\sum_{i\notin A} d(w,\phi_i) + \frac{1}{n}\cdot\frac{n-r}{n-r}\sum_{i\notin A} d(w,\phi_i) \\
&= \frac{1}{n-r}\sum_{i\notin A} d(w,\phi_i).
\end{aligned}$$

This is just the expectation over the choice of j under the permuted ordering:

$$\mathbb{E}_{\text{perm}}[d(w,\phi_j)] = \frac{1}{n-r}\sum_{i\notin A} d(w,\phi_i),$$

and so the result is proven. □

Theorem 5.5 and the two variants of it above gives us a convergence rate in terms of $\frac{1}{n}\sum_i d(w,\phi_i)$. It is not immediately obvious how this quantity relates to traditional measures of convergence such as $f(w) - f(w^*)$ or $\|w - w^*\|^2$. So we now relate $\frac{1}{n}\sum_i d(w,\phi_i)$ at step k to function suboptimality and at step 0 to gradient norm, to give a convergence rate comparable to traditional optimisation methods.

Theorem 5.8. *Assuming that we initialise with $\phi_i^0 = \phi^0$ for all i, the expected convergence rate of the MISO method is:*

$$\mathbb{E}\left[f(x^k) - f(x^*)\right] \leq \left(1 - \frac{\mu}{(\mu+L)n}\right)^{2k} \frac{2n}{\mu}\left\|f'(\phi^0)\right\|^2,$$

under each of the cyclic, permuted and random orderings.

Proof. We start by bounding the gradient norm of f:

$$\begin{aligned}
\left\|f'(w)\right\| &= \left\|\frac{1}{n}\sum_i f_i'(w)\right\| \\
&= \left\|\frac{1}{n}\sum_i \left[f_i'(w) - f_i'(\phi_i) + f_i'(\phi_i)\right]\right\| \\
&\leq \left\|\frac{1}{n}\sum_i f_i'(\phi_i)\right\| + \left\|\frac{1}{n}\sum_i \left[f_i'(w) - f_i'(\phi_i)\right]\right\| \\
&\leq L\left\|w - \bar{\phi}\right\| + \frac{1}{n}\sum_i \left\|f_i'(w) - f_i'(\phi_i)\right\| \\
&\leq L\left\|w - \bar{\phi}\right\| + \frac{L}{n}\sum_i \left\|w - \phi_i\right\|.
\end{aligned}$$

Now recall that $\left\|w - \bar{\phi}\right\|^2 = \frac{1}{n}\sum_i \left\|w - \phi_i\right\|^2 - \frac{1}{n}\sum_i \left\|\bar{\phi} - \phi_i\right\|^2$ by the variance decomposition. Therefore $\left\|w - \bar{\phi}\right\| \leq \sqrt{\frac{1}{n}\sum_i \left\|w - \phi_i\right\|^2}$. The L_2 norm is always no greater than the L_1 norm, so $\sqrt{\frac{1}{n}\sum_i \left\|w - \phi_i\right\|^2} \leq \sqrt{\frac{1}{n}}\sum_i \left\|w - \phi_i\right\|$. We have shown so far that:

$$\begin{aligned}
\left\|f'(w)\right\| &\leq \frac{L}{\sqrt{n}}\sum_i \left\|w - \phi_i\right\| + \frac{L}{n}\sum_i \left\|w - \phi_i\right\|, \\
&\leq \frac{2L}{\sqrt{n}}\sum_i \left\|w - \phi_i\right\|,
\end{aligned}$$

and since $2\mu\left[f(x) - f(x^*)\right] \leq \left\|f'(w)\right\|^2$, we get

$$\sqrt{2\mu\left[f(x) - f(x^*)\right]} \leq \frac{2L}{\sqrt{n}}\sum_i \left\|w - \phi_i\right\|,$$

$$2\mu\left[f(x) - f(x^*)\right] \leq \frac{4L^2}{n}\left(\sum_i \left\|w - \phi_i\right\|\right)^2,$$

$$\therefore \frac{2\mu}{4L^2 n}\left[f(x) - f(x^*)\right] \leq \left(\frac{1}{n}\sum_i \left\|w - \phi_i\right\|\right)^2 \leq \left(\frac{1}{n}\sum_i d(w, \phi_i)\right)^2.$$

Combining with one step convergence rate in Theorem 5.5:

$$\mathbb{E}\left[\frac{1}{n}\sum_i d(w^{k+1}, \phi_i^{k+1})\right] \leq \left(1 - \frac{\mu}{(\mu + L)n}\right)\frac{1}{n}\sum_i d(w, \phi_i),$$

squared and chained between 0 and $k - 1$, we get:

$$\mathbb{E}\left[f(x^k) - f(x^*)\right] \leq \left(1 - \frac{\mu}{(\mu+L)n}\right)^{2k} \frac{2L^2 n}{\mu} \left(\frac{1}{n}\sum_i d(w^0, \phi_i^0)\right)^2.$$

Now we use Jensen's inequality to bound $\left(\frac{1}{n}\sum_i d(w^0, \phi_i^0)\right)^2 \leq \frac{1}{n}\sum_i d(w^0, \phi_i^0)^2$:

$$\mathbb{E}\left[f(x^k) - f(x^*)\right] \leq \left(1 - \frac{\mu}{(\mu+L)n}\right)^{2k} \frac{2L^2 n}{\mu} \left(\frac{1}{n}\sum_i d(w^0, \phi_i^0)^2\right).$$

Now assuming that all the ϕ_i^0 start at the same value (ϕ^0) gives

$$\frac{1}{n}\sum_i d(w^0, \phi_i^0)^2 = \left\|w^0 - \phi^0\right\|^2 = \frac{1}{L^2}\left\|f'(\phi^0)\right\|^2.$$

The result follows:

$$\mathbb{E}\left[f(x^k) - f(x^*)\right] \leq \left(1 - \frac{\mu}{(\mu+L)n}\right)^{2k} \frac{2n}{\mu}\left\|f'(\phi^0)\right\|^2.$$

□

Chapter 6

Beyond Finite Sums: Learning Graphical Models

In the preceding chapters we considered incremental gradients methods whose applicability is limited to objectives that contain a finite sum structure. In the following chapters we consider problems with the other major function structure, a *graph* structure. We particularly focus on the simplest case, that of the Gaussian graphical model. We look at two sides of the problem, that of learning smaller complex structured models, and that of learning very large models. For smaller models, we introduce in Chapter 7 a method for learning graphs with the *scale-free* property, common in real world graphs. For large scale applications, we consider in Chapter 9 the use of the Bethe approximation for learning large Gaussian graphical models with known structure. When the structure is not known, it can be approximated using a variety of techniques. In Chapter 8 we give a fast variant of an existing technique which is highly scalable, and which often learns better structures than slower techniques.

6.1 Beyond the Finite Sum Structure

Not all loss minimisation problems in machine learning are suited to the application of the incremental gradient methods considered in the previous chapters. For some problems, there is shared structure between the losses that can be exploited in batch optimisation methods. Consider the probability density for a log linear model with p variables and d features:

$$P(x : \theta) = \frac{1}{Z(\theta)} \exp\left\{ -\sum_{r=1}^{d} \theta_r f_r(x) \right\},$$

where θ is a vector of feature weights and $Z(\theta)$ is the partition function whose value ensures that $\int_x P(x : \theta) = 1$. Now suppose we have a dataset $X\colon n \times p$ of n data-

points x_k. Using the negative log-likelihood gives the objective:

$$\begin{aligned} NLL(\theta) &= \frac{1}{n}\sum_{k=1}^{n}\left[-\log 1/Z(\theta) + \sum_{r=1}^{d}\theta_r f_r(x_k)\right] \\ &= \frac{1}{n}\sum_{k=1}^{n}\sum_{r=1}^{d}\theta_r f_r(x_k) + \log Z(\theta). \end{aligned} \tag{6.1}$$

While the objective does decompose as a sum of functions over individual data-points as we require for the application of incremental gradient methods, the $\log Z(\theta)$ term is shared by all the data-points. The cost of evaluating $NLL(\theta)$ is dominated by the evaluation of $\log Z(\theta)$, so it essentially costs the same to compute one full gradient as one incremental gradient in this framework.

Evaluating the NLL doesn't always require the full dataset. A set of empirical statistics known as the *sufficient statistics* can be extracted from the data, which contain sufficient information for evaluating the NLL and its gradient. These statistics can be substantially more compact than the full dataset.

Most applications of log-linear models in modern machine learning use *conditional* models, where instead each partition function Z is a function of a set of conditioning variables y_i as well as the parameters θ. Conditional models do not share the same partition function for each data-point, so evaluating the whole loss is much more expensive than the per-datum loss. The incremental gradient methods discussed in previous chapters are directly applicable to conditional models.

In the remainder of this work we focus on unconditional models. The main application of unconditional models in machine learning is in structure learning.

6.2 The Structure Learning Problem

Given a dataset $X : n \times p$, where we have n samples of p variables, the structure learning problem is the estimation of a network of p nodes, where an edge (i, j) between two nodes signifies that there is a *direct dependence* between the two variables i & j in the data. The most natural notion of direct dependence is that of conditional independence. Under the assumption that our data is Gaussian distributed, this task is precisely estimation of the sparsity pattern of the precision matrix of the data distribution. The assumption of Gaussianity is a standard approach to structure estimation, primarily because it results in a tractable optimisation problem. Even when the Gaussian assumption does not hold, it can be used as a subtask in the estimation of more complex models such as Gaussian Copulas (Dauwels et al., 2013).

This estimation task is known under a variety of names; the earliest references confusingly use the term "Covariance Selection" (Dempster, 1972), whereas some machine learning literature uses the more accurate but longer "Sparse Inverse Covariance Selection". We use the terms interchangeably in this work. The inverse of the

covariance matrix is also known as the precision matrix or the concentration matrix, and all three terms are used in the Covariance selection literature. This task is complicated by the fact that the sample covariance matrix C of the data is noisy and potentially low rank, so the sample precision matrix as a natural estimate of the data precision matrix may not even be well defined.

6.3 Covariance Selection

A Gaussian graphical model is an example of log-linear model of the above form. The feature set consists of singleton feature functions for each variable f_i, and feature functions f_{ij} defined over pairs of variables, with one feature per pair. The model has the following general structure:

$$P(x;\Theta) = \frac{1}{Z(\Theta)} \exp\left(-\sum_{i}^{p} \Theta_{ii} f_i(x_i) - \sum_{i}^{p} \sum_{j>i}^{p} \Theta_{ij} f_{ij}(x_i, x_j) \right). \tag{6.2}$$

We are using Θ instead of θ, as the weights are better thought of as having a symmetric matrix structure ($\Theta_{ij} = \Theta_{ji}$) rather than a flat vector structure. Additionally, in order that $Z(\Theta)$ exist, we will require a positive definiteness constraint on Θ, leading to a conic structure.

The unary features f_i penalise deviations of x_i from its average value:

$$f_i(x_i) = \frac{1}{2}(x_i - \mu_i)^2.$$

The pair-wise features penalise x_i and x_j if they vary from their respective means in the same direction:

$$f_{ij}(x_i, x_j) = (x_i - \mu_i)(x_j - \mu_j).$$

Note that *negative* values of Θ_{ij} encourage correlation, which might be the opposite of what would be expected. The reason for defining f_{ij} this way, instead of say $f_{ij}(x_i, x_j) = -(x_i - \mu_i)(x_j - \mu_j)$, is so that we are consistent with standard Gaussian distribution notation. To see this, notice that if we equate terms in Equation 6.2 with the definition of a multivariate Gaussian distribution in terms of the precision matrix:

$$P(x;\Theta) = \frac{1}{\sqrt{(2\pi)^n \det(\Theta^{-1})}} \exp\left(-\frac{1}{2} (x - \mu)^T \Theta (x - \mu) \right), \tag{6.3}$$

The feature weights Θ we have defined exactly form the precision matrix Θ of the Gaussian distribution. Note that the pair-wise features now appear twice due to the symmetry of Θ, in the forms Θ_{ij} and Θ_{ji} , which is why the weighting factor of half appears not just on the unary features.

In the following sections, we will discuss learning Θ given a dataset of points x_k. To this end, we now derive the maximum likelihood estimator of Θ. First we take the negation of the logarithm of Equation 6.3:

$$\begin{aligned}
-\log P &= -\log 1/\sqrt{(2\pi)^n \det(\Theta^{-1})} + \frac{1}{2}(x-\mu)^T \Theta (x-\mu) \\
&= \frac{1}{2}\log\left[(2\pi)^n \det(\Theta^{-1})\right] + \frac{1}{2}(x-\mu)^T \Theta (x-\mu) \\
&= \frac{n}{2}\log[2\pi] + \frac{1}{2}\log\left[\det(\Theta^{-1})\right] + \frac{1}{2}(x-\mu)^T \Theta (x-\mu) \\
&= \frac{n}{2}\log[2\pi] - \frac{1}{2}\log[\det(\Theta)] + \frac{1}{2}(x-\mu)^T \Theta (x-\mu).
\end{aligned}$$

Now we can drop the constant factor $\frac{n}{2}\log[2\pi]$, and the multiplicative factor $\frac{1}{2}$ to simplify the objective. Giving the single datapoint negative log-likelihood (NLL):

$$NNL(\Theta\colon x) = (x-\mu)^T \Theta (x-\mu) - \log\det(\Theta).$$

The full data NLL is the average of this over the data points: $\frac{1}{n}\sum_k^n NLL(x_k : \Theta)$. We can write this is a simple form using the Frobenius inner product notation for matrices $\langle\cdot,\cdot\rangle$, defined as $\langle X, Y\rangle = \sum_i \sum_j X_{ij} Y_{ij}$, together with the covariance matrix of the data C:

$$\begin{aligned}
NLL(\Theta\colon X) &= \frac{1}{n}\sum_k^n (x_k-\mu)^T \Theta (x_k-\mu) - \log\det(\Theta) \\
&= \frac{1}{n}\sum_k^n \sum_i \sum_j \Theta_{ij}(x_{ki}-\mu_i)(x_{kj}-\mu_j) - \log\det\Theta \\
&= \sum_i \sum_j \Theta_{ij}\left[\frac{1}{n}\sum_k^n (x_{ki}-\mu_i)(x_{kj}-\mu_j)\right] - \log\det\Theta \\
&= \sum_i \sum_j \Theta_{ij} C_{ij} - \log\det\Theta \\
&= \langle C, \Theta\rangle - \log\det\Theta.
\end{aligned}$$

The maximum likelihood problem is equivalent to minimisation of the NLL (the negative log-likelihood) over the set of matrices that form valid probability distributions, which is $\Theta \in S^N_{++}$, the cone of symmetric positive definite matrices. So we have:

$$\min_{\Theta \in S^N_{++}} \langle C, \Theta\rangle - \log\det\Theta. \tag{6.4}$$

The gradient of this objective is straight-forward:

$$\frac{d}{d\Theta}\left(\langle C, \Theta\rangle - \log\det\Theta\right) = C - \Theta^{-1}.$$

When C is an observed full-rank covariance matrix, taking the gradient to zero gives the feasable solution $\Theta = C^{-1}$. If C is low rank but PSD (positive semi-definite), then there will be a subspace of possible solutions. Since we are concerned with covariance matrices, we do not consider non-PSD C matrices further in this work.

We are more interested in the support of the precision matrix (the graphical model structure) than its entries, and using C^{-1} as an estimator of Θ does not lead to sparse graph structures. In order to induce sparsity a L_1 regulariser is typically used:

$$\min_{\Theta \in S^N_{++}} \langle C, \Theta \rangle - \log\det\Theta + \lambda \left\|\Theta\right\|_1 . \tag{6.5}$$

Where the L_1 norm is taken elementwise, and λ is a regularisation parameter. This formulation was first used for covariance selection by Banerjee et al. (2006). This objective is convex, and therefore tractable, although specialised optimisation algorithms needed to be developed for it as standard first or second order methods do not work well. The Θ^{-1} term in the gradient is very sensitive to changes in Θ, and the inverse operation highly couples the variables so standard optimisation methods make slow progress. The cone constraint S^N_{++} also complicates matters; it is an open set and the objective is sharply curved near the boundary.

The dual of Equation 6.5 is particularly simple. Let S be the matrix of dual variables. Then like other L_1 regularised problems, the L_1 norm turns into a box constraint in the dual:

$$\begin{aligned} &\max_{S \in S^N_{++}} \log\det S, \\ &\text{s.t. } \forall i, j\colon \left|S_{ij} - C_{ij}\right| \leq \lambda. \end{aligned} \tag{6.6}$$

6.3.1 Direct optimisation approaches

By our count there are over 35 papers published on distinct optimisation methods for the covariance selection objective. Early approaches applied block coordinate descent to the dual problem, with a block being the ith row and column (Friedman et al., 2007; Banerjee et al., 2006). These approaches are quadratic time per update, and can be very effective on small problems, or those with high levels of sparsity.

For medium sized problems, a proximal approach can be taken, where the optimisation method alternates between evaluating the proximal operator of the log det function and the L_1 norm (Scheinbert et al., 2010). These *alternating* approaches are easy to implement, converge rapidly and have strong convergence guarantees, but they fail for problems for which the eigenvalue decomposition at each step is too expensive.

For large scale problems, the QUIC framework is currently the state of the art among direct optimisation methods (Hsieh et al., 2011, 2013). It uses an approximate (proximal) Newton step with line search as the core component. Finding the Newton step

at each iteration is a separate optimisation problem, requiring sophisticated methods. The QUIC method is very complex compared to the other methods considered here.

A more complete review of optimisation approaches to covariance selection appears in Scheinberg and Ma (2012). It should be noted that some approaches do not regularise the diagonal of Θ, such as the SPICE method of Rothman et al. (2008), as there is no motivation for pushing diagonal elements towards zero, and regularisation of the diagonal seems to harm theoretical performance. Also, like all the methods we will discuss, the regularised maximum likelihood approach can be applied to the Pearson correlation matrix $\bar{C}$ instead of the covariance matrix. Rothman et al. (2008) are able show better theoretical performance for the correlation variant of their SPICE method than the covariance version.

6.3.2 Neighbourhood selection

Instead of joint maximum likelihood learning of all edges at once, another approach is to determine the dependence relations for each variable as a separate problem (Meinshausen and Bühlmann, 2006). This involves performing p L_1-regularised linear regression operations, working with the data matrix X instead of its covariance C. To write the method compactly, we introduce the subscript notation $(\neg i)$ to represent taking the subset of that the indices excluding the ith, and the notation $i*$ to represent the ith row and $*i$ the ith column.

For each row i of the precision matrix, the neighbourhood selection algorithm performs a separate minimisation:

$$\Theta_{i(\neg i)} = \arg\min_{\theta} \left[\frac{1}{n} \left\| X_{*i} - X_{*(\neg i)}\theta \right\|_2^2 + \lambda \left\| \theta \right\|_1 \right].$$

The resulting matrix Θ's support will not necessarily be symmetric, so further processing is required to determine a symmetric support. Considering the support only, conflicting edges can be combined by either a union (i.e. $\Theta_{ij} \neq 0 \cup \Theta_{ji} \neq 0$) or intersection operation; Meinshausen and Bühlmann (2006) show consistency results for both. In the case where $n \approx \sqrt{p}$, neighbourhood selection is among the fastest methods in theory. In practice, it requires a very efficient lasso implementation to be practical for large problems.

6.3.3 Thresholding approaches

As the sample covariance matrix is readily available, the technique of directly thresholding the absolute value of its entries can be used (Bickel and Levina, 2008). This technique can give better estimates of the true covariance matrix than directly using the

empirical covariance matrix for sparse Gaussians, however it doesn't necessarily reveal the network structure. In the case where the covariance matrix is full rank, the technique of inverse sample covariance matrix thresholding may be used (Dempster, 1972). This technique is not often used as the inverse empirical covariance matrix as an estimate of the precision matrix can be poor as the inversion is sensitive to small changes in the covariance matrix.

A better approach is thresholding pairwise mutual information. For Gaussian distributed variables x_i and x_j, the mutual information is given by:

$$I(x_i; x_j) = \frac{1}{2} \log \left(\frac{C_{ii} C_{jj}}{C_{ii} C_{jj} - C_{ij}^2} \right).$$

The well known Chow-Liu method (Chow and Liu, 1968) for learning the best-fitting *tree* structure relies on mutual information between variables, and mutual information thresholding is also widely used for general directed graphical model structure learning (Federer, 2011). Mutual Information thresholding is a form of independence testing, a standard technique in applied statistics. Indeed, the mutual information score is proportional to the χ^2 statistic up to first order (Koller and Friedman, 2009).

6.3.4 Conditional thresholding

A newer class of techniques consider for each entry a set of conditional covariance or conditional mutual information terms. Instead of thresholding the mutual information term $I(x_i; x_j)$, Anandkumar et al. (2011b) consider thresholding the minimum of the set of conditional mutual information's $I(x_i; x_j | x_S)$ where S is a set of variables not containing x_i or x_j. For tractability the minimisation is taken over subsets of size at most η:

$$w_{ij} = \min_{S \in V \setminus \{x_i, x_j\}, |S| \leq \eta} I(x_i; x_j | x_S).$$

Performing this minimisation takes time $O(p^\eta)$ per edge, so for thresholding all edges the running time is $O(p^{2+\eta})$. In applications this is only practical for $\eta = 1$ or possibly $\eta = 2$.

For the $\eta = 1$ case, we introduce some additional notation. We will subscript matrices by a set of indices to denote selection of the square submatrix containing the rows and columns in the set. E.g $C_{\{i,j\}}$ is the submatrix of C containing rows i, j and columns i, j. Using this notation, the conditional mutual information for variables x_i, x_j given x_k is given by:

$$I(x_i; x_j | x_k) = \frac{1}{2} \log \left(\frac{\det C_{\{i,k\}} \det C_{\{j,k\}}}{C_{kk} \det C_{\{i,k,j\}}} \right).$$

Anandkumar et al. (2011a) consider the case of conditional covariances, which behave better theoretically, as the number of samples required for correct reconstructions depends less on the strength of the data distributions dependencies. The conditional covariance of x_i, x_j given a set of variable indices S is:

$$Cov[x_i, x_j | x_S] = C_{ij} - C_{iS} C_{SS}^{-1} C_{Sj}.$$

As the conditional covariance can be negative, the minimisation is taken of its absolute value. Like in the mutual information case, the minimum over all subsets S of a particular size is used. Besides better theoretical bounds, the conditional covariance is faster to evaluate for small η, and its values are easier to interpret. The $C_{iS} C_{SS}^{-1} C_{Sj}$ term can be thought of as the transitive covariance contributed by the path between x_i and x_j through x_S. If C_{ij} is significantly above the transitive covariance over subset S, then it is likely due to a direct dependence between variables x_i and x_j.

6.4 Alternative Regularisers

The L_1 norm used in the maximum likelihood approach is known to encourage sparsity, but it also has a significant and potentially undesirable effect on the learned weights. One way to overcome this is to use a regulariser that is stronger in the vicinity of 0 than the L_1 norm, but weaker away from zero. Such a regulariser necessarily be nonconvex. Candes et al. (2008) suggest the use of a logarithmic regulariser, such as

$$\lambda \sum_{i,j} \log \left(\left| \Theta_{ij} \right| + \epsilon \right), \tag{6.7}$$

for some $\epsilon > 0$. The constant ϵ just prevents the log terms being infinity near 0. In order to efficiently solve this, the problem can be addressed using repeated linearisation of the log term. At each stage, a separate weight λ_{ij} is found for each entry of Θ_{ij} so that the tangent of $\lambda_{ij} \left| \Theta_{ij} \right|$ matches $\lambda \log \left(\left| \Theta_{ij} \right| + \epsilon \right)$ at the current Θ_{ij} value. Then the resulting "reweighted" L_1 regularised problem is solved, and the reweighted is repeated. This reweighted L_1 method falls within the class of majorisation-minimisation methods (Hunter and Lange, 2000), as on both sides of 0 the weighted L_1 regularised problem is an upper bound for the $\lambda \sum_{i,j} \log \left(\left| \Theta_{ij} \right| + \epsilon \right)$ regularised one (i.e. a majorisation), which we minimise at each stage.

This approach has been adapted by Liu and Ihler (2011) to encourage a *scale free* network structure (discussed in Chapter 7) using the following objective:

$$f(\Theta) = \langle \Theta, C \rangle - \log \det \Theta + \lambda \sum_i \log \left(\| \Theta_{i*} \|_1 - |\Theta_{ii}| + \epsilon \right) + \gamma \sum_i |\Theta_{ii}| . \tag{6.8}$$

The regulariser is split into a row term which is designed to encourage sparsity in the edge parameters, and a more traditional diagonal term. The row term $(\|\Theta_{i*}\|_1 - |\Theta_{ii}|)$ is in effect a continuous analogue to the degree of node i. The same kind of reweighting optimisation scheme can be applied as for Equation 6.7 to this objective.

The other major class of regularisers are those that encourage *group sparsity*. Group-sparse regularisers just encourage whole sets of variables to be zero or non-zero together (Bach et al., 2012). For graph structures the most common application is to encourage variable independence, by treating all edges incoming to a node as a group. The objective is of the form:

$$f(\Theta) = \langle \Theta, C \rangle - \log\det\theta + \lambda \sum_i \|\Theta_{i*}\|_2 \,.$$

This is effectively a sum of L_1 norms, one group per node i, where the group consists of edges adjacent to a node i. The groups overlap due to the symmetry constraint, as each edge is adjacent to two nodes.

Chapter 7

Learning Scale Free Networks

Structure learning for graphical models is a problem that arises in many contexts. In applied statistics, graphical models with learned structure can be used as a tool for understanding the underlying conditional independence relations between variables in a dataset. For example, in bioinformatics Gaussian graphical models are fitted to data resulting from micro-array experiments, where the fitted graph can be interpreted as a gene expression network (Dobra et al., 2004).

Recent research has seen the development of *structured* sparsity, where more complex prior knowledge about a sparsity pattern can be encoded. Examples include group sparsity (Yuan and Lin, 2007), where parameters are linked so that they are regularised in groups. More complex sparsity patterns, such as region shape constraints in the case of pixels in an image (Jenatton et al., 2010b), or hierarchical constraints (Jenatton et al., 2010a) have also been explored.

In this chapter we study the problem of recovering the structure of a Gaussian graphical model under the assumption that the graph recovered should be scale-free. Many real-world networks are known a priori to be scale-free and therefore enforcing that knowledge through a prior seems natural. Recent work has offered an approach to deal with this problem which results in a non-convex formulation (Section 6.4). Here we present a convex formulation. We show that scale-free networks can be induced by enforcing submodular priors on the network's degree distribution, and then using their convex envelope (the Lovász extension) as a convex relaxation.

The resulting relaxed prior has an interesting non-differentiable structure, which poses challenges to optimisation. We outline a few options for solving the optimisation problem via proximal operators, in particular an efficient dual decomposition method. Experiments on both synthetic data produced by scale-free network models and a real bioinformatics dataset suggest that the convex relaxation is not weak: we can infer scale-free networks with similar or superior accuracy than with the previous state-of-the-art.

An earlier version of the work in this chapter has been published as Defazio and Caetano (2012a).

7.1 Combinatorial Objective

Consider an undirected graph with edge set E and node set V, where n is the number of nodes. We denote the degree of node v as $d_E(v)$, and the complete graph with n nodes as K_n. We are concerned with placing priors on the degree distributions of graphs such as (V, E). By degree distribution, we mean the bag of degrees $\{d_E(v)|v \in V\}$.

We would like to place higher prior probability mass on graphs with scale-free structure. Scale-free graphs are simply graphs whose degree distribution follows a power law. In other words, the random draws from the bag of degrees of the graph has a distribution of the form:

$$p(i) \propto i^{-\alpha},$$

for some $\alpha > 1$, typically in the range 2 to 3. It is too much to ask that the empirical degree distribution of a graph exactly matches a power-law distribution, so in practice a graph is considered scale free if the tail of the degree distribution is significantly heavier, in the sense of having more probability mass, than the exponential distribution.

A natural prior on degree distributions can be formed from the family of exponential random graphs (Terry, 2005). Exponential random graph (ERG) models assign a probability to each n node graph using an exponential family model. The probability of each graph depends on a small set of sufficient statistics, in our case we only consider the degree statistics. A ERG distribution with degree parameterisation takes the form:

$$p(G = (V, E) \colon h) = \frac{1}{Z(h)} \exp\left\{\left[-\sum_{v \in V} h(d_E(v))\right]\right\},$$

The degree weighting function $h \colon \mathbb{Z}^+ \to \mathbb{R}$ encodes the preference for each particular degree. The function Z is chosen so that the distribution is correctly normalised over n node graphs.

A number of choices for h are reasonable; A geometric series $h(i) \propto 1 - \alpha^i$ with $\alpha \in (0, 1)$ has been proposed by Snijders et al. (2004) and has been widely adopted. However, for encouraging scale free graphs we require a more rapidly increasing sequence. Under the strong assumption that each node's degree is independent of the rest, h grows logarithmically for scale free networks. To see this, take a scale free model $p(i) \propto i^{-\alpha}$, with scale α; the joint distribution under the node degree independence simplification takes the form:

$$p(G = (V, E) \colon \epsilon, \alpha) = \frac{1}{Z(\epsilon, \alpha)} \prod_{v \in V} (d_E(v) + \epsilon)^{-\alpha},$$

where $\epsilon > 0$ is added to prevent infinite weights. Putting this into ERG form gives the weight sequence $h(i) = \alpha \log(i + \epsilon)$. We will consider this and other functions h

in Section 7.4. We intend to perform maximum a posteriori (MAP) estimation of a graph structure using such a distribution as a prior, so the object of our attention is the negative log-posterior, which we denote F:

$$F(E) = \sum_{v \in V} h(d_E(v)) + \text{const.}$$

So far we have defined a function on edge sets only, however in practice we want to optimise over a weighted graph, which is intractable when using discontinuous functions such as F. We now consider the properties of h that lead to a convex relaxation of F.

7.2 Submodularity

A set function $F\colon 2^E \to \mathbb{R}$ on E is a non-decreasing submodular function if for all $A \subset B \subset E$ and $x \in E \backslash B$ the following conditions hold:

$$F(A \cup \{x\}) - F(A) \geq F(B \cup \{x\}) - F(B) \qquad \text{(submodularity)}$$
$$\text{and } F(A) \leq F(B). \qquad \text{(non-decreasing)}$$

The first condition can be interpreted as a diminishing returns condition; adding x to a set A increases $F(A)$ by more than adding x to a larger set B, if B contains A. We now consider a set of conditions that can be placed on h so that F is submodular.

Proposition 7.1. *Denote h as tractable if h is non-decreasing, concave and $h(0) = 0$. For tractable h, F is a non-decreasing submodular function.*

Proof. First note that the degree function is a set cardinality function, and hence modular. A concave transformation of a modular function is submodular (Bach, 2010a), and the sum of submodular functions is submodular. □

The concavity restriction we impose on h is the key ingredient that allows us to use submodularity to enforce a prior for scale-free networks; any prior favouring long tailed degree distributions must place a lower weight on new edges joining highly connected nodes than on those joining other nodes. As far as we are aware, this is a novel way of mathematically modelling the "preferential attachment" rule (Barabasi and Albert, 1999) that gives rise to scale-free networks: through non-decreasing submodular functions on the degree distribution.

Let X denote a symmetric matrix of edge weights. A natural convex relaxation of F would be the convex envelope of $F(\text{Supp}(X))$ under some restricted domain. For tractable h, we have by construction that F satisfies the conditions of Proposition 1 in Bach (2010b), so that the convex envelope of $F(\text{Supp}(X))$ on the L_∞ ball is precisely

the Lovász extension evaluated on $|X|$. The Lovász extension for our function is easy to determine as it is a sum of "functions of cardinality" which are considered in Bach (2010b). Below is the result from Bach (2010b) adapted to our problem.

Proposition 7.2. *Let $X_{i,(j)}$ be the weight of the jth edge connected to i, under a decreasing ordering by absolute value (i.e. $|X_{i,(0)}| \geq |X_{i,(1)}| \geq ... \geq |X_{i,(n-1)}|$). The notation (i) maps from sorted order to the natural ordering, with the diagonal not included. Then the convex envelope of F for tractable h over the L_∞ norm unit ball is:*

$$\Omega(X) = \sum_{i=0}^{n} \sum_{k=0}^{n-1} (h(k+1) - h(k)) \left| X_{i,(k)} \right|.$$

This function is piece-wise linear and convex.

The form of Ω is quite intuitive. It behaves like a L_1 norm with an additional weight on each edge that depends on how the edge ranks with respect to the other edges of its neighbouring nodes.

7.3 Optimisation

We are interested in using Ω as a prior, for optimisations of the form

$$\text{minimize}_X \quad f(X) = g(X) + \alpha\Omega(X),$$

for a convex negative log likelihood g and prior strength parameter $\alpha \geq 0$, over symmetric X. We will focus on the simplest structure learning problem that occurs in graphical model training, that of Gaussian models. In which case we have

$$g(X) = \langle X, C \rangle - \log\det X,$$

where C is the observed covariance matrix of our data (see Section 6.3 for the derivation). The support of X will then be the set of edges in the undirected graphical model together with the node precisions. This function is a rescaling of the maximum likelihood objective. In order for the resulting X to define a normalisable distribution, X must be restricted to the cone of symmetric positive definite matrices. This is not a problem in practice as $g(X)$ is infinite on the boundary of the PSD cone, and hence the constraint can be handled by restricting optimisation steps to the interior of the cone. In fact X can be shown to be in a strictly smaller cone, $X^* \succeq aI$, for a constant a derivable from C (Lu, 2009). This restricted domain is useful as $g(X)$ is Lipschitz smooth over $X \succeq aI$ but not over all positive definite matrices (Scheinbert et al., 2010).

There are a number of possible algorithms that can be applied for optimising a convex non-differentiable objective such as f. Bach (2010b) suggests two approaches

to optimising functions involving submodular relaxation priors; a subgradient approach and a proximal approach.

Subgradient methods are the simplest class of methods for optimising non-smooth convex functions. They provide a good baseline for comparison with other methods. For our objective, a subgradient is simple to evaluate at any point, due to the piecewise continuous nature of $\Omega(X)$. Unfortunately (primal) subgradient methods for our problem will not return sparse solutions except in the limit of convergence. They will instead give intermediate values that oscillate around their limiting values.

An alternative is the use of proximal methods. Proximal methods exhibit superior convergence in comparison to subgradient methods, and produce sparse solutions. Proximal methods rely on solving a simpler optimisation problem, known as the *proximal operator* at each iteration:

$$\arg\min_X \left[\alpha\Omega(X) + \frac{1}{2}\|X - Z\|_2^2\right],$$

where Z is a variable that varies at each iteration. For many problems of interest, the proximal operator can be evaluated using a closed form solution. For non-decreasing submodular relaxations, the proximal operator can be evaluated by solving a submodular minimisation on a related (not necessarily non-decreasing) submodular function (Bach, 2010b).

Bach (2010b) considers several example problems where the proximal operator can be evaluated using fast graph cut methods. For the class of functions we consider, graph-cut methods are not applicable. Generic submodular minimisation algorithms can be as bad as $O(p^6)$ for p variables (Fujishige, 2005), giving $O(n^{12})$ for a n-vertex graph (optimizing over $O(n^2)$ edges), which is clearly impractical. We will instead propose a dual decomposition method for solving this proximal operator problem in Section 7.3.2.

For solving our optimisation problem, instead of using the standard proximal method (sometimes known as ISTA), which involves a gradient step followed by the proximal operator, we propose to use the alternating direction method of multipliers (ADMM), which has shown good results when applied to the standard L_1 regularised covariance selection problem (Scheinbert et al., 2010). Next we show how to apply ADMM to our problem.

7.3.1 Alternating direction method of multipliers

The alternating direction method of multipliers (ADMM) is one approach to optimising our objective. ADMM is a classical method (Gabay and Mercier 1976; Glowinski and Marrocco 1975), recently repopularised in Boyd et al. 2011.

ADMM has a number of advantages over the basic proximal method. Let U be the matrix of dual variables for the decoupled problem:

$$\begin{aligned} \text{minimize}_X \quad & g(X) + \alpha\Omega(Y), \\ s.t. \quad & X = Y. \end{aligned}$$

Following the presentation of the algorithm in Boyd et al. (2011), given the values $Y^{(l)}$ and $U^{(l)}$ from iteration l, with $U^{(0)} = 0_n$ and $Y^{(0)} = I_n$ the ADMM updates for iteration $l+1$ are:

$$\begin{aligned} X^{(l+1)} &= \arg\min_X \left[\langle X, C \rangle - \log\det X + \frac{\rho}{2} ||X - Y^{(l)} + U^{(l)}||_2^2 \right], \\ Y^{(l+1)} &= \arg\min_Y \left[\alpha\Omega(Y) + \frac{\rho}{2} ||X^{(l+1)} - Y + U^{(l)}||_2^2 \right], \\ U^{(l+1)} &= U^{(l)} + X^{(l+1)} - Y^{(l+1)}, \end{aligned}$$

where $\rho > 0$ is a fixed step-size parameter (we used $\rho = 0.5$). The advantage of this form is that both the X and Y updates are a proximal operation. It turns out that the proximal operator for g (i.e. the $X^{(l+1)}$ update) actually has a simple solution (Scheinbert et al., 2010) that can be computed by taking an eigenvalue decomposition $Q^T \Lambda Q = \rho(Y - U) - C$, where $\Lambda = \text{diag}(\lambda_1, \ldots, \lambda_n)$ and updating the eigenvalues using the formula

$$\lambda_i' := \frac{\lambda_i + \sqrt{\lambda_i^2 + 4\rho}}{2\rho},$$

to give $X = Q^T \Lambda' Q$. The stopping criterion we used was $\left\| X^{(l+1)} - Y^{(l+1)} \right\| < \epsilon$ and $\left\| Y^{(l+1)} - Y^{(l)} \right\| < \epsilon$. In practice the ADMM method is one of the fastest methods for L_1 regularised covariance selection. Scheinbert et al. (2010) show that convergence is guaranteed if additional cone restrictions are placed on the minimisation with respect to X, and small enough step sizes are used. For our degree prior regulariser, the difficultly is in computing the proximal operator for Ω, as the rest of the algorithm is identical to that presented in Boyd et al. (2011). We now show how we solve the problem of computing the proximal operator for Ω.

7.3.2 Proximal operator using dual decomposition

Here we describe the optimisation algorithm that we effectively use for computing the proximal operator. The regulariser Ω has a quite complicated structure due to the interplay between the terms involving the two end points for each edge. We can decouple these terms using the dual decomposition technique, by writing the

Algorithm 7.1 Dual decomposition main

input: matrix Z, constants α, ρ
input: step-size $0 < \eta < 1$
initialise: $X = Z$
initialise: $V = 0_n$
repeat
  for $l = 0$ **until** $n - 1$ **do**
    $X_{l*} = \text{solveSubproblem}(Z_{l*}, V_{l*})$ # *Algorithm 7.2*
  end for
  $V = V + \eta(X - X^T)$
until $||X - X^T|| < 10^{-6}$
$X = \frac{1}{2}(X + X^T)$ # *symmetrise*
round: any $|X_{ij}| < 10^{-15}$ to 0
return X

proximal operation for a given $Z = Y - U$ as:

$$\text{minimize}_X = \frac{\alpha}{\rho} \sum_i^n \sum_k^{n-1} (h(k+1) - h(k)) \left| X_{i,(k)} \right| + \frac{1}{2} ||X - Z||_2^2$$
$$s.t. \quad X = X^T.$$

The only difference so far is that we have made the symmetry constraint explicit. Taking the dual gives a formulation where the upper and lower triangle are treated as separate variables. The dual variable matrix V corresponds to the Lagrange multipliers of the symmetry constraint, which for notational convenience we store in an anti-symmetric matrix. The dual decomposition method is given in Algorithm 7.1.

We use the notation X_{i*} to denote the ith row of X. Since this is a dual method, the primal variables X are not feasible (i.e. symmetric) until convergence. Essentially we have decomposed the original problem, so that now we only need to solve the proximal operation for each node in isolation, namely the sub-problems:

$$\forall i.\ X_{i*}^{(l+1)} = \arg\min_x \frac{\alpha}{\rho} \sum_k^{n-1} (h(k+1) - h(k)) \left| x_{(k)} \right| + ||x - Z_{i*} + V_{i*}^{(l)}||_2^2. \tag{7.1}$$

Note that the dual variable has been integrated into the quadratic term by completing the square. As the diagonal elements of X are not included in the sort ordering, they will be minimised by $X_{ii} = Z_{ii}$, for all i. Each sub-problem is strongly convex as they consist of convex terms plus a positive quadratic term. This implies that the dual problem is differentiable (as the subdifferential contains only one subgradient), hence the V update is actually gradient ascent. Since a fixed step size is used, and the dual is Lipschitz smooth, for sufficiently small step-size convergence is guaranteed. In practice we used $\eta = 0.9$ for all our tests.

This dual decomposition sub-problem can also be interpreted as just a step within

the ADMM framework. If applied in a standard way, only one dual variable update would be performed before another expensive eigenvalue decomposition step. Since each iteration of the dual decomposition is much faster than the eigenvalue decomposition, it makes more sense to treat it as a separate problem as we propose here. It also ensures that the eigenvalue decomposition is only performed on symmetric matrices.

Each sub-problem in our decomposition is still a non-trivial problem. They do have a closed form solution, involving a sort and several passes over the node's edges, as described in Algorithm 7.2.

Proposition 7.3. *Algorithm 7.2 solves the sub-problem in Equation 7.1.*

Proof. See Section 7.6. The main subtlety is the grouping together of elements induced at the non-differentiable points. If multiple edges connected to the same node have the same absolute value, their subdifferential becomes the same, and they behave as a single point whose weight is the average. To handle this grouping, we use a disjoint-set data-structure, where each x_j is either in a singleton set, or grouped in a set with other elements, whose absolute value is the same. □

7.4 Alternative Degree Priors

Under the restrictions on h detailed in Proposition 7.1, several other choices seem reasonable. The scale free prior can be smoothed somewhat, by the addition of a linear term, giving

$$h_{\epsilon,\beta}(i) = \log(i + \epsilon) + \beta i,$$

where β controls the strength of the smoothing. A slower diminishing choice would be a square-root function such as

$$h_{\beta}(i) = (i + 1)^{\frac{1}{2}} - 1 + \beta i.$$

This requires the linear term in order to correspond to a normalisable prior.

Ideally we would choose h so that the expected degree distribution under the ERG model matches the particular form we wish to encourage. Finding such a h for a particular graph size and degree distribution amounts to maximum likelihood parameter learning, which for ERG models is a hard learning problem. The most common approach is to use sampling based inference. Approaches based on Markov chain Monte Carlo techniques have been applied widely to ERG models (Snijders, 2002) and are therefore applicable to our model.

Algorithm 7.2 Dual decomposition sub-problem (*solveSubproblem*)

input: vectors z, v
initialise: Disjoint-set datastructure with set membership function γ
$w = z - v$ # *w gives the sort order*
$u = 0_n$
build: sorted-to-original position function μ under descending absolute value order of w, excluding the diagonal
for $k = 0$ **until** $n - 1$ **do**
  $j = \mu(k)$
  $u_j = |w_j| - \frac{\alpha}{\rho}\left(h(k+1) - h(k)\right)$
  $\gamma(j)$.value $= u_j$
  r = k
  while $r > 1$ and $\gamma(\mu(r))$.value $\geq \gamma(\mu(r-1))$.value **do**
    join: the sets containing $\mu(r)$ and $\mu(r-1)$
    $\gamma(\mu(r))$.value $= \frac{1}{|\gamma(\mu(r))|}\sum_{i \in \gamma(\mu(r))} u_i$
    set: r to the first element of $\gamma(\mu(r))$ by the sort ordering
  end while
end for
for $i = 1$ **to** N **do**
  $x_i = \gamma(i)$.value
  if $x_i < 0$ **then**
    $x_i = 0$ # *negative values imply shrinkage to 0*
  end if
  if $w_i < 0$ **then**
    $x_i = -x_i$ # *Correct orthant*
  end if
end for
return x

7.5 Experiments

7.5.1 Reconstruction of synthetic networks

We performed a comparison against the reweighted L_1 method of Liu and Ihler (2011), and a standard L_1 regularised method, both implemented using ADMM for optimisation. Although Liu and Ihler (2011) use the glasso (Friedman et al., 2007) method for the inner loop, ADMM will give identical results, and is usually faster (Scheinbert et al., 2010). Graphs with 60 nodes were generated using both the Barabasi-Albert model (Barabasi and Albert, 1999) and a predefined degree distribution model sampled using the method from Bayati et al. (2009) implemented in the NetworkX software package. Both methods generate scale-free graphs; the BA model exhibits a scale parameter of 3.0, whereas we fixed the scale parameter at 2.0 for the other model.

To define a valid Gaussian model, edge weights of $X_{ij} = -0.2$ were assigned, and the node weights were set at $X_{ii} = 0.5 - \sum_{i \neq j} X_{ij}$ so as to make the resulting precision matrix diagonally dominant. The resulting Gaussian graphical model was sampled 500 times. The covariance matrix of these samples was formed, then normalised to have diagonal uniformly 1.0. We tested with the two h sequences described in Section 7.4. The parameters for the degree weight sequences were chosen by grid search on random instances separate from those we tested on. The resulting ROC curves for the Hamming reconstruction loss are shown in Figure 7.1. Results were averaged over 30 randomly generated graphs for each each figure.

We can see from the plots that our method with the square-root weighting presents results superior to those from Liu and Ihler (2011) for these datasets. This is encouraging particularly since our formulation is convex while the one from Liu and Ihler (2011) is not. Interestingly, the log based weights give very similar but not identical results to the reweighting scheme which also uses a log term. The only case where it gives inferior reconstructions is when it is forced to give a sparser reconstruction than the original graph.

7.5.2 Reconstruction of a gene activation network

A common application of sparse covariance selection is the estimation of gene association networks from experimental data. A covariance matrix of gene co-activations from a number of independent micro-array experiments is typically formed, on which a number of methods, including sparse covariance selection, can be applied. Sparse estimation is key for a consistent reconstruction due to the small number of experiments performed. Many biological networks are conjectured to be scale-free, and additionally ERG modelling techniques are known to produce good results on

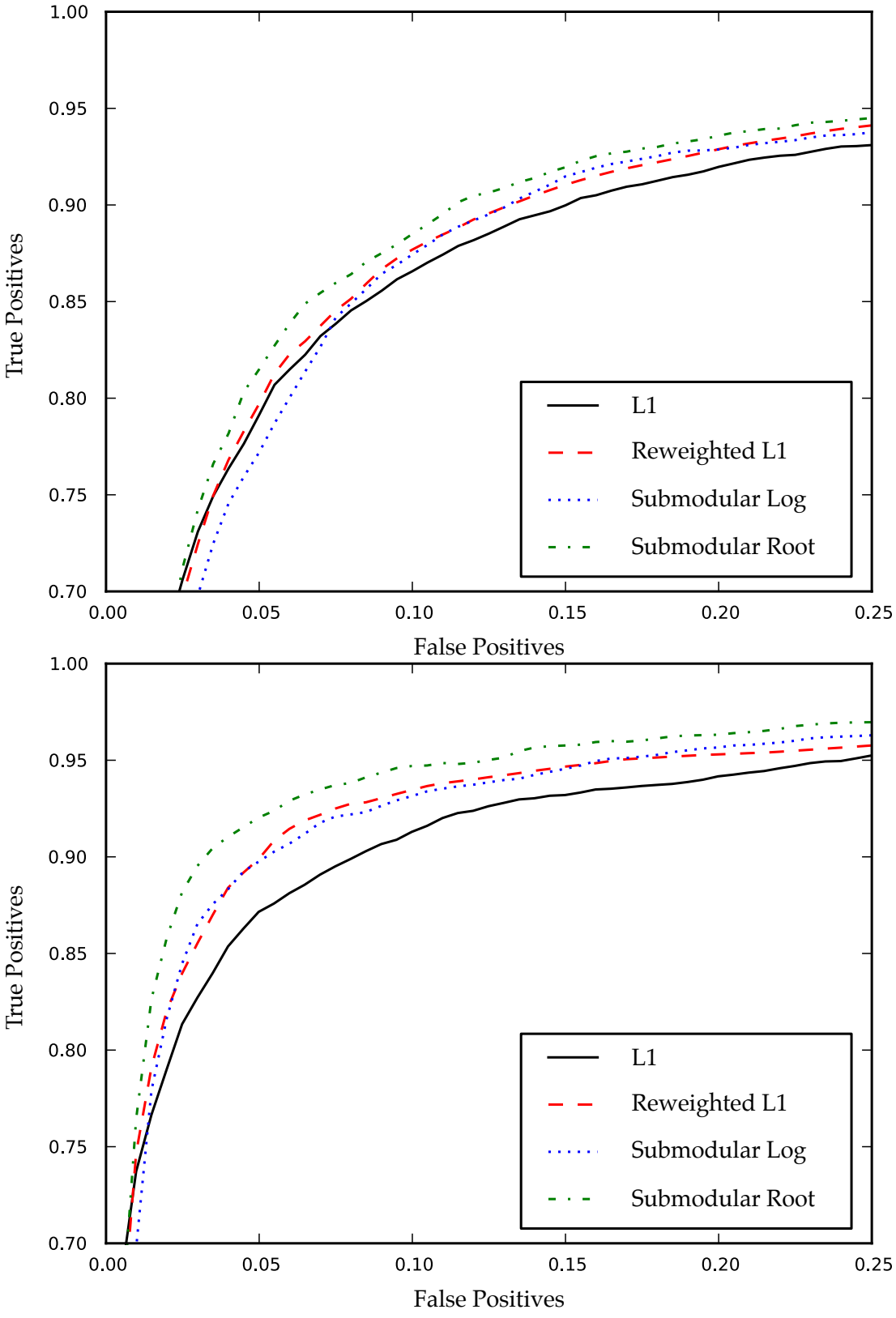

Figure 7.1: ROC curves for BA model (top) and fixed degree distribution model (bottom)

biological networks (Saul and Filkov, 2007). So we consider micro-array datasets a natural test-bed for our method. We ran the three methods considered on the first 500 genes from the GDS1429 dataset [1], which contains 69 samples for 8565 genes. The parameters for both methods were tuned to produce a network with near to 50 edges for visualisation purposes. The major connected component for each is shown in Figure 7.2.

While these networks are too small for valid statistical analysis of the degree distribution, the submodular relaxation method produces a network with structure that is commonly seen in scale free networks. The star subgraph centered around gene 60 is more clearly defined in the submodular relaxation reconstruction, and the tight cluster of genes in the right is less clustered in the L_1 reconstruction. The reweighted L_1 method produced a quite different reconstruction, with greater clustering.

7.5.3 Runtime comparison: different proximal operator methods

We performed a comparison against two other methods for computing the proximal operator: subgradient descent and the minimum norm point (MNP) algorithm. The MNP algorithm is a submodular minimisation method that can be adapted for computing the proximal operator (Bach, 2010b). We took the input parameters from the last invocation of the proximal operator in the BA test, at a prior strength of 0.7. We then plotted the convergence rate of each of the methods, shown in Figure 7.3. As the tests are on randomly generated graphs, we present only a representative example.

It is clear from this and similar tests that we performed that the subgradient descent method converges too slowly to be of practical applicability for this problem. Subgradient methods can be a good choice when only a low accuracy solution is required; for convergence of ADMM the error in the proximal operator needs to be smaller than what can be obtained by the subgradient method. The MNP method also converges slowly for this problem, however it achieves a low but usable accuracy quickly enough that it could be used in practice. The dual decomposition method achieves a much better rate of convergence, converging quickly enough to be of use even for strong accuracy requirements.

The time for individual iterations of each of the methods was 0.65ms for subgradient descent, 0.82ms for dual decomposition and 15ms for the MNP method. The speed difference is small between a subgradient iteration and a dual decomposition iteration as both are dominated by the cost of a sort operation. The cost of a MNP iteration is dominated by two least squares solves, whose running time in the worst case is proportional to the square of the current iteration number. Overall, it is clear that our dual decomposition method is significantly more efficient.

[1] http://www.ncbi.nlm.nih.gov/gds/1429

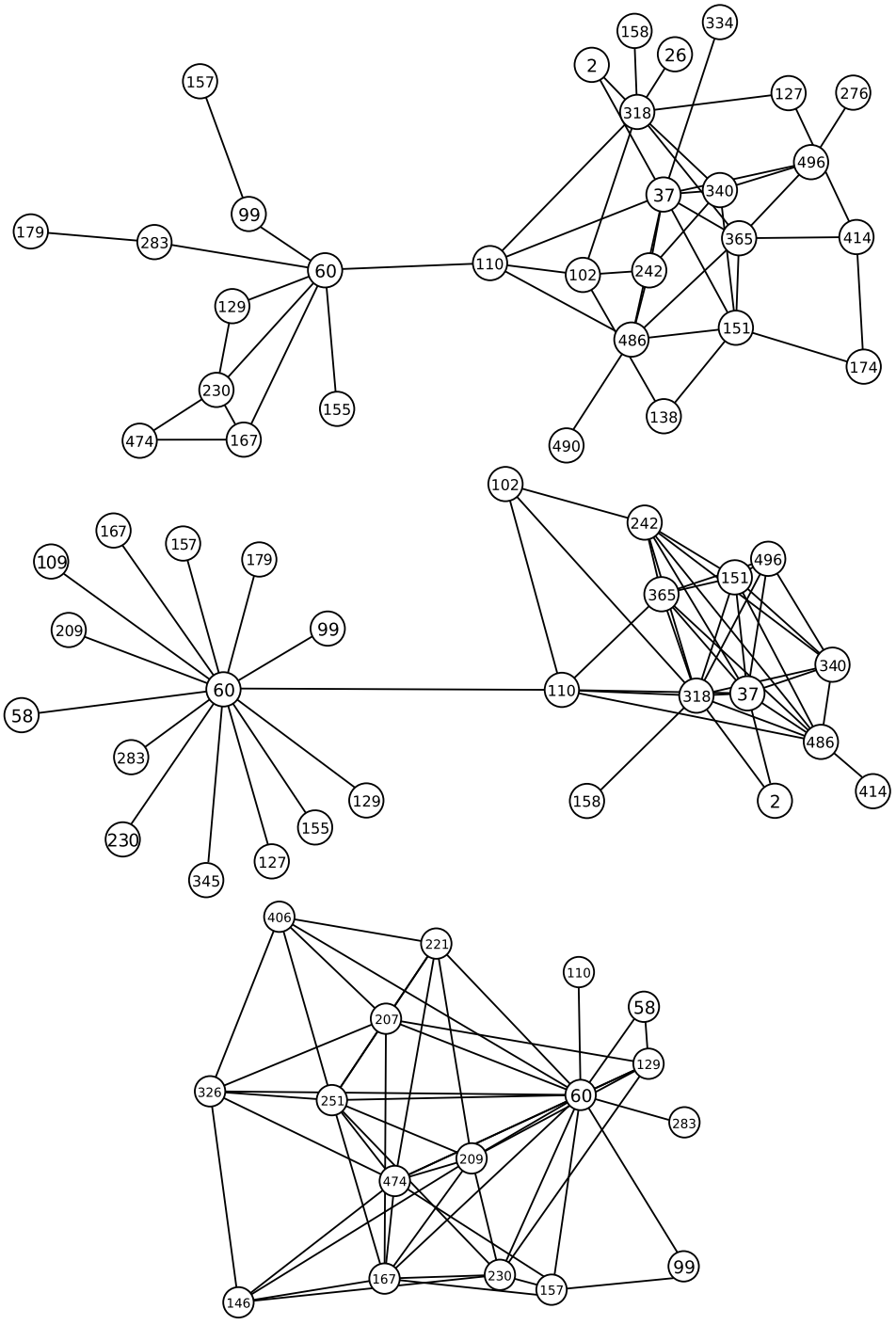

Figure 7.2: Reconstruction of a gene association network using L_1 (top), submodular relaxation (middle), and reweighted L_1 (bottom) methods

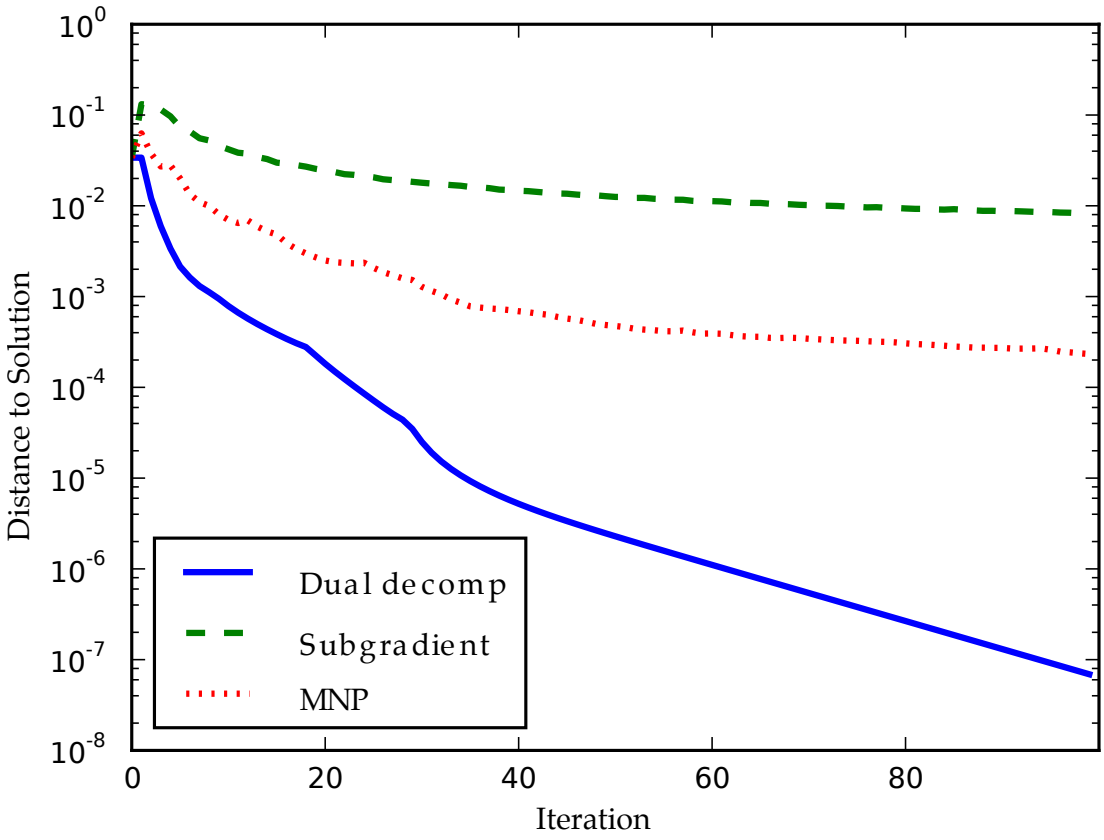

Figure 7.3: Comparison of proximal operators

7.5.4 Runtime comparison: submodular relaxation against other approaches

The running time of the three methods we tested is highly dependent on implementation details, so the following speed comparison should be taken as a rough guide. For a sparse reconstruction of a BA model graph with 100 vertices and 200 edges, the average running time per 10^{-4} error reconstruction over 10 random graphs was 16 seconds for the reweighted L_1 method and 5.0 seconds for the submodular relaxation method. This accuracy level was chosen so that the active edge set for both methods had stabilised between iterations. For comparison, the standard L_1 method was significantly faster, taking only 0.72 seconds on average.

7.6 Proof of Correctness

Proof. In this section we establish that Algorithm 7.2 solves Equation 7.1. First we note that the pseudo-code uses $\mu(i)$ instead of (i) to denote the mapping from sort order to storage order, to remove ambiguity. We also use object-oriented notation $\gamma(p)$ to represent the set containing p, with $\gamma(p)$.value denoting the value field of the set object. This value field is interpreted as the absolute value of each of the elements of the set, with a negative value implying zero. The value field is stored as an ancillary array in our implementation. We also need an operation that returns the "first" element of the set, which in our data structure is just the root of the tree that represents the set.

We start by simplifying the notation to

$$f(x) = \frac{\alpha}{\rho} \sum_{j=1}^{n} h'(j) \left| x_{(j)} \right| + \frac{1}{2} ||x - w_j||_2^2,$$

where $w_j = z_{(j)} - v_{(j)}$, and $h'(j) = h(j) - h(j-1)$. We want to find $\arg\min_x f(x)$. We consider the two main cases.

Unique valued x_j

First we take the gradient when x_j is not at the same value as another, and is non-zero:

$$\frac{\partial f}{\partial x_{(j)}} = \frac{\alpha}{\rho} h'(j) \mathrm{sgn}(x_{(j)}) + x_{(j)} - w_j.$$

Equating to zero gives:

$$|x_{(j)}| = |w_j| - \frac{\alpha}{\rho} h'(j), \tag{7.2}$$

when $|w_j| > \frac{\alpha}{\rho} h'(j)$, with $\mathrm{sgn}(x_{(j)}) = \mathrm{sgn}(w_j)$. If $|w_j| \leq \frac{\alpha}{\rho} h'(j)$, then clearly the gradient can not be equated to zero except at $x_{(j)} = 0$, where the subdifferential

needs to be considered. Considering the subdifferential at zero gives the requirement that

$$\frac{w_j}{\frac{\alpha}{\rho}h'(j)} \in [-1, 1],$$

which follows from $|w_j| \leq \frac{\alpha}{\rho}h'(j)$. So essentially if $|w_j| - \frac{\alpha}{\rho}h'(j) \leq 0$ we set $x_{(j)} = 0$. This is essentially the same shrinkage as performed in the proximal operator of a L_1 regulariser.

Non-unique x_j

The above update is used for singleton sets in Algorithm 7.2. Now when several $x_{(j)}$ have the same value, say a set Q of them, and none of them are zero, then equating the gradients to zero gives a set of equations, which can be solved to give

$$\forall j \in Q, \quad \text{sgn}(w_j)x_{(j)} = \frac{1}{|Q|}\sum_{i \in Q}\left(|w_i| - \frac{\alpha}{\rho}h'(i)\right). \tag{7.3}$$

One direct implication of this is that the sort ordering for equal variables doesn't effect the solution, so a stable sort is not necessary in Algorithm 7.2. The result for the singleton case where the value is negative follows also for the grouped together variables.

It suffices to show that at termination of Algorithm 7.2, these equations (7.2 or 7.3) are satisfied by the returned x^* for all j, as this implies that 0 is in the subdifferential at x^*. The assignments in Algorithm 7.2 clearly ensure that this is the case under the assumption that the sort ordering of $|w_j|$ is the same as the sort order of $|x_{(j)}|$ after termination of the algorithm, and likewise for the grouped variables. So we just need to show that the assignments to the $x_{(j)}$ result in that ordering. In particular since $x_i = \gamma(i)$.value for positive $x_i$and w_i, we need that for all p, q:

$$|w_p| > |w_q| \implies \gamma(\mu(p)).\text{value} > \gamma(\mu(q)).\text{value}.$$

We proceed by induction, with the inductive hypothesis at step k being that the ordering is correct for each group containing $\mu(l) < k$, i.e.

$$\forall \mu(p) < k, \mu(q) < k\text{:} \quad |w_p| > |w_q| \implies \gamma(\mu(p)).\text{value} > \gamma(\mu(q)).\text{value}.$$

The base case $k = 0$ doesn't trigger the while loop, it just finds $j = \mu(k)$, then sets u_j using Equation 7.2 and sets the singleton set containing j with that value also ($\gamma(j)$.value $= u_j$). Our inductive hypothesis holds since it is a vacuous statement for $k = 0$.

Assume now that at iteration $k - 1$ of the first loop in Algorithm 7.2 the inductive hypothesis holds. Then at iteration k, a new singleton set is created for $j = \mu(k)$, with value given by $|w_j| - \frac{\alpha}{\rho}h'(j)$. If $\gamma(j)$'s value is less than the value of $\mu(k-1)$, then by induction the ordering is correct. Otherwise, the algorithm proceeds by adding j to

set $\mu(k-1)$, and updating the value of j's new set to the average from Equation 7.3. This will increase the value of the set, which may cause its value to increase above that of another set. That case is handled by the repeated merging in the main while loop, in the same manner. It is clear that the while loop must terminate after no more than k steps, as it performs at one merge per iteration. At termination of the while loop the ordering is then correct up to k, as all changes in the set values that would cause the ordering to change instead have caused set merges. □

Chapter 8

Fast Approximate Structural Inference

In Chapter 6 we described how learning the structure of a Gaussian graphical model can be phrased as a regularised maximum likelihood learning problem. This formulation gives good results but scales poorly as the number of variables is increased. Intuitively, it seems overkill to find the values of all the edge weights when we are only concerned with the existence or non-existence of edges. In this chapter we consider the conditional covariance thresholding method (CCT, Anandkumar et al., 2011b) which only looks at a small neighbourhood of each edge when determining if it is part of the structure. The effect of distant parts of a graph decays exponentially, so for large graphs with high diameters, looking at just a neighbourhood can be a substantial saving. We give a modification of the CCT method that improves its running time by a factor of $O(\sqrt{p})$ for p variables, reducing it to $O(p^{2.5})$ in the important $\eta = 1$ case of the method. This allows the method to be applied to substantially larger problems in practice, essentially any problem for which the covariance matrix can be formed in memory.

Section 8.1 describes our algorithm, and discusses its running time in theory and practice. Our experiments in Section 8.3 cover the reconstruction of synthetically generated networks, as well as two practical problems: determining the conditional independence relations in stock-market prices and weather station data.

8.1 SHORTCUT

Recall the conditional covariance thresholding (CCT) method from Section 6.3.3. It starts by forming the following matrix W:

$$W_{ij} = \min_{S \subset V \setminus \{i,j\}, |S| \leq \eta} \left| Cov[x_i, x_j | x_S] \right|,$$
$$\text{where } Cov[x_i, x_j | x_S] = C_{ij} - C_{iS} C_{SS}^{-1} C_{Sj}.$$

The matrix W is then thresholded by a constant t to give the edge structure. The CCT method is only practical for $\eta = 1$ or $\eta = 2$ for moderately sized problems. In many applications the number of variables can be as large as 10,000 to 100,000, and in those cases even the $\eta = 1$ variant is too slow. SHORTCUT is fundamentally a variant of the conditional covariance thresholding method in the $\eta = 1$ regime. We propose to modify the minimisation:

$$\min_{k \in V \setminus \{i,j\}} \left| C_{ij} - \frac{C_{ik} C_{kj}}{C_{kk}} \right|,$$

to:

$$\max \left\{ 0 \,,\, \min_{k \in V \setminus \{i,j\}} \left| C_{ij} \right| - \operatorname{sgn}(C_{ij}) \frac{C_{ik} C_{kj}}{C_{kk}} \right\}.$$

We make this approximation to allow for more efficient algorithms for evaluating the inner minimisation. To understand this approximation, without loss of generality, consider the case where C_{ij} is positive. For positive C_{ij}, our modification is identical except when $\frac{C_{ik} C_{kj}}{C_{kk}} > C_{ij}$ for some k, in which case the approximation will return 0 instead of a small positive value. This special case only occurs if the transitive correlation over the path $i \to k \to j$ is nearly as strong as the direct correlation. Although this special case appears troubling at first glance, we show in Section 8.4 that the SHORTCUT method still gives structurally consistent reconstructions, under a similar set of problem instances as the CCT method.

The reason we make the above approximation is so we can rearrange the optimisation as:

$$\max \left\{ 0 \,,\, \sqrt{C_{ii} C_{jj}} \left(\left| \bar{C}_{ij} \right| - \max_{k \in V \setminus \{i,j\}} \operatorname{sgn}(\bar{C}_{ij}) \bar{C}_{ik} \bar{C}_{kj} \right) \right\}.$$

Where $\bar{C}_{ik} = C_{ik} / \sqrt{C_{ii} C_{kk}}$ is the correlation between x_i and x_k. This form allows us to use a fast method for computing the maximum of a set of pairwise products due to McAuley and Caetano (2011). This approach requires preprocessing, namely row-wise sorting of the correlation matrix entries, sans-diagonal. Under the assumption that the permutations that sorted row i and row j are independent, McAuley & Caetano's method performs the maximisation in expected time $O(\sqrt{p})$, which results in a reduction of the running time of the conditional covariance thresholding method to only expected time $O(p^{2.5})$. Note that the worst case is still $O(p^3)$. McAuley & Caetano's algorithm can only handle positive values, so it is necessary to run it twice, split by case; The specific method we use is shown in Algorithm 8.1; it assumes a threshold is given prescaled by $1/\sqrt{C_{ii} C_{kk}}$.

8.2 Running Time

The improvement in running time is not just theoretical. We find in practice that, for randomly generated covariance selection problems, less than $\sqrt{p}$ pairwise products

Algorithm 8.1 SHORTCUT algorithm

input: $p \times p$ Correlation matrix $\bar{C}_{ij}$, threshold t
initialise: Weight matrix W
for $i = 1$ **to** p **do**
  Build: P_i as the mapping that sorts the positive off-diagonal entries of row i of $\bar{C}$ in descending order
  Build: N_i as the mapping that sorts the negative off-diagonal entries of row i of $\bar{C}$ in ascending order
  Build: P_i^{-1} and N_i^{-1} as the inverse maps of P_i and N_i respectively
end for
for $i = 1$ **to** p, $j = 1$ **to** $i - 1$ **do**
  if $\bar{C}_{ij} >= 0$ **then**
    t_l := maxProduct($\bar{C}_{i*}$, $\bar{C}_{j*}$, P_i, P_j, P_i^{-1}, P_j^{-1})
    t_r := maxProduct($\bar{C}_{i*}$, $\bar{C}_{j*}$, N_i, N_j, N_i^{-1}, N_j^{-1})
    W_{ij} := max $\left(0, \bar{C}_{ij} - max(t_l, t_r)\right)$
  else
    t_l := maxProduct($\bar{C}_{i*}$, $|\bar{C}_{j*}|$, P_i, N_j, P_i^{-1}, N_j^{-1})
    t_r := maxProduct($|\bar{C}_{i*}|$, $\bar{C}_{j*}$, N_i, P_j, N_i^{-1}, P_j^{-1})
    W_{ij} := max $\left(0, |\bar{C}_{ij}| + max(t_l, t_r)\right)$
  end if
  $W_{ji} = W_{ij}$
end for
Threshold Set to zero any element (i, j) where $|W_{ij}| < t$
return W

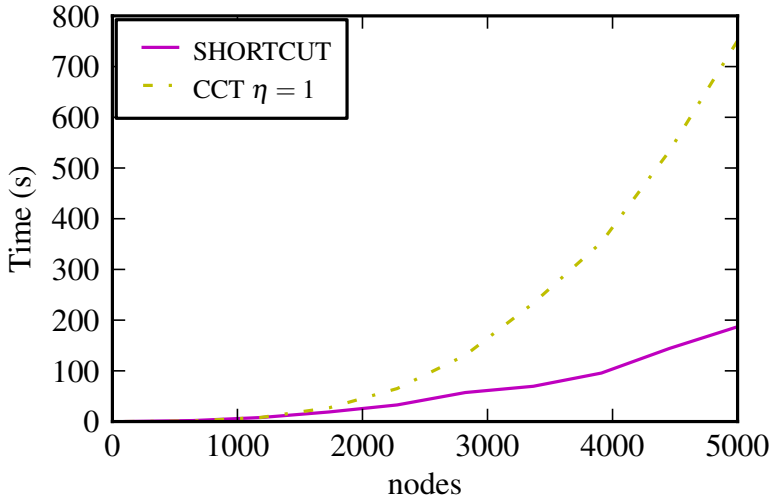

Figure 8.1: Running time of SHORTCUT on a representative problem

Algorithm 8.2 maxProduct algorithm

input: Sequences C_a, C_b, P_a, P_b, P_a^{-1}, P_b^{-1}.
initialise: start := 0, best = $P_a[0]$
initialise: max_seen := C_a [best] $\cdot$ C_b [best]
initialise: $\text{end}_a := P_a^{-1}[P_b[0]]$ and $\text{end}_b := P_b^{-1}[P_a[0]]$
// Check if $P_b[0]$ is a better starting point than $P_a[0]$
if $C_a[P_b[0]] \cdot C_b[P_b[0]] > \text{max\_seen}$ **then**
  best = $P_b[0]$
  max_seen := C_a [best] $\cdot$ C_b [best]
end if
while start $< \text{end}_a$ and start $< \text{end}_b$ **do**
  if $C_a[P_a[\text{start}]] \cdot C_b[P_a[\text{start}]] > \text{max\_seen}$ **then**
    best := P_a [start]
    max_seen := C_a [best] $\cdot$ C_b [best]
  end if
  $\text{end}_b := \min\left\{\text{end}_b, P_b^{-1}[P_a[\text{start}]]\right\}$
  // The following is the same as the 5 lines above but with a and b interchanged
  if $C_a[P_b[\text{start}]] \cdot C_b[P_b[\text{start}]] > \text{max\_seen}$ **then**
    best := P_b [start]
    max_seen := C_a [best] $\cdot$ C_b [best]
  end if
  $\text{end}_a := \min\{\text{end}_a, P_a^{-1}[P_b[\text{start}]]\}$
  start := start + 1
end while
return max_seen

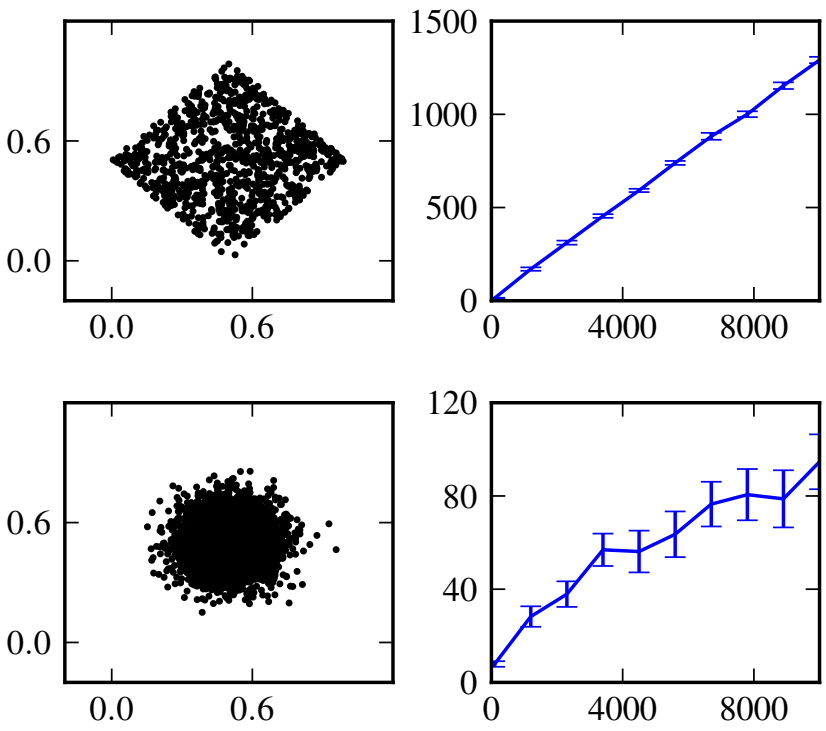

Figure 8.2: Empirical scaling of the max-product method on samples from the unit diamond and isotropic Gaussian distributions. The left hand plots are samples from the respective distributions, and the right hand plots show scaling in terms of entries examined as the number of samples increases.

per edge are required for each maxProduct invocation; the runtime is not hindered by any hidden multiplicative factors. The improvement in running time for building the conditional covariance matrix over the naive approach is illustrated in Figure 8.1, for implementations in compiled python. It behaves empirically as predicted by the asymptotic bound. The performance advantage is roughly a factor of 4 at 4000 nodes. Our method is aimed at problems with mid tens of thousands of nodes, where the advantage is much greater.

In general we have observed that the number of comparisons required (and hence the running time) is lower when the matrix entries are positively correlated within each row, although the speed-up is dependent on the distribution of the entries. For example, there exists distributions that have positive Pearson correlation coefficient, yet exhibit worst-case run-time behaviour. A simple example is uniform distribution over a diamond shape in the $[0-1]$ interval in 2 dimensions. Figure 8.2 shows the (worst-case) linear complexity of the fast max-product method on it. We have never observed this worst-case complexity when the max-product method is applied to correlation matrices, in fact they seem to closer to the ideal case.

8.3 Experiments

We ran a suite of experiments testing the SHORTCUT method against two CCT variants; CCT $\eta = 1$ which based on theoretical results should give similar results to SHORTCUT; and CCT $\eta = 2$ which should give better results at the expense of quartic running time. We also compared against correlation thresholding, which is often used by practitioners, L_1 regularised maximum likelihood on the correlation matrix, and the neighbourhood selection method discussed in Section 6.3.2 using both union and disjunction variants. Covariance thresholding was significantly inferior on our test problems, and covariance variants of the other methods performed worse than the correlation versions shown in the plots that follow.

8.3.1 Synthetic datasets

There is a substantial difficulty in doing a comprehensive evaluation of covariance selection methods due to the lack of ground truth structure information. We begin with a series of tests on synthetically generated data, using structures generated from two commonly used models: the Barabasi-Albert model (Barabasi and Albert, 1999) and the classical Erdos-Renyi model (Erdos and Renyi, 1959).

Generating synthetic data using walk summability

Walk summability is usually described in terms of a spectral condition on the matrix of partial correlation coefficients. For most practical purposes it is easier to work with the notion of *pairwise normalisability*. Maliotov et al. (2006) detail the equivalence of the two definitions. Suppose we have a Gaussian distribution with sparse precision matrix Θ. It is pairwise normalisable if Θ can be decomposed into a sum involving the precision matrices $A^{(i,j)}$ of 2D Gaussians, one for each edge, in particular:

$$\Theta_{ij} = \begin{cases} A_{ij}^{(i,j)} & \text{if } i \neq j \\ \sum_{k \in \text{ne}(i)} A_{ii}^{(i,k)} & \text{if } i = j \end{cases}.$$

Each precision matrix must be positive semidefinite, which is where the pairwise normalisable terminology comes from. This definition gives substantial insight into the properties of walk summable models. The condition is in a sense local, which is not at all clear from the spectral definition.

We can use this definition for generating walk-summable but not necessarily diagonally dominant test distributions. For our synthetic tests in Section 8.3, to choose the edge weights of our test matrices, we generated 2x2 precision matrices and then used the above summation. Each 2D precision matrix A was formed by sampling the

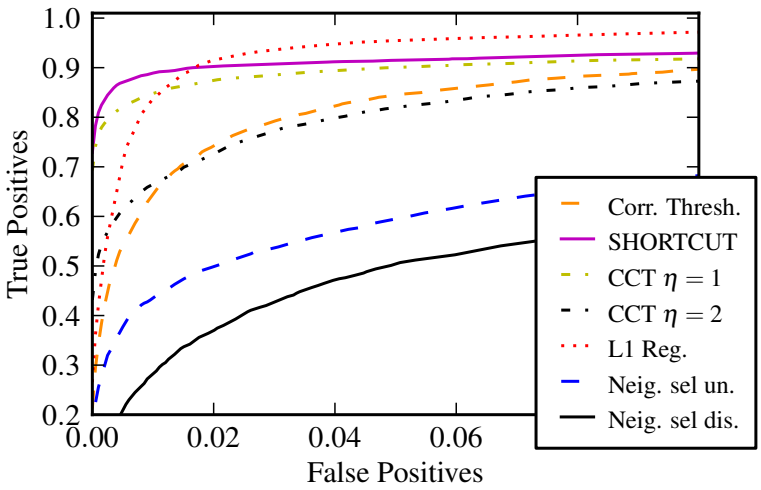

Figure 8.3: Synthetic data ROC curves for the BA model

off-diagonal element $A_{1,2}$ (chosen from a normal distribution with mean -0.2 and variance 1), then sampling a proportionality constant β and setting $A_{1,1} = \beta|A_{1,2}|$ and $A_{2,2} = \beta^{-1}|A_{1,2}|$. This gives a lopsided distribution that is harder to optimise against than typical diagonally dominant distributions.

For each plot in Figure 8.3, 30 sparse graphs were generated in each case with 60 nodes and 120 edges (in expectation). The shown line is the average over these graphs. Due to the $O(n^4)$ running time of the CCT $\eta = 2$ method, we were not able to test all methods on substantially larger graphs. For the cubic time methods, the shown trends were consistent for larger graphs. Edge weights were chosen so that the walk summable condition holds. The generation method is detailed in Section 8.3.1.

We can see in Figure 8.3 that the CCT $\eta = 2$ method performs very similarly to the $\eta = 1$ case. SHORTCUT performs similarly on the easier ER model, and slightly better on the BA model. As would be expected from the simplicity of the method, correlation matrix thresholding performs poorly. Interestingly, the L_1 regularised maximum likelihood method is out-performed by the thresholding methods for sparse reconstructions, but is able to capture a larger proportion of correct edges as the number of allowed false positives increases. It's notable that neighbourhood selection performs particularly badly on these synthetic problems. We were not able to determine a good reason for this. Their performance is more in line with the other methods on the real world datasets in the next section.

8.3.2 Real world datasets

In this set of experiments we used a different comparison methodology than in the synthetic case. Instead of comparing the structure learned we can compare the quality of the structure when used to fit a maximum likelihood model. Essentially we use

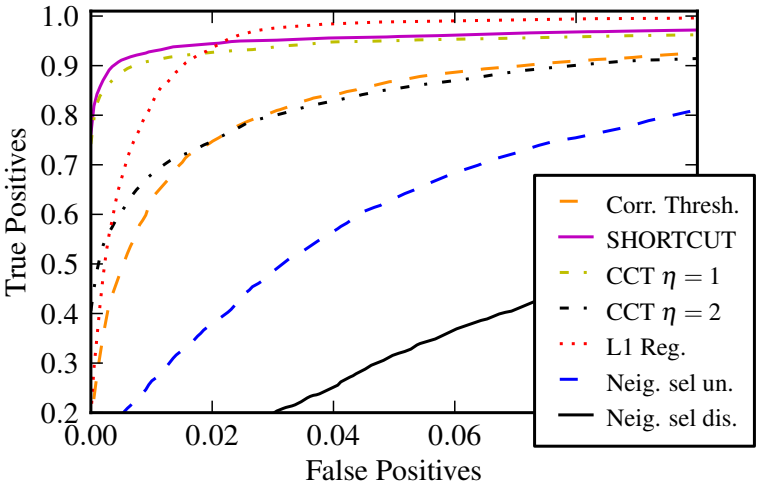

Figure 8.4: Synthetic data ROC curves for the ER model

each method as described, then we fit parameters to a model with each structure as fixed. We can then compare the likelihood of held out data, which gives us an idea of how well each structure captures the true dependencies in the data. This avoids the difficulty of requiring the ground truth structure. Instead of the likelihood, we plot the negation of the objective in Equation 6.4, which is a shifted and scaled negative log likelihood.

For our first real world dataset test we choose stock market data. We gathered the daily fractional change in value of each share in the ASX300 between Feb 1 2012 and 18 Dec 2012. We then removed any shares with missing data, or those that were not part of the ASX300 for the whole period. This left us with 235 shares over 250 days. We used a 125/125 train/test split. Figure 8.5 shows the resulting test likelihood on model trained on structure from each method, for varying number of edges.

We see that on this problem SHORTCUT performs better than L_1 regularised maximum likelihood, which is significantly better than correlation thresholding. As in the other tests, SHORTCUT performs similar to or better than the CCT $\eta = 1$ method. The neighbourhood selection methods give middle of the pack performance.

For our second test we used climate data. We extracted the maximum daily temperatures from all of the weather stations in NSW, Australia that reported temperatures for each day between Jan 1st 2012 and Dec 1st 2012. This gave us 171 stations with 336 temperature readings for each. As before, we use even split between test and training data.

On this particular problem the advantages of CCT with $\eta = 2$ is much more apparent. Figure 8.6 shows that it outperforms the other methods, at the expense of quite prohibitive running time. Like in the other cases, SHORTCUT performs similarly to CCT $\eta = 1$, but interestingly simple correlation thresholding is more effective than

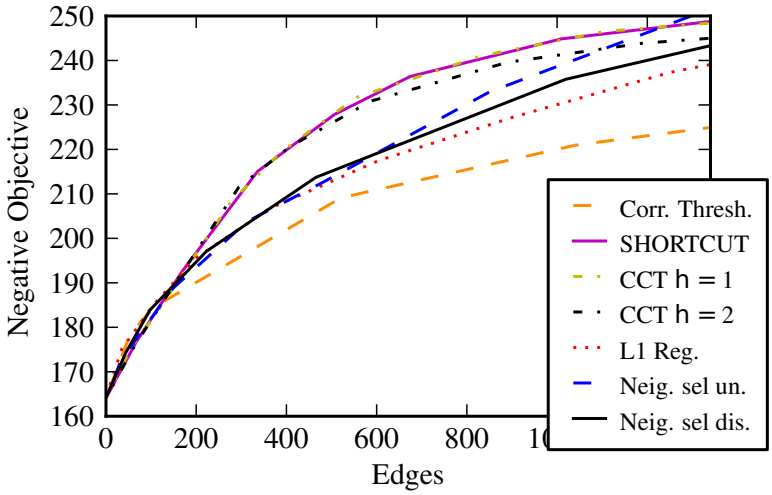

Figure 8.5: Comparison on stock market data

either for this problem. Neighbourhood selection performs very well using the union variant, and very poorly using the disjunction variant.

8.4 Theoretical Properties

Although our algorithm differs from the CCT method, we show in this section that our method has the same theoretical guarantees, although with slightly stronger assumptions required. Anandkumar et al. (2011a) are able to show that CCT provides reconstructions structurally consistent with the true model, under a set of asymptotic conditions. The key requirements are that the number of samples n scales with the number of nodes p as $n = \Omega\left(\Theta_{\min}^{-2} \log p\right)$, that the model be walk summable, and that a form of local-separation holds. See Anandkumar et al. (2011a, p10-11) for details. Their proof proceeds by considering the noise-free (exact covariance) case. They show that if nodes i and j are not neighbours, then the maximum absolute conditional covariance over nodes $k \in V \backslash \{i, j\}$ is bounded. They then show that if i and j are neighbours, then the *minimum* absolute conditional covariance over k is bounded away from zero. Thus the CCT method can separate the two cases successfully, with an appropriate choice of threshold.

Pairs of non-neighbouring nodes will be thresholded under both SHORTCUT and CCT, as the bounded distance from zero ensures that they would be beneath of threshold of CCT if they changed sign (recall that SHORTCUT only behaves differently for entries whose covariance's sign differs from the CC matrices sign). So we only need to consider the case of neighbouring nodes. The relevant lemma from the CCT proof is as follows:

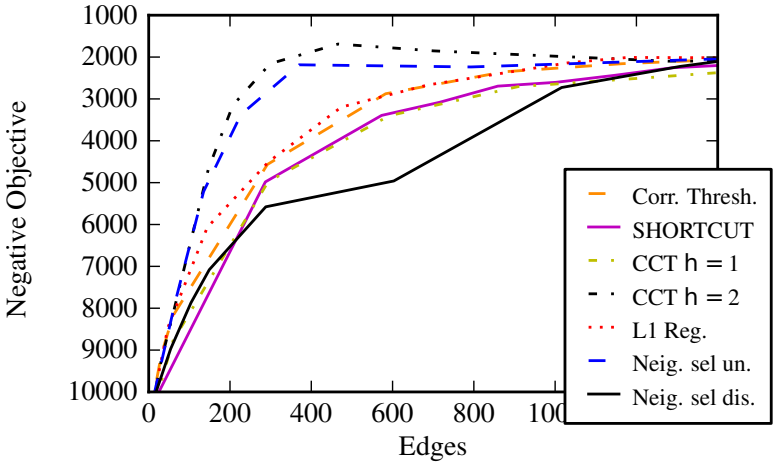

Figure 8.6: Comparison on climate data

Lemma 8.1. ***[Lemma 14 in Anandkumar et al. (2011a), p27]*** *For an α-walk summable graphical model satisfying*

$$D_{\min}(1-\alpha)\min_{(i,j)\in G}\frac{|\Theta_{ij}|}{K} > 1+\delta,$$

for some $\delta > 0$ (not depending on p), where $D_{\min} := \min_i \Theta_{ii}$ and $K = \left\|\Theta_{\{i,j\}(V\setminus\{i,j\})}\right\|^2$, and where $K > 2\Theta_{ii}\Theta_{jj}$. Then we have

$$|\Sigma(i,j|k)| = \Omega(\Theta_{\min}),$$

for any neighbouring (i,j) and any $k \in V\setminus\{i,j\}$, where $\Theta_{\min}$ is the minimum element of Θ.

The assumptions in this lemma are the key technical assumptions about the data. The bound on K is the additional assumption on top of those made by Anandkumar et al. (2011a). Note that the absolute value around Θ_{ij} is a correction of an apparent typo. We will modify their proof of this lemma to additionally show that the sign of $\Sigma(i,j|k)$ is the same as $\Sigma(i,j)$, so that the SHORTCUT method will not incorrectly threshold in the neighbouring case.

Proof. We use the notation $A = \{i,j\}$ and $B = V\setminus\{i,j,k\}$. Let $\tilde{\Sigma}$ denote the conditional covariance matrix of $A \cup B$ conditioned on k, it is formed by removing row and column k from Θ, then inverting. We are interested in the 2x2 sub-matrix $\tilde{\Sigma}_{AA}$, as it contains the conditional covariance value we are interested in. It can be expressed as part of block matrix inversion:

$$\tilde{\Sigma} = \begin{bmatrix} \Theta_{AA} & \Theta_{AB} \\ \Theta_{BA} & \Theta_{BB} \end{bmatrix}^{-1} = \begin{bmatrix} \left(\Theta_{AA} - \Theta_{AB}\Theta_{BB}^{-1}\Theta_{BA}\right)^{-1} & \cdots \\ \cdots & \cdots \end{bmatrix}.$$

So in order to bound $\Sigma(i,j|k) = \tilde{\Sigma}_{i,j}$ away from zero, we need to upper bound the absolute value of $\rho := \Theta_{AB}\Theta_{BB}^{-1}\Theta_{BA}$, so that $\tilde{\Theta}_{AA} := \Theta_{AA} - \rho$ is bounded away from zero.

Anandkumar et al. (2011a) establish that the maximum element of ρ is bounded by

$$\frac{\|\Theta_{AB}\|^2}{D_{\min}(1-\alpha)},$$

a constant, and thus since $\Theta_{i,j} > \Theta_{\min}$, we have that $\tilde{\Theta}_{ij} = \Omega(\Theta_{\min})$. It follows from 2x2 matrix inversion that

$$\Sigma(i,j|k) = \frac{-\tilde{\Theta}_{ij}}{\tilde{\Theta}_{ii}\tilde{\Theta}_{jj} - \tilde{\Theta}_{ij}^2} > \frac{-\tilde{\Theta}_{ij}}{\tilde{\Theta}_{ii}\tilde{\Theta}_{jj}} = \Omega(\Theta_{\min}).$$

We note that the above bound establishes that the sign of $\tilde{\Theta}_{ij}$ is the same as Θ_{ij}, and that $\Sigma(i,j|k)$ has the opposite sign to $\tilde{\Theta}_{ij}$. Therefore, in order to show that the sign of the non-conditional covariance coincides, we need to establish the sign of Θ_{ij}.

From Lemma 13 of Anandkumar et al. (2011a), we have that

$$\left|\Sigma_{ij} + \frac{\Theta_{ij}}{\Theta_{ii}\Theta_{jj} - \Theta_{ij}^2}\right| \leq \frac{2\alpha^2}{D_{\min}(1-\alpha)}.$$

Using this lemma, it is sufficient to establish that the right hand side here is bounded by $\frac{|\Theta_{ij}|}{\Theta_{ii}\Theta_{jj}-\Theta_{ij}^2}$. It follows from our initial assumption that:

$$\frac{1}{D_{\min}(1-\alpha)} \leq \frac{|\Theta_{ij}|}{K(1+\delta)},$$

therefore

$$\left|\Sigma_{ij} + \frac{\Theta_{ij}}{\Theta_{ii}\Theta_{jj} - \Theta_{ij}^2}\right| \leq 2\alpha^2 \frac{|\Theta_{ij}|}{K(1+\delta)}.$$

We can use our assumed bound on K and the fact that $\alpha < 1$ and $\delta > 0$ to simplify as:

$$\begin{aligned}\left|\Sigma_{ij} + \frac{\Theta_{ij}}{\Theta_{ii}\Theta_{jj} - \Theta_{ij}^2}\right| &\leq \frac{\alpha^2}{1+\delta} \cdot \frac{|\Theta_{ij}|}{\Theta_{ii}\Theta_{jj}} \\ &\leq \frac{|\Theta_{ij}|}{\Theta_{ii}\Theta_{jj} - \Theta_{ij}^2}.\end{aligned}$$

The last line follows from $\Theta_{ii}\Theta_{jj} - \Theta_{ij}^2$ being a minor of Θ. □

Chapter 9

Fast Approximate Parameter Inference

In this chapter we consider the problem of large scale learning of the parameters of a Gaussian graphical model. We assume the structure is known, perhaps using the techniques from Chapter 8. Our goal in machine learning is not learning for its own sake, but to learn predictive models. To this end, we consider a reasonable restriction of the class of all Gaussian models which ensures that prediction using all models in the class is tractable. In Section 9.2 we give a novel dual-decomposition learning procedure for this restricted class. We then introduce the collaborative filtering application domain, where a Gaussian graph structure naturally arises. In Section 9.8 we show promising empirical performance of our method on this domain.

An earlier version of the work in this chapter has been published as Defazio and Caetano (2012b).

9.1 Model Class

In this section we impose a number of restrictions of the class of precision matrices Θ that we will consider. These restrictions have multiple purposes. Primarily, we are looking to ensure that inference on the resulting model is tractable. A second reason for our structural assumptions is that they form a hypothesis class restriction. The approximation we use in Section 9.2 learns poor models without the additional restrictions used here.

9.1.1 Improper models

A proper Gaussian graphical model is one in which the function $Z(\Theta) \propto \log\det\Theta$ (the log determinant of the precision matrix) which plays the part of the normalisation constant is finite. In a sense proper models are those that can be normalised.

The requirement that a Gaussian graphical be proper is actually stronger than we require in our applications, and potentially difficult to enforce in practice. For Gaussian models, if Θ is positive definite than it is proper. An improper model is still required to have a symmetric positive semi-definite (PSD) Θ.

To see why we don't need a proper model, consider that our ultimate goal is to perform prediction using Bayesian inference. Inference in this case means conditioning on a subset of variables, then determining the expected values and variances of the remaining variables. For this purpose we just need that all of the principal minors of Θ are positive definite as they form the conditional sub-models which we need to be proper. We will discuss in the next section how to ensure this is the case.

9.1.2 Precision matrix restrictions

The first restriction we apply to Θ is to force it to be a member of the class of Z-matrices.

Definition 9.1. A Z-matrix is a matrix for which all off-diagonal entries are non-positive. I.e

$$\forall i \neq j \quad \Theta_{ij} \leq 0.$$

For a Gaussian graphical model, a negative Θ_{ij} value implies that (conditioned on all other variables) the variables i and j are positively correlated. So this restriction means that we can not model negative direct correlations in our model. Although this is a strong restriction, it is a natural one. When one thinks of a network of dependencies, edges are naturally assumed to imply correlation between the adjoined nodes rather than anti-correlation. In the collaborative filtering application area we consider, this assumption is reasonable. We discuss this further in Section 9.6. Note that this restriction to modelling negative correlations manifests in the covariance matrix Θ^{-1}; it can only contain non-negative entries for PSD $Z-$matrices.

The Z-matrix property together with the SPSD requirement implies quite a lot about Θ. The most important property for our purpose is the following:

Theorem 9.2. ***(Berman and Plemmons, 1994, Theorem 4.16 p156)*** *Suppose Θ is a SPSD Z-matrix. Then if Θ is an irreducible matrix, i.e. the support of Θ is a connected graph, then all principal minors of Θ are positive definite.*

So our requirement that conditional sub-models are proper is satisfied as long as we ensure that the graph structure of Θ is connected. This requirement is very weak in practice. In fact, non-connected models can still be handled by treating the connected components separately. When no values in a component are conditioned on then the predictions for that component are just the (unconditional) expectations of those variables.

The final restriction we place on Θ is the requirement that it is actively diagonally dominant:

Definition 9.3. A symmetric matrix Θ is *actively diagonally dominant* if:

$$\forall i \;\; |A_{ii}| = \sum_{j \neq i} \left|A_{ij}\right| .$$

This is a sub-class of the diagonally dominant matrices, where the above expression holds with inequality instead ($|A_{ii}| \geq \sum_{j \neq i} \left|A_{ij}\right|$).

In our case the Z-matrix restriction simplifies this condition to $A_{ii} = -\sum_{j \neq i} A_{ij}$. For general matrices diagonal dominance is a very strong restriction. In our setting, it is not as strong a requirement. Informally, in order that A be PSD, there needs to be sufficient weight on the diagonal to counter-act the off-diagonal entries. If the diagonal entries are of roughly similar magnitude, then diagonal dominance will hold. The purpose of the *active* constraint rather than the usual inequality is primarily a practical one. When optimising over the set of diagonally dominant matrices, the constraints are normally active during optimisation, so it simplifies the algorithm to enforce that they are always active. The active constraint also prevents the model from shrinking its predictions towards the mean, which is undesirable in some applications. Interestingly, this diagonal dominance condition is also implicitly assumed in other network models in the collaborative filtering domain. This is discussed further in Section 9.7.

One immediate consequence of the active diagonal dominance is the singularity of the matrix Θ. So in fact we are certain to not have a proper Gaussian graphical model.

9.2 An Approximate Constrained Maximum Entropy Learning Algorithm

For Gaussian models, the mean and covariance matrix form the sufficient statistics, so there is no need to work directly with the data points during learning. Let Σ be the empirical covariance matrix and μ the mean vector. We will apply an approximate maximum entropy approach to learning the parameters of a model under our class restriction.

9.2.1 Maximum Entropy Learning

In the previous chapter we discussed the method of maximum likelihood learning in the context of Gaussian models. When a L1 regulariser is used, the dual problem took the form:

$$\max_{C \in S^N_{++}} \log\det C,$$
$$\text{s.t. } \forall i,j\colon \left|C_{ij} - \Sigma_{ij}\right| \leq \lambda. \tag{9.1}$$

This is actually an instance of Maximum Entropy learning (ME). In general maximum likelihood problems have maximum entropy duals. The entropy nomenclature refers to the fact that the objective is a scaled and shifted form of the entropy of a Gaussian distribution:

$$H(\mathcal{N}(.,C)) = \frac{N}{2}\left(1 + \log(2\pi)\right) + \frac{1}{2}\log\det C.$$

In ME learning we need to place some sort of constraint on the allowed distributions so that the solution is well defined. For the L1 case that was a box constraint $\left|C_{ij} - \Sigma_{ij}\right| \leq \lambda$. For the unregularised case it would simply be $C = \Sigma$, which obviously gives the trivial solution for C. Once we have the ME solution we can recover a ML solution using the gradients of the Lagrangian. We give an example of this in Section 9.2.4.

For Gaussian models exact maximum entropy learning can be tractable. However, for the size of models we are considering it quickly becomes impractical. There is also a lack of robustness in the solutions. Instead, we will rely on the use of the Bethe approximation.

9.2.2 The Bethe Approximation

The Bethe approximation is better known as the implicit entropy approximation made by the standard belief propagation method. For parameter learning, we will work with the approximation more directly. Suppose we have a set of pairwise beliefs $b_{ij}(x_i, x_j)$ and unary beliefs $b_i(x_i)$. Beliefs in this context refers to probability distributions which we intend to (variationally) optimise over so that they become better approximations to the probabilities $p(x_i, x_j)$. Beliefs that are consistent on their overlap (i.e. $b_i(x_i) = \sum_y b_{ij}(x_i, y)$ for all i) encode the local properties of a probability distribution. The Bethe approximation is an entropy like function that is defined on such local information of a distribution. It has the following form for pairwise models (Koller and Friedman, 2009, Section 11.3.7), defined using the true entropy H as:

$$\begin{aligned} H_{\text{Bethe}}(b) &= \sum_{i}^{N}\sum_{j=i+1}^{N} H(b_{ij}) \\ &- (N-1)\sum_{i}^{N} H(b_i). \end{aligned}$$

The goal of this approximation is to approximate the full entropy using the entropy over the local beliefs b_{ij}. We can't just use the approximation $H_{\text{Bethe}}(b) = \sum_i^N \sum_{j=i+1}^N H(b_{ij})$ as each x_i appears N times as part of an entropy, essentially being over-counted $N-1$ times. The Bethe entropy deals with this over-counting by subtracting off $N-1$ copies of each unary entropy, resulting in each x_i being counted only once.

In a pairwise model over a graph structure, we only define beliefs that have matching factors (i.e. edges). So the Bethe entropy takes the form:

$$H_{\text{Bethe}}(b) = \sum_{(i,j)\in E} H(b_{ij}) - \sum_{i\in V} (\deg(i)-1) H(b_i).$$

9.2.3 Maximum entropy learning of unconstrained Gaussians distributions

In a Gaussian model, it is convenient to encode the beliefs in matrix form. Each belief b_{ij} is a 2D Gaussian (As marginals of Gaussian distributions must be Gaussian), and so its covariance matrix has parameters C_{ii}, C_{ij}, C_{jj}. Since we are only interested in consistent beliefs (those that agree on the overlap), two beliefs that share a variable (say x_1) will agree on the variance of it (C_{11}). So in fact we can write the full set of beliefs compactly as a sparse matrix C, which contains the covariance C_{ij} according to belief b_{ij} at location (i,j). The diagonal contains all the unary variances C_{ii} for each i.

The Bethe entropy approximation in this notation is:

$$\begin{aligned} H_{\text{Bethe}}(C) &= \sum_{(i,j)\in E} \log\left(C_{ii}C_{jj} - C_{ij}^2\right) \\ &\quad + \sum_{i\in V} (1-\deg(i)) \log C_{ii}. \end{aligned}$$

Using the Bethe approximation, we can now perform approximate maximum entropy learning. Recall that the maximum entropy objective has additional constraints requiring that the marginals of the learned distribution match the observed distribution. When using an approximation entropy, we just require that the beliefs match. We start by considering a model without the restrictions from Section 9.1. In our matrix notation, the maximum entropy objective is:

$$\begin{aligned} \underset{C}{\text{maximize}} \quad & H_{\text{Bethe}}(C) \\ \text{s.t. } & C = \Sigma. \end{aligned}$$

Stated this way, the solution is trivial as the constraints directly specify C. However, we are interested in learning the weights Θ, which are the Lagrange multipliers of

the equality constraints. The Lagrangian is

$$L_\Sigma(C, \Theta) = H_{\text{Bethe}}(C) + \langle \Theta, \Sigma - C \rangle \,, \tag{9.2}$$

where $\langle \cdot, \cdot \rangle$ is the standard inner product on matrices. The Lagrangian has derivatives:

$$\frac{\partial L_\Sigma(C, \Theta)}{\partial C} = \frac{\partial H_{\text{Bethe}}(C)}{\partial C} - \Theta,$$
$$\frac{\partial L_\Sigma(C, \Theta)}{\partial \Theta} = \Sigma - C.$$

Equating the gradients to zero, gives the following equation for Θ:

$$\Theta = \frac{\partial H_{\text{Bethe}}(C)}{\partial C}|_{C=\Sigma},$$

which has the closed form solution:

$$\begin{aligned} \Theta_{ij} &= \frac{-\Sigma_{ij}}{\Sigma_{ii}\Sigma_{jj} - \Sigma_{ij}^2} \\ \Theta_{ii} &= \frac{1}{\Sigma_{ii}} + \sum_{j \in ne(i)} \left(\frac{\Sigma_{jj}}{\Sigma_{ii}\Sigma_{jj} - \Sigma_{ij}^2} - \frac{1}{\Sigma_{ii}} \right). \end{aligned} \tag{9.3}$$

This kind of solution is also known as pseudo-moment matching (Koller and Friedman, 2009, 20.5.1.1 p963).

9.2.4 Restricted Gaussian distributions

If we were applying a vanilla Gaussian model, we could use Equation 9.3 directly. However, for our novel restricted class we have active diagonal dominance constraints as well. To handle these constraints, we use variable substitution, replacing Θ_{ii} with $\sum_{j \in ne(i)} \Theta_{ij}$. In particular:

$$\Theta_{ii} \left(\Sigma_{ii} - C_{ii} \right) \rightarrow \sum_{j \in ne(i)} \Theta_{ij} \left(\Sigma_{ii} - C_{ii} \right).$$

Grouping in terms of Θ, we have the following Lagrangian:

$$H_{\text{Bethe}}(C) + \sum_{(i,j) \in E} \Theta_{ij} \left(\Sigma_{ij} - \Sigma_{ii} - \Sigma_{jj} \right) - \sum_{(i,j) \in E} \Theta_{ij} \left(C_{ij} - C_{ii} - C_{jj} \right)$$

which we denote $L'_\Sigma(C, \Theta)$. It has gradients:

$$\begin{aligned}
\frac{\partial L'_\Sigma(C,\Theta)}{\partial C_{ij}} =& \frac{\partial H_{\text{Bethe}}(C)}{\partial C_{ij}} - \Theta_{ij}, \\
\frac{\partial L'_\Sigma(C,\Theta)}{\partial C_{ii}} =& \frac{\partial H_{\text{Bethe}}(C)}{\partial C_{ii}} + \sum_{j \in \text{ne}(i)} \Theta_{ij}, \\
\frac{\partial L'_\Sigma(C,\Theta)}{\partial \Theta_{ij}} =& \Sigma_{ij} - \Sigma_{ii} - \Sigma_{jj} - C_{ij} + C_{ii} + C_{jj}.
\end{aligned}$$

In order to optimise this constrained objective, we can take advantage of the closed form solution for the simpler unconstrained Gaussian. The procedure we use is given in Algorithm 9.1. It gives a quality solution in a small number of iterations (see Figure 9.1). The core idea is that if we fix the diagonal of C, the rest of the elements are determined. So we take a block coordinate ascent approach. One block is all off-diagonal entries. We do an exact solve for that block. The other block is the diagonal elements, for which we do a gradient step. The algorithm simply alternates between the two block updates.

The gradient of the diagonal elements can be computed easily from the dual variable matrix Θ, so we recompute that at each step. We use a $\alpha / \sqrt{k}$ step size regime for the gradient step, where k is the step number.

We have not discussed yet the non-positive restriction on the off diagonal elements (Section 9.1). When using the Bethe approximation, we can see from Equation 9.3 that Θ_{ij} is negative if C_{ij} is positive. Our restricted model class can only model covariance matrices with C_{ij} positive, so we do not need to consider negative C_{ij} at all. Algorithm 9.1 just clamps $C_{ij} = 0$ to be positive, which is a well founded way of enforcing a positivity constraint in a coordinate descent algorithm.

9.3 Maximum Likelihood Learning with Belief Propagation

In Section 9.2 we derived an efficient learning procedure for our restricted class of models. It is also possible to apply general black box optimisation methods to this problem, and we use such as method as a baseline for comparison.

Instead of working with a maximum entropy viewpoint, we will use a more standard maximum likelihood approach. Using the Bethe approximation to the entropy, we can form an approximate maximum likelihood objective as follows. First note that the Lagrangian (Equation 9.2) can be split as follows:

$$\begin{aligned}
L_\Sigma(\Theta, C) =& H_{\text{Bethe}}(C) + \langle \Theta, \Sigma - C \rangle \\
=& \langle \Theta, \Sigma \rangle - \left(\langle \Theta, C \rangle - H_{\text{Bethe}}(C) \right);
\end{aligned}$$

Algorithm 9.1 Diagonal ascent algorithm for approximate maximum entropy learning

input: covariance Σ, size N, step size α
$C = \Sigma$ and $k = 1$
repeat
  # *Compute* Θ*, needed for each* C_{ii} *gradient*
  for $i = 1$ **to** N **do**
    $\Theta_{ii} = \frac{1}{C_{ii}}$
  end for
  for $(i, j) \in E$ **do**
    if $C_{ii}C_{jj} - C_{ij}^2 > 0$ **then**
      $\Theta_{ij} = \frac{-C_{ij}}{C_{ii}C_{jj} - C_{ij}^2}$
      Θ_{ii} += $\frac{C_{jj}}{C_{ii}C_{jj} - C_{ij}^2} - \frac{1}{C_{ii}}$
    else
      $\Theta_{ij} = 0$
    end if
  end for
  # *Take a gradient step on each* C_{ii}
  for $i = 1$ **to** N **do**
    C_{ii} += $\frac{\alpha}{\sqrt{k}}(\Theta_{ii} + \sum_{j \in \mathrm{ne}(i)} \Theta_{ij})$
  end for
  # *Update the off-diagonal elements*
  for $(i, j) \in E$ **do**
    $C_{ij} = \Sigma_{ij} - \Sigma_{ii} - \Sigma_{jj} + C_{ii} + C_{jj}$
    $C_{ij} = \max(C_{ij}, 0)$
  end for
  $k = k + 1$
until sufficient convergence
return Θ

The dual is then formed by maximising in terms of C:

$$\begin{aligned} -\log p(\Sigma; \Theta) &\propto \max_C L_\Sigma(\Theta, C) \\ &= \langle \Theta, \Sigma \rangle - \min_C \left(\langle \Theta, C \rangle - H_{\mathrm{Bethe}}(C) \right); \end{aligned}$$

The term inside of the minimisation on the right is the Bethe free energy (Yedidia et al., 2000). By equating with the non-approximate likelihood, it can be seen that the log partition function is being approximated as:

$$\log Z(\Theta) = -\min_C \left(\langle \Theta, C \rangle - H_{\mathrm{Bethe}}(C) \right).$$

The value of $\log Z(\Theta)$ and a (locally) minimising C can be found efficiently using belief propagation (Cseke and Heskes, 2011). The C found by belief propagation is

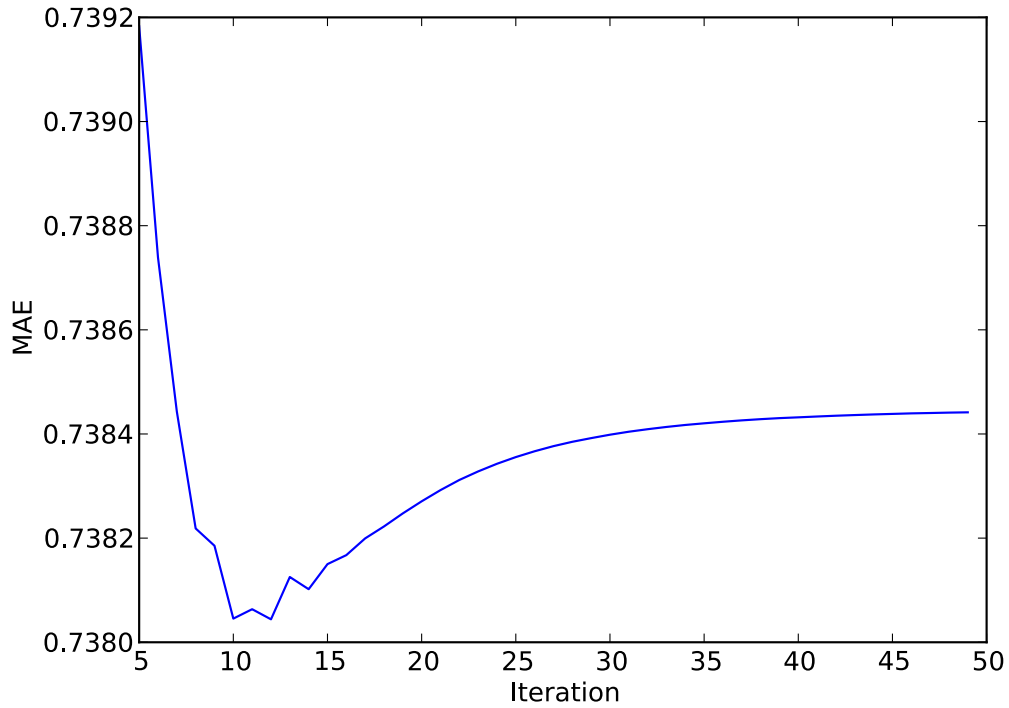

Figure 9.1: Test error as a function of the number of training iterations on the 100K MovieLens dataset. A mild over-fitting effect is visible.

the gradient of $\log Z(\Theta)$, so we can use a gradient based method on this approximate maximum likelihood objective.

For diagonally dominant Θ belief propagation can be shown to always converge (Weiss and Freeman, 2001). The diagonal constraints as well as the non-positivity constraints on the off diagonal elements of Θ ensure diagonal dominance in this case.

Maximum likelihood objectives for undirected graphical models are typically optimised using quasi-Newton methods, and that is the approach we took here. The diagonal constraints are easily handled by variable substitution, and the non-positivity constraints are simple box constraints. We used the L-BFGS-B algorithm (Zhu et al., 1997) – a quasi-Newton method that supports such constraints. The log-partition function $\log Z(\Theta)$ is convex if we are able to exactly solve the inner minimisation over C, which is not the case in general.

9.4 Collaborative Filtering

We will illustrate the application of our learning algorithm on the collaborative filtering (CF) problem domain. CF is the sub-field of recommendation systems that makes

use of information from all users that interact with a system in order to make personalised recommendations for each individual user. Early recommendation systems treated each user individually, but virtually all modern recommendation systems fall within the collaborative filtering category. We will use the standard setup, where a history of past *ratings* are known for each user. Each user u is associated with a set R_K of items, for which the user's rating r_{ui}, $i \in R_K$ is known. Ratings in our test problems are ordinal values in the range 1 to 5.

9.5 The Item Graph

We begin by introducing the foundations of graph based collaborative filtering. We are given a set of users and items, along with a set of real valued ratings of items by users. Classical item neighbourhood methods (Sarwar et al., 2001) learn a graph structure over items $i = 0 \dots N-1$, along with a set of edge weights $s_{ij} \in \mathbb{R}$, so that if a query user u is presented, along with his ratings for the neighbours of item i (r_{uj}, $j \in ne(i)$), the predicted rating of item i is

$$r_{ui} = \mu_i + \frac{\sum_{j \in ne(i)} s_{ji} \left(r_{uj} - \mu_j\right)}{\sum_{j \in ne(i)} s_{ji}}, \tag{9.4}$$

where $\mu_i \in \mathbb{R}$ represent average ratings for that item over all users. When the rating of all neighbouring items is not known, then the known subset is used in the prediction rule. See Figure 9.2 for an example of an actual neighbourhood for a movie recommendation system.

In order to use the above method, some principle or learning algorithm is needed to choose the neighbour weights. The earliest methods use the Pearson correlation between the items as the weights. In our notation, the Pearson correlation between two items is defined as

$$s_{ij} = \frac{\sum_u (r_{ui} - \mu_i)(r_{uj} - \mu_j)}{\sqrt{\sum_u (r_{ui} - \mu_i)^2} \sqrt{\sum_u (r_{uj} - \mu_j)^2}}.$$

The set of neighbours of each item is chosen as the k most similar, under the same similarity measure used for prediction. More sophisticated methods were developed for the NetFlix competition, including the work of Bell and Koren (2007), which identified the following problems with the above:

- Bounded similarity scores can not handle deterministic relations;
- Interactions among neighbours are not accounted for, which greatly skews the results;

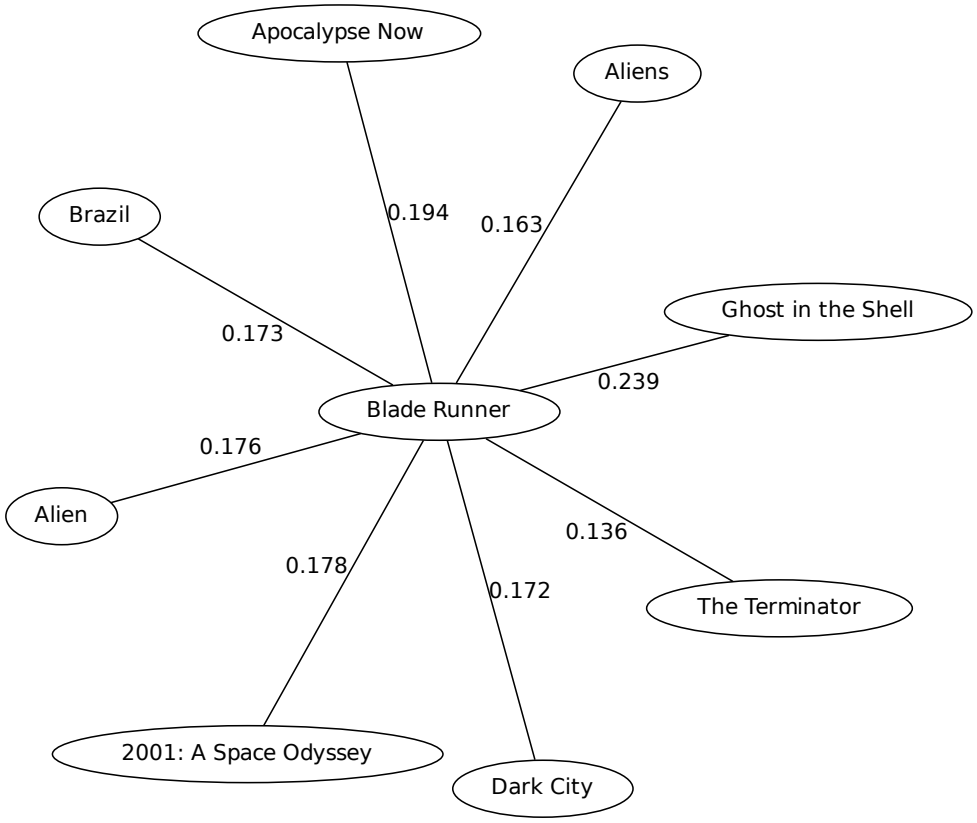

Figure 9.2: Neighbourhood of "Blade Runner" found using the item field method (Section 9.6) on the MovieLens 1M dataset

- The weights s_{ij} cause over-fitting when none of the neighbours provide useful information.

Learning the weights s_{ij} under an appropriate model can alleviate all of these problems, and provide superior predictions (Bell and Koren, 2007), with the only disadvantage being the computational time required for training the model. Learning the neighbourhood structure for such a model is not straightforward due to the potentially quadratic number of edges. In this work we take the approach used by other neighbourhood methods, and assume that the neighbourhood structure is chosen by connecting each item to its k most similar neighbours, using Pearson correlation as the similarity measure. We denote this undirected edge set E. The approach detailed in Chapter 8 would give a more principled way of choosing the edge set, but would make comparison against results in the existing literature harder.

9.5.1 Limitations of previous approaches

The classical prediction rule in Equation 9.4 has a number of disadvantages. Suppose we wish to predict a rating for a user u on item i. If user u has only rated a small number (possibly 0) of the items neighbouring item i, then the classical prediction rule gives poor results. Ideally in such cases we want to use indirect information, say from distance 2 or 3 in the graph, in order to make the predictions. Another limitation of the classical approach is that it gives points estimates of the predicted value. Ideally we would like to take a probabilistic approach, and output a distribution over the possible values.

We show in the next section that the restricted Gaussian class of models yields a model that fixes both these deficiencies. In fact it gives a prediction rule that generalises the classical one. When ratings for all items in a neighbourhood are known, it uses the classical prediction rule with weights $s_{ji} = \Theta_{ji}$:

$$r_{ui} = \mu_i + \frac{\sum_{j \in ne(i)} s_{ji} \left(r_{uj} - \mu_j\right)}{\sum_{j \in ne(i)} s_{ji}}. \tag{9.5}$$

However, when fewer items are known the unknown items are marginalised out in the probability model, yielding a well-founded prediction rule that captures the additional uncertainty in such cases.

9.6 The Item Field Model

We will now define a natural pairwise log-linear model over the item graph structure. Recall that a log-linear model is defined by a set of feature functions over subsets of variables, where the functions return a local measure of compatibility. For pairwise models, these subsets are just pairs of neighbouring variables in the graph structure. In our case the set of variables is simply the set of items, whose values we treat as continuous variables in the range 1 to 5. For any particular user, given the set of their items ratings (R_K), we will predict their ratings on the remaining items (R_U) by conditioning on this distribution, namely computing expectations over $P(R_U|R_K)$.

Recall the form of a pairwise log-linear model (Section 6.1) :

$$P(r;\Theta) = \frac{1}{Z(\Theta)} \exp\left(- \sum_{i \in V} \Theta_{ii} f_i(r_i) - \sum_{(i,j) \in E} \Theta_{ij} f_{ij}(r_i, r_j) \right).$$

Here Θ is a matrix of features weights, and Z is the partition function, whose value depends on the parameters Θ, and whose purpose is to ensure the distribution is

correctly normalised. We want functions that encourage smoothness, so that a discrepancy between the ratings of similar items is penalised. We propose the use of (negated) squared difference features:

$$f_{ij}(r_i, r_j) \quad = \quad -\frac{1}{2}((r_i - \mu_i) - (r_j - \mu_j))^2.$$

These features, besides being intuitive, have the advantage that for any choice of parameters Θ we can form a Gaussian log-linear model that defines that same distribution.

In a Gaussian log-linear model, pairwise features are defined for each edge as $f_{ij}(r_i, r_j) = (r_i - \mu_i)(r_j - \mu_j)$, and unary features as $f_i(r_i) = \frac{1}{2}(r_i - \mu_i)^2$. The pairwise feature weights Θ_{ij} correspond precisely with the off diagonal entries of the precision matrix (that is, the inverse of the covariance matrix). The unary feature weights θ_i correspond then to the diagonal elements. Now notice that we can write the squared difference features as:

$$f_{ij}(r_i, r_j) = -\frac{1}{2}(r_i - \mu_i)^2 + (r_i - \mu_i)(r_j - \mu_j) - \frac{1}{2}(r_j - \mu_j)^2.$$

Thus, we can map the squared difference features to a constrained Gaussian log-linear model, where the diagonal elements are constrained so that for all i,

$$\Theta_{ii} = -\sum_{j \in ne(i)} \Theta_{ji}.$$

As discussed in Section 9.1, we impose an additional constraint on the allowable parameters, that each off-diagonal element Θ_{ij} is non-positive. Our choice of squared-difference features was also motivated by our model class restriction; As we just showed, they yield an actively diagonally dominant Θ matrix.

9.7 Prediction Rule

The feature functions defined in the previous section seem the natural choice under our computational considerations. We now derive the associated predictive distributions under that model. Consider the case of predicting a rating r_{ui}, where for user u all ratings r_{uj}, $j \in \text{ne}(i)$ are known. These neighbours form the Markov blanket of node i. Using standard formulas for manipulating Gaussian distributions (Bishop, 2006, p86 Eq 2.73/2.75), we find that the conditional distribution under the item field model is:

$$\mathcal{N}\left(r_{ui}\,;\, \mu_{i|-i}, \frac{1}{\sigma^2} = \sum_{j \in ne(i)} \Theta_{ji}\right), \text{ where}$$

$$\mu_{i|-i} = \mu_i - \frac{\sum_{j \in ne(i)} \Theta_{ji} \left(r_{uj} - \mu_j\right)}{\sum_{j \in ne(i)} \Theta_{ji}}.$$

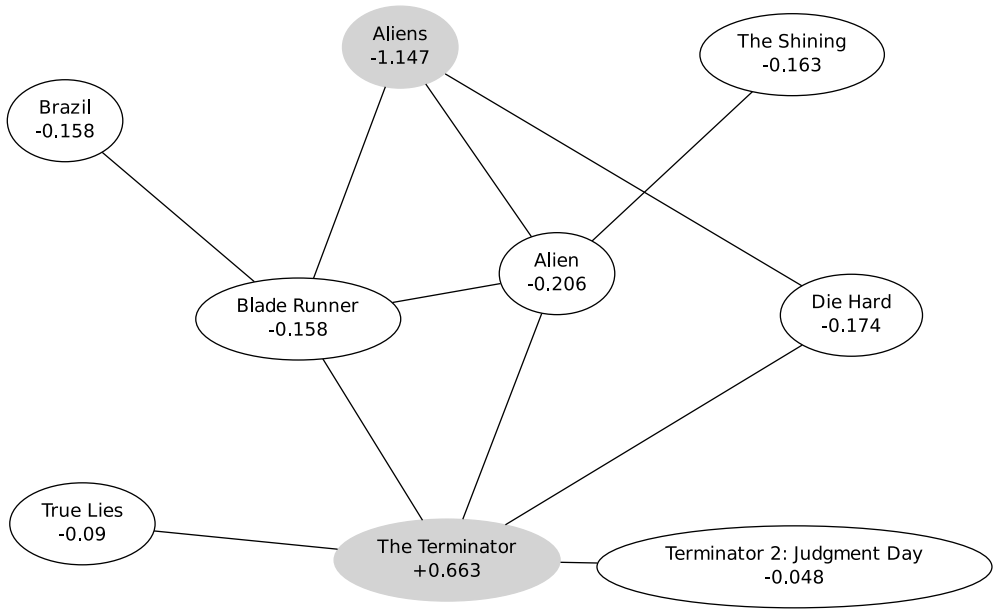

Figure 9.3: Diffusion of ratings, shown as deltas from the item means, for a user that has rated only the shaded items. A hand chosen subgraph of the item graph generated for the 100K MovieLens dataset is shown.

This is a univariate Gaussian distribution, whose mean matches Equation 9.5, the traditional neighbourhood method prediction rule. In practice we rarely have ratings information for each item's complete neighbourhood, so this special case is just for illustrating the link with existing approaches.

In the general case, conditioning on a set of items K with known ratings r_K, with the remaining items denoted U, we have:

$$\mathcal{N}\left(r_U\,;\,\mu_{U|K}, \Theta_{UU}\right), \text{ where}$$

$$\mu_{U|K} = \mu_U - \left[\Theta_{UU}\right]^{-1}\Theta_{UK}\left(r_K - \mu_K\right).$$

Thus computing the expected ratings requires nothing more than a few fast sparse matrix operations, including one sparse solve. If the prediction variances are required, both the variances and the expected ratings can be computed using belief propagation, which often requires fewer iterations than the sparse solve operation (Shental et al., 2008).

The linear solve in this prediction rule has the effect of diffusing the known ratings information over the graph structure, in a transitive manner. Figure 9.3 shows this effect which is sometimes known as spreading activation. Such transitive diffusion

has been explored previously for collaborative filtering, in a more ad-hoc fashion (Huang et al., 2004).

Note that this prediction rule is a bulk method, in that for a particular user, it predicts their ratings for all unrated items at once. This is the most common case in real world systems, as all item ratings are required in order to form user interface elements such as top 100 recommendation lists.

9.8 Experiments

For our comparison we tested on 2 representative datasets. The 1M ratings MovieLens dataset[1] consists of 3952 items and 6040 users. As there is no standard test/training data split for this dataset, we took the approach from Stern et al. (2009), where all data for 90% of the users is used for training, and the remaining users have their ratings split into a 75% training set and 25% test set. The 100K ratings MovieLens dataset involves 1682 items and 943 users. This dataset is distributed with five test/train partitions for cross validation purposes which we made use of.

All reported errors use the mean absolute error (MAE) measure ($\frac{1}{N}\sum_i^N |\mu_i - r_i|$). All 2 datasets consist of ratings on a discrete 1 to 5 star scale. Each method we tested produced real valued predictions, and so some scheme was needed to reduce the predictions to real values in the interval 1 to 5. For our tests the values were simply clamped. Methods that learn a user dependent mapping from the real numbers into this interval have been explored in the literature (Stern et al., 2009).

Table 9.1 shows the results for the two MovieLens datasets. Comparisons are against our own implementation of a classical cosine neighbourhood method (Sarwar et al., 2001); a typical latent factor model (similar to Funk (2006) but with simultaneous stochastic gradient descent for all factors) and the neighbourhood method from Koren (2010) (the version without latent factors), which uses a non-linear least squares objective. All implementations were in python (using cython compilation), so timings are not comparable to fast implementations. We also show results for various methods of training the item field model besides the maximum entropy approach, including exact maximum likelihood training.

The item field model outperforms the other neighbourhood methods when sparse (10 neighbour) models are used. Increasing the neighbourhood size past roughly 10 actually starts to degrade the performance of the item field model: at 50 neighbours using maximum entropy training on the 1M dataset the MAE is 0.6866 v.s. 0.6772 at 10 neighbours. We found this occurred with the other training methods as well. This may be caused by an over-fitting effect as restricting the number of neighbours is a form of regularisation.

[1] http://grouplens.org/datasets/movielens/

Method	MAE	Precomputation (s)	Training (s)
100K MovieLens			
Maximum Entropy (k=10)	0.7384	18.9	0.12
Cosine Neigh. (k=10)	0.8107	18.7	0
Bethe Maximum Likelihood (k=10)	0.7390	18.9	28
Exact Maximum Likelihood (k=10)	0.7398	18.9	99
Least Squares Neighbours (k=10)	0.7510	18.9	90
Maximum Entropy (k=50)	0.7439	19	1.7
Least Squares Neighbours (k=50)	0.7340	19	288
Latent Factor Model (50 factors)	0.7321	0	215
1M MovieLens			
Maximum Entropy (k=10)	0.6772	514	0.64
Cosine Neigh. (k=10)	0.7421	513	0
Bethe Maximum Likelihood (k=10)	0.6767	514	75
Exact Maximum Likelihood (k=10)	0.6755	514	2795
Least Squares Neighbours (k=10)	0.6826	514	1369
Maximum Entropy (k=50)	0.6866	517	7.17
Least Squares Neighbours (k=50)	0.6756	517	4551
Latent Factor Model (50 factors)	0.6683	0	4566

Table 9.1: Comparison of a selection of models against the item field model with approximate maximum likelihood, exact maximum likelihood and maximum entropy approaches

The latent factor model and the least squares neighbourhood model both use stochastic gradient descent for training. They required looping over the full set of training data each iteration. The maximum entropy method only loops over a sparse item graph each iteration which is why it is roughly two thousand times faster to train. Note that the dataset still has to be processed once to extract the neighbourhood structure and covariance values, the timing of which is indicated in the precomputation column. This is essentially the same for all the neighbourhood methods we compared. In an on-line recommendation system the covariance values can be updated as new ratings stream in, so the precomputation time is amortised. Training time is more crucial as multiple runs from a cold-start with varying regularisation are needed to get the best performance (due to local minima).

9.9 Related Work

There has been previous work that applies undirected graphical models in recommendation systems. Salakhutdinov et al. (2007) used a bipartite graphical model, with binary hidden variables forming one part. This is essentially a latent factor model, and due to the hidden variables, requires different and less efficient training methods than those we apply in the present paper. They apply a fully connected

bipartite graph, in contrast to the sparse, non-bipartite model we use. Multi-scale conditional random fields models have also been applied to the more general social recommendation task with some success (Xin et al., 2009). Directed graphical models are commonly used as a modelling tool, such as in Salakhutdinov and Mnih (2008). While undirected models can be used in a similar way, the graph structures we apply in this work are far less rigidly structured.

Several papers propose methods of learning weights of a neighbourhood graph (Koren, 2010) (Bell and Koren, 2007), however our model is the first neighbourhood method we are aware of which gives distributions over its predictions. Our model uses non-local, transitive information in the item graph for prediction. Non-local neighbourhood methods have been explored using the concept of spreading activation, typically on the user graph (Griffith et al., 2006) or on a bipartite user-item graph (Lie and Wang, 2007).

The closest probabilistic approach to ours is the work of Truyen et al. 2007. They form an undirected network with one node per user/item pair, instead of the one node per item approach that characterises neighbourhood methods. Instead of the squared difference features we use, they apply absolute deviation features. For learning they apply a pseudo-likelihood learning approach together with stochastic gradient descent.

9.10 Extensions

There are a few clear avenues for extension of the collaborative filtering model we have described.

9.10.1 Missing Data & Kernel Functions

The training methods proposed take as input a sparse subset of a covariance matrix Σ, which contains the sufficient statistics required for training. It should be emphasised that we do not assume that the covariance matrix is sparse, rather our training procedure only needs to query the entries at the subset of locations where the precision matrix is assumed to be non-zero.

As our samples are incomplete (we do not know all item ratings for all users), the true covariance matrix is unknown. For our purposes, we form a covariance matrix by assuming the unrated items are rated at their item mean. More sophisticated methods of imputation are possible; we explored an Expectation-Maximisation (EM) approach, which did not result in a significant improvement in the predictions made. It did however give better prediction covariances.

In general a kernel matrix can be used in place of the covariance matrix, which would allow the introduction of item meta-data through the kernel function. We left this avenue for future work.

9.10.2 Conditional Random Field Variants

Much recent work in Collaborative filtering has concerned the handling of additional user meta-data, such as age and gender information usually collected by on-line systems (Stern et al., 2009). These attributes are naturally discrete, and so integrating them as part of the MRF model results in mixed discrete/continuous model. Approximate inference in such as model is no longer a simple linear algebra problem, and convergence becomes an issue. User attributes are better handled in a conditional random field (CRF) model, where the conditional distributions involve the continuous item variables only.

Unfortunately the optimisation technique described above does not extend readily to CRF models. Approximate maximum entropy training using Difference-of-convex methods has been applied to CRF training successfully (Granapathi et al., 2008), although such methods are slower than maximum likelihood. We explored CRF extensions using maximum likelihood learning, and while they did give better ratings predictions, training was slow due to the large number of belief propagation calls. While practical if the computation is distributed, the training time was still several hundred times slower than any of the other methods we tested.

Chapter 10

Conclusion and Discussion

We have covered a number of new algorithms in this work that address open problems in the intersection of machine learning and numerical optimisation. Although these algorithms are of wide applicability, we have focused on a limited set of experiments to validate each method, as this is primarily a theoretical thesis. In this chapter we will attempt to put our contributions in a wider context, discussing related problems and remaining open problems.

10.1 Incremental Gradient Methods

10.1.1 Summary of contributions

Our work on fast incremental gradient methods has tied together a number of disparate methods. Our primary method, SAGA, has an interesting role as a midpoint between two of the three major fast incremental gradient methods. In relation to SAG, we showed that it is the natural extension of SAG to having unbiased gradient estimates. The primary problem with SAG is the difficulty of theoretical analysis of variants of it. This has prevented the development of proximal and accelerated versions of SAG. SAGA resolves this issue, having a much simpler and more flexible analysis. In relation to SVRG, SAGA has been shown to be a natural extension from its memory-less formulation to a version with memory. The analysis techniques are similar but allow for improved constants and a simplified convergence rate statement.

The SDCA method is not directly related to SAGA, but we have shown an indirect relation, going from SAGA to Finito, then to Prox-Finito. The later two methods were introduced in this work. This ties together all the known fast incremental gradient methods as natural transformations of each other.

The SAGA and Finito methods have a number of properties that make them well suited to practical application. We established in our experiments that none of the

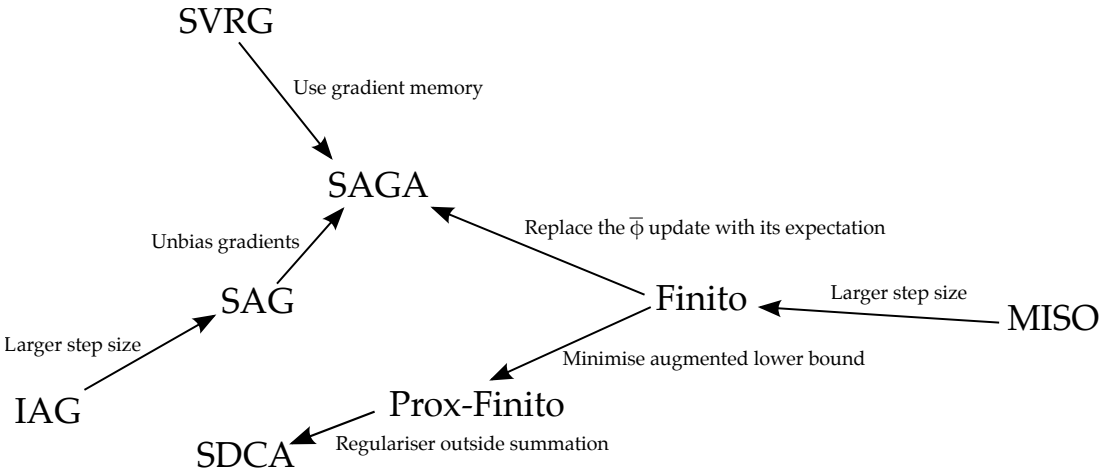

Figure 10.1: Incremental gradient methods

discussed methods has a clear advantage in all cases. The choice in practice of what method to use depends more on the properties of the methods than the actual speed of convergence. The Finito method we introduced has a substantial advantage for dense valued problems over the other methods. Unfortunately it is missing theory covering the use of L_1 and other non-differentiable regularisers. The existing SDCA method is favoured in strongly convex problems with simple loss functions, but it is problematic (but not impossible) to apply it on complex losses or non-strongly convex problems. The SAGA method appears to be better than SAG in all situations covered by the theory, but SAG can be sped-up by aggressive heuristics, whereas such approaches have not yet be applied to SAGA. SAGA is the clear method of choice for non-strongly convex problems.

Besides the introduction of new incremental gradient methods, we have also made contributions to their theoretical foundations. We discussed the importance of strong convexity, and how it is the key that allows faster convergence than traditional black-box methods. In finite sums, for the purposes of optimisation the amount of strong convexity is in a sense amplified by the number of terms in the sum. In convergence rates μn replaces μ. In contrast, we established that without additional restrictions non-strongly convex problems with summation structures are no easier to optimise than the non-summation (black-box) case.

We discussed in detail the importance of randomisation in fast incremental gradient methods. The effect of randomisation appears to be a key differentiator between fast and slow incremental gradient methods. All known fast methods require randomisation to work, whereas slow methods do not necessarily. For a number of methods, both fast and slow methods are known that only differ by the step size used. Even in those cases, the method will converge empirically and theoretically without randomisation for small steps sizes, whereas only the randomised variant will converge with large step sizes. We have provided a further example of this, by establishing

theoretically for the small-step size case of Finito (MISO) a rate of a convergence for randomised and non-randomised versions.

10.1.2 Applications

The fast incremental gradient methods we have described are primarily of interest in statistics and machine learning problems, for a number of reasons. Recall that the Lipschitz constant in their proven convergence rates depends on the properties of each individual term f_i, and so is different from the whole loss Lipschitz smoothness constant L_f, which applies to the average $\frac{1}{n}\sum f_i$. The applicability of fast incremental gradient methods depends on how similar the full gradient Lipschitz constant is to the term one L. It is when they are of comparable magnitude that methods like SAGA are most effective. Problems in engineering and physics such as discretisations of partial differential equations unfortunately do not usually have the required uniformity.

There is an interesting middle ground of problems for which both coordinate descent methods and incremental gradient methods could be applicable. These are the problems that have a summation structure where each term in the summation only involves a small number of variables. An example is MAP inference in graphical models, where terms correspond to factors in the graphical model (Koller and Friedman, 2009, Sec. 13.5). We are not aware of any work applying fast incremental gradient methods to such problems so far.

In machine learning most state-of-the-art methods use non-convex loss minimisation objectives. For the primal incremental gradient methods there is no principled reason why they can not be applied to such problems. Any theoretical guarantees are likely to be weak though. Some theoretical results appear in the literature for the MISO method already (Mairal, 2014). There is also some very preliminary experiments apply the SVRG method to neural networks (Johnson and Zhang, 2013). The primary difficulty with applying most fast incremental gradient methods is the storage requirements. Other than SVRG, all the known methods require storing a set of gradients, one per datapoint, which for neural networks and other popular models can be on the order of thousands of times larger than the input datapoints. Storing such gradients slows the optimisation down by as much as 50 times[1] compared to SGD, making application fairly impractical. For SVRG, the computational overhead is only between 2-3 times, making it an attractive option that deserves further experimental validation.

[1]The slowdown is roughly proportional to the ratio of memory bandwidth to computational throughput on the hardware used, sometimes called the *machine balance(Callahan et al., 1988).* For reference, an Intel i7 processor has roughly 40-100 gigaflops computational throughput versus roughly 10 gigabytes per second memory bandwidth.

We predict a large volume of literature in the future on the application of various fast incremental gradient methods in areas outside of the loss minimisation framework. The ease of implementation of the SAG/SAGA/SVRG/Finito methods is likely to spur their future use, just as it has for the classical stochastic gradient descent method. The SDCA method is not well presented in the current literature, which may limit its future application, although it is actually the most suited to be embedded within software libraries due to the minimal tuning it requires. It is already in use within the popular *liblinear* library (Fan et al., 2008) for instance.

10.1.3 Open problems

The fast incremental gradient framework suggests a number of interesting open problems, a few of which have already been discussed in Section 5.1.4. The understanding of randomness is really the key problem. All the currently know fast incremental gradient methods require that data-points be accessed randomly both for their theoretical and practical convergence rates. Is this a fundamental limitation or can it be overcome? The current lower complexity bounds are deterministic, but perhaps more sophisticated lower complexity bounds are possible. The understanding of permuted (without-replacement) random access rates is of equal interest. Even for classical SGD there is no theory supporting the use of without-replacement sampling. For some methods it gives faster convergence, and for some methods it causes slower convergence. What property of these methods induces such behaviour? It is likely new analytical tools will be needed to fully understand such permuted orders, as the standard expected case analysis techniques fail.

The randomness in each fast incremental gradient method is not necessarily a problem in practice. When we have a large number of data-points, the random effects are sufficiently averaged over that convergence is quite predictable. Perhaps the biggest problem is an implementation one. Modern hardware is much slower under random access patterns than in-order patterns. Fortunately, for many large dense problems, the latency induced by random access is of the order of 100 nanoseconds [2], and is small compared to the cost of the gradient evaluation at each step, which can be >1000 nanoseconds. For sparse problems, there may only be 50 or less active elements in a data-point vector, and so that 100 nanosecond delay will result in the method being up-to 5 times slower than in-order access. The development of non-randomised incremental gradient methods may fix this problem, but at the moment the best solution is to use hardware data pre-caching using a separate thread. As far as we are aware, for Intel processors this is only possible on processors with hyper-threading, and is very difficult to implement correctly.

The acceleration of incremental gradient methods is a major open problem. Most optimisation methods can be accelerated using a double-loop procedure, and this is

[2] See https://software.intel.com/en-us/articles/intelr-memory-latency-checker

approach taken in the ASDCA method. We believe the same techniques are applicable to the other fast incremental gradient methods. Such double-loop constructions are unsatisfying though. They are particularly fragile to the values of the Lipschitz and strong convexity parameters, and they introduce a log term to the convergence rate which is almost certainly improvable. The development of simple single loop primal incremental gradient methods is the next logical step, and we expect so see them appear over the next few years.

The requirement of the knowledge of the strong convexity or Lipschitz constants is an issue with incremental gradient methods. This is not an issue with regular gradient descent, where a line-search can be used instead of knowledge of the Lipschitz smoothness constant. Gradient descent is also automatically adaptive to the level of strong convexity of the problem, just like SAG and SAGA. The accelerated gradient descent method can also be made to work without prior knowledge of the Lipschitz and strong convexity constants, however a rather unsatisfying procedure involving keeping estimates of the strong convexity constant during the course of optimisation is required (Gonzaga and Karas, 2013). While such an approach does work, an approach that doesn't explicitly estimate μ would be a huge improvement.

It would be a remarkable development to see a primal fast incremental gradient method that didn't require knowledge of the Lipschitz constant or estimation of it. Likewise, for the dual case a method that doesn't require explicit knowledge of the amount of regularisation (or running estimates of it) would be an improvement.

We have largely ignored the case of non-differentiable loss functions in this work. The case of non-differentiable regularisers is easy to cover using proximal methods, such as we do for the SAGA method, however for primal methods at least, it is not clear how to handle non-differentiable losses. For dual methods, the non-differentiable case is quite straight-forward, and a $O(1/k)$ rate is established for the convergence of SDCA on L_2 regularised problems. This is the same rate known for black-box methods. We would like to see a primal method that makes use of the proximal operator of the loss in order to achieve a similar rate, likely using techniques from the theory of mirror-descent and primal-dual optimisation.

Distributed optimisation has been a hot topic in optimisation research in the last few years. The theory of distributed SGD has greatly expanded, both with its use in gigantic applications and with theoretical advances. There has been some preliminary results on the application of SDCA in a distributed setting (Yang, 2013). It is not clear in what settings an improvement in convergence rate is possible for incremental gradient methods, especially primal ones. The theoretical analysis is complicated by the need for a model of distributed machines, which tends to require specific assumptions about hardware, latency and network topology. A simple map-reduce style framework is provably not sufficient.

10.2 Learning Graph Models

10.2.1 Summary of contributions

This thesis introduced new methods for structure and parameter learning for graphical models. We primarily focused on the Gaussian graphical model case, where the goal is to learn the direct dependencies between variables in a dataset in the form of a graph structure over the variables. For the task of learning the structure, we proposed the SHORTCUT method, a modification of the existing Conditional Covariance Thresholding (CCT) method which has an improved expected case running time, reduced from $O(n^3)$ to $O(n^{2.5})$.

Given a fixed known structure, we also proposed a new method for learning the parameters (edge weights) in a model. It uses the Bethe approximation, together with dual decomposition followed by coordinate descent. Our formulation is careful to restrict the class of models that can be learned to those for which later inference tasks using the model are tractable.

For more advanced structure learning, we proposed a method that can make use of prior knowledge that the true graph structure is scale-free. This method makes use of sophisticated submodular regularisation techniques to ensure the resulting optimisation problem is convex.

In combination, the methods we proposed comprise are a powerful tool-set for Gaussian graphical model learning. We have addressed both very large scale learning via approximations as well as improvements to the reconstruction quality for smaller scale models.

10.2.2 Applications

Learning graph structures is common outside of machine learning for the purpose of data analysis. Graph structures are one of the primary ways to visualise the dependencies between variables in a dataset. A common application of Gaussian graphical model learning is in bioinfomatics, where the interactions between gene expressions are modelled as a graph structure (Davidson and Levin, 2005) . We included such a dataset in our experiments. Another potential application is in modelling social network structures which are not observed directly. For instance, the propagation of reposts of news articles between sites can be modelled in such as way (Yang and Leskovec, 2010).

Graph structure learning can sometimes be used in place of clustering. When a strong L_1 regulariser is used, the resulting graph can be unconnected, with the components playing the roles of clusters. As an example, in political science the voting

decisions of politicians are sometimes modelled as a unconnected graph structure (Jakulin and Buntine, 2004), and our methods could be applied to such networks as well.

We tested our parameter learning method on a recommendation system problem, where we modelled a set of movies with a graph structure. The edge weight between two movies (i, j) indicated how predictive the rating for movie i by a user is on for their rating of movie j, and vice-versa. Another approach to recommendation is to instead form a graph over users instead of items. Such user graph approaches were used in some of the first recommendation systems, but when large amounts of item ratings information is available, they proved less effective than item graph approaches. User graph approaches are making a resurgence lately (Wang et al., 2010), as we now have known graph structures such as the user graph in FaceBook that previously we had to estimate. Additionally, the user graph structure has greater utility when we don't have large numbers of numerical ratings for items. For instance, the small numbers of Boolean ratings that result from "likes" on social network posts (Sedhain et al., 2014). Our parameter learning algorithm could potentially be used for large-scale learning on such networks.

10.2.3 Open Problems

Despite their basis in well understood Gaussian distribution theory, Their are still many open problems relating to Gaussian graphical models. Scaling the L_1 regularised maximum likelihood learning problem up to larger problem instances is still an area of active research. In theory fast matrix multiplication methods can be used to also speed-up the inversion problem, but it is not clear if such approaches will ever lead to practical algorithms. This would probably require further advances towards the conjectured $O(n^{2+\epsilon})$ rate for fast matrix multiplication to occur.

It is well known that the Bethe approximation we apply for parameter learning can be extended to an approximation over higher-order cliques. It would be interesting to see if such an extension resulted in better results in applications such as the recommender system example we use. The dual decomposition approach may not be a practical approach with higher-order cliques.

We briefly mentioned extensions to CRF variants of the recommender system "item field" model. The traditional *collaborative filtering* datasets we had access to did not have a lot of additional information that could have been conditioned on, but in the *social* recommendation space large amounts of biographic information are often available for each user. Extending our dual decomposition approach to conditional models is an interesting possibility for future extension.

For our scale free network learning method, we make use of exponential random graph models. These are still not well understood. Indeed, just determining the

expected degree distribution under an ERG model currently requires the use of a slow MCMC sampling procedure. ERG models are still a subject of active research, and we expect that the classes of ERG models that induce scale free structures will be better understood in the near future.

The ADMM learning procedure we use in our scale-free formulation is not known to handle large problems well. In theory it should be possible to adapt the current large-scale state-of-the-art Newton methods to use my scale-free inducing regulariser instead of an L_1 regulariser. It is not clear if this can be done without losing efficiently though.

Appendix A

Basic Convexity Theorems

The theory of convex analysis is large and we make no attempt to cover it in depth in this appendix. We can get away with this sin as our theory in the preceding chapters only concerns convex functions defined on the whole of $\mathbb{R}^d$, mapping to the (non-extended) real numbers $\mathbb{R}$. Such functions are particularly well behaved as most of the complexity of analysis of convex functions occurs on the boundary of their domain, or in regions where their values are $\pm\infty$. For example, all such functions are continuous (Corollary 10.1.1, Rockafellar, 1970). Most of the theorems in this section are standard; we provide references to textbooks for these results.

A.1 Definitions

- We use the angle bracket notation $\langle x, y \rangle$ to denote the inner product between two vectors x and y.
- The **proximal operator** $\text{prox}_\gamma^f(v) \colon \mathbb{R}^d \times \mathbb{R}^d$ is defined as:

$$\text{prox}_\gamma^f(v) = \min_x \left\{ \gamma f(x) + \frac{1}{2} \|x - v\|^2 \right\}.$$

- A function f is **convex** if for all $x, y \in \mathbb{R}^d$ and $\alpha \in [0, 1]$:

$$f(\alpha x + (1 - \alpha) y) \leq \alpha f(x) + (1 - \alpha) f(y).$$

  Additionally, f is **strictly convex** if this inequality is strict.

- A function f is **strongly convex** with constant $\mu \geq 0$ if for all $x, y \in \mathbb{R}^d$ and $\alpha \in [0, 1]$:

$$f(\alpha x + (1 - \alpha) y) \leq \alpha f(x) + (1 - \alpha) f(y) - \alpha (1 - \alpha) \frac{\mu}{2} \|x - y\|^2.$$

when we say a function is strongly convex colloquially, we usually mean that $\mu > 0$. Typically, theorems about strongly convex functions also hold for $\mu = 0$, but sometimes become vacuous statements.

- A function f has **Lipschitz continuous gradients** with constant L, or equivalently is L**-smooth** if it is differentiable and for all $x, y \in \mathbb{R}^d$:

$$\left\|f'(x) - f'(y)\right\| \leq L \left\|x - y\right\|.$$

We will virtually always make this assumption when working with differentiable convex functions.

- The **condition number** of f is the ratio L/μ of its smoothness and strong convexity constants.

- The **directional derivative** of a function at $x \in \mathbb{R}^d$ in direction $v \in \mathbb{R}^d$ is the quantity:

$$\Delta_v f(x) = \lim_{h \to 0} \frac{f(x + hv) - f(x)}{h}.$$

This is related to the gradient through the relation $\Delta_v f(x) = \langle f'(x), v \rangle$.

A.2 Useful Properties of Convex Conjugates

The convex conjugate $f^* \colon \mathbb{R}^d \to \mathbb{R}^+$ of a convex function $f \colon \mathbb{R}^d \to \mathbb{R}$ is defined as:

$$f^*(u) = \max_x \left\{\langle u, x \rangle - f(x)\right\}.$$

We will call the set of points u such that $f^*(u) < \infty$ the dual space X^* of f. The derivatives of a function are also in X^*, so we can often think of dual points u with finite $f^*(u)$ as being derivatives of f at some (unknown) location. We can avoid the use of the extended real numbers if we restrict ourselves to X^* when evaluating f^*. Note also in our definition of the convex conjugate we have used max instead of sup, as they are equivalent for convex f with the domain $\mathbb{R}^d$.

The following properties of convex conjugates are particularly useful:

1. f^* is convex.
2. **Fenchel–Moreau theorem** If f is convex and continuous, then the conjugate-of-the-conjugate (known as the biconjugate) is the original function:

$$f = f^{**}.$$

3. **The Legendre transform property** For strictly convex differentiable functions, the gradient of the convex conjugate maps a point in the dual space into the point at which it is the gradient of. I.e.

$$f^{*\prime}(\big(f^{\prime}(x)\big) = x. \tag{A.1}$$

This result is quite surprising at first glance. It often lets one transform proofs involving a function into a result about it's conjugate. Note that when strict convexity does not hold, the conjugate may not be differentiable at the given dual point $f'(x)$. The value x is still in the sub-differential though. For general differentiable functions f, a function g whose gradient is the inverse map of f' is known as a Legendre transform of f. For strictly convex problems, Equation A.1 implies that $g(x) = f^*(x)$ for all $x \in X^*$, i.e. The Legendre transform is just the convex conjugate restricted to X^* where it is finite.
Another way of interpreting this result is to see the gradient and the conjugate's gradient as the mappings to and from the dual space respectively for a given function.

4. **Fenchel-Young Inequality** Given a dual point u and a primal point x, it holds that:

$$f(x) + f^*(u) \geq \langle x, u \rangle .$$

This inequality becomes an equality when $u = f'(x)$, or for non-differentiable functions, if u is any subgradient at x:

$$f(x) + f^*(f'(x)) = \left\langle f'(x), x \right\rangle .$$

This inequality is useful for computing the conjugate function value. Together with the previous inequality, it is the main tool used to convert proofs to their conjugate version.

5. **Moreau decomposition** For convex f, the proximal operator of the convex conjugate function f^* can be computed trivially from the function's proximal operator using the following equality:

$$\text{prox}_{\gamma}^{f^*}(x) = x - \text{prox}_{\gamma}^{f}(x).$$

This result is surprising, as the conjugate function value is not necessarily this easy to compute.

6. If f has Lipschitz continuous gradients with constant L, then f^* is strongly convex with constant $1/L$. Likewise if f is strongly convex with constant μ, then f^* is Lipschitz smooth with constant $1/\mu$. It follows that the condition number of f^* is the same as f, namely L/μ.

A.3 Types of Duality

The main use of convex conjugates is in forming the *dual problem* of a given convex optimisation problem. This terminology can be ambiguous, as there are several types of duals can potentially be formed. Here we review three types:

Fenchel duality Given a minimisation problem of the form $f(x) - g(x)$, where f is convex and g is concave, the Fenchel dual problem is:

$$\max_u \{g^*(u) - f^*(u)\}.$$

Wolfe duality Given a constrained minimisation problem for the function f with constraints $g_i(x) \leq 0$ for each $i = 1 \dots m$, the Wolfe dual is the following:

$$\max_{x,u_i} f(x) + \sum_j^m u_j g_j(x),$$

$$\text{s.t. } f'(x) + \sum_j^m u_j g_j(x) = 0,$$

$$u_i \geq 0, \quad i = 1, \dots, m.$$

This is the least practical of the discussed duals to work with. The objective is biconvex, and the constraints potentially non-convex.

Lagrangian duality Given a constrained minimisation problem for the function f with constraints $g_i(x) \leq 0$ for each $i = 1 \dots m$, the Lagrange dual is the following:

$$\max_u \min_x \left(f(x) + \sum_j^m u_j g_j(x) \right),$$

$$\text{s.t. } u_i \geq 0, \quad i = 1, \dots, m.$$

When applying this dual, the inner minimisation is usually solved analytically.

A.4 Properties of Differentiable Functions

When proving properties about convex functions, it is cumbersome to work directly with the definitions of differentiability in terms of limits. Instead, we can often use one of the following higher-level theorems.

Theorem A.1. ***(Second fundamental theorem of Calculus)****. Let $f : \mathbb{R} \to \mathbb{R}$ be a differentiable function. Then:*

$$f(y) = f(x) + \int_x^y f'(z)dz.$$

Corollary A.2. *Since we are almost exclusively concerned with vector valued functions, we tend to use this theorem along intervals in a vector space. i.e. let $x, y \in \mathbb{R}^d$ and $f\colon \mathbb{R}^d \to \mathbb{R}$, then*

$$f(y) = f(x) + \int_0^1 \left\langle f'(x + \tau(y - x)),\, y - x \right\rangle d\tau. \tag{A.2}$$

The theorem is also useful when used for functions of the form $f\colon \mathbb{R}^d \to \mathbb{R}^d$, such as derivatives, where it is applied over an interval, but separately for each coordinate. For example, assuming f is twice differentiable:

$$f'(y) = f'(x) + \int_0^1 f''\left(x + \tau(y - x)\right)(y - x)\, d\tau.$$

This appears in proofs of local convergence of Newton's method, where $x = x^*$, and y is the current iterate x_k.

Theorem A.3. ***(Mean value theorem).*** *Let $f\colon \mathbb{R} \to \mathbb{R}$ be a continuously differentiable function and $a, b \in \mathbb{R}$ with $a < b$. Then there exists a $c \in (a, b)$ such that:*

$$f'(c) = \frac{f(b) - f(a)}{b - a}.$$

A.5 Convexity Bounds

This section gives full proofs of a number of basic results in convexity theory. These proofs often appear in the literature in condensed form, or are omitted as exercises. Most theorems in this section can also be proved in the twice differentiable case by arguments involving the Hessian.

A.5.1 Taylor like bounds

Theorem A.4. *(Nesterov, 1998, Thm 2.1.8)* Let f be $\mu \geq 0$ strongly convex and differentiable. Then for all $x, y \in \mathbb{R}$:

$$f(y) \geq f(x) + \left\langle f'(x), y - x \right\rangle + \frac{\mu}{2} \|x - y\|^2.$$

When $\mu = 0$, this is the familiar convexity lower bound $f(y) \geq f(x) + \langle f'(x), y - x\rangle$, which applies for general convex functions.

Proof. From the definition of strong convexity $f(\alpha x + (1-\alpha)y) \leq \alpha f(x) + (1-\alpha) f(y) - \alpha(1-\alpha)\frac{\mu}{2}\|x - y\|^2$ we have:

$$f(\alpha x + (1-\alpha)y) - \alpha f(x) + \alpha(1-\alpha)\frac{\mu}{2}\|x - y\|^2 \leq (1-\alpha) f(y),$$

$$\begin{aligned}
\therefore f(y) &\geq \frac{1}{1-\alpha}\left[f\left(\alpha x+(1-\alpha)y\right)-\alpha f(x)\right]+\alpha\frac{\mu}{2}\left\|x-y\right\|^2 \\
&= f(x)+\frac{1}{1-\alpha}\left[f\left(\alpha x+(1-\alpha)y\right)-f(x)\right]+\alpha\frac{\mu}{2}\left\|x-y\right\|^2 \\
&= f(x)+\frac{1}{1-\alpha}\left[f\left(x+(1-\alpha)(y-x)\right)-f(x)\right]+\alpha\frac{\mu}{2}\left\|x-y\right\|^2. \quad \text{(A.3)}
\end{aligned}$$

Now recall the definition of the directional derivative as a limit:

$$\Delta_v f(x)=\lim_{h\to 0}\frac{f(x+hv)-f(x)}{h}.$$

The second term of our expression A.3 has this form for $h=1-\alpha$ and $v=y-x$, so we take the limit as $\alpha\to 1$, and use the fact that directional derivatives obey $\Delta_v f(x)=\langle f'(x),v\rangle$:

$$\lim_{\alpha\to 1}\frac{1}{1-\alpha}\left[f\left(x+(1-\alpha)(y-x)\right)-f(x)\right]=\Delta_{y-x}f(x)=\left\langle f'(x),y-x\right\rangle,$$

We also need to take the limit of the term $\alpha\frac{\mu}{2}\left\|x-y\right\|^2$ as $\alpha\to 1$, which is trivially $\frac{\mu}{2}\left\|x-y\right\|^2$. Leaving us with:

$$f(y)\geq f(x)+\left\langle f'(x),y-x\right\rangle+\frac{\mu}{2}\left\|x-y\right\|^2.$$

□

Theorem A.5. ***(Lipschitz upper bound)*** *(Nesterov, 1998, Thm 2.1.5) If f is convex and L-smooth, then for all $x,y\in\mathbb{R}^d$:*

$$f(y)\leq f(x)+\left\langle f'(x),y-x\right\rangle+\frac{L}{2}\left\|x-y\right\|^2.$$

Proof. Using the second fundamental theorem of calculus, in the interval form of Equation A.2, we have:

$$\begin{aligned}
f(y) &= f(x)+\int_0^1\left\langle f'(x+\tau(y-x)),y-x\right\rangle d\tau \\
&= f(x)+\left\langle f'(x),y-x\right\rangle+\int_0^1\left\langle f'(x+\tau(y-x))-f'(x),y-x\right\rangle d\tau \\
&\leq f(x)+\left\langle f'(x),y-x\right\rangle+\int_0^1\left\|f'(x+\tau(y-x))-f'(x)\right\|\left\|x-y\right\|d\tau \text{ (Cauchy-Schwarz)} \\
&\leq f(x)+\left\langle f'(x),y-x\right\rangle+\int_0^1\tau L\left\|x-y\right\|^2 d\tau \quad \text{(Lipschitz condition)} \\
&= f(x)+\left\langle f'(x),y-x\right\rangle+\frac{L}{2}\left\|x-y\right\|^2.
\end{aligned}$$

□

A.5.2 Gradient difference bounds

Theorem A.6. *If f is strongly convex with constant μ, then for all $x, y \in \mathbb{R}^d$:*

$$f(y) \leq f(x) + \langle f'(x), y - x \rangle + \frac{1}{2\mu} \left\| f'(x) - f'(y) \right\|^2 .$$

Proof. Let u and v be points in the dual space of f. As noted in point 6 of the properties of convex conjugates in Section A.2, f^* has Lipschitz continuous gradients with constant $1/\mu$. So:

$$f^*(v) - f^*(u) - \langle f^{*\prime}(u), u - v \rangle \leq \frac{1}{2\mu} \|u - v\|^2 .$$

Now take $v = f'(x)$ and $u = f'(y)$. We replace each f^* with f using The Fenchel-Young equality $f(x) + f^*(f'(x)) = \langle f'(x), x \rangle$:

$$\langle f'(x), x \rangle - f(x) - \langle f'(y), y \rangle + f(y) - \langle f^{*\prime}(f'(y)), f'(x) - f'(y) \rangle \leq \frac{1}{2\mu} \left\| f'(x) - f'(y) \right\|^2 .$$

The remaining dual quantity obeys $f^{*\prime}(f'(y)) = y$ (See point 3 in Section A.2), so we can simplify further to get the result:

$$f(y) - f(x) + \langle f'(x), x - y \rangle \leq \frac{1}{2\mu} \left\| f'(x) - f'(y) \right\|^2 .$$

□

Remark A.7. This bound in full generality rarely appears in the literature. It is more often seen in the special case of $x = x^*$ and $y = x$ in the form:

$$\left\| f'(x) \right\|^2 \geq 2\mu \left[f(x) - f(x^*) \right] ,$$

which is used in proving convergence of gradient descent for strongly convex functions in terms of function value.

Theorem A.8. *(Nesterov, 1998, Thm 2.1.5) If f is convex and L-smooth, then for all $x, y \in \mathbb{R}^d$:*

$$f(y) \geq f(x) + \langle f'(x), y - x \rangle + \frac{1}{2L} \left\| f'(x) - f'(y) \right\|^2 .$$

Proof. Define $g(y) = f(y) - \langle f'(x), y \rangle$. Then g is convex and has gradient $g'(y) = f'(y) - f'(x)$. Clearly the gradient is zero at x, so its minimiser is $y^* = x$. Now consider the gradient step $y - \frac{1}{L} g'(y)$. We apply the Lipschitz upper bound (Theorem A.5) to g at $y - \frac{1}{L} f'(y)$ around y.

$$\begin{aligned} g\left(y - \frac{1}{L} g'(y) \right) &\leq g(y) + \left\langle g'(y), y - \frac{1}{L} g'(y) \right\rangle + \frac{L}{2} \left\| -\frac{1}{L} g'(y) \right\|^2 \\ &= g(y) - \frac{1}{2L} \left\| g'(y) \right\|^2 . \end{aligned}$$

We know that y^* gives as least as small a function value as any other point, i.e. $g(y^*) \leq g(y - \frac{1}{L}g'(y))$. Given that $y^* = x$, we thus have:

$$g(x) \leq g(y) - \frac{1}{2L} \left\| g'(y) \right\|^2.$$

Therefore, by plugging in f:

$$f(x) - \left\langle f'(x), x \right\rangle \leq f(y) - \left\langle f'(x), y \right\rangle - \frac{1}{2L} \left\| f'(y) - f'(x) \right\|^2,$$

$$\therefore -f(y) \leq -f(x) + \left\langle f'(x), x - y \right\rangle - \frac{1}{2L} \left\| f'(y) - f'(x) \right\|^2.$$

Negating gives the result. □

Remark A.9. This proof follows Nesterov (1998). It can also be proved using the techniques used in Theorem A.6, which gives a less mysterious but more straightforward proof.

A.5.3 Inner product bounds

All (continuously-differentiable) convex functions satisfy the basic inequality $\left\langle f'(x) - f'(y), x - y \right\rangle \geq 0$ for any x, y (See Nesterov, 1998, Thm 2.1.3). This inequality can be strengthened for the classes of functions we consider, using the following theorems.

Theorem A.10. *(Nesterov, 1998, Thm 2.1.5) If f is L-smooth and convex, then for all $x, y \in \mathbb{R}^d$:*

$$\left\langle f'(x) - f'(y), x - y \right\rangle \geq \frac{1}{L} \left\| f'(x) - f'(y) \right\|^2.$$

Proof. From Theorem A.14 we have: $f(y) \geq f(x) + \left\langle f'(x), y - x \right\rangle + \frac{1}{2L} \left\| f'(x) - f'(y) \right\|^2$. Add this to the same inequality but with x and y reversed and we get:

$$f(y) + f(x) \geq f(x) + f(y) + \left\langle f'(x), y - x \right\rangle + \left\langle f'(y), x - y \right\rangle + \frac{1}{L} \left\| f'(x) - f'(y) \right\|^2,$$

$$\therefore \left\langle f'(x) - f'(y), x - y \right\rangle \geq \frac{1}{L} \left\| f'(x) - f'(y) \right\|^2.$$

□

Theorem A.11. *(Nesterov, 1998, Thm 2.1.9) If f is strongly convex with constant μ, then for all $x, y \in \mathbb{R}^d$:*

$$\left\langle f'(x) - f'(y), x - y \right\rangle \geq \mu \left\| x - y \right\|^2.$$

Proof. Same as previous theorem, using the strong convexity lower bound. □

A.5.4 Strengthened bounds using both Lipschitz and strong convexity

Theorem A.12. *(Nesterov, 1998, Thm 2.1.11) If f is strongly convex with constant μ and L-smooth, then for all $x, y \in \mathbb{R}^d$:*

$$\left\langle f'(x) - f'(y), x - y \right\rangle \geq \frac{\mu L}{\mu + L} \left\| x - y \right\|^2 + \frac{1}{\mu + L} \left\| f'(x) - f'(y) \right\|^2.$$

Proof. Define the function g as $g(x) = f(x) - \frac{\mu}{2} \left\| x \right\|^2$. Then the gradient is $g'(x) = f'(x) - \mu x$, and g is $(L - \mu)$-smooth. From Theorem A.10 we have:

$$\left\langle g'(x) - g'(y), x - y \right\rangle \geq \frac{1}{L - \mu} \left\| g'(x) - g'(y) \right\|^2.$$

Now replacing g with f:

$$\left\langle f'(x) - f'(y) - \mu \left(x - y \right), x - y \right\rangle \geq \frac{1}{L - \mu} \left\| f'(x) - f'(y) - \mu \left(x - y \right) \right\|^2.$$

So:

$$\begin{aligned}
\left\langle f'(x) - f'(y), x - y \right\rangle &\geq \mu \left\| x - y \right\|^2 + \frac{1}{L - \mu} \left\| f'(x) - f'(y) - \mu \left(x - y \right) \right\|^2 \\
&= \mu \left\| x - y \right\|^2 + \frac{1}{L - \mu} \left\| f'(x) - f'(y) \right\|^2 \\
&\quad - \frac{2\mu}{L - \mu} \left\langle f'(x) - f'(y), x - y \right\rangle + \frac{\mu^2}{L - \mu} \left\| x - y \right\|^2 \\
\left(1 + \frac{2\mu}{L - \mu} \right) \left\langle f'(x) - f'(y), x - y \right\rangle &\geq \left(\mu + \frac{\mu^2}{L - \mu} \right) \left\| x - y \right\|^2 + \frac{1}{L - \mu} \left\| f'(x) - f'(y) \right\|^2 \\
\frac{L - \mu + 2\mu}{L - \mu} \left\langle f'(x) - f'(y), x - y \right\rangle &\geq \frac{(L - \mu)\mu + \mu^2}{L - \mu} \left\| x - y \right\|^2 + \frac{1}{L - \mu} \left\| f'(x) - f'(y) \right\|^2 \\
\frac{L + \mu}{L - \mu} \left\langle f'(x) - f'(y), x - y \right\rangle &\geq \frac{\mu L}{L - \mu} \left\| x - y \right\|^2 + \frac{1}{L - \mu} \left\| f'(x) - f'(y) \right\|^2.
\end{aligned}$$

Multiplying through by $\frac{L - \mu}{L + \mu}$ gives the result. □

Remark A.13. This inequality allows us to get the RHS from both inner product inequalities from Section A.5.3 added together, while only losing about a multiplicative $\frac{\mu}{L}$ factor on each. We can also achieve the same result by interpolating between the two inequalities, but that loses a factor of $\frac{1}{2}$ for each. Since the constants are more complex in this combined inequality, it leads to more technical but stronger proofs.

Theorem A.14. *If f is strongly convex with constant μ and L-smooth, then for all $x, y \in \mathbb{R}^d$:*

$$\begin{aligned} f(x) \quad \geq \quad & f(y) + \langle f'(y), x - y \rangle + \frac{1}{2(L-\mu)} \left\| f'(x) - f'(y) \right\|^2 + \frac{\mu L}{2(L-\mu)} \left\| x - y \right\|^2 \\ & + \frac{\mu}{(L-\mu)} \langle f'(x) - f'(y), y - x \rangle . \end{aligned}$$

Proof. Define the function g as $g(x) = f(x) - \frac{\mu}{2} \left\| x \right\|^2$. Then the gradient is $g'(x) = f'(x) - \mu x$. g has a Lipschitz continuous gradient with constant $L - \mu$. By convexity we have:

$$g(x) \geq g(y) + \langle g'(y), x - y \rangle + \frac{1}{2L} \left\| g'(x) - g'(y) \right\|^2 .$$

Now replacing g with f:

$$\begin{aligned} f(x) - \frac{\mu}{2} \left\| x \right\|^2 \quad \geq \quad & f(y) - \frac{\mu}{2} \left\| y \right\|^2 + \langle f'(y) - \mu y, x - y \rangle \\ & + \frac{1}{2(L-\mu)} \left\| f'(x) - \mu x - f'(y) + \mu y \right\|^2 . \end{aligned}$$

Note that

$$\begin{aligned} \frac{1}{2(L-\mu)} \left\| f'(x) - \mu x - f'(y) + \mu y \right\|^2 \quad = \quad & \frac{1}{2(L-\mu)} \left\| f'(x) - f'(y) \right\|^2 \\ & + \frac{\mu^2}{2(L-\mu)} \left\| y - x \right\|^2 \\ & + \frac{\mu}{(L-\mu)} \langle f'(x) - f'(y), y - x \rangle , \end{aligned}$$

so:

$$\begin{aligned} f(x) \quad \geq \quad & f(y) + \langle f'(y), x - y \rangle + \frac{1}{2(L-\mu)} \left\| f'(x) - f'(y) \right\|^2 + \frac{\mu^2}{2(L-\mu)} \left\| y - x \right\|^2 \\ & + \frac{\mu}{2} \left\| x \right\|^2 - \frac{\mu}{2} \left\| y \right\|^2 + \frac{\mu}{(L-\mu)} \langle f'(x) - f'(y), y - x \rangle - s \langle y, x - y \rangle . \end{aligned}$$

Now using:

$$\frac{\mu}{2} \left\| x \right\|^2 - \mu \langle y, x \rangle = -\frac{\mu}{2} \left\| y \right\|^2 + \frac{\mu}{2} \left\| x - y \right\|^2 ,$$

we get:

$$\begin{aligned} f(x) &\geq f(y) + \langle f'(y), x-y\rangle + \frac{1}{2(L-\mu)}\left\|f'(x)-f'(y)\right\|^2 + \frac{\mu^2}{2(L-\mu)}\|x-y\|^2 \\ &\quad -\mu\|y\|^2 + \frac{\mu}{2}\|x-y\|^2 + \frac{\mu}{(L-\mu)}\langle f'(x)-f'(y), y-x\rangle + \mu\langle y, y\rangle. \end{aligned}$$

Note the norm y terms cancel, and:

$$\begin{aligned} \frac{\mu}{2}\|x-y\|^2 + \frac{\mu^2}{2(L-\mu)}\|x-y\|^2 &= \frac{(L-\mu)\mu+\mu^2}{2(L-\mu)}\|x-y\|^2 \\ &= \frac{\mu L}{2(L-\mu)}\|x-y\|^2. \end{aligned}$$

So:

$$\begin{aligned} f(x) &\geq f(y) + \langle f'(y), x-y\rangle + \frac{1}{2(L-\mu)}\left\|f'(x)-f'(y)\right\|^2 + \frac{\mu L}{2(L-\mu)}\|y-x\|^2 \\ &\quad + \frac{\mu}{(L-\mu)}\langle f'(x)-f'(y), y-x\rangle. \end{aligned}$$

□

Remark A.15. This inequality uses the same proof technique as Theorem A.12, and indeed that theorem can be proved using this one, using a similar proof technique as Theorem A.10. I'm not aware of this theorem appearing in the literature previously, although it is too simple to be novel.

Theorem A.16. *If f is twice differentiable, strongly convex with constant μ and L-smooth, then for all $x, y \in \mathbb{R}^d$.*

$$\left\|x-y+t\left(f'(y)-f'(x)\right)\right\| \leq \max\left\{|1-tL|, |1-t\mu|\right\}\|x-y\|.$$

Proof. We start by applying Corollary A.2:

$$f'(y)-f'(x) = \int_0^1 f''\left(x+\tau(y-x)\right)(y-x)\,d\tau.$$

Therefore:

$$\begin{aligned}
\left\|x - y + t\left(f'(y) - f'(x)\right)\right\| &= \left\|x - y + t\int_0^1 f''\left(x + \tau(y-x)\right)(y-x)\,d\tau\right\| \\
&= \left\|\int_0^1 \left(tf''\left(x + \tau(y-x)\right) - I\right)(y-x)\,d\tau\right\| \\
&\leq \int_0^1 \left\|\left(tf''\left(x + \tau(y-x)\right) - I\right)(y-x)\right\| d\tau \\
&\leq \int_0^1 \left\|tf''\left(x + \tau(y-x)\right) - I\right\| \|x-y\|\,d\tau \\
&\leq \max_z \left\|tf''(z) - I\right\| \|x-y\|.
\end{aligned}$$

Consider the eigenvalues of $f''(z)$. The minimum one is at least μ and the maximum at least L. An examination of the possible eigenvalues of $(tf''(z) - I)$ then gives the result. □

Remark A.17. This lemma gives a straightforward proof of the convergence of gradient descent for strongly convex problems. Suppose we use $x^{k+1} = x^k - \frac{2}{L+\mu}f'(x^k)$. Then

$$\begin{aligned}
\left\|x^{k+1} - x^*\right\| &= \left\|x^k - x^* + \frac{2}{L+\mu}\left(f'(x^*) - f'(x^k)\right)\right\| \\
&\leq \max\left\{\left|1 - \frac{2}{L+\mu}L\right|, \left|1 - \frac{2}{L+\mu}\mu\right|\right\}\left\|x^k - x^*\right\|
\end{aligned}$$

Now note that

$$\left|1 - \frac{2}{L+\mu}L\right| = \left|1 - \frac{2L+2\mu-2\mu}{L+\mu}\right| = \left|1 - 2 + \frac{2}{L+\mu}\mu\right| = \left|1 - \frac{2}{L+\mu}\mu\right|$$

so the two parts of the max operation are balanced. The rate can also be written as:

$$1 - \frac{2}{L+\mu}\mu = \frac{L+\mu}{L+\mu} - \frac{2\mu}{L+\mu} = \frac{L-\mu}{L+\mu}.$$

So we have:

$$\left\|x^k - x^*\right\| \leq \left(\frac{L-\mu}{L+\mu}\right)^k \left\|x^0 - x^*\right\|.$$

Miscellaneous Lemmas

In this Appendix we summarise a number of standard lemmas. These are well known in some research circles and obscure in others. We omit proofs when they are overly technical.

Lemma B.1. *For any vectors $a, b \in \mathbb{R}^d$, and constant $\beta > 0$:*

$$\|a+b\|^2 \leq (1+\beta)\|a\|^2 + \left(1+\frac{1}{\beta}\right)\|b\|^2.$$

Proof. We start by expanding the quadratic:

$$\begin{aligned}\|a+b\|^2 &= 2\langle a, b\rangle + \|a\|^2 + \|b\|^2 \\ &= 2\left\langle \sqrt{\beta}a, \frac{1}{\sqrt{\beta}}b\right\rangle + \|a\|^2 + \|b\|^2.\end{aligned}$$

Now by expanding the quadratic $\left\|\sqrt{\beta}a + \frac{1}{\sqrt{\beta}}b\right\|^2$ we get: $2\left\langle \sqrt{\beta}a, \frac{1}{\sqrt{\beta}}b\right\rangle \leq \beta\|a\|^2 + \frac{1}{\beta}\|b\|^2$. So combining we have:

$$\|a+b\|^2 \leq (1+\beta)\|a\|^2 + \left(1+\frac{1}{\beta}\right)\|b\|^2.$$

□

Remark B.2. This lemma is a rather interesting strengthened version of the more commonly used lemma $\|a+b\|^2 \leq 2\|a\|^2 + 2\|b\|^2$. It can be seen as the most natural generalisation of the triangle inequality to squared norms. Since in optimisation theory we virtually always work with squared norms, this kind of result is quite useful.

Lemma B.3. *For any $x \in \mathbb{R}$:*

$$\exp(1+x) \geq 1+x,$$

$$\textit{and for } x > -1,\ \log(1+x) \leq 1+x.$$

Proof. We apply the convexity lower bound around $x = -1$ to $\exp(1+x)$:

$$\begin{aligned}\exp(1+x) &\geq e^0 + \langle e^0, x+1 \rangle \\ &\geq 1 + x.\end{aligned}$$

Similarly, for $\log(1+x)$ we apply the concavity upper bound at $x = 0$:

$$\begin{aligned}\log(1+x) &\leq \log(1) + \left\langle \frac{1}{1}, x - 0 \right\rangle \\ &= x \\ &\leq 1 + x.\end{aligned}$$

□

Lemma B.4. ***(Bernoulli's Inequality)*** *For any $\alpha \in [0, 1)$ and integer $k \geq 0$:*

$$(1-\alpha)^k \geq 1 - k\alpha.$$

Proof. This can easily be proved by induction. The base case $k = 0$ is trivial. Suppose it holds for k. Then:

$$\begin{aligned}(1-\alpha)^{k+1} = (1-\alpha)^k(1-\alpha) &\geq (1-k\alpha)(1-\alpha) \\ &= 1 - \alpha - k\alpha + k\alpha^2 \\ &= 1 - (k+1)\alpha + k\alpha^2 \\ &\geq 1 - (k+1)\alpha.\end{aligned}$$

□

Remark B.5. Notice that the terms that prevent this from being an equality are of the form $\sum_i^k i\alpha^2 \leq k^2\alpha^2$. If $\alpha \ll \frac{1}{k}$, then it holds approximately as an equality.

Lemma B.6. ***(Bernoulli's Inequality for roots)*** *For any real numbers$\alpha \leq 1$ and $r \in (0, 1)$:*

$$(1-\alpha)^r \leq 1 - r\alpha.$$

I.e. The direction of inequality for Bernoulli's inequality flips when using roots instead of powers.

Proof. The functions $f(\alpha) = (1-\alpha)^r$ and $g(\alpha) = 1 - r\alpha$ have the same derivative at 0. Since $g(\alpha)$ is linear and $g(0) = f(0)$, it is the tangent line of $f(\alpha)$ at $\alpha = 0$. The $f(\alpha)$ function is concave for $r \in (0, 1)$, so it is upper bounded by its tangent, so $f(\alpha) \leq g(\alpha)$. □

Lemma B.7. *For any α and $k \geq 0$:*

$$(1-\alpha)^k \leq \exp(-k\alpha).$$

Proof. In Lemma B.3, we established that $\exp(1+x) \geq 1+x$. Raising both sides to the power k will give the result. □

Remark B.8. This inequality bounds the same quantity as Bernoulli's inequality, but with an upper bound instead of a lower bound. Like Bernoulli's inequality this can hold with close to equality, but instead in the setting where α is similar in magnitude to $\frac{1}{k}$; indeed the error in such an approximation goes to zero asymptotically. This is essentially the well known limiting definition of e:

$$\left(1-\frac{1}{n}\right)^n \to \frac{1}{e}, \text{ and } \left(1+\frac{1}{n}\right)^n \to e.$$

This converges fairly quickly for our purposes. For example it is only 2% off at $n = 30$, and for $n = 1000$, we get $0.367\mathbf{7}\ldots$ compare to $1/e = 0.367\mathbf{8}\ldots$. In optimisation proofs n is approximately the amount of data, so $n \gg 1000$ is typical.

This lemma is convenient for converting bounds on the error that a k step procedure gives, to a bound on the number of steps required to ensure at most some error level. For example, suppose we have a bound on the error after k steps of the form:

$$\epsilon \leq (1-\alpha)^k,$$

Then using Lemma B.7 we get $\epsilon \leq \exp(-\alpha k)$. Now suppose we want to ensure our error is less than ξ ($\epsilon \leq \xi$). If we take $k \geq -\alpha^{-1}\log\xi$, then

$$\begin{aligned} \epsilon &\leq \exp(-\alpha k) \\ &\leq \exp(\log\xi) \\ &\leq \xi, \end{aligned}$$

as required. These two ways of stating the convergence of an iterative algorithm are essentially equivalent, and different literature uses different styles. The lower bound k style is more common when constants are not considered important, as it is easily used in conjunction with Big-O notation, like $k = O\left(-\alpha^{-1}\log\xi\right)$. We use the explicit error bound style in this work as it is better suited to the careful style of our analysis. We do not use Big-O notation in our proofs, instead we explicitly compute the values of the extra constants.

Lemma B.9. *(Decomposition of variance)*

We can decompose $\mathbb{E}_x \|y-x\|^2$ as:

$$\mathbb{E}_x \|y-x\|^2 = \|y-\mathbb{E}_x[x]\|^2 + \mathbb{E}_x \|\mathbb{E}_x[x]-x\|^2.$$

Taking $y = 0$ gives the useful equality: $\mathbb{E}[\|x - \mathbb{E}[x]\|^2] = \mathbb{E}[\|x\|^2] - \|\mathbb{E}[x]\|^2$.

Proof.

$$\begin{aligned}
\mathbb{E}_x \|y - x\|^2 &= \mathbb{E}_x \|y - \mathbb{E}_x[x] + \mathbb{E}_x[x] - x\|^2 \\
&= \|y - \mathbb{E}_x[x]\|^2 + \mathbb{E}_x \|\mathbb{E}_x[x] - x\|^2 + 2\mathbb{E}_x \langle y - \mathbb{E}_x[x], \mathbb{E}_x[x] - x\rangle \quad \text{(B.1)} \\
&= \|y - \mathbb{E}_x[x]\|^2 + \mathbb{E}_x \|\mathbb{E}_x[x] - x\|^2 + 2 \langle y - \mathbb{E}_x[x], \mathbb{E}_x[x] - \mathbb{E}_x[x]\rangle \\
&= \|y - \mathbb{E}_x[x]\|^2 + \mathbb{E}_x \|\mathbb{E}_x[x] - x\|^2 . \quad \text{(B.2)}
\end{aligned}$$

□

References

Anandkumar, A.; Tan, V. Y. F.; and Willsky, A. S., 2011a. High-dimensional gaussian graphical model selection: Walk summability and local separation criterion. Technical report, University of California Irvine. (cited on pages 108, 137, 138, and 139)

Anandkumar, A.; Tan, V. Y. F.; and Willsky, A. S., 2011b. High-dimensional graphical model selection: Tractable graph families and necessary conditions. *NIPS*, (2011). (cited on pages 107 and 129)

Andrew, G. and Gao, J., 2007. Scalable training of l1-regularized log-linear models. *ICML*, (2007). (cited on page 2)

Bach, F., 2010a. Convex analysis and optimization with submodular functions: a tutorial. Technical report, INRIA. (cited on page 113)

Bach, F., 2010b. Structured sparsity-inducing norms through submodular functions. *NIPS*, (2010). (cited on pages 113, 114, 115, and 122)

Bach, F.; Jenatton, R.; Mairal, J.; and Obozinski, G., 2012. *Optimization for Machine Learning*, chap. Convex Optimization with Sparsity-Inducing Norms, 19–49. MIT press. (cited on page 109)

Banerjee, O.; Ghaoui, L. E.; d'Aspremont, A.; and Natsoulis, G., 2006. Convex optimization techniques for fitting sparse gaussian graphical models. *ICML*, (2006). (cited on page 105)

Barabasi, A.-L. and Albert, R., 1999. Emergence of scaling in random networks. *Science*, 286 (1999), 509–512. (cited on pages 113, 120, and 134)

Bayati, M.; Kim, J. H.; and Saberi, A., 2009. A sequential algorithm for generating random graphs. *Algorithmica*, 58 (2009). (cited on page 120)

Beck, A. and Teboulle, M., 2009. A fast iterative shrinkage-thresholding algorithm for linear inverse problems. *SIAM Journal on Imaging Sciences*, 2, 1 (2009), 183–202. (cited on page 4)

Beck, A. and Tetruashvili, L., 2013. On the convergence of block coordinate descent type methods. *SIAM Journal on Optimization*, 23:4 (2013), 2037–2060. (cited on page 93)

Bell, R. and Koren, Y., 2007. Scalable collaborative filtering with jointly derived neighborhood interpolation weights. In *IEEE International Conference on Data Mining*. (cited on pages 150, 151, and 157)

Berman, A. and Plemmons, R. J., 1994. *Nonnegative matrices in the mathematical sciences*. Society for Industrial and Applied Mathematics. (cited on page 142)

Bertsekas, D. P., 2012. Incremental gradient, subgradient, and proximal methods for convex optimization: A survey. In *Optimization for Machine Learning*. MIT Press. (cited on page 13)

Bickel, P. J. and Levina, E., 2008. Covariance regularization by thresholding. *Annals of Statistics*, (2008). (cited on page 106)

Bishop, C. M., 2006. *Pattern recognition and machine learning*. Springer. (cited on pages 10 and 153)

Blatt, D.; Hero, A. O.; and Gauchman, H., 2007. A convergent incremental gradient method with a constant step size. *SIAM Journal of Optimization*, (2007). (cited on page 19)

Boyd, S.; Parikh, N.; Chu, E.; Peleato, B.; and Eckstein, J., 2011. Distributed optimization and statistical learning via the alternating direction method of multipliers. *Foundations and Trends in Machine Learning*, 3 (2011). (cited on pages 115 and 116)

Callahan, D.; Cocke, J.; and Kennedy, K., 1988. Estimating interlock and improving balance for pipelined architectures. *Journal of Parallel and Distributed Computing*, (1988). (cited on page 161)

Candes, E. J.; Wakin, M. B.; and Boyd, S. P., 2008. Enhancing sparsity by reweighted l1 minimization. *Journal of Fourier Analysis and Applications*, (2008). (cited on page 108)

Chow, C. and Liu, C., 1968. Approximating discrete probability distributions with dependence trees. *IEEE Transaction on Information Theory*, (1968). (cited on page 107)

Combettes, P. and Pesquet, J.-C., 2011. *Proximal Splitting Methods in Signal Processing. In Fixed-Point Algorithms for Inverse Problems in Science and Engineering*. Springer. (cited on pages 33 and 56)

Cseke, B. and Heskes, T., 2011. Properties of bethe free energies and message passing in gaussian models. *JAIR*, 40 (2011). (cited on page 148)

Dauwels, J.; Yu, H.; Xu, S.; and Wang, X., 2013. Copula gaussian graphical model for discrete data. In *International Conference on Acoustics, Speech and Signal Processing*. (cited on page 102)

de Klerk, E. and Pasechnik, D. V., 2006. Approximation of the stability number of a graph via copositive programming. *SIAM Journal on Optimization*, (2006). (cited on page 2)

Dean, J.; Corrado, G. S.; Rajat Monga, K. C.; Devin, M.; Le, Q. V.; Mao, M. Z.; Ranzato, M.; Senior, A.; Tucker, P.; Yang, K.; and Ng, A. Y., 2012. Large scale distributed deep networks. *NIPS*, (2012). (cited on page 2)

Defazio, A.; Bach, F.; and Lacoste-Julien, S., 2014a. Saga: A fast incremental gradient method with support for non-strongly convex composite objectives. *Advances in Neural Information Processing Systems 27 (NIPS 2014)*, (2014). (cited on pages 8, 55, and 59)

Defazio, A. and Caetano, T., 2012a. A convex formulation for learning scale-free networks via submodular relaxation. *Advances in Neural Information Processing Systems 25 (NIPS 2012)*, (2012). (cited on pages 8 and 111)

Defazio, A. and Caetano, T., 2012b. A graphical model formulation of collaborative filtering neighbourhood methods with fast maximum entropy training. *The 29th International Conference on Machine Learning (ICML 2012)*, (2012). (cited on pages 8 and 141)

Defazio, A.; Caetano, T.; and Domke, J., 2014b. Finito: A faster, permutable incremental gradient method for big data problems. *The 31st International Conference on Machine Learning (ICML 2014)*, (2014). (cited on pages 8 and 23)

Dempster, A. P., 1972. Covariance selection. *Biometrics*, 28 (1972), 157–175. (cited on pages 102 and 107)

Dobra, A.; Hans, C.; Jones, B.; Nevins, J. R.; and West, M., 2004. Sparse graphical models for exploring gene expression data. *Journal of Multivariate Analysis*, (2004). (cited on page 111)

Erdos, P. and Renyi, A., 1959. On random graphs. *Publicationes Mathematicae*, (1959). (cited on page 134)

Fan, R.-E.; Chang, K.-W.; Hsieh, C.-J.; Wang, X.-R.; and Lin, C.-J., 2008. Liblinear: A library for large linear classification. *Journal of Machine Learning Research*, (2008). (cited on page 162)

Federer, A., 2011. *Estimating networks using mutual information*. Master's thesis, Swiss Federal Institute of Technology Zurich. (cited on page 107)

Friedman, J.; Hastie, T.; and Tibshirani, R., 2007. Sparse inverse covariance estimation with the graphical lasso. *Biostatistics*, (2007). (cited on pages 105 and 120)

Fujishige, S., 2005. *Submodular Functions and Optimization*. Elsevier. (cited on page 115)

Funk, S., 2006. Netflix update: Try this at home. http://sifter.org/~simon/journal/20061211.html. (cited on page 155)

Gabay, D. and Mercier, B., 1976. A dual algorithm for the solution of nonlinear variational problems via finite element approximations. *Computers and Mathematics with Applications*, (1976). (cited on page 115)

Glowinski, R. and Marrocco, A., 1975. Sur l'approximation, par éléments finis d'ordre un, et la résolution, par pénalisation-dualité d'une classe de problèmes de dirichlet non linéares. *Revue Française d'Automatique, Informatique, et Recherche Opérationelle*, (1975). (cited on page 115)

Gonzaga, C. and Karas, E., 2013. Fine tuning nesterov's steepest descent algorithm for differentiable convex programming. *Mathematical Programming*, 138, 1-2 (2013), 141–166. doi:10.1007/s10107-012-0541-z. http://dx.doi.org/10.1007/s10107-012-0541-z. (cited on page 163)

Granapathi, V.; Vickrey, D.; Duchi, J.; and Koller, D., 2008. Constrained approximate maximum entropy learning of markov random fields. In *UAI*. (cited on page 158)

Griffith, J.; O'Riordan, C.; and Sorensen, H., 2006. A constrained spreading activation approach to collaborative filtering. In *Knowledge-Based Intelligent Information and Engineering Systems*. (cited on page 157)

Hinton, G. E., 2002. Training products of experts by minimizing contrastive divergence. *Neural computation*, 14, 8 (2002), 1771–1800. (cited on page 1)

Hsieh, C.-J.; Sustik, M. A.; Dhillon, I.; Ravikumar, P.; and Poldrack, R., 2013. Big & quic: Sparse inverse covariance estimation for a million variables. In *Advances in Neural Information Processing Systems 26* (Eds. C. Burges; L. Bottou; M. Welling; Z. Ghahramani; and K. Weinberger), 3165–3173. http://papers.nips.cc/paper/4923-big-quic-sparse-inverse-covariance-estimation-for-a-million-variables.pdf. (cited on page 105)

Hsieh, C.-J.; Sustik, M. A.; Dhillon, I. S.; and Ravikumar, P., 2011. Sparse inverse covariance matrix estimation using quadratic approximation. *NIPS*, (2011). (cited on page 105)

Huang, Z.; Chen, H.; and Zeng, D., 2004. Applying associative retrieval techniques to alleviate the sparsity problem in collaborative filtering. *ACM Transactions on Information Systems*, (2004). (cited on page 155)

Hunter, D. R. and Lange, K., 2000. Quantile regression via an mm algorithm. *Journal of Computational and Graphical Statistics*, 9 (2000). (cited on page 108)

Jakulin, A. and Buntine, W., 2004. Analyzing the us senate in 2003: Similarities, networks, clusters and blocs. (cited on page 165)

Jenatton, R.; Mairal, J.; Obozinski, G.; and Bach, F., 2010a. Proximal methods for sparse hierarchical dictionary learning. *ICML*, (2010). (cited on page 111)

Jenatton, R.; Obozinski, G.; and Bach, F., 2010b. Structured sparse principal component analysis. *AISTATS*, (2010). (cited on page 111)

Johnson, R. and Zhang, T., 2013. Accelerating stochastic gradient descent using predictive variance reduction. *NIPS*, (2013). (cited on pages 20, 59, 65, and 161)

Koller, D. and Friedman, N., 2009. *Probabilistic Graphical Models: Principles and Techniques*. MIT Press. (cited on pages 107, 144, 146, and 161)

Konečný, J. and Richtárik, P., 2013. Semi-Stochastic Gradient Descent Methods. *ArXiv e-prints*, (Dec. 2013). (cited on pages 20, 21, and 64)

Koren, Y., 2010. Factor in the neighbors: Scalable and accurate collaborative filtering. *ACM Trans. Knowl. Discov. Data*, (2010). (cited on pages 155 and 157)

Lie, J.-G. and Wang, B.-H., 2007. Improved collaborative filtering via information transformation. *CoRR*, (2007). (cited on page 157)

Liu, D. C. and Nocedal, J., 1989. On the limited memory bfgs method for large scale optimization. *Mathematical programming*, 45, 1-3 (1989), 503–528. (cited on page 2)

Liu, Q. and Ihler, A., 2011. Learning scale free networks by reweighted l1 regularization. *AISTATS*, (2011). (cited on pages 108 and 120)

Lu, Z., 2009. Smooth optimization approach for sparse covariance selection. *SIAM J. Optim.*, (2009). (cited on page 114)

Mairal, J., 2013. Optimization with first-order surrogate functions. *ICML*, (2013). (cited on pages 27 and 30)

Mairal, J., 2014. Incremental majorization-minimization optimization with application to large-scale machine learning. Technical report, INRIA Grenoble RhÃt'ne-Alpes / LJK Laboratoire Jean Kuntzmann. (cited on pages 30, 93, and 161)

Maliotov, D. M.; Johnson, J. K.; and Willsky, A. S., 2006. Walk-sums and belief propagation in gaussian graphical models. *Journal of Machine Learning Research*, (2006), 2031–2064. (cited on page 134)

McAuley, J. J. and Caetano, T. S., 2011. Faster algorithms for max-product message-passing. *JMLR*, (2011). (cited on page 130)

Meinshausen, N. and Bühlmann, P., 2006. High dimensional graphs and variable selection with the lasso. *Annals of Statistics*, (2006). (cited on page 106)

Nedic, A. and Bertsekas, D., 2000. Convergence rate of incremental subgradient algorithms. *Stochastic Optimization: Algorithms and Applications*, (2000), 263–304. (cited on page 93)

Nemirovsky, A. S. and Yudin, D. B., 1983. *Problem Complexity and Method Efficiency in Optimization*. Wiley-Interscience. (cited on pages 3 and 86)

Nesterov, Y., 1988. On an approach to the construction of optimal methods of minimization of smooth convex functions. *Ekonomika i Mateaticheskie Metody*, 24 (1988), 509–517. (cited on page 86)

Nesterov, Y., 1998. *Introductory Lectures On Convex Programming*. Springer. (cited on pages 3, 87, 89, 171, 172, 173, 174, and 175)

Nesterov, Y., 2005. Smooth minimization of non-smooth functions. *Math. Program. Ser. A*, 103 (2005). (cited on page 3)

Nesterov, Y., 2010. Efficiency of coordinate descent methods on huge-scale optimization problems. Technical report, CORE. (cited on page 36)

Nesterov, Y. and Nemirovski, A., 1994. *Interior-Point Polynomial Algorithms in Convex Programming*. SIAM Studies in Applied Mathematics. (cited on page 2)

Nocedal, J., 1980. Updating quasi-newton matrices with limited storage. *Mathematics of Computation*, 35 (1980), 773–782. (cited on pages 2 and 5)

Nutini, J.; Schmidt, M.; Laradji, I.; Friedlander, M.; and Koepke, H., 2015. Coordinate descent converges faster with the gauss-southwell rule than random selection. In *Proceedings of the 32nd International Conference on Machine Learning (ICML-15)*, 1632–1641. JMLR Workshop and Conference Proceedings. http://jmlr.org/proceedings/papers/v37/nutini15.pdf. (cited on page 93)

Proceedings of the National Academy of Sciences, 2005. *Spell issue on Gene regulatory networks*, vol. 102(14). http://www.pnas.org/content/102/14/4935.full.pdf.

Recht, B. and Re, C., 2012. Beneath the valley of the noncommutative arithmetic-geometric mean inequality: conjectures, case-studies, and consequences. Technical report, University of Wisconsin-Madison. (cited on page 94)

Richtarik, P. and Takac, M., 2011. Iteration complexity of randomized block-coordinate descent methods for minimizing a composite function. Technical report, University of Edinburgh. (cited on page 3)

Robbins, H. and Monro, S., 1951. A stochastic approximation method. *Ann. Math. Statist.*, 22, 3 (09 1951), 400–407. doi:10.1214/aoms/1177729586. http://dx.doi.org/10.1214/aoms/1177729586. (cited on page 4)

Rockafellar, R. T., 1970. *Convex Analysis*. Princeton Paperbacks. (cited on page 167)

Rothman, A.; Bickel, P.; Levina, E.; and Zhi, J., 2008. Sparse permutation invariant covariance estimation. *Electronic Journal of Statistics*, (2008). (cited on page 106)

Rumelhart, D. E.; Hinton, G. E.; and Williams, R. J., 1986. Learning representations by back-propagating errors. *Nature*, 323 (1986), 533–536. (cited on page 13)

Salakhutdinov, R. and Mnih, A., 2008. Bayesian probabilistic matrix factorization using mcmc. In *ICML*. (cited on page 157)

Salakhutdinov, R.; Mnih, A.; and Hinton, G., 2007. Restricted boltzmann machines for collaborative filtering. In *Twenty-fourth International Conference In Machine Learning*. (cited on page 156)

Sarwar, B.; Karypis, G.; Konstan, J.; and Riedl, J., 2001. Item-based collaborative filtering recommendation algorithms. In *WWW10*, 285–295. (cited on pages 150 and 155)

Saul, Z. M. and Filkov, V., 2007. Exploring biological network structure using exponential random graph models. *Bioinformatics*, (2007). (cited on page 122)

Scheinberg, K. and Ma, S., 2012. *Optimization for Machine Learning*, chap. Optimization Methods for Sparse Inverse Covariance Selection, 455–477. MIT Press. (cited on page 106)

Scheinbert, K.; Ma, S.; and Goldfarb, D., 2010. Sparse inverse covariance selection via alternating linearization methods. In *NIPS*. (cited on pages 105, 114, 115, 116, and 120)

Schmidt, M.; Roux, N. L.; and Bach, F., 2013. Minimizing finite sums with the stochastic average gradient. Technical report, INRIA. (cited on pages 4, 18, 26, 27, 36, 58, and 61)

Sedhain, S.; Sanner, S.; Braziunas, D.; Xie, L.; and Christensen, J., 2014. Social collaborative filtering for cold-start recommendations. *In Proceedings of the ACM Conference on Recommender Systems*, (2014). (cited on page 165)

Shalev-Shwartz, S. and Zhang, T., 2013a. Accelerated proximal stochastic dual coordinate ascent for regularized loss minimization. Technical report, The Hebrew University, Jerusalem and Rutgers University, NJ, USA. (cited on pages 16, 17, and 32)

Shalev-Shwartz, S. and Zhang, T., 2013b. Stochastic dual coordinate ascent methods for regularized loss minimization. *JMLR*, (2013). (cited on pages 4, 6, 8, 13, and 26)

Shental, O.; Bickson, D.; Siegel, P. H.; Wolf, J. K.; and Dolev, D., 2008. Gaussian belief propagation solver for systems of linear equations. In *IEEE Int. Symp. on Inform. Theory (ISIT)*. Toronto, Canada. (cited on page 154)

Snijders, T., 2002. Markov chain monte carlo estimation of exponential random graph models. *Journal of Social Structure*, (2002). (cited on page 118)

Snijders, T. A.; Pattison, P. E.; and Handcock, M. S., 2004. New specifications for exponential random graph models. Technical report, University of Washington. (cited on page 112)

Stern, D.; Herbrich, R.; and Graepel, T., 2009. Matchbox: large scale online bayesian recommendations. In *WWW* (Madrid, Spain, 2009). (cited on pages 155 and 158)

Terry, A., 2005. *Exponential random graphs*. Master's thesis, University of York. (cited on page 112)

Truyen, T. T.; Phung, D. Q.; ; and Venkatesh, S., 2007. Preference networks: Probabilistic models for recommendation systems. *Sixth Australasian Data Mining Conference (AusDM)*, (2007). (cited on page 157)

Wainwright, M. J.; Jaakkola, T. S.; and Willsky, A. S., 2003. Tree-reweighted belief propagation algorithms and approximate ml estimation by pseudo-moment matching. *AISTATS*, (2003). (cited on page 1)

Wang, Z.; Tan, Y.; and Zhang, M., 2010. Graph-based recommendation on social networks. *APWEB*, (2010). (cited on page 165)

Weiss, Y. and Freeman, W. T., 2001. Correctness of belief propagation in gaussian graphical models of arbitrary topology. *Neural Computation*, 13 (2001), 2173–2200. (cited on page 149)

Widrow, B. and Hoff, M. E., 1960. Adaptive switching circuits. *Institute of Radio Enginners, Western Electronic Show and Convention*, 4 (1960), 96–104. (cited on page 13)

Xiao, L. and Zhang, T., 2014. A proximal stochastic gradient method with progressive variance reduction. Technical report, Microsoft Research, Redmond and Rutgers University, Piscataway, NJ. (cited on page 66)

Xin, X.; King, I.; Deng, H.; and Lyu, M. R., 2009. A social recommendation framework based on multi-scale continuous conditional random fields. In *CIKM*. (cited on page 157)

Yang, J. and Leskovec, J., 2010. Modeling information diffusion in implicit networks. *ICDM*, (2010). (cited on page 164)

Yang, T., 2013. Trading computation for communication: Distributed stochastic dual coordinate ascent. *NIPS*, (2013). (cited on page 163)

Yedidia, J. S.; Freeman, W. T.; and Weiss, Y., 2000. Bethe free energy, kikuchi approximations and belief propagation algorithms. Technical report, Mitsubishi electric research laboratories. (cited on pages 1 and 148)

Yuan, M. and Lin, Y., 2007. Model selection and estimation in regression with grouped variables. *Journal of the Royal Statistical Society*, (2007). (cited on page 111)

Zhu, C.; H.Byrd, R.; Lu, P.; and Nocedal, J., 1997. L-bfgs-b: Algorithm 778: Fortran routines for large scale bound constrained optimization. *ACM TOMS*, (1997). (cited on page 149)